Universitat Autònoma de Barcelona

Role of Nr4a2 transcription factor in hippocampal synaptic plasticity. Possible therapeutic target for Alzheimer's disease

Judit Català Solsona

Institut de Neurociències
Departament de Bioquímica i Biologia Molecular
Unitat de Bioquímica, Facultat de Medicina
Universitat Autònoma de Barcelona

Role of Nr4a2 transcription factor in hippocampal synaptic plasticity. Possible therapeutic target for Alzheimer's disease.

Judit Català Solsona

PhD in Neurosciences

Bellaterra, 2020

Institut de Neurociències
Departament de Bioquímica i Biologia Molecular
Unitat de Bioquímica, Facultat de Medicina
Universitat Autònoma de Barcelona

Role of Nr4a2 transcription factor in hippocampal synaptic plasticity. Possible therapeutic target for Alzheimer's disease.

Paper del factor de transcripció Nr4a2 en la plasticitat sinàptica hipocampal. Possible diana terapèutica per la malaltia d'Alzheimer.

Memòria de tesi doctoral presentada per Judit Català Solsona per optar al grau de Doctora en Neurociències per la Universitat Autònoma de Barcelona.

Treball realitzat al Departament de Bioquímica i Biologia Molecular i a l'Institut de Neurociències de la Universitat Autònoma de Barcelona sota la direcció del Dr. José Rodríguez Álvarez.

El treball realitzat en aquesta tesis doctoral ha estat finançat pels projectes de recerca del Ministerio de Ciencia, Innovación y Universidades (SAF2014-59697-R, SAF2017-89271-R), Centro de Investigación Biomédica en Red en enfermedades Neurodegenerativas –CIBERNED– (CB06/05/0042), Fundació La Marató TV3 (TV3-20143610), Generalitat de Catalunya (SGR2017-749) i per una beca predoctoral del Ministerio de Ciencia, Innovación y Universidades (Formación Profesorado Europeo, FPU14/05392).

Bellaterra, 6 de març de 2020

Doctoranda — Director de tesis

Judit Català Solsona — José Rodríguez Álvarez

"Travel isn't always pretty. It isn't always comfortable. Sometimes it hurts, it even breaks your heart. But that's okay. The journey changes you; it should change you. It leaves marks on your memory, on your consciousness, on your heart, and on your body. You take something with you. Hopefully, you leave something good behind."

Anthony Bourdain

CONTENTS

I. ABSTRACT

Effective strategies to prevent or treat Alzheimer's pathology remain elusive. To confront a disease with such a long prodromal phase is crucial to understand the mechanisms altered at early stages. Hippocampal synaptic dysfunction, broadly accepted to be caused by soluble forms of amyloid-β peptide (oAβ), strongly correlates with the cognitive decline observed in Alzheimer's disease (AD) patients and is thought to underlie its initial development. Postsynaptic forms of hippocampal long-term potentiation (LTP) and long-term depression (LTD) processes are widely believed to underlie some forms of learning and memory. These changes in synaptic efficacy are tightly regulated by ionotropic glutamate receptors (iGluRs) levels at the synapse and activity-induced gene transcription. In this regard, nuclear receptors subfamily 4 group A (Nr4a) have emerged as possible modulators of hippocampal synaptic and cognitive functions, although the underlying molecular mechanisms remain unknown. The aim of this study is to investigate at the molecular, synaptic and behavioral level the potential role of Nr4a2 in the synaptic failure occurring at early stages of AD, focusing on the functions of Nr4a2 transcription factor in hippocampal synaptic plasticity. We observed that, in mature hippocampal-cultured neurons, Nr4a2 expression increased upon neuronal stimulation in a mechanism dependent on calcium entry though iGluRs and on the activation of the CREB/CRTC1 signaling pathway and the phosphatase calcineurin. Notably, protein levels and extracellular release of BDNF, as well as GluA1-AMPAR and GluN1-NMDAR subunit protein levels were reduced in absence of Nr4a2 and increased with its activation. In addition, Nr4a2 activation was also able to upregulate postsynaptic AMPAR levels in CA1 pyramidal neurons and to block LTD at Schaffer collateral to CA1 synapses. Importantly, the activity-dependent increase of Nr4a2 protein levels was disrupted in mature hippocampal-cultured neurons exposed to oAβ, and the activation of Nr4a2 was able to block the oAβ-mediated depression as well as the oAβ-dependent LTP impairments. We also examined the effects of virally mediated Nr4a2 hippocampal overexpression in the $APP_{Sw,Ind}$ mouse model of AD by using a battery of tests to explore the Behavioral and Psychological Symptoms of Dementia (BPSD)-like behaviors, the abolishment of daily living activities and the cognitive deficits in an early and moderate stage of the pathology. Remarkably, we found that Nr4a2 hippocampal overexpression not only partly ameliorated the cognitive deficits but also significantly rescued the increased anxiety-related behaviors in the $APP_{Sw,Ind}$ mouse model of AD at both ages. Altogether, our findings strongly support that Nr4a2 transcription factor is involved in glutamatergic synaptic plasticity associated to hippocampal-dependent learning and memory events, opening the possibility to emerge as a possible disease-modifying therapy targeting the synaptic dysfunction that occurs at early stages of AD.

II. RESUM

Actualment no existeixen estratègies efectives per prevenir o curar la patologia d'Alzheimer. Per combatre una malaltia amb una fase prodròmica tant llarga, és crucial entendre els mecanismes alterats en estadis inicials. Actualment es creu que les formes solubles oligomèriques del pèptid β-amiloide (oAβ) generen la disfunció sinàptica hipocampal, la qual correlaciona amb el deteriorament cognitiu que s'observa en pacients amb la malaltia d'Alzheimer i podria ser subjacent a l'inici de la patologia. Les formes post-sinàptiques hipocampals de potenciació a llarg termini (LTP) i depressió a llarg termini (LTD) es troben a la base d'alguns processos d'aprenentatge i memòria dependents d'hipocamp. Aquests canvis en l'eficàcia sinàptica estan fortament regulats pels nivells dels receptors ionotròpics de glutamat (iGluRs) a la sinapsi i per la transcripció gènica induïda per activitat. En aquest context, la subfamília 4 grup A de receptors nuclears (Nr4a) han emergit com a possibles moduladors de les funcions sinàptiques i cognitives hipocampals, encara que no es coneixen els mecanismes moleculars implicats. L'objectiu d'aquest estudi es basa en investigar a nivell molecular, sinàptic i conductual el potencial rol de Nr4a2 en la fallida sinàptica que té lloc en estadis inicials de la malaltia d'Alzheimer, basant-nos en les funcions d'aquest factor de transcripció en la plasticitat sinàptica hipocampal. Vam observar que, en neurones hipocampals madures en cultiu, l'expressió de Nr4a2 incrementava amb l'estimulació neuronal a través d'un mecanisme dependent de l'entrada de calci a través dels iGluRs i de l'activació de la via de senyalització CREB/CRTC1 i la fosfatasa calcineurina. A destacar es troba el fet que els nivells proteics i l'alliberació extracel·lular de BDNF, així com els nivells proteics de les subunitats GluA1-AMPAR i GluN1-NMDAR es van trobar disminuïts en absència de Nr4a2 i incrementats amb la seva activació. A més, l'activació de Nr4a2 també va augmentar els nivells d'AMPARs post-sinàptics en neurones piramidals de CA1 i va bloquejar la LTD a les sinapsis col·laterals de Schaffer a CA1. Cal ressaltar que els oAβ van afectar l'augment dels nivells proteics de Nr4a2 dependents d'activitat en neurones hipocampals madures en cultiu, mentre que l'activació de Nr4a2 va se capaç de bloquejar la depressió sinàptica causada pels oAβ així com el deteriorament que els oAβ generen sobre la LTP. També vam examinar els efectes de la sobreexpressió hipocampal de Nr4a2 utilitzant vectors virals en el model transgènic de ratolí $APP_{Sw,Ind}$ utilitzant una bateria de tests per avaluar els símptomes conductuals i psicològics de la demència, coneguts amb les sigles BPSD en anglès, la cessació de les activitats diàries i els dèficits cognitius en una etapa inicial i moderada de la patologia. Sorprenentment, vam observar que la sobreexpressió hipocampal de Nr4a2 no només va pal·liar els dèficits cognitius, sinó que també va reduir significativament el comportament ansiós dels ratolins $APP_{sw,ind}$ a ambdues edats. En conjunt, els nostres resultats recolzen el paper del factor de transcripció Nr4a2 en la plasticitat sinàptica glutamatèrgica associada als processos d'aprenentatge i memòria dependents d'hipocamp, obrint la possibilitat d'emergir com una possible diana terapèutica per combatre la disfunció sinàptica que té lloc en estais inicials de la malaltia d'Alzheimer.

III. LIST OF ABBREVIATIONS

4-AP	4-aminopyridine
AAV	Adeno-associated viral vector
Aβ	Amyloid-beta
ACSF	Artificial cerebrospinal fluid
AD	Alzheimer's disease
ADDL	Aβ-derived diffusible ligands
AF	Activation function
AICD	Amyloid intracellular domain
AKAP150	A kinase anchor protein 150
AMPA	α-amino-3-hydroxy-5-methylisoxazole-4-propionic acid
AMPAR	AMPA receptor
ANOVA	Analysis of variance
AP-1	Activating protein 1
ApoE	Apolipoprotein E
APP	Amyloid precursor protein
AQ	Amodiaquine
Arc	Activity-regulated cytoskeleton-associated
A.U.	Arbitrary units
BACE-1	Beta-site amyloid precursor protein-cleaving enzyme 1
BDNF	Brain derived neurotrophic factor
Bic	Bicuculline
Bp	Base pairs
BPSD	Behavioral and psychological symptoms of dementia
BSA	Bovine Serum Albumin
CA	Cornu ammonis
CaMK	Ca^{2+}/calmodulin-dependent protein kinase
cAMP	Cyclic adenosine monophosphate
CAPS	N-cyclohexul-3-aminopropanesulfonic acid
CBP	CREB binding protein
C/EBP	CCAAT enhancer binding protein
CERAD	Consortium to Establish a Registry for Alzheimer's disease
CFC	Contextual fear conditioning
ChIP	Chromatin immunoprecipitation
CNS	Central nervous system
COX5β	Cyclooxigenase 5β
CQ	Chloroquine
CREB	cAMP-response element binding protein

CRTC1	CREB-regulated transcription coactivator 1
CSF	Cerebrospinal fluid
CT	Corner test
CTD	C-terminal domain
CTF	C-terminal fragment
DAT	Dopamine transporter
DBD	DNA-binding domain
DG	Dentate gyrus
DI	Discrimination index
DIV	Days *in vitro*
DMEM	Dulbecco's modified Eagle's medium
DMSO	Dimethyl sulfoxide
DNA	Deoxyribonucleic acid (cDNA, complementary DNA)
DNase I	Deoxyribonuclease I
EC	Entorhinal cortex
EDTA	Ethylenediaminetetraacetic acid
Egr	Early growth response
EGTA	Ethylene glycol tetraacetic acid
EPSC	Excitatory postsynaptic current (mEPSC, miniature EPSC)
EPSP	Excitatory postsynaptic potential (fEPSP, field EPSP)
ER	Endoplasmic reticulum
FAD	Familial AD
FBS	Fetal Bovine Serum
FDA	Food and Drug Administration
FDUR	Fluoro deoxyuridine
FRAP	Fluorescence recovery after photobleaching
FSK	Forskolin
GAPDH	Glyceraldehyde-3-phosphate dehydrogenase
GFP	Green fluorescent protein
GSK-3β	Glycogen synthase kinase 3β
H1	Histone 1
HDAC	Histone deacetylase
HEK 293T	Human embryonic kidney 293T
HFIP	Hexafluor-2-propanol
HFS	High frequency stimulation
HSV	Herpes simplex virus
IDE	Insulin-degrading enzyme
iGluRs	Ionotropic glutamate receptors

IR	Insulin receptor
IRES	Internal ribosomal entry site
KDa	Kilodalton
LBD	Ligand-binding domain
LFS	Low frequency stimulation
LOAD	Late onset AD
LTD	Long term depression (cLTD, chemical LTD)
LTP	Long term potentiation (cLTP, chemical LTP)
MAPK	Mitogen-activated protein kinase
MARCKS	Myristoylated alanine-rich C kinase substrate
MB	Marble-burying
MCI	Mild cognitive impairment
MEM	Minimum essential medium
MTL	Medial temporal lobe
MWM	Morris Water Maze
nAChR	Nicotinic acetylcholine receptor
NBRE	Nerve growth factor-inducible-β-binding response element
NES	Nuclear export signal
NF-κB	Nuclear Factor κB
NFT	Neurofibrillary tangles
NMDA	N-methyl-D-aspartate
NMDAR	NMDA receptor
NMDG	N-Methyl-d-glucamin
NLS	Nuclear localization signal
NOR	Novel Object Recognition
NP-40	Nonidet P-40
Nr4a	Nuclear receptor subfamily 4 group A
NTD	N-terminal domain
NurRE	Nur-response element
oAβ	Aβ oligomers or soluble forms of Aβ peptide
OF	Open Field
ORM	Object recognition memory
p38 MAPK	p38 mitogen-activated protein kinase
PBS	Phosphate-buffered saline
PCR	Polymerase chain reaction
PD	Parkinson’s disease
PDGF β	Platelet-derived growth factor β
PDL	Poly-D-lysine

PFA	Paraformaldehyde
PI3K	Phosphatidylinositol 3-kinase
PK	Protein kinase
PMD	Postmortem delay
PMSF	Phenylmethylsulfonyl
PP	Protein phosphatase
PPIA	Peptidylpolyl isomerase A
PPR	Paired-pulse ratio
PrP^{C}	Cellular prion protein
PS/PSEN	Presenilin
PSD	Post-synaptic density
PTEN	Phosphatase and tensin homolog
PTX	Picrotoxin
RIN	RNA integrity number
RNA	Ribonucleic acid (mRNA, messenger RNA)
RRID	Research resource identifier
RT-qPCR	Quantitative real-time polymerase chain reaction
RXR	Retinoic X receptor
SD	Standard deviation
SDS	Dodecyl sulfate
SEM	Standard error of the mean
shRNA	Short hairpin RNA
SIK	Salt-inducible kinase
SOD1	Sodium oxide dismutase 1
TAP	Thal Aβ phase
TARP	Transmembrane AMPAR regulatory protein
TBS	Tris-HCl buffered saline; Theta burst stimulation (depending on the context)
TH	Tyrosine hydroxylase
TrkB	Tyrosine receptor kinase B
TSFM	Ts translation elongation factor mitochondrial
TTX	Tetrodotoxin
UbC	Ubiquitin C
UTR	Untranslated region
VDCC	Voltage-dependent calcium channel
VMAT	Vesicular amine transporter 2
WR	Wall rearing
WT	Wild type

IV. Introduction

Preface

In 1906, Aloysius *Alois* Alzheimer described the neuropathology of the disease that was to bear his name; a disease that has become the most prevalent cause of dementia and currently affects more than 40 million people worldwide. Despite major efforts to understand its basic biology and clinical pathophysiology, with more than 100,000 published articles concerning this disorder and more than 450 failed clinical trails so far, strategies to prevent or treat Alzheimer's pathology are still far from being effective.

The structure of the brain is enormously complex. It contains about 100 billion nerve cells or neurons that are intertwined in an intricate network through thousand trillion connections, the so-called synapses. Long-lasting changes of synaptic efficacy are mediated by activity-induced gene transcription and are essential for neuronal plasticity and memory. Synaptic dysfunction, occurring several years before symptoms become evident, is widely accepted to underlie the cognitive decline that will lead to dementia in Alzheimer's disease. Therefore, understanding the molecular pathways regulating gene expression profiles may help to identify new synaptic therapeutic targets. In this scenario, transcription factors have emerged as pivotal players underlying synaptic plasticity and the modification of neural networks required for memory formation and consolidation. Among them, the Nr4a family of transcription factors has been reported to have a role in multiple processes altered in Alzheimer's pathology.

The aim of this study is to investigate the functions of Nr4a2 in hippocampal synaptic plasticity and its involvement in the synaptic failure occurring early in Alzheimer's pathology to ultimately use Nr4a2 activation as a possible therapeutic approach to prevent or delay the progression of this devastating disease.

Initially, the conceptual basis of this project will be discussed, with a revision of Alzheimer's neuropathology focusing on hippocampal synaptic dysfunction as a key-triggering factor. Then, differential gene expression in Alzheimer's hippocampus with special emphasis on transcription factors will be reported to eventually introduce Nr4a2 activation as a potential effective disease-modifying therapy for the treatment of Alzheimer's pathology.

1. Alzheimer's disease

1.1. General features: triggers, progression and clinical pathology

Alzheimer's disease (AD) is a multifactorial neurodegenerative disorder characterized by severe synaptic and neuronal loss and two major histopathological hallmarks: amyloid plaques and neurofibrillary tangles (NFTs). Amyloid plaques consist in extracellular deposits of aggregated amyloid-β (Aβ) peptides, which are typically surrounded by neurons with dystrophic neurites. Otherwise, NFTs are inclusions of filamentous aggregates of hyperphosphorylated tau protein species formed in neuronal cell bodies, which are referred to as threads if they are formed in dendrites or axons (Blennow, Leon & Zetterberg, 2006) **(figure 1).**

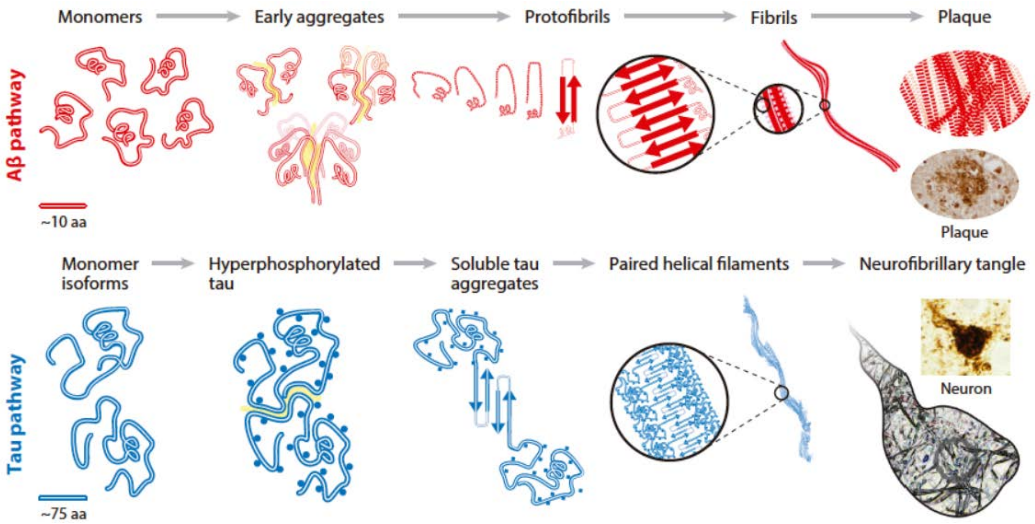

Figure 1. Main histopathological hallmarks of AD. *Top panel:* monomers of amyloid-β (Aβ) leading to amyloid plaques. Aβ monomers spontaneously self-assemble to form aggregates and then protofibrils, which ultimately form insoluble amyloid plaques. *Bottom panel:* monomers of tau leading to neurofibrillary tangles (NFT). Soluble tau aggregates of hyperphosphorylated species (shown by blue spots) assemble to paired helical filaments that will eventually form intracellular NFT or threads. Modified from Graham, Bonito-Oliva & Sakmar, 2017.

The neuropathology in AD comprises a broad range of alterations including dysregulation of calcium homeostasis (Demuro et al., 2005), increased oxidative stress (De Felice et al., 2007, de la Monte & Wands, 2006), mitochondrial dysfunction (Alberdi et al., 2010; Paula-Lima et al., 2011), inhibition of axonal transport of vesicles, neurotrophins and organelles (Decker et al., 2010b; Pigino et al., 2009; Poon et al., 2011), endoplasmic reticulum (ER) stress (Umeda et al., 2011), impaired protein-folding function and deficient proteasome-mediated and autophagic-mediated clearance of damaged proteins (Hoozemans et al., 2005; Tseng et al., 2008), cell cycle re-entry (Varvel et al., 2008) and recruitment of

astrocytes and microglia (Maezawa et al., 2011; Tomiyama et al., 2010). These events, either directly or indirectly, contribute to the severe synaptic and neuronal loss observed in AD.

Current research identifies three stages of the pathology: presymptomatic or preclinical AD, which can last for years in which the pathophysiological process has started but the clinical symptoms are not still present (Sperling, Mormino, & Johnson, 2014), mild cognitive impairment (MCI) due to AD, which can also last for years, and dementia due to AD **(figure 2).** Approximately 15-20% of people older than 65 years have MCI, an intermediate stage from normal cognition to dementia that identifies a spectrum of diseases that include impairment in both memory and non-memory cognitive domains (Roberts & Knopman, 2013). MCI due to AD links the MCI syndrome to a specific etiology by the use of biomarkers for AD. From those patients with MCI due to AD, around 30% will develop dementia due to AD in the next 5 years. This reflects the slow, insidious and uncertain progression of AD. Compensation processes may explain the delay between initial signs of synaptic loss and the clinical manifestation of memory deficits (Katzman, 2004). For simplicity purposes, in the rest of the text MCI will refer to MCI due to AD, and AD will refer to dementia due to AD.

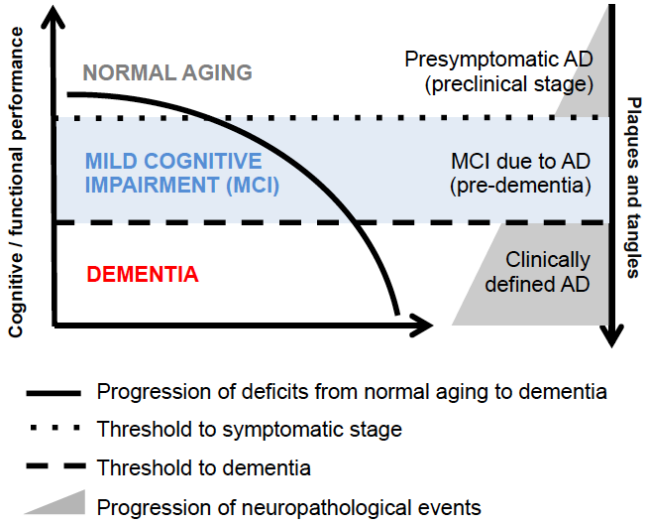

Figure 2. Schematic representation of the relationship between the progression of cognitive function and the neuropathological events in the transition from presymptomatic AD to MCI and dementia due to AD. Modified from Forlenza, Diniz & Gattaz, 2010.

Typically, the symptoms of the disease begin with insidious episodic memory difficulties and gradually progress towards a prominent impairment in memory, executive functions, visuospatial abilities, language and other domains of cognition and behavior. Agitation, hallucinations, delusions, depressive symptoms (changes in sleeping habits, irritability and

aggressiveness) and other behavioral disturbances can also appear as the disease progresses (Voisin & Vellas, 2009). Cognitive and behavioral deficits interfere with complex activities of daily life and the pathology eventually becomes incapacitating.

1.1.1. APP processing and amyloid cascade hypothesis

Amyloid plaques, one of the main histopathological features of the disease, are primarily composed by Aβ peptides (Glenner & Wong, 1984), which originate from proteolysis of the type I integral membrane glycoprotein amyloid precursor protein (APP) (Kang et al., 1987; for review Querfurth & Laferla, 2010). The human *APP* gene is located on chromosome 21 with three major isoforms arising from alternative splicing, APP695, APP751 and APP770, with APP695 being predominantly expressed in neurons. Although APP has been the subject of much study since its identification, its physiological function remains largely undetermined. A role for APP has been suggested in various processes such as neurite outgrowth and synaptogenesis, neuronal trafficking, transmembrane signal transduction, cell adhesion or calcium metabolism (Zheng & Koo, 2006).

Two mutually exclusive pathways process APP, the anti-amyloidogenic and the pro-amyloidogenic processing. The anti-amyloidogenic cleavage of APP is initiated by the α-secretase ADAM10 (Kuhn et al., 2010; Lammich et al., 1999), which releases a large soluble APP ectodomain (sAPPα) and leaves an 83-residue C-terminal fragment (α-CTF). α-CTF is then digested by γ-secretase, giving rise to an extracellular p3 and the amyloid intracellular domain (AICD), which has been implicated in gene transcription and calcium signaling (Huifang et al., 2007). sAPPα has an important role in neuronal plasticity and survival, and it is protective against excitotoxicity (Furukawa et al., 1996).

Conversely, the pro-amyloidogenic processing of APP is accomplished by two-step proteolitic cleavage initiated by the β-secretase beta-site amyloid precursor protein-cleaving enzyme 1 (BACE-1) (Vassar et al., 1999), which cleaves near the N-terminus of the Aβ domain of APP to generate secreted sAPP-β and leaves a membrane bound β-CTF containing the entire Aβ domain. Although sAPP-β only differs from sAPPα by lacking the Aβ1-16 region in the carboxyl-terminus, sAPP-β has been reported to mediate axonal pruning and neuronal cell death (Nikolaev et al., 2009). The Aβ domain is further cleaved by γ-secretase, a protein complex with presenilin 1 as its catalytic core, giving rise to AICD and different Aβ peptides of varying lengths (39 to 43 amino acids) depending on the site of cleavage **(figure 3).** Therefore, Aβ monomers are natural products of metabolism, being $A\beta_{40}$ and $A\beta_{42}$ peptides the ones that aggregate *in vivo* and have

pathogenic effects. $A\beta_{40}$ monomers are much more prevalent and less prone to aggregate than $A\beta_{42}$ species.

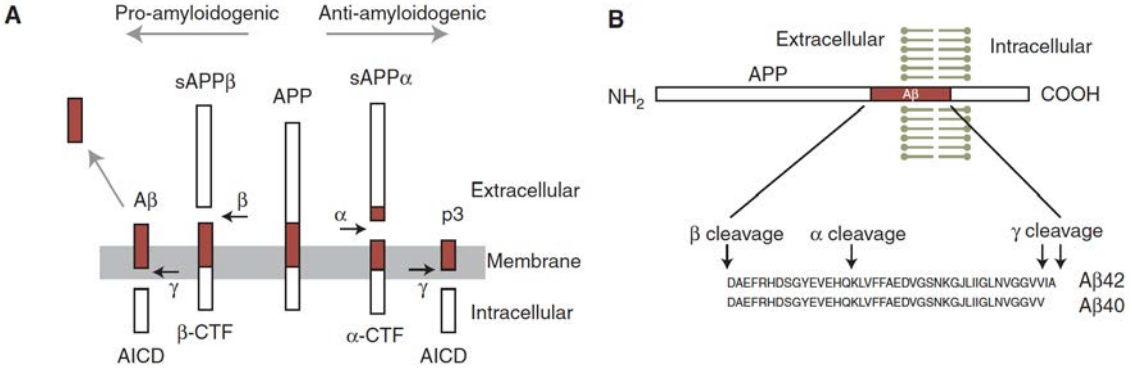

Figure 3. Amyloid precursor protein processing and the formation of amyloid-β peptides. A) Pro-amyloidogenic and anti-amyloidogenic processes of APP. Sequence of events are detailed in the main text. **B)** Schematic structure of APP and sequence of $A\beta_{40}$ and $A\beta_{42}$ peptides, with secretase cleavage sites indicated with arrows. Aβ, amyloid β; AICD, amyloid intracellular domain; APP, amyloid precursor protein; CTF, C-terminal fragment; sAPP, soluble APP. Modified from Sheng, Sabatini & Su, 2015.

$A\beta_{42}$ spontaneously self-aggregates into multiple coexisting forms. Aβ oligomers or soluble forms of Aβ peptide (oAβ) include dimers, trimers, Aβ*56 (a putative dodecameric Aβ assembly, 56 kda), spices immunoreactive to Aβ-derived diffusible ligands (ADDLs) (docecamers, 35-60 kda)/globulomers (dodecamers, 38-48 kda) antibodies, and annular protofibrils (Wang et al., 2016b). oAβ follow a trimer-based expansion in size under physiological conditions, but in pathological conditions monomeric Aβ becomes misfolded into dimers, which can rapidly expand to create dimer-based protofibrils, ultimately arranging themselves into β-sheets to form insoluble fibers constituting the amyloid plaques.

The amyloid cascade hypothesis, formulated in 1991 (Hardy & Allsop, 1991), broadly posited that an imbalance between production and clearance, with the consequent aggregation of Aβ peptides, caused Aβ to accumulate into amyloid plaques, which was thought to be the primary cause of AD (Hardy & Higgins, 1992; Hardy & Selkoe, 2002). The original formulation of the amyloid hypothesis was based in part on the discovery that the *APP* gene was on chromosome 21, implying that individuals with Down's syndrome (trisomy of chromosome 21) developed typical AD neuropathology because they produced more Aβ (Kolata, 1985). Evidence was also built on the overproduction of Aβ peptides in nearly all familiar forms of AD (see section 1.1.3 introduction).

The precise meaning of the amyloid hypothesis changed over years due to poor correlation between amyloid plaque load and cognitive functions in AD patients (Roth,

Tomlinson & Blessed, 1966; Terry, 1996). The original amyloid cascade hypothesis of AD switched to the oligomer hypothesis of AD, which specifically points out the oAβ as the neurotoxic forms causing synaptic toxicity and leading to synaptic dysfunction and eventual loss (Cleary et al., 2005; Klein, Krafft, & Finch, 2001; Lesne et al., 2006; Shankar et al., 2007, 2008; for review Selkoe & Hardy, 2016; Walsh & Selkoe, 2007) **(figure 4).**

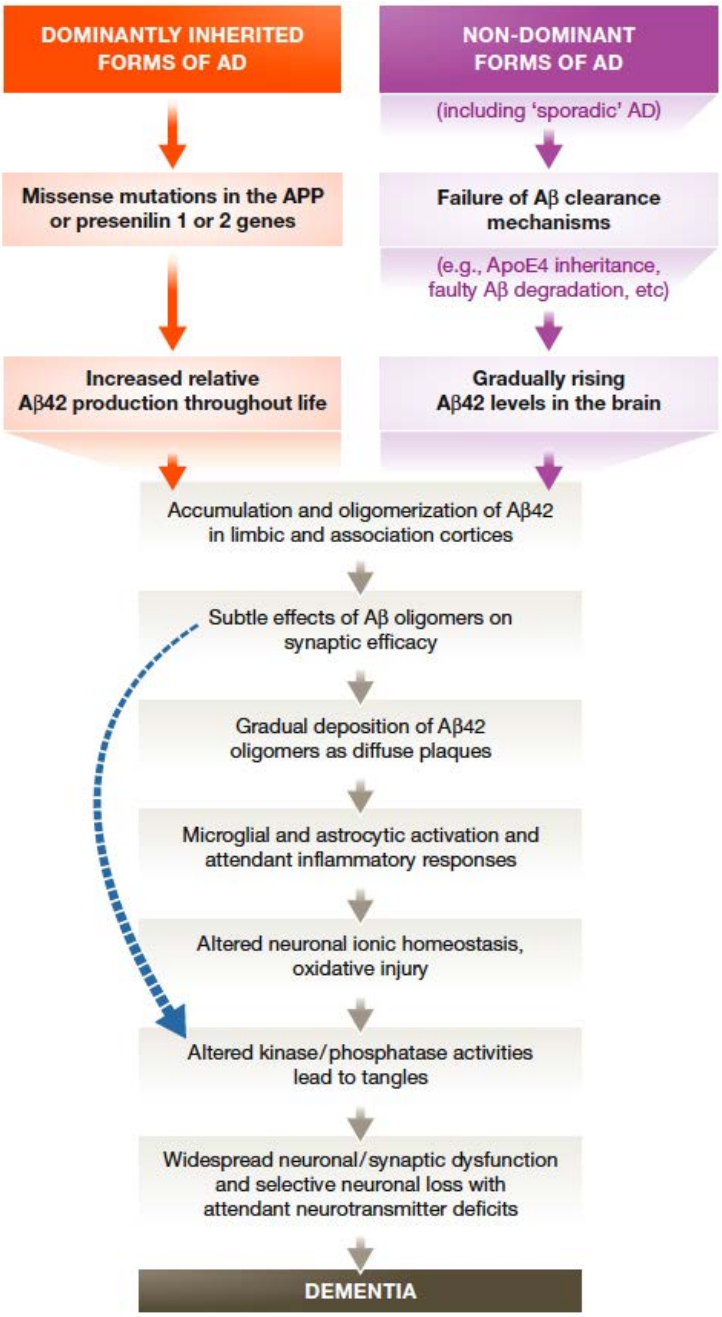

Figure 4. Sequence of major pathogenic events leading to dementia due to AD proposed by the oligomer cascade hypothesis. Both dominantly inherited and non-dominant forms of AD (reviewed in section 1.1.3 introduction) lead to accumulation of oAβ, synaptotoxins able to directly injure synapses in addition to cause neuroinflammation, oxidative stress and other neuropathological insults that will eventually cause selective neuronal loss and dementia. From Selkoe & Hardy, 2016.

Cognitive impairments, beginning early in the disease, have been attributed to oAβ-induced disruption of synaptic plasticity, with later stages of dementia attributed to oAβ-induced synapse and cellular degeneration and death (Ferreira & Klein, 2011). Indeed, oAβ levels strongly correlate with synaptic loss (Koffie et al., 2009; Lue et al., 1999) and the severity of the disease (Mc Donald et al., 2010; McLean et al., 1999). Synaptotoxic effects of oAβ have been mainly demonstrated in transgenic mice that express human mutant APP and overproduce human $A\beta_{40/42}$ and in slices from wild-type (WT) mice that are acutely exposed to various preparations of Aβ aggregates (Sheng et al., 2015; reviewed in detail in sections 1.3.4 and 1.3.5 of the introduction).

Although the oligomer hypothesis is currently supported by more than a decade of further investigation, it also arises some concerns. A longstanding debate exists about the neurotoxic properties of oAβ. It has been reported that mouse models with high levels of both $A\beta_{40}$ and $A\beta_{42}$ without APP overexpression do not show either neuronal loss nor cognitive deficits (Kim et al., 2013), indicating that Aβ peptide, including oAβ, was not cytotoxic. In addition, various immunotherapies targeting Aβ in AD patients have been effective decreasing its deposition but have not lead to improvement of cognitive symptoms or decreased accumulation of tau protein (Doody et al., 2014; Giacobini & Gold, 2013; Salloway et al., 2014; see also introduction, section 1.2).

1.1.2. Tau hypothesis

Hyperphosphorylation and consequent aggregation of tau is the other main histopathological hallmark of AD. Tau is a soluble, unfolded microtubule-associated protein that regulates the cytoskeletal dynamics of neurons, promoting assembly of tubulin and stabilizing microtubules (Trinczek et al., 1995). Although tau is primarily an axonal cytoplasmic protein, it has also been found at both the pre- and post-synapse in human brains (Tai et al., 2012). Interestingly, tau directly interacts with synaptic proteins, suggesting a role for tau in regulating intracellular signaling pathways (Pooler & Hanger, 2010). Extracellularly, tau is also found in brain fluids such as interstitial and cerebrospinal fluid (CSF; Arai et al., 1998; Yamada et al., 2011).

In AD brains, tau is mis-localized from axons to cell bodies and dendrites and it is accumulated in a hyperphosphorylated state in pathological inclusions (Goedert, 1993), the so-called NFT or threads, affecting selectively vulnerable brain regions that are essential for learning and memory (Hyman et al., 1984). Moreover, several studies have demonstrated active secretion and interneuronal transfer of tau in different AD models (de Calignon et al., 2012; L. Liu et al., 2012; Saman et al., 2012). Tau pathology is associated

with loss of synaptic proteins (Kopeikina et al., 2013) and neurodegeneration (Hutton et al., 1998; for review Iqbal et al., 2005). Spreading of tau is strongly correlated with the extent of cognitive and clinical symptoms (Bejanin et al., 2017). The tau hypothesis posits this protein as the principle causative substance for AD pathology.

Of interest is to mention that both oligomers of Aβ and tau are thought to spread through the brain in a way much like misfolded cellular prion protein (PrP^C) (Kim & Holtzman, 2010; Novak, Prcina & Kontsekova, 2011; Prusiner, 1984). Misfolded Aβ and tau have a seeding effect, and can induce normal Aβ and tau to misfold, spread and become toxic (de Calignon et al., 2012; Harris et al., 2010; Kane et al., 2000; Liu et al., 2012), so the disease seems to become self-propagating once it has started. Therefore, AD can be regarded as a disease that harbors two proteins with prion-like behavior (Nussbaum, Seward & Bloom, 2013).

What is indubitable is that increasing evidences are displacing the unitary view of AD as a disease with a single sequential pathological pathway, in which Aβ or tau are considered the only initial and/or causal event, towards a more complex picture in which AD is considered as a multiparameter pathology (Chetelat, 2013; Kametani & Hasegawa, 2018).

1.1.3. AD forms: familial and sporadic

Familial AD (FAD) is a very rare (estimated less than 0.5% of cases) autosomal dominant disease with early onset, caused by multiple point mutations in the *APP* or in presenelin-1 (*PSEN1*) or presenelin-2 (*PSEN2*) genes, being *PSEN1* mutations the most common cause of FAD (Bekris et al., 2010). APP mutations are clustered near β-secretase or γ-secretase cleavage sites and are associated with either an increase in Aβ production and/or a shift in the $Aβ_{42}/Aβ_{40}$ ratio toward the more pro-amyloidogenic form $Aβ_{42}$. As aforementioned, presenilins are the catalytic component of the γ-secretase complex, responsible for APP cleavage. Beyond that, they have a multitude of functions involving synaptic function and neurodegeneration (Pimplikar et al., 2010; Saura et al., 2004; Shen & Kelleher, 2007).

The vast majority of AD cases are sporadic, with age being the greatest risk factor. AD prevalence rises exponentially after 65 years old (Blennow, Leon & Zetterberg, 2006). However, it is important to stress that Alzheimer's dementia is not a normal part of aging (Nelson & Schmitt, 2011) and that older age alone is not sufficient to cause AD. Another risk factor is family history of AD, with an extent of heritability of almost 80% (Gatz et al., 2006).

There are also genes implicated in sporadic AD. The most firmly established genetic risk factor for sporadic AD is the allele e4 of the apolipoprotein E (*ApoE*) gene (Corder et al., 1993), which increases the risk to develop AD threefold to fourfold in heterozygous dose and around fifteen times in homozygous (Kim, Basak & Holtzman, 2009). ApoE-e4 allele is associated with deficient clearing of Aβ from the brain (Castellano et al., 2011; Robert et al., 2017) and increased tau-mediated neurodegeneration and neuroinflammation (Shi et al., 2017). Other biological processes also confer risk to develop AD such as inflammation or endosomal vesicle recycling (Jones et al., 2010; for review Selkoe & Hardy, 2016).

Pathogens as possible risk factors for AD have also been profoundly debated (Harris & Harris, 2015). Indeed, growing evidences have suggested that infection with herpes simplex virus (HSV)-1 may play a role in the progression of AD (Itzhaki, 2014). HSV viral deoxyribonucleic acid (DNA) has been found in AD brains (Readhead et al., 2018), being HSV-1 viral DNA associated with Aβ plaques (Wozniak, Mee, & Itzhaki, 2009), meanwhile an association between ApoE-e4 and HSV-1 has also been established (Corder, Lannfelt, & Mulder, 1998). Furthermore, epidemiological studies have provided evidence that a previous infection or a recent HSV-1 reactivation in elderly individuals increases the risk of developing AD (Letenneur et al., 2008; Tzeng et al., 2018).

Although some controversies exist, distinct environmental factors such as education, physical, cognitive and social activities, diet, sleep, circadian rhythm and cardiovascular risk factors (especially diabetes, obesity, smoking and hypertension) are also thought to affect sporadic AD as they influence the risk for dementia (Baumgart et al., 2015; for review James & Bennett, 2019). Of especial interest is the interrelation between AD and diabetes. Indeed, although not widely accepted as a clinical diagnosis, the term “type 3 diabetes” has been proposed to describe people who suffer from type 2 diabetes and they are also diagnosed with dementia due to AD (de la Monte & Wands, 2008; Kandimalla, Thirumala & Reddy, 2017). This condition has also been used to describe a form of brain-specific diabetes, suggesting that a brain-specific insulin resistance and insulin-like growth factor (IGF) signaling dysfunction represent early and progressive abnormalities that could account for the majority of molecular, biochemical and histopathological lesions in AD (Steen et al., 2005). Specifically, it has been demonstrated that induction of diabetes in rabbits leads to brain oAβ accumulation and tau hyperphosphorylation (Bitel et al., 2012) and, importantly, glucose concentrations observed in diabetic patients facilitate Aβ oligomerization (Kedia, Almisry & Bieschke, 2017).

1.2. Lack of effectiveness in AD therapies

Despite several decades of research and investment, no therapeutic strategy for AD treatment has demonstrated long-term efficacy to date. The U.S. Food and Drug Administration (FDA) approved four drugs that are currently marketed for the treatment of AD. Three of these drugs, donezepil, galantamine and rivastigmine, act on central nervous system (CNS) cholinergic pathways, severely affected in AD. All three drugs have anticholinesterase activity, and galantamine is also active as an allosteric modulator of nicotinic acetylcholine receptors (nAChRs). Memantine is the most recently approved drug, in 2013, which targets N-methyl-D-aspartate (NMDA) receptors (Winblad & Poritis, 1999). Evidence exists for both cholinergic and glutamatergic involvement in the etiology of AD (Francis, 2005).

In addition, non-pharmacological therapies are often utilized with the goal of maintaining or improving cognitive function, the ability to perform daily living activities or overall quality of life in AD patients. They are also used to reduce behavioral symptoms such as depression, apathy, wandering, sleep disturbances, agitation and/or aggression. Among these non-pharmacological therapies, regular physical exercise and cognitive training have been found modestly beneficial to AD patients (Groot et al., 2016; Hill et al., 2017; Zucchella et al., 2018).

Currently approved drugs are merely symptomatic if so, whose efficacy is limited in magnitude and by disease stage. Effective strategies to prevent and/or treat AD remain elusive despite major efforts to understand its basic biology and clinical pathophysiology. Given the involvement of oAβ in the synaptic dysfunction and memory impairment, researchers have focused their efforts, but not limited to, in finding therapeutic agents that prevent the production of oAβ or eliminate them. Various candidate drugs have been tested so far, including γ-secretase or BACE1 inhibitors to modulate Aβ production, Aβ immunotherapies to increase Aβ clearance, Aβ fibrillisation inhibitors, and also drugs to target hyperphosphorylated or specific conformations of tau protein, anti-inflammatory drugs, cholesterol-lowering drugs, oestrogens or antioxidants, among others (Cline et al., 2018; Graham et al., 2017; Sun & Alkon, 2019).

Even these attempts, more than 450 clinical trials have failed since the last drug for AD was approved and is more than evident that new approaches are needed (Cummings, Morstorf & Zhong, 2014). The high failure rate to develop successful disease-modifying therapies might be due, in part, to the advance stage of the patients enrolled in clinical trials because of the lack of early biomarkers for diagnosis, and also to the complexity of measuring drug efficacy in a disease with a long prodromal phase, often-insidious onset,

rates of progression that vary widely from individual to individual, and high-probability of co-morbidities (Sperling et al., 2014).

Moreover, one frustrating issue with clinical trials is their inability to therapeutically target the pathophysiological core underlying the dementia, which is the structural and functional deficits in synapses, known to strongly correlate with cognitive decline in AD patients (Bereczki et al., 2016; DeKosky & Scheff, 1990; Masliah et al., 2001; Scheff et al., 2006, 2007; Terry et al., 1991).

The continuous failures of AD clinical trials over the last decades unquestionably indicate that in order to find promising disease-modifying therapeutic agents an evaluation of the field is necessary.

1.3. Hippocampal synaptic dysfunction as a key-triggering factor for AD

1.3.1. Hippocampal pathology in AD

Prior to dementia due to AD, network dysfunctions occur in the medial temporal lobe (MTL) and related cortical areas essential for memory encoding and storage and collectively known as the default network (Hyman et al., 1984; Reitz et al., 2009; Sperling et al., 2010). The MTL includes the hippocampal formation (cornu ammonis –CA– field, divided into different subfields comprising CA1 to CA3, dentate gyrus –DG– and subiculum), amygdala and adjacent cortical regions (entorhinal cortex –EC–, perirhinal and parahippocampal cortices). The EC receives cortical sensory information and projects axons (perforant path) to DG granule cells. Axons from the lateral and medial EC innervate the outer and middle third of the granule cells dendritic tree, respectively. Glutamatergic granule cells of the DG project, through their axons (mossy fibers), to the proximal apical dendrites of CA3 pyramidal cells. The mossy fibers extend through the polymorphic layer, also known as hilus. In turn, CA3 pyramidal neurons project to ipsilateral CA1 pyramidal cells through Schaffer collaterals and to contralateral CA3 and CA1 pyramidal cells through commissural connections. In addition to this sequential trisynaptic circuit, there is also a dense associative network interconnecting CA3 cells on the same side. CA3 and CA1 pyramidal neurons are also innervated by direct inputs of the layer II and III of the EC, respectively **(figure 5).**

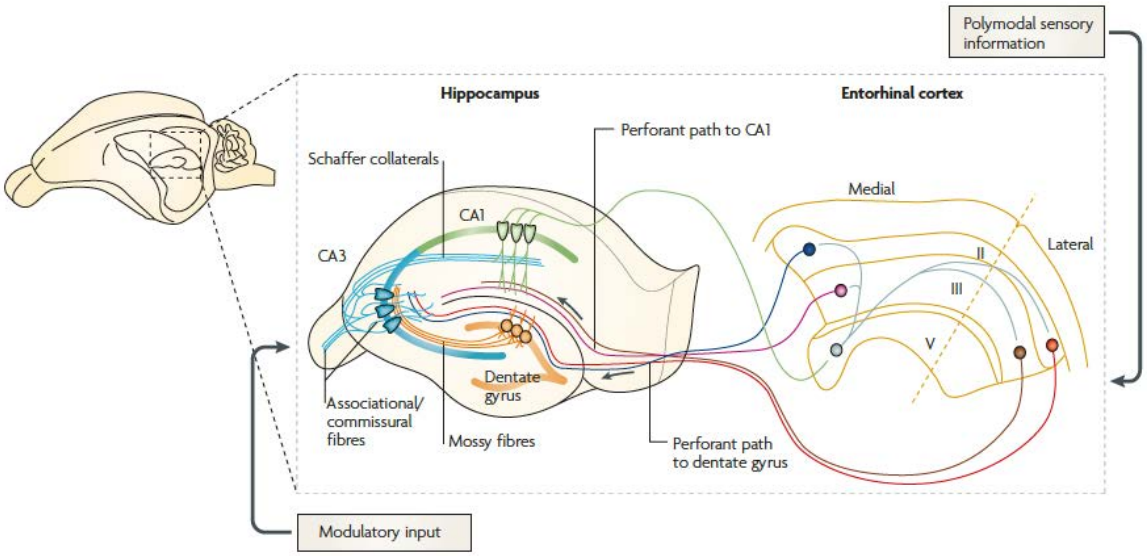

Figure 5. Basic connections of the hippocampus. Hippocampal connectivity is defined by a trisynaptic loop. Sensory information is carried by axons of the entorhinal cortex (perforant path) to granule cells of the dentate gyrus. Granule cells project their axons (mossy fibers) to CA3 pyramidal cells, which, in turn, project to ipsilateral CA1 pyramidal cells through Schaffer collaterals and to contralateral CA3 and CA1 pyramidal cells through commissural connections. For simplicity, inhibitory neurons and different modulatory inputs to hippocampal neurons are not depicted. From Neves, Cooke & Bliss, 2008.

Based on tau pathology, Braak and Braak distinguished six AD stages that can be summarized in three: entorhinal, limbic and isocortical (Braak & Braak, 1991). Specifically, tau pathology starts in the EC and continues to CA1 prior to clinical symptoms (Braak stages I-II). Next, tau pathology accumulates in limbic structures such as the subiculum of the hippocampal formation, amygdala and thalamus (Braak stages III-IV). Finally, pathological inclusions of tau spread to all isocortical areas with the associative areas being affected prior and more severely than the primary sensory, motor and visual areas (Braak stages V-VI) (Serrano-Pozo, Frosch, Masliah & Hyman, 2011) **(figure 6)**. In addition to the tau staging scheme, there are also other scoring systems based on Aβ pathology such as the Consortium to Establish a Registry for Alzheimer's disease (CERAD) and the Thal Aβ phase (TAP) (Hyman et al., 2012).

Hippocampal formation, affected very early in the disease process, is required for consolidation of long-term declarative or explicit memories (Jeneson & Squire, 2011), which can be divided into episodic (referring to the ability to recall personally experienced events) and semantic memories (regarding the meaning of words and concepts). Functional magnetic resonance imaging studies reported increased activity of cortical and temporal lobe regions, particularly the hippocampus, during memory tasks in preclinical and MCI patients, meanwhile decreased activity and connectivity of the hippocampus,

temporal and prefrontal cortices during episodic memory tasks was found in AD patients (Dickerson & Sperling, 2009; Setti, Hunsberger & Reed, 2017).

A decrease in the number of synapses by 25-30% in the frontal and temporal cortices has been reported in AD brain biopsies (Davies et al., 1987), primarily affecting the hippocampus (Coleman & Yao, 2003; Scheff et al., 2006, 2007). Synaptic loss has been shown to not only happen in degenerating neurons but also in the still surviving neurons (Masliah et al., 2001), and the major synaptic loss occurs very early in the AD process. Noteworthy, hippocampus, and specially CA1 subfield, undergoes atrophy, with reduced spine density (Perez-Cruz et al., 2011) and hypometabolism not only in dementia but also in MCI due to AD (Mosconi et al., 2005; La Joie et al., 2013).

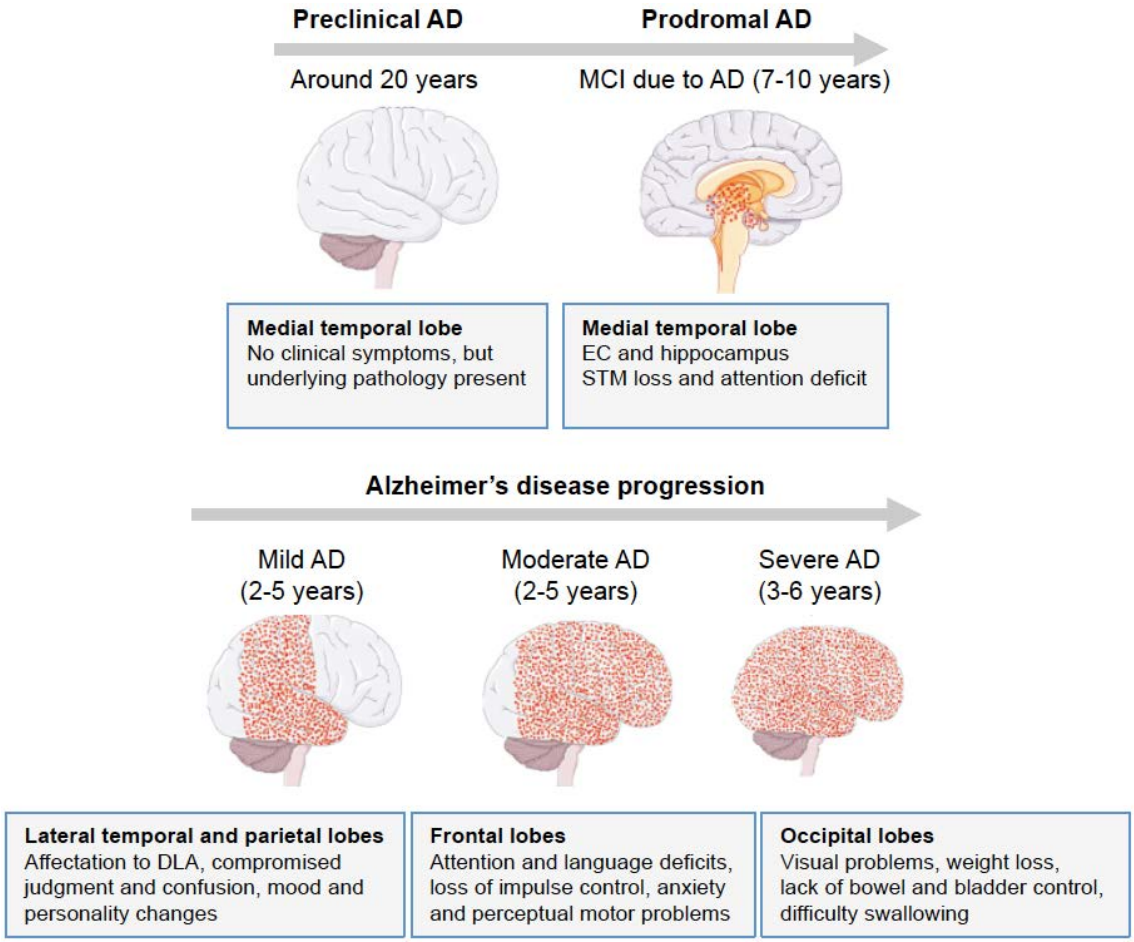

Figure 6. Schematic representation of the brain areas affected during AD progression and the consequent clinical manifestations. DLA, daily living activities; EC, entorhinal cortex, STM, short-term memory. Modified from Govindarajulu et al., 2018.

1.3.2. Hippocampal synaptic plasticity

Generally, plasticity refers to the ability of the nervous system to dynamically modulate its function in response to ongoing internal activities or external experiences (Jackson et al., 2019). Plasticity can be classified into different levels of function, from biochemical events to integrated behavioral responses. Structural plasticity refers to the physical morphology and number of synapses and the term synaptic plasticity describes persistent and activity-dependent changes in synaptic strength. These changes occur globally during homeostatic scaling or locally at individual synapses during Hebbian plasticity (Morris, 1999).

Long term potentiation (LTP) and long term depression (LTD) are the most actively studied forms of Hebbian plasticity that are thought to represent cellular correlates of particular types of learning and memory (Bliss & Lomo, 1973; Malenka & Bear, 2004; for review Nicoll, 2017). The specific cellular and molecular mechanisms mediating these processes depend on the synapses and circuits that are being activated and the specific pattern of activity. Changes in the properties and postsynaptic abundance of α-amino-3-hydroxy-5-methylisoxazole-4-propionic acid (AMPA) and NMDA receptors (AMPAR and NMDAR, respectively) underlie these forms of synaptic plasticity of excitatory transmission in the hippocampus (Bliss & Collingridge, 2013), besides for LTP occurring between mossy fiber synapses onto CA3 pyramidal dendrites, which is independent of NMDAR and is entirely expressed pre-synaptically (Nicoll & Schmitz, 2005).

NMDARs are heterotetrameric complexes formed by different assemblies of seven subunits (GluN1, GluN2A-D and GluN2A-B), being most native NMDARs composed of two GluN1 and two GluN2 subunits (Hansen et al., 2018). NMDARs activation has a central role in excitatory synaptic plasticity, as it can induce either LTP or LTD depending on the downstream activation of specific intracellular cascades in response to the extent of intracellular calcium rise in the dendritic spines (Kasai et al., 2010). The best-characterized form of both LTP and LTD occurs between CA3 and CA1 pyramidal neurons of the hippocampus. Both are expressed post-synaptically, require NMDARs activation, involve trafficking of existing AMPARs (Malenka & Bear, 2004) and require additional transcription and translation mechanisms.

LTP and LTD processes can be induced by a variety of electrical paradigms (Kumar, 2011). In acute hippocampal slices, LTP can be induced by high-frequency stimulation (HFS) protocols that typically comprise delivery of one or several trains of pulses at 50-100 Hz for 1 second or by theta burst stimulation (TBS). TBS is considered a better physiological way to induce LTP since it mimics the electroencephalogram theta waves

(theta rhytm: 5-10 Hz), an oscillation pattern found in the mammalian hippocampus when it is engaged in exploratory behavior and spatial memory processing (Colgin et al., 2013). These protocols cause a strong temporal summation of excitatory postsynaptic potentials (EPSPs) and the resultant large depolarization of the postsynaptic cell, which is sufficient to relieve the Mg^{2+} block of NMDARs and consequently allow a large amount of calcium to enter the postsynaptic cell during the induction protocol. Conversely, low frequency stimulation (LFS) of presynaptic axons is used to induce LTD, with a protocol that typically involves stimulation at 1-3 Hz for 5-15 minutes. This causes only a modest but prolonged increase in postsynaptic calcium due to modest and repetitive activation of NMDARs.

LTP and LTD processes can also be reproduced chemically. In hippocampal slices or culture cells, chemical LTP (cLTP) has been commonly induced by the increase of intracellular cyclic adenosine monophosphate (cAMP) levels by the application of the adenylyl ciclase activator forskolin (FSK) and the phosphodiesterase inhibitor rolipram (Molnár, 2011), meanwhile chemical LTD (cLTD) has been extensively studied by brief application (2 to 5 minutes) of NMDA (Ehlers, 2000; Lee et al., 1998).

1.3.3. AMPARs in hippocampal synaptic plasticity

Rapid but sustained changes in synaptic efficacy are mediated by AMPARs, which are mobile and recycle between the cytoplasm and the cell membrane. AMPARs are tetrameric, cation-permeable ionotropic glutamate receptors formed by assemblies of two dimers of four homologous pore-forming subunits (GluA1-GluA4), with GluA1/GluA2 heteromers comprising around 80% of all hippocampal synaptic AMPARs (Lu et al., 2009). Each AMPAR subunit consists of an extracellular region containing a N-terminal domain (NTD) and a ligand binding domain (LBD) followed by the transmembrane region, which forms the ion-conducting pore, and the cytosolic C-terminal domain (CTD) (Greger, Watson & Cull-Candy, 2017) **(figure 7).** Upon binding of glutamate, the pore opens to allow the influx of Na^+ ions along with K^+ efflux to depolarize the postsynaptic compartment, a requisite to fully relieve the Mg^{2+} block of NMDARs.

It is worth to note that depending on the subunit composition and the ribonucleic acid (RNA) editing, AMPARs can also permit Ca^{2+} influx. In the adult brain, most GluA2 subunits undergo RNA editing that replaces a glutamine with a positively charged arginine in the pore-forming region, preventing Ca^{2+} influx. In contrast, GluA2-lacking AMPARs are calcium permeable, mainly constituted by homomers of the GluA1 subunit (Luscher & Malenka, 2012).

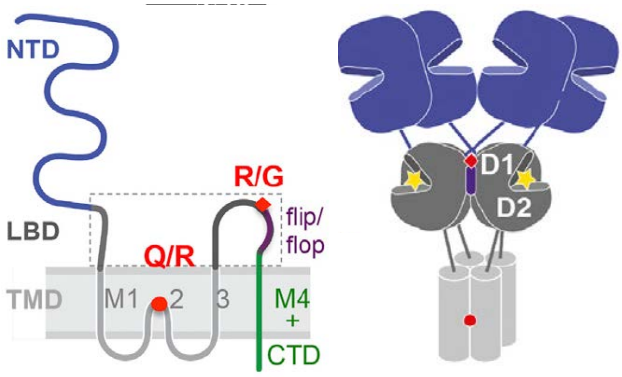

Figure 7. Schematic representation of AMPA receptor (AMPAR) structure. *Left:* AMPAR structural diagram. NTD (blue), LBD (gray; dashed square) and CTD (green) are depicted. mRNA processing sites (red; Q/R, R/G, and flip/flop) as well as the 4 transmembrane domains (M1-M4) are also indicated. *Right:* 3D AMPAR scheme. Sites of RNA editing in subunit interfaces (red, as in left) as well as agonist docking (yellow star) between LBD lobes (D1/2) are drawn. NTD, N-terminal domain; LBD, ligand-binding domain; CTD, C-terminal domain. Modified from Greger et al., 2017.

AMPARs are synthesized in the ER and transit through the Golgi apparatus. Some discrepancies exist about the assembly of AMPARs complexes. Schwenk and colleagues reported that AMPARs assembly into tetramers occurred in the ER in discrete steps determined by ER-resident proteins (Schwenk et al., 2019). However, other evidences exist showing that GluA1 and GluA2 monomers and dimers can enter and exit from synaptic regions, concluding that AMPARs are metastable, instantaneously falling apart into monomers, dimers or trimmers, which readily form tetramers again (Morise et al., 2019).

AMPARs can be inserted into the plasma membrane either at the soma or at synapses, and receptors inserted somatically travel to synaptic sites via lateral diffusion (Adesnik, Nicoll & England, 2005) **(figure 8).** Notably, AMPARs can also be synthetized locally at dendrites. Messenger RNA (mRNA) coding for GluA1 and GluA2 (Gria1 and Gria2, respectively) AMPAR subunits can be detected in dendrites together with protein translation machinery (Grooms et al., 2006; Shepherd & Huganir, 2007).

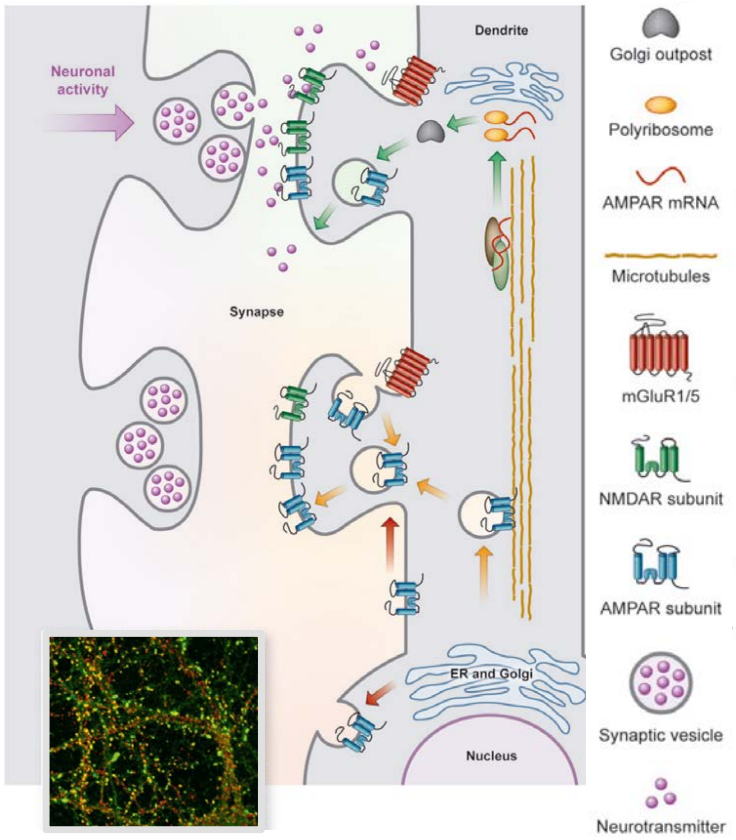

Figure 8. AMPA receptor (AMPAR) trafficking. AMPARs are synthetized in the ER and Golgi apparatus in the cell body and are inserted into the plasma membrane either at the soma (red arrows) or at synapses (yellow arrows). Receptors can also be synthetized locally at dendrites (green arrows). The inset at lower left shows cultured hippocampal neurons stained with PSD-95 (green) and surface GluA1 (red) markers. ER, endoplasmic reticulum. Modified from Shepherd & Huganir, 2007.

A major mechanism for the expression of LTP and LTD involves increasing or decreasing, respectively, the number of AMPARs in the plasma membrane at synapses via activity-dependent changes in AMPARs trafficking (Bredt & Nicoll, 2003; Malinow & Malenka, 2002; Song & Huganir, 2002; Watson, Ho & Greger, 2017). AMPARs postsynaptic recruitment comes either from neighboring extra synaptic receptors or from intracellular reserve pools by exocytosis (Penn et al., 2017). AMPARs exocytosis to synapses is mediated by SNARE proteins meanwhile synaptic receptors are removed from synapses by dynamin-dependent endocytosis (Chater & Goda, 2014; Jurado et al., 2013).

A part from the number of AMPARs at the synapse, LTP and LTD processes are also modulated by subunit-specific protein interactions, auxiliary proteins and posttranslational modifications in its cytosolic c-tail including phosphorylation, ubiquitination, glycosylation, palmitoylation and s-nitrosylation (Diering & Huganir, 2018; Huganir & Nicoll, 2013). Notably, GluA1-AMPARs cytosolic c-tail has been postulated to be both necessary and sufficient for hippocampal LTP (Zhou et al., 2018). Specifically, phosphorylation of the

cytosolic c-tail is a critical determinant of AMPARs trafficking and function (Esteban et al., 2003; W. Lu & Roche, 2012; Wang et al., 2014). AMPARs are substrates for a wide range of kinases including protein kinase A (PKA), protein kinase G (PKG), protein kinase C (PKC), Ca^{2+}/calmodulin-dependent kinase II (CaMKII), casein kinase II, PAK3 and Src family of tyrosine kinases on over 20 different phosphorylation sites, three to five sites per subunit (Diering & Huganir, 2018; Huganir & Nicoll, 2013).

In general, kinase activity resulting in AMPARs phosphorylation is associated with LTP whereas phosphatase activity and dephosphorylation is linked to LTD (Banke et al., 2000). For LTP, there is strong evidence that opening NMDARs increases calcium concentration sufficiently in the dendritic spine to activate CaMKII/PKC, which phosphorylate a wide range of substrates involved in plasticity (Soderling, 2000) including AMPARs themselves at serine 831 (Ser831) residue of GluA1 subunit, increasing GluA1 single-channel conductance and promoting GluA1 targeting to the post-synaptic density (PSD) **(figure 9).** Phosphorylation of Ser831 and Ser845 residues of GluA1 subunit are both strongly associated with LTP. Ser845-GluA1 is phosphorylated by PKA, which can be activated by Ca^{2+}-sensitive adenyl-ciclase or downstream of neuromodulators signaling through their Gs-coupled receptors, such as the β-adrenergic receptor or D1-type dopamine receptors (Joiner et al., 2010; Sun, Zhao & Wolf, 2005). Phosphorylation of Ser845-GluA1 increases single-channel open probability and also promotes GluA1 targeting or retention to the cell surface (Man, Sekine-Aizawa & Huganir, 2007).

Gene knockin mice lacking both Ser831 and Ser845 phosphorylation sites of GluA1-AMPARs showed faster decaying of LTP and a deficit in LTD (Lee et al., 2003). Later, it was described that Ser831 mutants displayed normal LTP and LTD, whereas Ser845 mutants had a specific deficit in LTD, concluding that Ser845 site is critical for LTD expression whereas both phosphorylation sites may support LTP (Lee et al., 2010). Mounting evidences suggest that indeed, PKA-mediated phosphorylation of Ser845-GluA1-AMPARs promotes its surface trafficking, lowering the threshold needed to induce LTP. However, additional signaling from CaMKII is needed to promote GluA1-AMPARs targeting to the PSD for maximal LTP (Esteban et al., 2003).

Ser845-GluA1 dephosphorylation is critical for NMDAR-dependent hippocampal LTD. A population of perisynaptic calcium permeable AMPARs (GluA1 homomers) are transiently recruited to the synapse during the induction of LTD in a PKA-dependent manner. Transient signaling from synaptic calcium permeable AMPARs is required for the full expression of LTD. During the progression of LTD, calcium permeable AMPARs signal their own removal through activation of the protein phosphatase calcineurin (also known as protein phosphatase 2B –PP2B–). GluA1-AMPARs undergo dephosphorylation of

threonine 840 and Ser845 during LTD by PP1/PP2A and calcineurin/PP2B, respectively (Sanderson, Gorski & Dell'Acqua, 2016) **(figure 9)**.

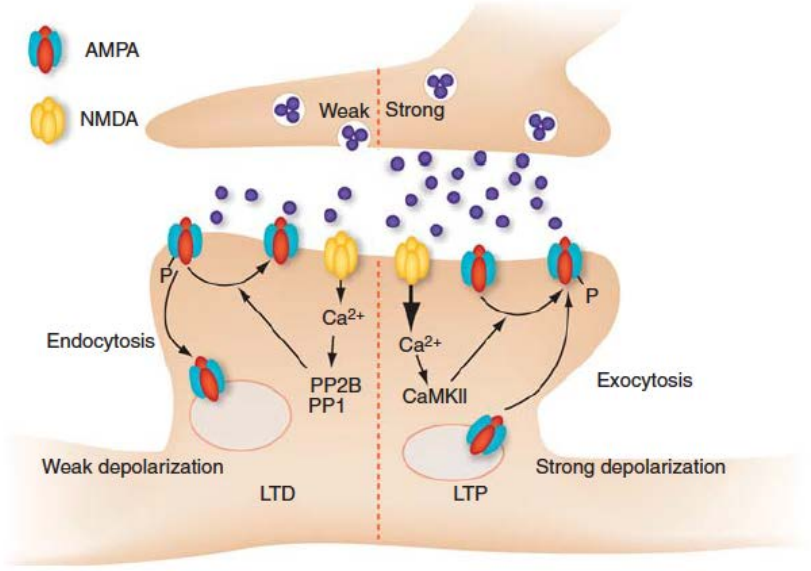

Figure 9. Postsynaptic expression mechanisms of LTP and LTD. LTD is caused by weak activity of the presynaptic neuron that leads to modest post-synaptic depolarization and calcium influx through NMDARs. This preferentially activates phosphatases (PP1/PP2A and calcineurin/PP2B) that dephosphorylate AMPARs, thus promoting their endocytosis. Conversely, LTP is generated by strong pre-synaptic activity paired with strong post-synaptic depolarization that activates protein kinases such as PKA and CaMKII, which phosphorylate AMPARs promoting their exocytosis. CaMKII, Ca^{2+}/calmodulin-dependent kinase II; LTD, long term depression; LTP, long term potentiation; PP, protein phosphatase. From Luscher & Malenka, 2012.

Protein-protein interactions also play a crucial role in AMPARs trafficking. A large family of proteins associates with AMPARs to regulate their mobility and biophysical properties as well as their stabilization within the PSD (Sheng & Kim, 2011). The best studied of those are the transmembrane AMPAR regulatory proteins (TARPs) γ2 (also known as stargazin), γ3, γ4, γ5, γ7 and γ8 (Tomita et al., 2003) and the cornichon-like proteins CNIH2/CNIH3 (Schwenk et al., 2009), which regulate AMPARs channel properties and cellular and synaptic trafficking (Jacobi & von Engelhardt, 2017). TARPs stabilize AMPARs both on the cell surface and at synapses through binding with PSD-95 (Sheng et al., 2018), the major component of the PSD. PSD-95 contains modular protein-protein motifs called PDZ domains that serve as scaffolding proteins at synapses. PSD-95 is attached to the postsynaptic membrane directly by palmitoylation and indirectly by PDZ interactions with NMDARs and the aforementioned TARP proteins, exerting then a pivotal role in "slotting" receptors to the synapse (Buonarati et al., 2019).

Both LTP and LTD are accompanied with synaptic morphological changes. LTP undergoes with growth of new dendritic spines, enlargement of preexisting spines and

their associated PSDs, and the splitting of single PSDs and spines into two functional synapses (Matsuzaki et al., 2004; Yuste & Bonhoeffer, 2001). Conversely, LTD is accompanied with spine shrinkage and eventual loss (Zhou, Homma & Poo, 2004).

Ultimately, long-term synaptic plasticity not only causes structural changes in synapses, but its maintenance also requires new protein synthesis and gene transcription (Frey et al., 1988). Both local dendritic and nuclear transcription and somatic translation are believed to synthesize the proteins required for the maintenance of functional and structural plasticity (Martin, Barad & Kandel, 2000; Tsokas et al., 2005). Several families of transcription factors, including cAMP response element binding protein (CREB), CCAAT enhancer binding protein (C/EBP), activating protein 1 (AP-1), early growth response factor (Egr) and Rel/Nuclear Factor κB (Rel/NF-κB), have been shown to exert essential functions for hippocampal long-term synaptic plasticity and long-term memory formation (Alberini, 2009). Moreover, although a large number of proteins have been identified as being altered in their expression following long-term synaptic plasticity, only a very few of these such as brain derived neurotrophic factor –BDNF– (Mei et al., 2011), protein kinase Mζ (Pastalkova et al., 2006), CaMKII (Lisman, Yasuda & Raghavachari, 2012) or activity-regulated cytoskeleton-associated protein –arc– (Guzowski et al., 2000) have been implicated in the maintenance of long-term synaptic plasticity.

Importantly, further evidences for a transcriptional role in long-term synaptic plasticity come from studies of its epigenetic regulation. For example, histone deacetylases (HDACs) are potent negative regulators of gene expression and it has been demonstrated that HDAC inhibitors enhance hippocampal long-term synaptic plasticity through CREB transcription factor (Vecsey et al., 2007). Similarly, DNA methylation is a potent stabilizer of gene expression, and enhanced DNA methylation potently inhibits LTP (Levenson et al., 2006).

1.3.4. Hippocampal synaptic plasticity deficits in AD

Hippocampal synaptic dysfunction and eventual loss is a key feature in many neurodegenerative diseases including dementia and, in particular, AD, where the number of synapses disproportionately drops relative to neurons. Evidences from epidemiological studies show that synapse loss strongly correlates with the cognitive deficits seen in AD patients (Bereczki et al., 2016; DeKosky & Scheff, 1990; Terry et al., 1991) as well as reflects the synaptic dysfunction that underlies the initial development of the disease (Masliah et al., 2001; Scheff et al., 2006, 2007).

Several lines of transgenic mice have been generated to study the hippocampal synaptic plasticity deficits occurring in AD (for review Marchetti & Marie, 2011), including APP-derived, that over-express the human *APP* gene mutated in one or more sites; PS1-derived, that over-express the human *PSEN1* gene encoding a FAD mutation; APP/PS1, 3xTg, which over-express human APP_{swe} and tau MAPTP301L and encode a knock-in of PS1M146V (Oddo et al., 2003) and 5xTg models, that harbor three *APP* and *PSEN2* (M146V and L286V) mutations that are causally related to FAD (Oakley et al., 2006).

Although conflicting results exist, several transgenic mouse models of AD have highlighted impairments of hippocampal long-term synaptic plasticity associated with the progression of the disease (Mango et al., 2019; Marchetti & Marie, 2011; Spires-Jones & Knafo, 2012). In APP-derived models, significant alterations in hippocampal synaptic plasticity at excitatory glutamatergic synapses have been described. Specifically, age-dependent reduction in LTP, both in CA1 (Balducci et al., 2011) and DG regions of the hippocampus (Jacobsen et al., 2006; Palop et al., 2007), has been reported. Moreover, enhanced LTD along with enhanced calcineurin-dependent dephosphorylation of Ser845-GluA1-AMPARs have also been described (Cavallucci et al., 2013; D'Amelio et al., 2011). Similarly, 6-month-old 3xTg mice displayed impaired hippocampal LTP well before plaque and tangle pathology appeared (Oddo et al., 2003) and 5xFAD mice showed reduced basal synaptic transmission and LTP deficits at Schaffer collateral to CA1 synapses (Crouzin et al., 2013).

It is essential to stress that some of the previous mentioned studies have showed synaptic impairments in AD transgenic mice not only long before the appearance of amyloid plaques and NFT, but also prior to the appearance of learning and memory deficits.

1.3.5. Effects of oAβ on hippocampal synaptic plasticity

oAβ have been reported to potently and selectively disrupt hippocampal excitatory synaptic plasticity, inhibiting hippocampal NMDAR-dependent LTP (Barghorn et al., 2005; Jürgensen et al., 2011; Klyubin et al., 2008; Li et al., 2011; Rammes et al., 2011; Shankar et al., 2007, 2008; Walsh et al., 2002) and enhancing hippocampal LTD (Hsieh et al., 2006; Li et al., 2009a; Shankar et al., 2008).

Impairments of hippocampal synaptic plasticity have been studied both *in vitro* and *in vivo* using different sources of oAβ, including synthetic oAβ (Barghorn et al., 2005; Jürgensen et al., 2011; Li et al., 2011), cell-derived oAβ (Li et al., 2009a, 2011; Shankar et al., 2007; Walsh et al., 2002), human-derived oAβ from CSF (Klyubin et al., 2008) or AD brains (Li et al., 2009a, 2011; Shankar et al., 2008), and also APP-derived transgenic mice with high

levels of oAβ, as stated in the previous section. Importantly, inhibitors that block Aβ oligomerization prevented the oAβ-impairment in LTP (Walsh et al., 2005) and insoluble Aβ plaques from human brains did not impair LTP unless they were first solubilized to release oAβ (Shankar et al., 2008).

A major challenge in AD research has been and continues to be the elucidation of whether the deleterious impact of oAβ on synaptic plasticity is mediated by one or more specific receptors. oAβ have been proposed to bind a range of synaptic proteins, which include, but are not limited to, glutamate transporters (Li et al., 2009a), NMDARs (Decker et al., 2010a), GluA2/3-containing AMPARs (Reinders et al., 2016; Zhao et al., 2010), mGluR5 receptors (Renner et al., 2010), α7nAChR (Nery et al., 2013), the p75 neurotrophin receptor (Knowles et al., 2009), the receptor for advanced glycation end products (Sturchler et al., 2008), Frizzled receptor (Magdesian et al., 2008), ephrin type B receptor 2 (Cissé et al., 2011) and PrP^{C} (Caetano et al., 2011) **(figure 11).** Another longstanding debate is whether oAβ present at synapses originate from intracellular or extracellular sources, and there is evidence supporting either view (Iulita et al., 2014; Takeda et al., 2013).

Despite several studies, the underlying molecular mechanisms by which oAβ disrupt hippocampal synaptic plasticity remain incompletely understood. It is known that oAβ-induced synaptic depression requires NMDARs activation (Shankar et al., 2007), which triggers the removal of AMPARs from synapses (Hsieh et al., 2006). oAβ also increase AMPARs ubiquitination (Guntupalli et al., 2017; Rodrigues et al., 2016; for review Widagdo et al., 2017) and reduce its phosphorylation at Ser845-GluA1 residue, occurring simultaneously to AMPARs removal from the plasma membrane (Miller et al., 2014; Miñano-Molina et al., 2011). According to the requirement of NMDAR activation, oAβ-mediated removal of synaptic AMPARs has been proposed to share common signaling pathways with Hebbian LTD, including downstream effectors such as calcineurin, p38 mitogen-activated protein kinase (p38 MAPK), glycogen synthase kinase 3β (GSK-3β) or phosphatase and tensin homolog (PTEN) signaling pathways (Li et al., 2009a; Miller et al., 2014; Miñano-Molina et al., 2011; Wang et al., 2004; Zhao et al., 2010; for review Jurado, 2018) **(figure 10).** Internalization of synaptic receptors and LTD enhancement has also been shown to be dependent on oAβ-mediated caspase-3 activation (Chen et al., 2013; D'Amelio et al., 2011).

oAβ can also affect LTP induction by altering CaMKII synaptic localization (Cook et al., 2019; Gu, Liu & Yan, 2009) and/or promoting endocytosis of synaptic NMDARs (Snyder et al., 2005). Moreover, not only synaptic NMDARs are involved in oAβ-mediated impairments in hippocampal synaptic plasticity, but also over-activation and consequent

endocytosis of extrasynaptic GluN2B-NMDAR may also play a role (Li et al., 2009a, 2011). Another route that oAβ may utilize to interfere with LTP appears to be interfering with BDNF-dependent pathways required for AMPARs synaptic insertion (Peng et al., 2009).

Thus, the overall impact of oAβ is depressed synaptic output, which causes dysfunctional trafficking of ionotropic and metabotropic glutamate receptors (Gong et al., 2003; Lacor et al., 2004) and synapse pruning and eventual loss. Binding to functional excitatory synapses, oAβ have been shown to reduce dendritic spines in dissociated cultured neurons (Calabrese et al., 2007; Evans et al., 2008; Lacor et al., 2007), organotypic hippocampal slices cultures (Hsieh et al., 2006; Shankar et al., 2007; Shrestha et al., 2006) and transgenic mouse and nonhuman primate models of AD (Beckman et al., 2019; Bittner et al., 2010; Forny-Germano et al., 2014; Jacobsen et al., 2006; Spires et al., 2005). Importantly, the blockade of AMPARs endocytosis prevents the loss of dendritic spines induced by oAβ (Hsieh et al., 2006) denoting that removal of synaptic AMPARs is necessary and sufficient for oAβ-induced pruning of dendritic spines. Noteworthy, as outlined above regarding impairments in synaptic plasticity, spine loss was also prevented by modulators of oAβ aggregation (Shankar et al., 2007).

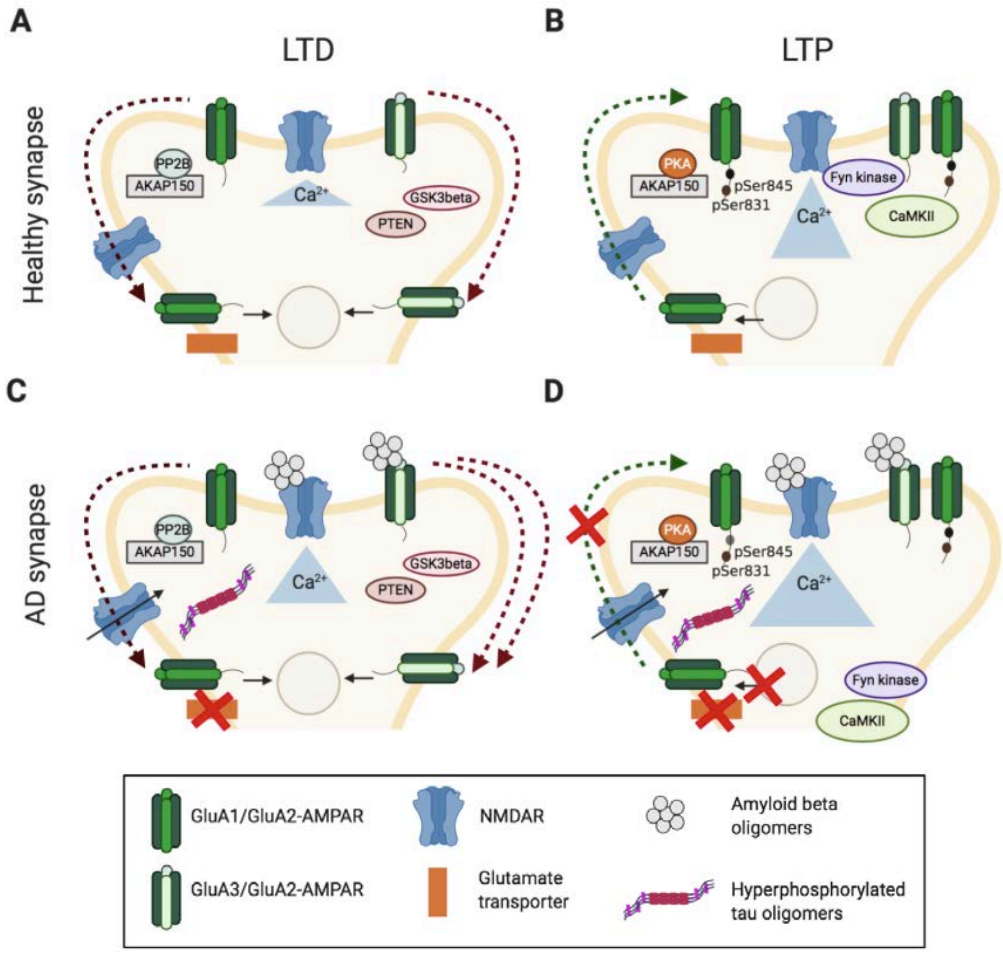

Figure 10. Synaptic plasticity deficits in AD. A) *AMPARs internalization during LTD in a healthy synapse.* Mild calcium influx through NMDARs causes calcineurin/PP2B-dependent dephoshorylation of Ser845-GluA1-AMPARs, destabilizing the interaction of AMPARs with PSD (not shown) and ultimately leading to endocytosis. **B)** *AMPARs insertion during LTP in a healthy synapse.* High frequency stimulation induces a strong activation of NMDARs sufficient to recruit CaMKII to the synapse where it phosphorylates Ser831-GluA1-AMPARs. AKAP150 translocation to synapses allows PKA phosphorylation of Ser845-GluA1-AMPARs, leading to its exocytosis. **C)** *AMPARs internalization during LTD in AD synapses.* Aβ and tau oligomers enhance AMPARs endocytosis. It is also depicted the affectation of glutamate transport, activation of extrasynaptic GluN2B-NMDARs and calcium dyshomeostasis. **D)** *AMPARs insertion during LTP in AD synapses.* oAβ prevent CaMKII from reaching synaptic localization and therefore block AMPARs phosphorylation and consequent exocytosis. Hyperphoshporylated tau is missorted to dendritic spines and prevents Fyn kinase from reaching synaptic localization, which in turns affects phosphorylation levels of both AMPARs and NMDARs. AKAP150, A kinase anchor protein 150; CamKII, Ca^{2+}/calmodulin-dependent protein kinase; GSK-3β, glycogen synthase kinase 3β; PKA, protein kinase A; PP2B; protein phosphatase 2B; PTEN; phosphatase and tensin homolog.

Concomitantly to synaptic AMPARs removal and dendritic spine loss, oAβ also affect other synaptic proteins, both extracellular and intracellular, including synaptic scaffolding proteins. For example, it has been reported that oAβ decrease PSD-95 protein levels in cultured-neurons through a proteasome-dependent pathway (Almeida et al., 2005; Roselli et al., 2005). Interestingly, data from our group also demonstrate that oAβ lead to degradation of the scaffolding protein AKAP150 in hippocampal-cultured neurons (Miñano Molina, Cheng and Rodríguez-Álvarez; unpublished). Those affectations in synaptic proteins also contribute to synaptic dysfunction and eventual loss (Ding et al., 2019).

Importantly, oAβ also alter functionally and structurally cells other than neurons, including microglia, astrocytes and the endothelial and smooth muscle cells of cerebral blood vessels (De Strooper & Karran, 2016). This affectation occurs simultaneously as the disease progresses and contributes to the synaptic affectation.

It is also worth to mention that, although numerous reports indicate that oAβ impair synaptic plasticity, there are paradoxical lines of evidence from *in vitro* and *in vivo* studies showing that increased synaptic activity induces Aβ secretion (Cirrito et al., 2008; Kamenetz et al., 2003). Based on these reports, it has been speculated that though excessive production of Aβ is synaptotoxic, at lower concentrations it may actually serve as a physiological molecule that regulates normal synaptic plasticity and memory (Morley & Farr, 2014). Indeed, recent studies indicate not only that Aβ is indispensable for normal learning and memory, but also that, at picomolar concentrations, oAβ markedly enhance hippocampal LTP (Puzzo et al., 2008) associated with a presynaptic activation of α7nAChR (Gulisano et al., 2019).

A large number of synaptic proteins, mainly cytoskeleton-associated proteins including tau, are phosphorylated in presence of oAβ (Mendes et al., 2018; Wu et al., 2018). Direct

experimental evidence in living cells also shows that oAβ are able to convert normally folded tau into a conformation thought to predominate in toxic tau aggregates (Rudenko et al., 2019). These findings suggest that oAβ may be the initiators of synaptotoxicity, while tau is a downstream executer (Liao, Miller & Teravskis, 2014; Oddo et al., 2003; Palop et al., 2007; Rapoport et al., 2002). Consistently, several studies have shown that tau deletion can protect from the damaging effects of oAβ on synaptic and cognitive functions in several mice models of AD (Ittner et al., 2010; Miller et al., 2014; Roberson et al., 2011).

oAβ-mediated tau hyperphosphorylation compromise its binding to microtubules, disrupting the normal axonal transport of organelles such as mitochondria and receptors to synapses (Eckert et al., 2014). As previously stated, hyperphosphorylated tau can be localized not only in axonal microtubules but it can also be missorted to postsynaptic densities (Hoover et al., 2010), where it can contribute to the synaptotoxic role of oAβ (Zempel et al., 2010). Approximately one third of synapses in AD patients demonstrate colocalization of oAβ and tau (Fein et al., 2008). At PSDs, hyperphosphorylated tau can dysregulate AMPARs trafficking and disrupt postsynaptic targeting of Fyn kinase, subsequently increasing NMDAR activity and enhancing oAβ-mediated neurotoxicity (Bhaskar, Yen & Lee, 2005; Ittner et al., 2010). It can also activate the phosphatase calcineurin, which then dephosphorylates and/or inactivates CaMKIV and CREB signaling pathways, eventually resulting in synaptic and memory impairments (Yin et al., 2016).

The oAβ-mediated hippocampal synaptic dysfunction and eventual loss directly contributes to the cognitive deficits observed in AD. The presumptive causal link between synaptic plasticity and memory was formalized by Morris and colleagues as the synaptic plasticity and memory hypothesis: “activity-dependent synaptic plasticity is induced at appropriate synapses during memory formation, and is both necessary and sufficient for the information storage underlying the type of memory mediated by the brain area in which that plasticity is observed” (Martin, Grimwood & Morris, 2000). Thus, LTP and LTD processes are thought to represent cellular correlates of particular types of learning and memory (Collingridge et al., 2010; Lynch, 2004; Malenka & Bear, 2004; Neves, Cooke & Bliss, 2008; Nicoll, 2017).

Compelling evidences utilizing synthetic, natural, and human AD-derived Aβ have indicated that pathological concentrations of oAβ are both necessary and sufficient to disrupt normal learning and memory function and consolidation (Cleary et al., 2005; Freir et al., 2011; Lesne et al., 2006; Shankar et al., 2008). Consistently, mouse models of AD with high levels of oAβ show cognitive deficits such as impairments in specific spatial learning (Koistinaho et al., 2001; Miñano-Molina et al., 2011) as well as murine models

treated with oAβ from human brains present disrupted memory (Shankar et al., 2008). Noteworthy, oAβ cause cognitive impairment in the absence of neurodegeneration (Cleary et al., 2005; Haass & Selkoe, 2007; Lesne et al., 2006) and multiple APP-derived transgenic mice show both hippocampal synaptic plasticity deficits and memory impairments prior plaque pathology, suggesting that disruption of memory neuronal circuits is independent of plaque deposition (Gruart et al., 2008; Jacobsen et al., 2006).

It is also important to mention that, a part from the impairment in hippocampal synaptic plasticity leading to learning and memory deficits, oAβ also contribute to emotional psychiatric disturbances by disrupting glutamatergic excitatory/GABAergic inhibitory neurotransmission in the basolateral amygdala (España et al., 2010a).

1.3.6. oAβ and neurotoxicity

Through binding to different synaptic proteins, oAβ can directly or indirectly initiate distinct aberrant downstream signaling cascades leading to neuronal dysfunction. Moreover, oAβ can also directly insert to lipid bilayers, causing neuronal damage acting as a pore (Demuro et al., 2005; for review Drolle et al., 2014).

Furthermore, pathologically elevated oAβ levels at the synapse enhance the pre-synaptic release of glutamate together with the simultaneous blockade of glutamate uptake by astrocytes through glutamate transporters (Li et al., 2009a; Proctor, Coulson & Dodd, 2011). The consequent excitotoxic levels of glutamate in the synaptic cleft diffuse and activate extrasynaptic GluN2B-NMDARs, whose prolonged stimulation leads to aberrant redox events and calcium overload, increased oxidative/nitrosative stress, mitochondrial dysfunction with consequent bioenergetics compromise, dysregulation of synaptic neurotransmission and abnormal neuronal network activity (for review Cline et al., 2018; Tu et al., 2014) **(figure 11).**

oAβ have also been identified to bind around one hundred molecules in human CSF primarily involved in lipid transport and metabolism, the complement system and hemostasis, suggesting that they may affect multiple cellular functions through a wide range of potential binding partners (Rahman et al., 2015).

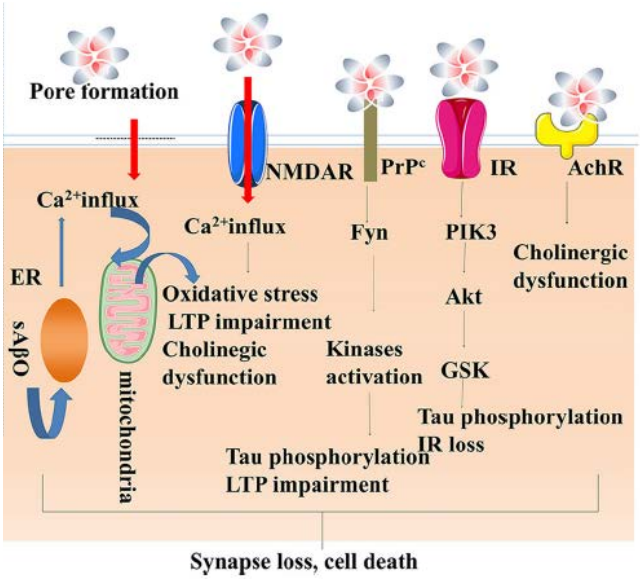

Figure 11. oAβ-mediated synaptotoxic effects through binding to different synaptic partners. oAβ may bind with high affinity and specificity to a broad range of receptors, which then indirectly or directly initiates distinct aberrant downstream signaling cascades leading to neuronal dysfunction. AChR, acetylcholine receptor; APP, amyloid precursor protein; ER, endoplasmic reticulum; GSK, glycogen synthase kinase; IR, insulin receptor; LTP, long term potentiation; PI3K, phosphatidylinositol 3-kinase; PrP^{C}, cellular prion protein. Modified from Wang et al., 2016b.

2. Differential gene expression in AD hippocampus

2.1. Synaptic genes altered in AD hippocampus

In humans, altered expression of genes related to energy metabolism, synapse, and transcriptional regulation processes exacerbates in the brain during the progression of AD pathology contributing likely to cognitive decline (Berchtold et al., 2014; Blalock et al., 2004; Liang et al., 2008; Miller, Oldham & Geschwind, 2008; Silva et al., 2012; Tan et al., 2010; Yao et al., 2003). MCI patients show widespread upregulation of genes associated with biosynthetic and energy production, specifically genes related to protein biosynthesis, turnover and trafficking, mitochondrial energy generation and, to a lesser degree, synaptic signaling and structure (Berchtold et al., 2014). This synaptic and neuronal compensation does happen very early in the disease, but this attempt probably fails due to the lack of appropriate neurotrophic support (Baazaoui & Iqbal, 2018). Contrary to gene upregulation in MCI stage, microarray analysis of hippocampal tissue (Berchtold et al., 2014) or single cell microarray analysis of CA1 neurons (Ginsberg, Alldred & Che, 2012; Ginsberg et al., 2010) revealed downregulation of multiple synaptic genes in AD. Specifically, these studies from AD human brain found significant expression changes in genes regulating vesicle trafficking and release, neurotransmitter receptors, postsynaptic function and cell adhesion. A summary of hippocampal synaptic genes altered in AD human hippocampus is shown in **table 1.**

Table 1. Summary of hippocampal synaptic genes altered in AD human patients.

Function	Symbol	Name	Model	Levels	References
Cell adhesion	*Cdh2*	N-cadherin	AD	Down	Ando et al., 2011
Neurotransmission	*Scg2*	Secretogranin II	AD	Down	Marksteiner et al., 2002
Neurotransmitter transporters	*Slc1A1*	GABA transporter 1	AD	Down	Ginsberg et al., 2012
	Slc6a1	Excitatory aminoacid transporter 3	AD	Down	Ginsberg et al., 2012
Neurotrophins	*Bdnf*	Brain-derived neurotrophic factor	AD	Down	Ferrer et al., 1999 Colangelo et al., 2002 Connor et al., 1997
Neurotrophin receptors	*TrkA*	Tropomyosin receptor kinase A,B,C	MCI,AD	Down	Margaret Fahnestock & Shekari, 2019
	TrkB		MCI,AD	Down	Ferrer et al., 1999; Ginsberg et al., 2012,2010
			AD	Unchanged Down	Wong et al., 2012
	TrkC		AD		Ginsberg et al., 2012,2010
Synapse structure and strength	*Arc*	Activity-regulated cytoskeleton-associated protein	AD	Down	Ginsberg et al., 2012
			AD I-IV	Down	Parra-Damas et al., 2014
	Grip2	Glutamate receptor interacting protein 2	AD	Down	Ginsberg et al., 2012
	Homer1	Homer1	MCI,AD	Down	Counts et al., 2014
	Kal7	Kalirin 7	AD	Down	Cissé et al., 2017
	Nrx1	Neurexin 1	AD	Down	Berchtold et al., 2014 Ravetti et al., 2010
	PSD95	Postsynaptic density 95	AD	Down	Ginsberg et al., 2012
	Synpo	Synaptopodin	MCI,AD	Down	Counts et al., 2014
Synaptic transmission	*Gabra1*	GABA-Aα_1	AD	Down	Limon, Reyes-Ruiz, & Miledi, 2012
	Gria	GluA1,2	AD	Down	Ginsberg et al., 2012
	Grin	GluN2B	AD	Down	Ginsberg et al., 2012
Vesicle trafficking	*Chga*	Chromogranin A	AD	Down	Marksteiner et al., 2002
	Rab	Rab5,7	MCI	Up	Ginsberg et al., 2010
		Rab4,24	AD	Up	Ginsberg et al., 2010
	SNAP25	Synaptosomal-associated protein 25KDa	MCI	Up	Berchtold et al., 2014
			AD	Down	Berchtold et al., 2014
	Stx	Syntaxin 1A,4,7	MCI,AD	Down	Counts et al., 2014
		Syntaxin 4A,6,18	AD	Down	Ginsberg et al., 2012 Berchtold et al., 2014
	Syn	Synapsin	MCI,AD	Down	Counts et al., 2014
	Syngr1	Synaptogyrin 1	MCI,AD	Down	Counts et al., 2014 Ginsberg et al., 2012
	Syp	Synaptophysin	MCI,AD	Down	Ginsberg et al., 2012
	Syt	Synaptotagmin 1,3,5,6,11,12	AD	Down	Ginsberg et al., 2012
	VAMP	Synaptobrevin or VAMP1,2,3,4	MCI,AD	Down	Counts et al., 2014 Ginsberg et al., 2012

Downregulation of specific neurotrophin receptors was also specifically found within CA1 neurons, including a significant downregulation of tyrosine receptor kinase B (TrkB) both in MCI and AD stages and a downregulation of TrkC receptor in AD stage (Ginsberg et al., 2010). Not only changes in neurotrophin receptors, but also changes in several neurotrophic factors have also been reported in AD patients (Fahnestock et al., 2002, 2011). In both MCI and AD stages, levels of BDNF are depressed (Peng et al., 2005). Moreover, recent reports have provided mechanistic evidence demonstrating that

BDNF/TrkB deficiency elevates δ-secretase, resulting in elevated cleavage of both APP and tau and therefore promoting AD pathology (Wang et al., 2019; Xiang et al., 2019). Conversely, BDNF treatment in rodents and non-human primates models of AD has been reported to support neuronal survival, synaptic function and memory processes (Nagahara et al., 2009, 2013).

Remarkably, downregulation of synaptic gene transcripts in CA1 hippocampal neurons of MCI/AD brains correlates with pathological cognitive status (Counts et al., 2014; Ginsberg et al., 2012). In contrast to the widespread loss of synaptic genes, transcripts encoding other genes relevant for AD such as *APP* were not differentially expressed in CA1 neurons in AD brains. Taken together, these data suggest that CA1 synaptic gene dysregulation occurs early in the cascade of pathogenic molecular events and underlies the progressive cognitive decline in AD (Berchtold et al., 2014; Liang et al., 2010).

In several AD mice models, transcriptome profile studies have also revealed deregulation of common cellular pathways including mitochondrial function, metabolism, insulin signaling, calcium homeostasis, inflammation, and synaptic plasticity. Several synaptic genes are significantly reduced in the hippocampus of AD transgenic mice coinciding with memory deficits (Dickey et al., 2003; Parra-Damas et al., 2014). In some studies, altered gene expression was restricted to amyloid-containing brain regions (Dickey et al., 2003). A summary of the hippocampal synaptic genes altered in AD mice models is shown in **table 2.**

Table 2. Summary of hippocampal synaptic genes altered in AD mice models.

Function	Symbol	Name	Model	Levels	References
Cell adhesion	*Cdh2*	N-cadherin	3xTg	Down	Gatta et al., 2014
Neurotransmission	*Scg2*	Secretogranin II	$APP_{Sw,Ind}$	Down	Parra-Damas et al., 2014
Neurotrophins	*Bdnf*	Brain-derived neurotrophic factor	$APP_{Sw,Ind}$	Down	Parra-Damas et al., 2014
Neurotrophin receptors	*TrkB*	Tropomyosin receptor kinase B	$APP_{Sw,Ind}$	Down	Parra-Damas et al., 2014
Synapse structure and strength	*Arc*	Activity-regulated cytoskeleton-associated protein	$APP_{Sw,Ind}$	Down	España et al., 2010b Parra-Damas et al., 2014
			APP/PS1	Down	Dickey et al., 2003
	Homer 1a	Homer 1a	APP/PS1	Down	Dickey et al., 2003
	Kal7	Kalirin 7	3xTg	Down	Cissé et al., 2017
	Neff	Neurofilament	$APP_{Sw,Ind}$	Down	Parra-Damas et al., 2014
			APP/PS1	Down	Dickey et al., 2003
	PSD95				
Synaptic plasticity	*Ophn1*	Oligophrenin 1	3xTg	Down	Gatta et al., 2014
Synaptic transmission	*Gabra1*	GABA-Aα_1	3xTg	Down	Gatta et al., 2014 Dickey et al., 2003
	Gria	GluA1	APP/PS1	Down	Parra-Damas et al., 2014 Cantanelli et al., 2014
		GluA2,3	3xTg	Down	Dickey et al., 2003
	Grin	GluN2B	APP/PS1	Down	
Vesicle trafficking	*Chga*	Chromogranin A	$APP_{Sw,Ind}$	Down	Parra-Damas et al., 2014
	SNAP25	Synaptosomal-associated protein 25KDa	3xTg	Down	Gatta et al., 2014

	Stx	Syntaxin 4A,18	$APP_{Sw,Ind}$	Down	Parra-Damas et al., 2014
	Syt	Synaptotagmin 4	$APP_{Sw,Ind}$	Down	Parra-Damas et al., 2014

It is also worth to mention that synaptic genes shown in table 1 and 2 are limited to neurons, but deregulation of genes in other cell types also occurs. For example, the levels of both glutamate transporters EAAT1 and EAAT2, which are responsible for the majority of glutamate uptake in glial cells, are downregulated in the hippocampus of AD patients (Jacob et al., 2007). In astrocytes, deregulation of genes associated with cytoskeleton, proliferation, apoptosis, and ubiquitin-mediated proteolysis also occurred at early AD, while altered regulation of intracellular signaling pathways, including insulin, phosphatidylinositol 3-kinase (PI3K/Akt), and MAPK pathways are primarily associated with late pathological stages (Simpson et al., 2011).

Downregulation of activity-dependent genes involved in synaptic plasticity and memory are associated with learning and memory deficits in APP transgenic mice (España et al., 2010b) and changes in the expression of these genes parallels altered activity of memory circuits, thus indicating a close relationship between neuropathology, transcriptional deregulation and activity of susceptible memory circuits in AD **(figure 12).**

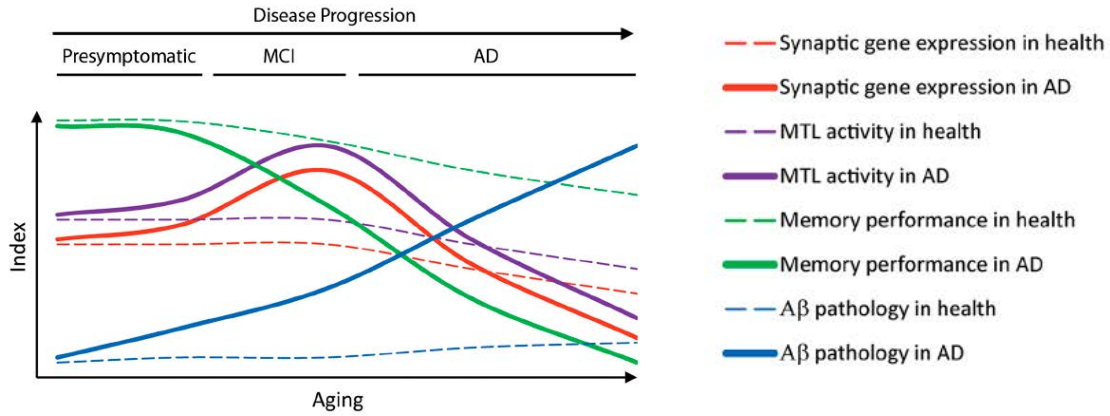

Figure 12. Temporal progression of pathological, transcriptional and functional changes in aging and AD. Schematic representation of the hypothetical temporal progression of Aβ pathology, synaptic gene expression, medial temporal lobe activity and memory performance both in healthy and AD brains. MTL. medial temporal lobe. From Saura, Parra-Damas & Enriquez-Barreto, 2015.

2.2. Synaptic plasticity-related transcription factors altered in AD hippocampus

As previously described, cognitive decline is associated with gene expression changes in the brain, but the regulatory transcriptional mechanisms underlying those changes in AD are largely unknown. In this regard, several transcription factors have been proposed to have a role in the pathogenesis of AD. A summary of the synaptic plasticity-related transcription factors that might have a role in AD pathogenesis is shown in **table 3.**

CREB is one of the transcription factors most extensively studied in AD, being disrupted by oAβ and leading to synaptic plasticity and memory deficits in AD (Saura & Valero, 2011; Vitolo et al., 2002). As previously mentioned, CREB is necessary for hippocampal LTP maintenance, suggesting that CREB-induced genes might play a role in long-lasting synaptic plasticity and memory processes (Alberini, 2009). Accordingly, CREB activation ameliorates synaptic and memory impairments in APP transgenic mice (Smith et al., 2009; Yiu, Rashid & Josselyn, 2011).

Moreover, CREB transcription factor represent the crossroad of different synapse-to-nucleus pathways associated with changes in gene expression that underlie memory decline in AD (Marcello, Di Luca & Gardoni, 2018). For example, oAβ induce nuclear accumulation of Jacob, a messenger that couple CREB shut-off following activation of GluN2B-containing extrasynaptic NMDARs (Grochowska et al., 2017; Rönicke et al., 2011). Other transcription factors related to CREB are also involved in AD pathology. For example, ATF4, which belongs to the ATF/CREB transcription factor family, is a CREB repressor and its levels are upregulated in mouse models of AD (Devi & Ohno, 2014) and the brains of AD patients (Lewerenz & Maher, 2009) **(table 3).**

CREB-regulated transcription coactivator-1 (CRTC1) is another example of a synapse-to-nucleus messenger controlling CREB pathway and involved in AD. CRTC1 localizes to synapses and undergoes activity-dependent nuclear translocation to regulate the transcription of CREB target genes. CRTC1 levels and CRTC1-dependent genes are reduced in AD human hippocampus at intermediate AD stages (Parra-Damas et al., 2014) **(table 3).** Both spatial memory and context-associative learning trigger calcineurin-mediated CRTC1 dephosphorylation, nuclear translocation and CRTC1-dependent transcription in the hippocampus (Parra-Damas et al., 2014, 2017a). These events are impaired in transgenic AD rodent models at early AD stages (Parra-Damas et al., 2014, 2017a; Wilson et al., 2016). Consistently, reduced calcineurin activity and expression was also reported in AD transgenic mice and the brains of AD patients (Celsi et al., 2007; Lian et al., 2001). Importantly, CRTC1 hippocampal overexpression rescued the early transcriptional changes and memory impairments in APP transgenic mice by restoring a specific subset of CRTC1 target genes (Parra-Damas et al., 2014).

Indeed, genome-wide transcriptome profile analyses of AD transgenic mice hippocampus revealed deregulation of a transcriptional program dependent on CREB/CRTC1. Specifically, $APP_{Sw,Ind}$ mice at 6 months of age shown downregulation of diverse genes compared with WT mice after spatial training. These genes include some participating in neurotransmission (*Scg2*, *Syt4*, *Stx4A*, *Stx18*, *Gria1*, *Chga*), neuritogenesis (*Nefl*) and synaptic plasticity and memory such as *Arc*, *c-fos*, *Bdnf* and also the *Nr4a* family of

transcription factors (Parra-Damas et al., 2014; Saura, Parra-Damas & Enriquiz-Barrero, 2015).

Among the latest, the Nr4a family of nuclear orphan receptors have emerged as promising candidates for the development of novel therapeutic approaches to target early AD synaptic failure (see introduction, section 4.3.3) due to their implication on hippocampal synaptic plasticity (see introduction, section 4.3.1 and below) and their ability to be modulated by diverse molecular activators (see introduction, section 4.4).

Table 3. Summary of synaptic plasticity-related transcription factors altered in the hippocampus of Alzheimer's disease patients and mice models.

Symbol	Name	Model	Change	References
ATF4	Activating transcription factor 4	Human AD midfrontal cortex 5XFAD	Up Up	Devi & Ohno, 2014 Lewerenz & Maher, 2009
C/EBPβ	CCAAT-enhancer binding protein β	Human AD	Up	Wang et al., 2019
c-Fos	c-Fos	$APP_{Sw,Ind}$	Down	Parra-Damas et al., 2014
c-Jun	c-Jun	Human AD hip	Increased phoshorylation	Thakur et al., 2007
c-Myc	c-Myc	Human AD brain	Increased phoshorylation	Ferrer et al., 2001
CREB	cAMP-response element binding protein	$APP_{Sw,Ind}$	Decrease in transcription-dependent genes	Saura & Valero, 2011
CRTC1	CREB-regulated transcription coactivator-1	$APP_{Sw,Ind}$ Human AD hip	Decrease in transcription-dependent genes	Parra-Damas et al., 2014
KCTD2	Potassium channel tetramerization domain 2	Human AD hip	Change in transcription-dependent genes	Potashkin et al., 2019
KLF9	Krüppel like factor 9	Human AD hip	Change in transcription-dependent genes	Potashkin et al., 2019
NFκB	Nuclear factor κ-light chain-enhancer of activated B cells	Human AD hip (CA1)	Up	Colangelo et al., 2002
NFAT	Nuclear factor of activated T cells	Human MCI hip Human AD hip	Increased nuclear NFAT1 Increased nuclear NFAT3	Abdul et al., 2009
Nr4a1	Nuclear receptor subfamily 4 group A member 1	$APP_{Sw,Ind}$ APP/PS1	Down Up	Parra-Damas et al., 2014 Zhao et al., 2018
Nr4a2	Nuclear receptor subfamily 4 group A member 2	$APP_{Sw,Ind}$ Human AD III-VI hip Human AD hip Human LOAD hip	Down Down Down Up	Parra-Damas et al., 2014 Parra-Damas et al., 2014 Moon et al., 2019 Annese et al., 2018
Nr4a3	Nuclear receptor subfamily 4 group A member 3	APP/PS1	Down	Dickey et al., 2003
Egr1	Early growth response protein 1	APP/PS1	Down	Dickey et al., 2003
XBP-1	X-box binding protein 1	APP/PS1, 5XFAD	Down	Reinhardt et al., 2014

LOAD, late onset AD.

3. Role of Nr4a2 in hippocampal synaptic plasticity

3.1. Nr4a subfamily of transcription factors

Within the nuclear receptor superfamily, nuclear receptor subfamily 4, group A (Nr4a), consists in a family of close-related three immediate early genes that encode three orphan nuclear receptors (Nr4a1/NGFI-B, Nr4a2/Nurr1 and Nr4a3/NOR-1). They are expressed in a wide variety of metabolically demanding and energy dependent tissues, such as skeletal muscle, adipose, heart, kidney, T-cells, liver and distinct but overlapping regions of the brain (Zetterström et al., 1996). The three members exhibit tissue-specific expression and hence their roles are context as well as tissue-specific.

Nr4a proteins function as transcription factors that recognize DNA response elements to regulate the expression of a variety of genes involved in multiple biological processes including proliferation, metabolism, immunity, cellular stress, apoptosis, DNA repair and angiogenesis (Safe et al., 2016). Nr4a transcriptional activity depends mainly on gene expression, miRNA targeting, alternative splicing, posttranslational modifications, subcellular localization and interaction with other nuclear receptors (Maxwell & Muscat, 2006). Depending on the cellular context, these transcriptional regulators may be stably expressed or induced as immediate early genes in response to a wide range of physiological signals, including synaptic activity (Pegoraro et al., 2010). The ability to sense and rapidly respond to changes in the cellular environment appears to be a hallmark of this subfamily of orphan nuclear receptors.

These receptors are involved in the onset and progression of various diseases such as various types of cancer, inflammation, atherosclerosis and obesity (Ranhotra, 2015). Notably, Nr4a transcription factors have also emerged as essential mediators of neuronal functions such as DNA repair of double strand breaks in neurons (Malewicz et al., 2011; Munnur et al., 2019) or neuronal survival (Volakakis et al., 2010).

3.2. Nr4a2 transcription factor

Nuclear receptor subfamily 4, group A, member 2 (Nr4a2), which belongs to the Nr4a subfamily of transcription factors, is primarily expressed in neurons of diverse areas of the CNS, particularly in the substantia nigra pars compacta, ventral tegmental area and limbic area (Zetterström et al., 1996). Moreover, it is also expressed in the hippocampus, subiculum, temporal cortex, olfactory bulb, cerebellum, posterior hypothalamus and habenuclear nuclei (Quina et al., 2009; Saucedo-Cardenas & Conneely, 1996). Nevertheless, Nr4a2 is expressed not only in neurons, but also in non-neuronal cells such as microglia, astrocytes or endothelial cells (Fan et al., 2009; Saijo et al., 2009) and it is

found not only in the CNS but also in other tissues, including the bone, synovial tissues, adrenal gland or the intestine.

Nr4a2 structure is composed by a modulator domain, referred to as the activation function (AF)-1 or the NTD, a conserve DNA-binding domain (DBD) and a LBD containing its transactivation-dependent AF-2 in the CTD (Ichinose et al., 1999) **(Figure 13A).**

Nr4a2 is known as an orphan nuclear receptor as no endogenous ligand has been identified so far. The Nr4a2 LBD lacks a cavity as a result of the tight packing of side chains from several bulky hydrophobic residues in the region normally occupied by agonists, and therefore lacks a “classical” binding site for coactivators, and adopts a canonical protein fold resembling that of an agonist-bound, transcriptionally active LBD (Wang et al., 2003). Classically, nuclear receptor activation is accomplished by the binding of a lipophilic ligand in a hydrophobic pocket within the LBD. By contrast, Nr4a2 transcriptional activity is independent of the LBD and appears to be reliant on the AF-1 domain. Thus, a major difference between Nr4a2 and classical nuclear receptors is ligand-independent regulation, and its activity is regulated at the level of gene expression and protein stability (Maxwell & Muscat, 2006).

Nr4a2 protein regulates both positively and negatively the transcription of its target genes by directly binding to response elements in their promoters. Two zinc fingers of the highly conserved DBD as a monomer or homodimer are able to bind the nerve growth factor-inducible-β-binding response element (NBRE; 5’-AAAGGTCA-3’) or as homodimer or heterodimer with Nr4a1 to attach to the nur-response element (NurRE; 5’-TGACCTTT-N6-AAAGGTCA-3’). Moreover, as monomer, homodimer or heterodimer, Nr4a2 can dimerize with the retinoic X receptor (RXR) and bind to a motif referred to as DR5 **(Figure 13B).** This union is permissive; meaning that ligand binding of RXR typically causes full activation of the entire heterodimer (Jiang et al., 2019).

Nr4a2 is mostly nuclear. It contains a bipartite nuclear localization signal (NLS) within its DBD and three leucine-rich nuclear export signals (NES) in its LBD. Together, these signals regulate Nr4a2 shuttling in and out of the nucleus (García-Yague et al., 2013).

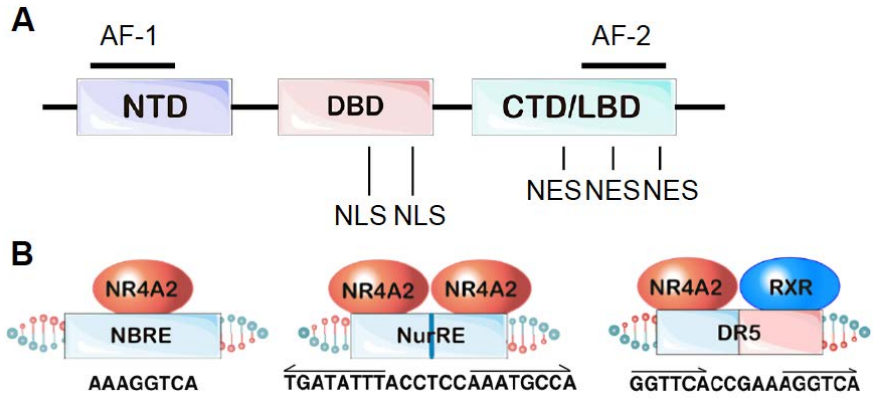

Figure 13. Nr4a2 structure and binding to target genes. A) Structural domains of Nr4a2, which include NTD, DBD and LBD. Modulator domains (AF-1 and AF-2) and localization signals (NLS and NES) are also depicted. **B)** Nr4a2 DNA-binding sites as monomers at NBRE sites, as dimers (homodimers or heterodimers, not shown) at NurRE sites and as heterodimers with RXR at DR5 sites. AF, activation function; CTD, C-terminal domain; DBD, DNA-binding domain; LBD, ligand-binding domain, NBRE, nerve growth factor-inducible-β-binding response element; NES, nuclear export signal; NLS, nuclear localization signal, NTD, N-terminal domain; NurRE, nur-response element; RXR, retinoic X receptor. Modified from Jakaria et al., 2019.

Nr4a2 is an early response gene whose transcriptional activity is rapidly induced by various physiological and pathological stimuli, including cAMP, calcium, inflammatory signals, stress, hormones and growth factors. In a study performed by Tokuoka and colleagues, they found that Nr4a2 was regulated by neuronal activity through voltage-dependent calcium channels (VDCC) and the phosphatase calcineurin in cultured-hippocampal and cerebral cortical neurons (Tokuoka et al., 2014). The neuronal activity-dependent induction of Nr4a2 mRNA has also been reported using other stimulus such as potassium chloride (KCl) or FSK (España et al., 2010b; Parra-Damas et al., 2014, 2017a,b).

Nr4a2 contains a ”half-CRE” site in its promoter, being controlled by the CREB signaling pathway in many systems, which is a cascade critical for transcription of diverse plasticity- and memory-related genes as previously stated (Barneda-Zahonero et al., 2012; Volakakis et al., 2010). Although CREB binds with higher affinity to the full 8-base consensus CRE site, it also binds to several variations of this sequence, including the so-called “half-CRE” site (5’CGTCA-3’ and 5’-TGACG-3’), which may be found in many promoters of CREB target genes including Nr4a2 (Zhang et al., 2005). Furthermore, selective gene transcription by CREB is highly modulated by the recruitment of specific coactivators such as CRTC1. It has been described that neuronal activity induces a significant binding of CRTC1 to the proximal CRE promoter region of Nr4a2, meanwhile CREB is already bound in the absence of neuronal stimulation (Parra-Damas et al., 2017b).

3.3. Nr4a2 in hippocampal synaptic plasticity: memory-enhancing effects of Nr4a2

Previous reports have highlighted a role for the Nr4a family of transcription factors in hippocampal synaptic plasticity and cognitive functions, although the underlying molecular mechanisms are still poorly understood.

Hippocampal slices from Nr4a dominant negative mutant mice, with the consequent attenuation of Nr4a-mediated transcription, did not present deficits in basal properties of Schaffer collateral to CA1 synapses or the stability of synaptic transmission, but they showed strongly impaired transcription-dependent hippocampal LTP maintenance (Bridi & Abel, 2013). Conversely, pharmacological activation of the Nr4a subfamily enhances hippocampal LTP (Bridi et al., 2017). This long-lasting form of synaptic plasticity shares many of its underlying molecular mechanisms with long-term memory. Both are enhanced by the pharmacological inhibition or genetic ablation of HDAC enzymes, which produce increases in histone acetylation that are dependent on CREB transcription factor (Vecsey et al., 2007). Importantly, HDAC inhibition failed to enhance LTP in hippocampal slices from Nr4a dominant negative mutant mice, indicating that Nr4a transcription factors are necessary for mediating the effects of HDAC inhibition on synaptic plasticity (Bridi & Abel, 2013).

Previous reports have also implicated the Nr4a family of transcription factors in the formation and expression of several types of memory. Nr4a transcription factors are expressed in the hippocampus immediately after memory-inducing activities, such as learning or other hippocampus-dependent tasks, or memory enhancement by HDAC inhibition (Hawk et al., 2012). Consistently, memory enhancement by HDAC inhibition was blocked in Nr4a dominant negative mutant mice, as well as blocking Nr4a activity in memory-supporting brain regions impaired long-term memory. These results demonstrated the contribution of Nr4a family in memory formation.

Recent studies addressing specifically the potential role of the Nr4a2 transcription factor in hippocampal synaptic plasticity and memory processes have also been published. Knocking out HDAC3 enhanced long-term memory as well as increased Nr4a2 expression, and this memory enhancement was specifically abolished by intrahippocampal delivery of Nr4a2 small interfering RNA (McQuown et al., 2011). Specific increase of Nr4a2 in the hippocampus has also been found after different memory-inducing activities. Intracranial self-stimulation treatment immediately after the acquisition session of a two-way active avoidance conditioning showed both increased Nr4a2 protein levels and improved retention (Aldavert-Vera et al., 2013). Relatedly, training in a contextual fear conditioning increased Nr4a2 mRNA expression and promoter acetylation

in a CREB/CREB binding protein (CBP)-dependent manner (Bridi et al., 2017; Oliveira et al., 2018; Vecsey et al., 2007) as well as learning in a spatial discrimination task leads to increased expression of Nr4a2 mRNA in the CA1 and CA3 subregions of the dorsal hippocampus (McNulty et al., 2012; Peña De Ortiz, Maldonado-Vlaar & Carrasquillo, 2000).

Accordingly, cumulative data suggest that disrupting Nr4a2 function impairs hippocampal memory formation. Mice lacking one copy of *Nr4a2* gene had impaired long-term memory for the hippocampus-dependent passive avoidance task (Rojas et al., 2007). In addition, injection of antisense oligodeoxynucleotides targeting Nr4a2 into the hippocampus impaired long-term memory and reversal learning in an appetitive spatial learning task (Colón-Cesario et al., 2006). Likewise, hippocampal knockdown of Nr4a2 affected performance both in the object location and object recognition tasks (McNulty et al., 2012).

Moreover, Nr4a2 transcription factor regulates several genes implicated in hippocampal synaptic plasticity and memory formation (Hawk et al., 2012; Volpicelli et al., 2007). One example is *Fosl2*, a member of the AP-1 family of transcription factors, a family that is known to be important for memory storage (Fleischmann et al., 2003). Other intriguing Nr4a2 target genes include two receptor protein tyrosine phosphatases, a class of molecules implicated in excitatory synapse formation (Dunah et al., 2005) and the myristoylated alanine-rich C kinase substrate (*MARCKS*), which can modulate memory formation (McNamara et al., 2005).

Of particular interest as a candidate by which Nr4a2 influences synaptic plasticity and memory is BDNF, a neurotrophic factor that regulates synaptic plasticity (Zagrebelsky & Korte, 2014) and contributes to the formation and long-term persistence of hippocampus-dependent memories (Bekinschtein, Cammarota & Medina, 2014; Miranda et al., 2019). BDNF regulates the expression and synaptic delivery of AMPARs and NMDARs in hippocampal neurons (Caldeira, et al., 2007a,b) and has a critical role in translation-dependent LTP both *in vitro* and *in vivo* (Lu, Christian & Lu, 2008). Remarkably, BDNF also has the ability to activate local dendritic translation of proteins promoting cellular processes of memory consolidation (Bramham, 2008).

3.4. Nr4a2 in AD

It has been reported that Nr4a2 expression is negatively regulated by HDAC3 in the aged hippocampus (Hawk et al., 2012). Moreover, Nr4a2 significantly and gradually decreases in the gerbil hippocampus with increasing age, indicating that Nr4a2 decrease may be associated with the normal aging process and a decline in hippocampus-dependent cognitive function (Ahn et al., 2018). However, a specific reduction of Nr4a2 levels in Alzheimer's pathology has also been proposed. Nr4a2 mRNA has been found decreased in $A\beta_{1-42}$-treated neuronal cells (Terzioglu-Usak et al., 2017), AD mouse models ($APP_{Sw,Ind}$ and 5XFAD) (España et al., 2010b; Moon et al., 2015; Parra-Damas et al., 2014) and postmortem brains of human AD patients, specifically the frontal cortex and the hippocampal formation (Moon et al., 2019).

Furthermore, Nr4a2 protein was reported to be prominently expressed in brain areas with Aβ accumulation in the 5XFAD mouse model of AD and, notably, it was found highly co-expressed with Aβ at mice ages mimicking early stages of the disease. In addition, the number of Nr4a2-expressing cells significantly declined in the 5XFAD mouse in an age-dependent manner, accompanied by increased plaque deposition, suggesting a possible causal-effect relation between Nr4a2 levels and AD progression (Moon et al., 2015). Moreover, in a recent study performed by the same lab, they found that knockdown of Nr4a2 significantly aggravated AD pathology while its overexpression alleviated it, including effects on Aβ accumulation, neuroinflammation and neurodegeneration (Moon et al., 2019).

Some evidences pointing out a role for other member of the Nr4a subfamily, Nr4a1, in AD pathology have also been reported. Contrary to Nr4a2, Nr4a1 was found increased in prefrontal cortex of AD patients compared to control subjects and transcriptionally active Nr4a1 correlated with measures of synaptic loss and cognitive impairment. The potential role of Nr4a1 in AD pathogenesis was also addressed in another study in which Nr4a1 promoted the pro-amyloidogenic processing of APP and accelerated tau hyperphosphorylation (Zhao et al., 2018). By contrast, Nr4a1 was also postulated to have a beneficial role in synaptic plasticity and cognition, since its expression was induced by learning tasks in the hippocampus (Von Hertzen & Giese, 2005) meanwhile Nr4a1 loss-of-function caused deficits in synaptic plasticity and long-term memory formation (Bridi & Abel, 2013). Moreover, in a recent study performed by Chen and colleagues, activity-induction of Nr4a1 was required for normal synapse distribution and function in CA1 pyramidal neurons (Chen et al., 2014).

3.5. Nr4a2 pleiotropic functions. Neuroprotective, anti-inflammatory and neurogenic effects.

Nr4a2 also plays a role in the pathogenesis of different CNS disorders including neuroinflammation (Chen et al., 2018), multiple sclerosis (Montarolo et al., 2019), schizophrenia (Rojas et al., 2007; Torretta et al., 2020; Vuillermot et al., 2011), depression (Rojas et al., 2010), intellectual disability (Lévy et al., 2018; Ramos et al., 2019), drug abuse (López et al., 2019) and Parkinson's disease (PD) (Chu et al., 2006; Li et al., 2018; Qian et al., 2020; Spathis et al., 2017). Moreover, it plays a role in rheumatoid arthritis and it regulates inflammatory processes in synovial cells (Davies et al., 2005; Rodríguez-Calvo, Tajes & Vázquez-Carrera, 2017). In addition, Nr4a2 is involved in the progression of various cancers, such as skin cancer, breast cancer, prostate cancer, and pancreatic ductal adenocarcinoma (Boakye et al., 2013; Ji et al., 2017; Llopis et al., 2013; Wang et al., 2013).

In the CNS, Nr4a2 has been mostly studied in PD, which results from the degeneration of midbrain dopaminergic neurons. Mutations in Nr4a2 have been associated with PD (Grimes et al., 2006; Sleiman et al., 2009; Xu et al., 2002) and Nr4a2 gene expression has been found reduced in postmortem brain tissue and peripheral blood of PD patients (Le et al., 2008; Montarolo et al., 2016). Nr4a2 is known to be a key regulator of the midbrain dopaminergic neurons differentiation, maintenance and survival (Jo et al., 2009; Saucedo-Cardenas et al., 1998; Sousa et al., 2007), being responsible for the transcription of several genes involved in the dopaminergic neuronal phenotype, ranging from genes regulating dopaminergic metabolism, differentiation and neurotransmission (tyrosine hydroxylase –*TH*–, vesicular amine transporter 2 –*VMAT*–, dopamine transporter –*DAT*–), mitochondrial function (sodium oxide dismutase 1 –*SOD1*–, Ts translation elongation factor mitochondrial –*TSFM*–, cyclo-oxigenase 5β –*COX5β*–) and dopaminergic neuronal survival (*Ret*) (Decressac et al., 2013; Kadkhodaei et al., 2013).

In dopaminergic neurons, Nr4a2 has an essential role in the neuroprotection and anti-inflammatory responses after exposure to neuropathological stress or insults. It was reported that Nr4a2-null heterozygous dopaminergic neurons exhibited greater vulnerability to neurotoxins (Le et al., 1999). Nr4a2 protects dopaminergic neurons from neuroinflammation insults not only through its function in neurons, but also glial cells (Bensinger & Tontonoz, 2009), since it is able to suppress inflammatory gene expression in microglia and astrocytes trough transcriptional repression of the NFκB transcription factor, essential to induce inflammatory responses (Saijo et al., 2009). Moreover, Nr4a2 not only inhibits the production of inflammatory factors, but also promotes the expression of neurotrophic factors such as BDNF (Chen et al., 2018).

Nr4a2 neuroprotective effects are not limited to dopaminergic neurons. In glutamatergic neurons, Nr4a2 also mediates CREB-induced neuroprotection in response to stress by increasing BDNF levels in cerebellar granule cells (Barneda-Zahonero et al., 2012) or upregulating an anti-apoptotic gene program in hippocampal neurons (Volakakis et al., 2010). Furthermore, Nr4a2 has also been described to play a role in hippocampal neurogenesis. Nr4a2 is abundantly expressed in adult hippocampal neural precursor cells, and it stimulates the proliferation and differentiation of adult hippocampal neural precursor cells both *in vitro* and *in vivo* (Kim et al., 2016).

4. Therapeutic potential of Nr4a2 activation for the treatment of AD

Nuclear transcription factors are increasingly being investigated for their role in synaptic plasticity and memory, and the potential of some nuclear receptors to serve as therapeutic targets in disorders of cognition including AD has been also reported (Mandrekar-Colucci & Landreth, 2011; Skerrett, Malm & Landreth, 2014). Likewise, interventions that rely on the regenerative capacity of the brain such as the modulation of the inherent neurogenesis and neuronal plasticity also represent a promising therapeutic strategy (Baazaoui & Iqbal, 2018). Consistently, agents showing promising therapeutic potential against AD tend to possess a similar pattern of multiple pharmacological profiles, such as antioxidant, anti-inflammatory, pro-BDNF, and pro-synaptic remodeling/regeneration (Sun & Alkon, 2019). In this regard, in this doctoral thesis we will explore the potential therapeutic role of Nr4a2 transcription factor in AD, which accomplishes all the pharmacological features previously listed.

4.1. Nr4a2 agonists

Several small molecules have been identified to activate Nr4a2 through its various domains **(Table 4).** Of special interest are the antimalarial drugs amodiaquine (AQ) and chloroquine (CQ), which increase the transcriptional function of Nr4a2 interacting with its LBD through direct physical binding. Both drugs increase the transcriptional activation of midbrain dopaminergic specific genes and enhance the transrepression of neurotoxic proinflammatory gene expression in microglia. In addition, these compounds meaningfully improve behavioral deficits in rat models of PD without any noticeable sign of dyskinesia-like behavior (Nguyen et al., 2015). Autophagic-lysosomal blockade has also been reported as one of their functions (Qiao et al., 2013). Recently, AQ has also been reported to enhance cognitive functions by increasing adult hippocampal neurogenesis (Kim et al.,

2016) and/or by inhibiting Aβ-mediated pathology in AD mouse models (Moon et al., 2019).

Concerning various studies, different compounds, including dopaminergic agonists, memantine, retinoic acid-loaded polymeric nanoparticles, and phyto-bioactive compounds as well as herbal extracts, have also been reported to increase Nr4a2 expression. However, their binding sites to Nr4a2 have not been confirmed (Jakaria et al., 2019; Wei et al., 2016).

Table 4. Features of Nr4a2 agonists.

Compound	Targeted region	Model	Outcomes	References
6-Mercaptopurine	AF-1 domain (N-terminus Nr4a2)	CV-1 cells	Activation of both Nr4a2 and Nr4a3	Ordentlich, et al., 2003 Wansa et al., 2003
		pMCAO model	Decreased TNFα and IL-1 Attenuated ischemic brain injury	Chang, Kwan, & Howng, 2010
Cloroquine **Amodiaquine** **Glafenine**	Putative LBD residues (C-terminus Nr4a2)	DA neurons, PC12 cells	Increased expression of DA genes; anti-inflammatory response and neuroprotection	Nguyen et al., 2015
		6-OHDA lesioned rats (PD model)	Improved behavioral deficits	
		C57BL/6 mice	Enhanced adult hippocampal neurogenesis, improved cognition	Kim et al., 2016
		5XFAD mice (AD model)	Inhibited Aβ-mediated pathology; improved cognitive functions	Moon et al., 2019
Benzimidazole–based	Putative LBD residues (C-terminus Nr4a2)	None	Activated Nr4a2 by increased luciferase activity	Dubois, Hengerer, & Mattes, 2006
Bexarotene	RXR	5XFAD mice (AD model)	Clearance of intraneuronal Aβ deposits, reduced inflammation, improved neuronal survival and memory	Mariani et al., 2017
		APP/PS1ΔE9 (AD model)	Decreased interstitial fluid Aβ, reversal of memory deficits in an apoE-dependent manner	Cramer et al., 2012
		6-OHDA lesioned rats (PD model)	Reduced DA neuron cell death and reversed behavioral deficits	McFarland et al., 2013
BRF110	Nr4a2:RXRα	SH-SY5Y PD patients iPSC-derived DA neurons	Increased expression of DA genes; neuroprotection	Spathis et al., 2017
		PD mice models	Increase expression of DA genes, neuroprotection and symptomatic relief	
C-DIM analogs	Both N- and C-terminus Nr4a2; direct binding not supported	N2A, N27	Neuroprotection	Hammond, Safe, & Tjalkens, 2015
		BV-2 cells	Supressed NFκB-induced genes	De Miranda et al., 2015a
		MPTP	Increased expression of DA	De Miranda et al.,

		lesioned rats (PD model)	genes; anti-inflammatory response and neuroprotection	2015b Hammond et al., 2018
		C57BL/6 mice	Enhanced long-term spatial memory in young mice, rescued memory deficits in aged mice	Chatterjee et al., 2020
		C57BL/6 mice	Enhanced hippocampal LTP and long-term contextual fear memory	Bridi et al., 2017
Daphnane and phorbol diterpenes	Unknown	SH-SY5Y cells BV-2 cells 6-OHDA lesioned rats (PD model)	Neuroprotection Anti-inflammatory response Reduced DA neuron cell death and ameliorated behavioral deficits	Han et al., 2017
IP7e **IP7e analalog: SH1**	Putative LBD residues (C-terminus Nr4a2)	Multiple sclerosis models Lactacystin lesioned mice	Inhibited expression of NFκB (attenuated inflammation and neurodegeneration) Improved rotarod performance; increased expression of DA genes; anti-inflammatory response and neuroprotection	Montarolo et al., 2014 Zhang et al., 2012
SA00025 and	Unknown	6-OHDA lesioned rats (PD model)	Increased expression of DA genes; anti-inflammatory response and neuroprotection	Smith et al., 2015
IRX4204	RXR	Mesencephalic cultures 6-OHDA lesioned rats (PD model)	DA neuron survival Attenuated neurochemical and motor deficits	Wang et al., 2016a

In order of appearance in the table: pMCAO, permanent middle cerebral artery occlusion; DA, dopaminergic; PD, Parkinson's disease; AD, Alzheimer's disease; RXR, retinoic X receptor; C-DIM, 1,1-Bis (30-Indolyl)-1-(Aromatic) methane; IP7e, isoxazolo-pyridinone 7e; NFκB: nuclear factor κB. Modified from Dong et al., 2016.

The existence of Nr4a2 agonists already in use in pre-clinical studies and the promising results observed in other neurodegenerative disorders broadens the perspective to study their translation to AD human patients.

4.2. Therapeutic potential of Nr4a2 activation in AD models

As discussed above, Nr4a2 is induced after learning and memory tasks in the mouse hippocampus, and reduced Nr4a2 levels cause impairments in synaptic plasticity and specific forms of hippocampal-dependent learning and memory (Bridi & Abel, 2013; Colón-Cesario et al., 2006; Hawk & Abel, 2011; Hawk et al., 2012; McNulty et al., 2012; McQuown et al., 2011; Rojas et al., 2007). Together, these data suggest that Nr4a2 may be a key factor that promotes preserved cognitive function, and recent reports have supported this idea. *Nr4a2* has been identified as a key gene that fails to be induced by learning in the hippocampus of cognitively impaired aged rats (Kwapis et al., 2019) and

mice models of AD (Parra-Damas et al., 2014). Conversely, specific overexpression of Nr4a2 in the dorsal hippocampus of male mice ameliorated age-related impairments in object location memory (Kwapis et al., 2019). Kim and colleagues showed that Nr4a2 activation promoted cognitive function probably by elevating adult hippocampal neurogenesis (Kim et al., 2016) and recently, Chaterjee and colleagues reported that Nr4a2 activation enhanced long-term spatial memory in young mice and rescued memory deficits in aged mice (Chatterjee et al., 2020).

Importantly, 5XFAD mice treated with AQ showed robust reduction in typical AD features including deposition of Aβ plaques, neuronal loss, microgliosis, and impairment of adult hippocampal neurogenesis, leading to significant improvement of cognitive function in the Y-maze, which is widely accepted as a behavioral paradigm for evaluating spatial working memory. For the first time, this same study also showed that AQ treatment significantly inhibited γ-secretase activity and enhanced degradation of Aβ via up-regulation of insulin-degrading enzyme (IDE), an Aβ-degrading protease (Moon et al., 2019).

The involvement of Nr4a2 in regulating neuronal survival, neuroinflammation, neurogenesis and synaptic plasticity, as well as its ability to be drug-targeted, postulates it as an attractive and promising therapeutic avenue for Alzheimer's pathology **(figure 14).**

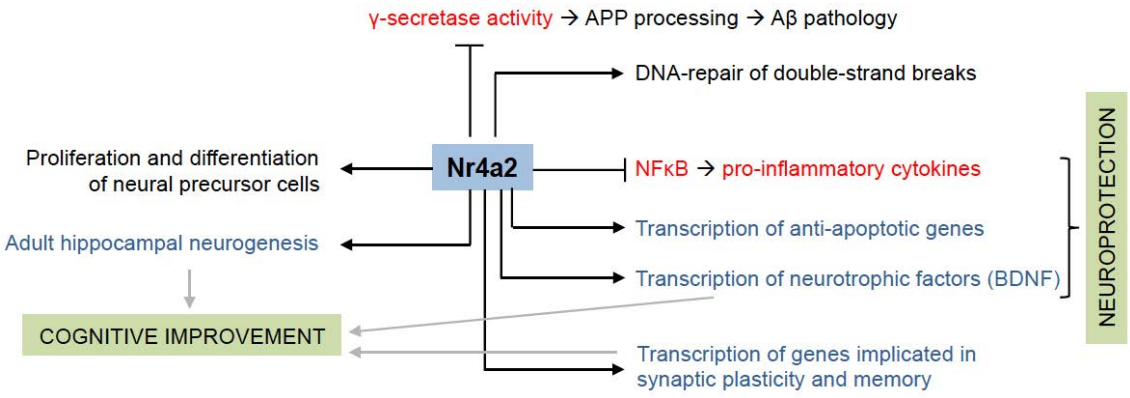

Figure 14. Schematic summary of Nr4a2 pleiotropic functions targeting AD pathology. Genes or processes up-regulated or down-regulated in AD are indicated in red and blue, respectively.

The evidences reported so far pointed us to study the role of Nr4a2 in hippocampal synaptic plasticity in order to shed light on the possible involvement of this transcription factor in the synaptic impairment occurring at early stages of AD. This will allow further pursuing whether Nr4a2 activation could mitigate the synaptic failure and consequently, the cognitive decline observed at early stages of Alzheimer's pathology.

V. Working hypothesis and objectives

The hypothesis of this study postulates that a decrease in hippocampal levels of Nr4a2 transcription factor caused by pathologic concentrations of soluble forms of amyloid-β peptide participates in the synaptic failure observed at early stages of Alzheimer's disease. As hippocampal synaptic dysfunction highly correlates with cognitive deficits, Nr4a2 activation could emerge as a potential therapeutic target to prevent, delay or even restore the cognitive decline observed in Alzheimer's disease patients.

To address this hypothesis, objectives were planned as follows:

1. To examine the role of Nr4a2 in hippocampal synaptic plasticity.

2. To check whether hippocampal Nr4a2 protein levels are altered in Alzheimer's disease.

3. To study whether Nr4a2 activation is able to ameliorate the Aβ-dependent synaptic dysfunction associated to early cognitive decline in Alzheimer's disease.

VI. Materials and methods

1. Experimental models

Animal handling and use for primary neuronal cultures and behavioral studies was performed in accordance to Animal Care facility and Bioethics Committee of the Universitat Autònoma de Barcelona (protocol CEEAH 2896, Generalitat de Catalunya DMAH8787) following the European Union guidelines.

1.1. Primary neuronal cultures

1.1.1. Primary cortical cultures

Cortical neurons were obtained from C57BL/6JRccHsd (Envigo) embryos of 14.5-15.5 days (E14.5-15.5).

Media, solutions and reagents:

Solution 1: Krebs-Ringer buffer 1X containing (in mM) 121 NaCl, 4.8 KCl, 1.2 KH_2PO_4, 25.5 $NaHCO_3$, 14.3 glucose and supplemented with 0.3% bovine serum albumin (BSA) and 0.03% $MgSO_4$.

Solution 2: solution 1 supplemented with 0.025% trypsin (Sigma).

Solution 3: solution 1 supplemented with 0.052% trypsin inhibitor (Thermo Fisher Scientific), 0.008% Deoxyribonuclease I (DNase I) (Sigma) and 0.04% $MgSO_4$.

Solution 4: solution 1 supplemented with 16% solution 3.

Solution 5: solution 1 supplemented with 0.03% $MgSO_4$ and 0.0014% $CaCl_2$.

Phosphate-buffered saline (PBS) 1X (in mM): 136.89 NaCl, 2.68 KCl, 8.1 Na_2HPO_4, 1.47 KH_2PO_4 supplemented with 30 mM glucose and 100,000 U penicillin / 0.1 g streptomycin; pH 7.4.

Dulbecco's modified Eagle's medium (DMEM) (Thermo Fisher Scientific) supplemented with 10% heat inactivated fetal bovine serum (FBS), 30 mM glucose and 50,000 U penicillin / 0.05 g streptomycin.

Neurobasal medium (Thermo Fisher Scientific) supplemented with 2% B27 (Thermo Fisher Scientific), 50,000 U penicillin / 0.05 g streptomycin and 1X glutaMAX™-I (Thermo Fisher Scientific).

Box 1. Composition of media, solutions and reagents used for primary cortical cultures.

To prepare primary cultures of cortical neurons, mice were sacrificed by cervical dislocation and embryos were extracted and placed into cold supplemented PBS 1X. Brains were removed, hemispheres were separated and meninges were detached. Cortices were dissected out and transferred to a sterile centrifuge tube containing 10 ml of supplemented Krebs-Ringer buffer (solution 1) and centrifuged for 30 seconds at 400 x g. After discarding the supernatant, tissue was enzymatically dissociated in trypsin (solution 2) at 37ºC during 10 minutes. The digestion reaction was stopped by adding trypsin inhibitor (solution 3) and centrifuged for 30 seconds at 400 x g. The supernatant was

discarded and tissue was mechanically dissociated in solution 4 using a Pasteur pipette and filtered through a nylon mesh (40 µm pore size). The filtered cell suspension was then transferred to a tube containing solution 5 and centrifuged at 200 x g for 5 minutes. The supernatant was discarded and the pellet was resuspended in supplemented DMEM. Neurons were counted in a Neubauer hemocytometer using trypan blue and plated in supplemented DMEM.

Neurons were maintained at 37ºC in a humidifier incubator with 5%CO_2 / 95%air. Three hours after seeding, medium was replaced by supplemented Neurobasal. Every 4-5 days, half of the conditioned medium was changed for fresh Neurobasal medium.

Neurons were plated in poly-D-lysine (PDL) mixture (0.01 mg/mL PDL in 0.1 M Sodium Borate Buffer, pH 8.4) pre-coated plates (65,790 neurons/cm^2 in 12-well plates for molecular and biochemical assays and 76,923 neurons/cm^2 in 60 mm diameter plates for chromatin immunoprecipitation assays). Experiments were performed when cortical neurons were mature, at 13-15 days *in vitro* (DIV).

1.1.2. Primary hippocampal cultures

Hippocampal neurons were obtained from C57BL/6JRccHsd (Envigo) newborn mice pups from postnatal day 0-2 (P0-P2).

Media, solutions and reagents:

Dissection Solution (in mM): 160 NaCl, 4.96 KCl, 1 $MgSO_4$, 3.87 $CaCl_2$, 5 HEPES, 5.55 glucose, 5.64 x 10^{-3} phenol red.

Serum Media: Minimum Essential Medium (MEM) w/ Earle's salts w/o L-glutamine (Thermo Fisher Scientific) supplemented with 5% FBS, 21 mM glucose and 1 ml mito+ serum extender (Corning, being 1 bottle resuspended in 10 ml sterile H_2O).

Enzymatic Solution, for 10 mL: 10 mL of dissection solution supplemented with 2 mg L-cysteine, 100 µl ethylenediaminetetraacetic acid (EDTA) (50 mM, pH 8), 100 µl $CaCl_2$ (100 mM), 15 µl NaOH (1N), 100 µl papain (100 units) (Worthington) and 100 µl DNase I (300 – 450 Kunitz / ml) (Sigma).

Inactivation Solution, for 10 mL: 10 mL of serum media supplemented with 25 mg BSA and 100 µl DNase I.

Neurobasal- A medium (Thermo Fisher Scientific) supplemented with 2% B27.

Fluoro deoxyuridine (FDUR): 100 mg 5-Fluoro-2'Deoxyuridine (Sigma) and 250 mg uridine (Sigma) in 50 ml MEM w/ Earle's salts w/o L-glutamine.

Box 2. Composition of media, solutions and reagents used for primary hippocampal cultures.

To prepare primary cultures of hippocampal neurons, mice pups were decapitated and placed into cold dissection solution. Brains were extracted, hemispheres were separated and meninges were removed. Hippocampi were dissected out and transferred into sterile

pre-warmed enzymatic solution. Tissue was enzymatically dissociated with enzymatic solution containing papain during 30 minutes at 37ºC in rocking conditions. After that, supernatant was discarded and inactivation solution was added during 2 minutes. Then, the supernatant was removed and tissue was mechanically dissociated in pre-warmed serum media using a Pasteur pipette and filtered through a nylon mesh (40 µm pore size). The filtered cell suspension was centrifuged at 200 x g for 5 minutes. The supernatant was discarded and the pellet was resuspended in serum media. Neurons were counted in a Neubauer hemocytometer and plated in supplemented Neurobasal-A medium.

Neurons were maintained at 37ºC in a humidifier incubator with 5%CO_2 / 95%air. One day after seeding, half of the medium was replaced by fresh supplemented Neurobasal-A medium, and then every 6-7 days. The mitotic inhibitor FDUR was added at 3 DIV to inhibit proliferation of non-neuronal cells (5 µl to 1 ml of medium).

Neurons were plated at specific densities in PDL mixture pre-coated plates (62,500 neurons/cm^2 in 24-well plates for luciferase assays, 65,780 neurons/cm^2 in 12-well plates for molecular and biochemical experiments and 76,923 neurons/cm^2 in 60 mm diameter plates for subcellular fractionation studies). For immunocytochemistry experiments, neurons were plated at 37,500 neurons/cm^2 in PDL pre-coated 24-well plates containing coverslips. Coverslips were previously treated with 3% fuming HCl overnight, washed and kept in absolute ethanol. Experiments were performed when hippocampal neurons were mature, at 17-21 DIV.

1.2. Hippocampal slices

Animal handling and use for hippocampal slices preparation followed a protocol approved by the Animal Care and Use Committee of Albert Einstein College of Medicine (20160412) in accordance with the National Institutes of Health guidelines.

P17 to P27 Sprague-Dawley rats and P49 to P57 C57BL/6J mice (Charles River Labs) of either sex were used for hippocampal slice preparation.

Solutions:

Cutting solution (in mM): 215 sucrose, 2.5 KCl, 26 $NaHCO_3$, 1.6 NaH_2PO_4, 1 $CaCl_2$, 4 $MgCl_2$, 4 $MgSO_4$ and 20 D-glucose.

NMDG-based cutting solution (in mM): 93 N-Methyl-d-glucamin, 2.5 KCl, 1.25 NaH_2PO_4, 30 $NaHCO_3$, 20 HEPES, 25 D-glucose, 2 Thiourea, 5 Na-Ascorbate, 3 Na-Pyruvate, 0.5 $CaCl_2$, 10 $MgCl_2$.

ACSF recording solution (in mM): 124 NaCl, 2.5 KCl, 26 $NaHCO_3$, 1 NaH_2PO_4, 2.5 $CaCl_2$, 1.3 $MgSO_4$ and 10 D-glucose.

Box 3. Composition of solutions used for hippocampal slices.

After rats were deeply anesthetized with isoflurane, they were decapitated and the brain rapidly removed into chilled cutting solution. Hippocampi were dissected out and cut into transverse hippocampal slices (300 µm thick) using a VT1200 Leica microslicer. At 15 minutes post-sectioning, the cutting solution was gradually switched to extracellular artificial cerebrospinal fluid (ACSF) recording solution. Slices were then incubated for at least 45 minutes in the recording solution and kept at room temperature before recording.

Slices from mice (400 µm thick) were prepared using NMDG-based cutting solution. These slices were directly transferred into ACSF and incubated for at least 45 minutes at room temperature before recording. All solutions were equilibrated with 95% O_2 and 5% CO_2 (pH 7.4).

1.3. $APP_{Sw,Ind}$ transgenic mouse

For behavioral studies, we used $APP_{Sw,Ind}$ transgenic mice (line J9; C57BL/6J background) expressing the mutant human APP695 isoform harboring the FAD-linked Swedish (K670N/M671L) and Indiana (V717F) mutations under the expression of the neuronal platelet-derived growth factor β (PDGFβ) promoter (Hsia et al., 1999).

Mice were age-matched littermate males obtained by crossing heterozygous $APP_{Sw,Ind}$ to non-transgenic WT mice (C57BL/6J background).

$APP_{Sw,Ind}$ phenotype includes age dependent Aβ pathology, reduced CREB-dependent gene expression, altered synaptic plasticity and hippocampal-dependent memory deficits (Cheng et al., 2007; España et al., 2010b; Mucke et al., 2000; Saganich et al., 2006; Wright et al., 2013) **(figure 15).**

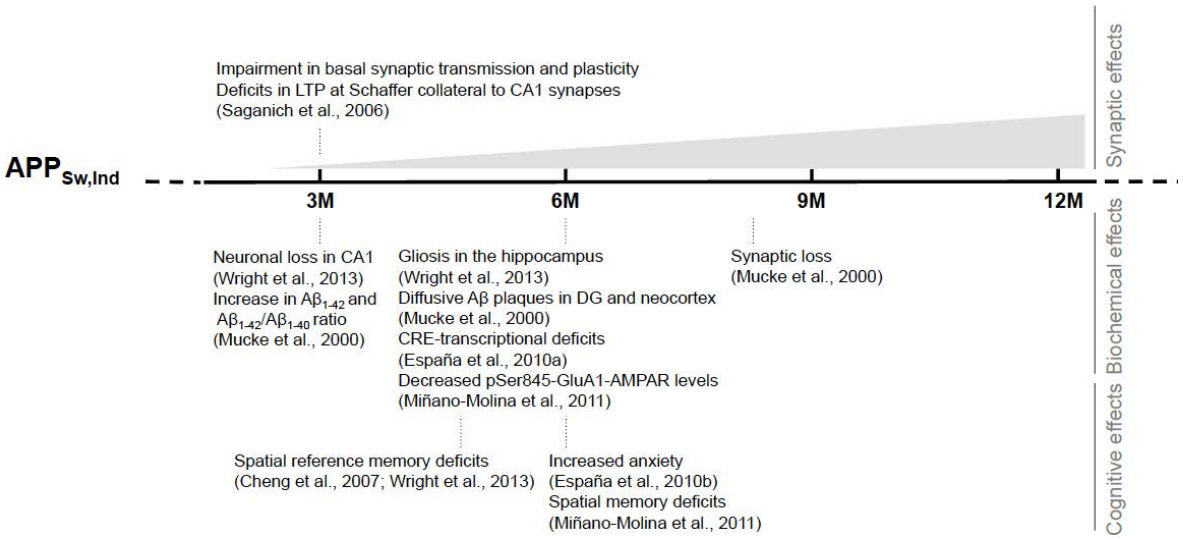

Figure 15. Summarized diagram of $APP_{Sw,Ind}$ synaptic, biochemical and cognitive deficits at different ages. DG, dentate gyrus; LTP, long term potentiation.

1.3.1. Mice genotyping

For mice genomic DNA extraction, a small portion of tail (1-2mm) was incubated overnight at 56ºC in 0.5 ml of digestion buffer containing (in mM): 100 Tris pH 8.5, 5 EDTA, 200 NaCl, 0.2% dodecyl sulfate (SDS) and supplemented with 0.1 mg/ml of proteinase K (Sigma). Samples were then centrifuged at 13,400 x g for 5 minutes. Supernatant was collected and mixed vigorously with 0.5 ml of isopropanol. After, samples were centrifuged at 13,400 x g for 10 minutes and 0.5 ml of 70% ethanol was added to the DNA pellet. Once dried, the DNA pellet was resuspended in 100 µl of TE buffer (10 mM Tris-HCl, 1 mM EDTA, pH 8) and incubated overnight at room temperature at 150 rpm in a thermomixer (Eppendorf).

For DNA amplification by polymerase chain reaction (PCR), 2 µl of genomic DNA was added in a mix containing 0.5 µM for each primer, 1X Display Buffer, 2 mM $MgCl_2$, 0.2 mM dNTP and Taq polymerase (1 unit) in a final volume of 25 µl. PCR was performed in a thermal cycler (PTC-100 Peltier Thermal Cycler, MJ Research) using the following program: 94ºC for 5 minutes and 40 cycles of 10 seconds at 94ºC, 10 seconds at 63ºC and 30 seconds at 72ºC.

Sequences for the specific primers used are shown in **table 5.**

Table 5. Sequences for the specific primers used for the polymerase chain reaction (PCR).

Gene	Forward sequence	Reverse sequence
Human APP	5'-GGT GAG TTT GTA AGT GAT GCC -3'	5'-TCT TCT TCT TCC ACC TCA GC -3'
Mouse APP	5'-CAA ATG TTG CTT GTC TGG TG -3'	5'-GTC AGT CGA GTG CAC AGT TT -3'

15 µl of the PCR product was resolved in 2% agarose-TAE gel (TAE buffer consisting in 40 mM Tris-acetate and 1 mM EDTA, pH 8.2) adding 1X GelRed Nucleic acid gel stain (Biotium). DNA bands were detected in a UV transiluminator (Gene genius, Syngene, Bio imaging system, GVT01A).

1.4. Human brain tissue

Postmortem human brain tissue analyzed in this study was provided by brain banks of Fundación CIEN (Instituto de Salud Carlos III, Madrid), Fundación Hospital Alcorcón (Madrid), Hospital Clínic-IDIBAPS (Barcelona) and Hospital Bellvitge (Barcelona).

We analyzed hippocampal tissue samples from control subjects and patients diagnosed as Braak I-II (corresponding to presymptomatic AD stage), Braak III-IV (corresponding to MCI due to AD) or Braak V-VI (corresponding to dementia due to AD).

Information of sex, age and postmortem delay (PMD) is shown in **table 6.**

Table 6. Demographic and clinical information of human hippocampal tissue samples.

	Control	Braak II	Braak III-IV	Braak V-VI
Cohort size	13	13	13	28
Sex (W/M)	6/7	5/8	5/8	18/10
Age (years) Mean ± SD (range)	58.77 ± 12.87 (43-79)	70 ± 10.43 (52-86)	81.15 ± 12.77 (46-98)	81.5 ± 6.12 (67-92)
PMD (h) Mean ± SD (range)	7.7 ± 4.23 (2-16)	5.46 ± 2.2 (3-9.75)	6.75 ± 3.24 (2-14)	8.4 ± 4.87 (2-20.5)

Results are expressed as mean ± SD for each group, range (min-max). PMD, postmortem delay.

2. Plasmids construction

Plasmids used for the experiments were either previously designed or generated for the first time.

shCRTC1 and shCREB were cloned into the pLVTHM vector (Dr. Didier Trono, Addgene) (see **annex 1**). Constructions were generated as previously described (Barneda-Zahonero et al., 2012; España et al., 2010b) and kindly provided by Dr. Carlos A. Saura, Universitat Autònoma de Barcelona.

Complementary oligonucleotides for mouse CREB and CRTC1 short hairpin RNA (shRNA) were as follows:

sh-CRTC1 forward:
5'gatccccGCAGCGTGACAATCGACCTATttcaagagaATAGGTCGATTGTCACGCTGCttttt-3'
sh-CRTC1 reverse:
5'-agctaaaaaGCAGCGTGACAATCGACCTATtctcttgaaATAGGTCGATTGTCACGCTGCggg-3'

sh-CREB forward:
5'-gatccccCTGAAGAAGCAGCACGAAAttcaagagaCTGAAGAAGCAGCACGAAAtctcttgaa-3'
sh-CREB reverse:
5' agctaaaaaCTGAAGAAGCAGCACGAAAtctcttgaaTTTCGTGCTGCTTCTTCAGggg-3'

2.1. FUGW-shNr4a2

To silence Nr4a2, a shRNA against the 3'-untranslated region (3'-UTR) of Nr4a2 was cloned previously in the lab into a modified version of the original FUGW vector backbone (kindly provided by Dr. Robert C. Malenka, Stanford University) (Jurado et al., 2013) (see **annex 1**).

Fisher Scientific RNAi designer web tool was used to design the specific oligonucleotides (Thermo Fisher Scientific) against mouse Nr4a2, as follows:

sh-Nr4a2 forward:
5'-GATCCCCGGGCACAAGTATCAGTACATTGGAATTCAAGAGATTCCAATGTACTGATACTT
GTGCCCTTTTTG-3'
sh-Nr4a2 reverse:
5'-CTAGCAAAAAGGGCACAAGTATCAGTACATTGGAATCTCTTGAATTCCAATGTACTGATA
CTTGTGCCCGGG-3'

Briefly, shNr4a2 oligonucleotides were resuspended in RNase/DNase free H_2O to a final concentration of 100 µM. Each oligonucleotide was phosphorylated by T4 polynucleotide kinase (New England BioLabs) in a reaction containing 10 µl of oligonucleotides (100 µM), 1 µl of enzyme, 2 µl of 10X T4 DNA ligase buffer containing ATP (New England BioLabs) in a final reaction of 20 µl for 30 minutes at 37ºC. Complementary strands were annealed by mixing 20 µl of each oligonucleotide and incubating from 95ºC to room temperature overnight, obtaining a final concentration of 25 µM.

FUGW vector was digested using the NheI and BamHI restriction enzymes (New England BioLabs). 10 µg of FUGW vector, 5 µl of NheI, 5 µl of enzyme buffer and 30 µl of RNase/DNase free water were incubated at 37ºC for 1 hour, and then incubated for 30 minutes more after adding 5 µl of BamHI. Then, 1 µl of the CIAP phosphatase enzyme (10U/µl; New England BioLabs) was added to prevent religation of the digested vector. 50 µl of the digested vector was resolved in 1% agarose-TAE gel. DNA band was visualized in a UV transiluminator (Syngene, GVM20), cut and purified using the NucleoSpin Gel and PCR clean-up (Macherey-Nagel) kit following supplier's recommendations.

To introduce the shNr4a2 oligonucleotides into the FUGW vector, a mixture containing 2 µl of insert, 5 µl of vector, 2 µl of 10X T4 DNA ligase buffer, 1 µl of DNA ligase T4 (New England BioLabs) and 10 µl of RNase/DNase free H_2O was incubated at 16ºC overnight in a thermal cycler. Afterwards, the ligation reaction was incubated at 65ºC for 15 minutes to inactivate the ligase enzyme and kept at 4ºC until transformation. The relation vector:insert was of 1:3 to ensure high efficiency of the ligation.

The DNA plasmid (1 µl) was transformed into 30 µl of DH5α competent cells (Thermo Fisher Scientific) using the heat shock method (incubation 30 minutes at 4ºC, 1 minute at 42ºC and 2 minutes at 4ºC). Each transformation reaction was diluted in 1 ml of LB medium (10 g bacto tryptone, 5 g bacto yeast extract, 10 g NaCl in 1 L distilled water; pH 7) and incubated at 37ºC for 1 hour. Bacterial cells were centrifugued 3 minutes at 100 x g and resuspended in 75 µl of LB medium before being plated on ampicillin-containing LB agar plates (LB medium supplemented with 1.2% bacto agar) and incubated overnight at

37ºC. Individual isolated colonies were picked and grown in 6 ml of ampicillin-containing LB medium at 37ºC and 250 rpm for 12 hours. Plasmid DNA was isolated using the plasmid DNA purification NucleoSpin Plasmid kit (Macherey-Nagel) following supplier's recommendations. The presence of the shNr4a2 into the FUGW vector was confirmed by sequencing (Servei de Genòmica i Bioinformàtica – SGB –, Universitat Autònoma de Barcelona).

DNA plasmid was transformed again and individual isolated colonies were grown in 6 ml of ampicillin-containing LB medium at 37ºC and 250 rpm for 12 hours. Then, they were decanted to 250 ml of ampicillin-containing LB medium and incubated overnight in the same conditions. Plasmid DNA purification and amplification was performed using the plasmid DNA Purification Nucleobond Xtra Maxi EF kit (Macherey-Nagel) following supplier's recommendations. The schematic construction of the shNr4a2 introduced in the FUGW vector is shown in **figure 16.**

2.2. FUGW-shNr4a2+Nr4a2 and pWpi+Nr4a2

To generate a construct to overexpress Nr4a2, we used the In-Fusion HD Cloning Kit (Clontech) following supplier's recommendations. Vectors were linearized by restriction enzyme digestion as previously described. FUGWshNr4a2 vector was digested using AgeI restriction enzyme (New England BioLabs) and pWpi vector using PmeI restriction enzyme (New England BioLabs). 50 µl of the digested vector was resolved in 1% agarose-TAE gel and DNA band was visualized in a UV transiluminator, cut and purified using the NucleoSpin Gel and PCR clean-up kit as previously.

Nr4a2 coding sequence was obtained from pcDNA3.1Nr4a2V5HisB plasmid (see **annex 1**) kindly provided by Dr. Ángel Juan García Yagüe, Instituto de Investigaciones Biomédicas "Alberto Sols", Madrid.

To amplify the Nr4a2 coding sequence, we designed specific primers following In-Fusion ND Cloning kit recommendations. PCR primers consisted in 15 base pairs (bp) extensions (5') complementary to the end of the linearized vector (including the restriction enzyme site) and 25 bp extensions (3') that were specific to the insert (Nr4a2 coding sequence), as follows:

FUGWshNr4a2+Nr4a2 forward:
5'-ATCCCCGGGTACCGGATGCCTTGTGTTCAGGCGCAGTATG-3'
FUGWshNr4a2+Nr4a2 reverse:
5'-CATGGTGGCGACCGGCGTAGAATCGAGACCGAGGAGAG-3'

pWpi+Nr4a2 forward:
5'-CTAGCCTCGAGGTTTATGCCTTGTGTTCAGGCGCAGTATG-3'
pWpi+Nr4a2 reverse:
5'-TGCAGCCCGTAGTTTCGTAGAATCGAGACCGAGGAGAG-3'

The PCR reaction consisted in a mix containing 15 µg of each pair or primers, 100 ng of DNA (pcDNA3.1Nr4a2V5HisB), 1.5 mM $MgSO_4$, 0.3 mM dNTPs, 1X PCR buffer Pfx polymerase and 1.25 units of Taq polymerase Platinum-Pfx (Thermo Fisher Scientific) in a final volume of 50 µl. The program used was 2 minutes at 94ºC, 35 cycles of 30 seconds at 94ºC, 45 seconds at 50ºC and 1 minute at 72, and finally 10 minutes at 72ºC. 50 µl of the PCR product was resolved in 1% agarose-TAE gel to confirm the presence of a band of 1796 kb using a UV transilluminator. The band was cut and purified using the NucleoSpin Gel and PCR clean-up kit as previously.

To introduce the Nr4a2 coding sequence into the vectors, a mixture containing 100 ng of insert, 200 ng of linearized vector, 2 µl of 5X In-Fusion HD enzyme premix and distilled water up to 20 µl was incubated for 15 minutes at 50ºC. 2.5 µl of the In-Fusion reaction mixture were transformed into Stellar Competent Cells (Clontech) using the heat shock method as previously described. Each transformation reaction was diluted in SOC medium and incubated at 37ºC for 1 hour before seeding on ampicillin-containing LB agar plates. Plasmid DNA from individual isolated colonies was amplified as previously indicated. PCR and posterior sequencing confirmed the presence of the insert into the vectors. The schematic construction of the Nr4a2 coding sequence introduced into the FUGWshNr4a2 and pWpi vectors is shown in **figure 16.**

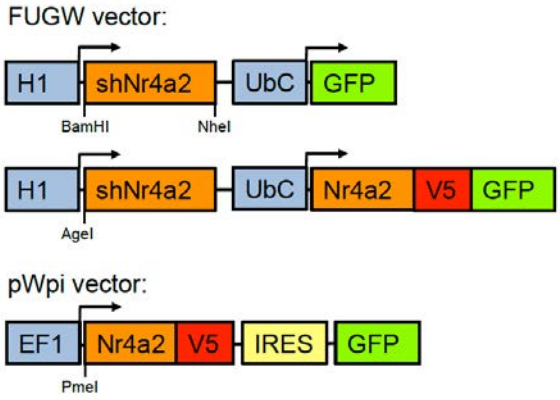

Figure 16. Schematic representation of the constructions used to silence and overexpress Nr4a2. GFP, green fuorescent protein; H1, histone 1; IRES, internal ribosomal entry site; UbC, ubiquitin C.

2.3. Transfection and lentiviral vector production and titration

Human embryonic kidney 293T (HEK293T) cells were grown in supplemented DMEM medium (Thermo Fisher Scientific) (box 1). At 70% of confluence, HEK293T cells were transfected using the CalPhos Mammalian Transfection kit (Clontech) following supplier's recommendations. We used 3 dishes of 100 mm of diameter per condition.

Briefly, HEK293T cells medium was supplemented with 25 μM chloroquine (Sigma) in order to increase the transfection efficiency. For empty FUGW, FUGWshNr4a2 or FUGWshNr4a2 +Nr4a2 lentiviral vectors generation, for each dish of 100 mm of diameter, a mixture containing 20 μg of specific DNA, 10 μg DNA of each of pVSVG, pREV and pRRE plasmids (kindly provided by Dr. Robert C. Malenka, Stanford University; see **annex 1**) and 250 mM $CaCl_2$ (in a final volume of 500 ul) mixed drop wise with 2X HBS was prepared. After 20 minutes at room temperature, the DNA mixture solution was added drop wise to HEK293T cells and incubated for 8 hours at 37ºC in a humidifier incubator with 5%CO_2 / 95%air. Then, medium was replaced by fresh supplemented DMEM.

For LVTHM, shCREB, shCRTC1, pWpi and pWpi+Nr4a2 lentiviral vectors generation, the DNA mixture consisted in 20 μg of specific DNA and 10 μg each of psPax2 and pMD2.G plasmids (from Dr. Didier Trono, Addgene; see **annex 1**).

HEK393T culture medium was collected 24, 36 and 48 hours after transfection and filtered through a 0.45 μm pore size filter to remove cellular debris. Then, medium was spun at 47,000 x g for 2 hours at 4ºC to concentrate the lentiviral vector particles, which were resuspended in 100 μl cold PBS 1X without supplements (box 1) and kept at 4ºC overnight with soft shaking before being aliquot and stored at -80ºC.

Biological titers of the viral preparations expressed as a number of transducing units per milliliter were assessed by transducing HEK293T cells with serial dilutions and checking the percentage of green fluorescent protein (GFP)-positive cells by flow cytometry (Cytomics FC 500, Beckman Coulter).

Hippocampal-cultured neurons were transduced at 7DIV with lentiviral vectors (1-2 transducing units/cell).

3. Cell treatments

3.1. Drugs

If not otherwise stated, drugs were directly added to cell culture media diluted at the proper final concentration using distilled H_2O. A summary of the drugs used is shown in **table 7.**

Table 7. List of drugs used in this study.

Drug	Action	Source	Concentration
4-aminopyridine (4-AP)	Non-selective voltage-dependent potassium-channel blocker	Sigma	50 µM
Amodiaquine dihydrochloride dehydrate (AQ)	Nr4a2 agonist	Sigma	10 µM (biochemistry) 60 µM (electrophysiology)
ANA-12(#)	TrkB antagonist	Sigma	25 µM
BAPTA-AM	Intracellular calcium quelator	Tocris	20 µM
BDNF(&)	TrkB agonist	R&D Systems	50 ng/ml
Bicuculline methiodide (Bic)	Classical $GABA_A$ receptor antagonist	Tocris	50 µM
Chloroquine diphosphate salt (CQ)	Nr4a2 agonist	Sigma	10 µM (biochemistry) 30 µM (electrophysiology)
FK-506 monohydrate	Calcineurin inhibitor	Sigma	10 µM
Forskolin (FSK)(*)	Protein kinase A agonist	Tocris	50 µM
MK-801 maleate	Selective and non-competitive NMDA receptor antagonist	Tocris	10 µM
MG-132	Proteasome inhibitor	Tocris	10 µM
NBQX disodium salt	Selective and competitive AMPA/kainate receptor antagonist	Tocris	10 µM
Nifedipine	L-type calcium channel blocker	Tocris	10 µM
N-Methyl-D-aspartate (NMDA)(*)	NMDA receptor agonist	Tocris	50 µM
Rolipram(*)	Phosphodiesterase-4 inhibitor	Sigma	0.1 µM

List in alphabetical order, indicating its action, source and the final concentration used. Specific identifiers are shown in key resources table (see annex 2). *Drugs marked with an asterisk were diluted in ACSF; #ANA-12 was diluted in culture medium; &BDNF was diluted in PBS 1X supplemented with 0.1% BSA.

3.2. cLTP and cLTD protocols

Before cLTP or cLTD induction, hippocampal-cultured neurons were incubated in ACSF buffer containing (in mM): 125 NaCl, 2.5 KCl, 1 $MgCl_2$, 2 $CaCl_2$, 33 D-glucose and 25 HEPES pH 7.3 for 30 minutes at 37ºC.

For cLTD induction, after 30 minutes of ACSF incubation, hippocampal neurons were stimulated for 5 minutes with NMDA 50 µM in ACSF in absence of $MgCl_2$. After that, cells were maintained 55 minutes in complete ACSF before lysis.

For cLTP induction, after 30 minutes of ACSF incubation, hippocampal neurons were stimulated for 10 minutes with FSK 50 µM and Rolipram 0.1 µM in ACSF in absence of $MgCl_2$. Afterwards, cells were maintained 50 minutes (for 1 hour of cLTP treatment) or 3 hours and 50 minutes (for 4 hours of cLTP treatment) in complete ACSF before lysis.

A detailed scheme for the cLTD and cLTP protocols is included in the results section **(figure 38 and 48)**.

3.3. Amyloid-β oligomerization

Synthetic $A\beta_{1-42}$ protein was purchased as a lyophilisate (Bachem or GenicBio). The lyophilisate was kept at room temperature for 30 minutes and dissolved in cold hexafluor-2-propanol (HFIP) to obtain a concentration of 1 mM $A\beta_{1-42}$. After homogenization (1 to 3 hours at room temperature in agitation), it was aliquoted in protein low-binding tubes (4 aliquots of 50 µl) and evaporated in a speed-vac at 800 x g <25ºC for 20 minutes. The precipitate was stored at -80ºC until use (stable during 6 months).

The precipitated $A\beta_{1-42}$ protein was dissolved in 20 µl of 100% dimethyl sulfoxide (DMSO) to get a stock of 5 mM. To allow oligomerization, $A\beta_{1-42}$ was diluted to a final concentration of 100 µM by adding DMEM F-12 phenol-red free media (Life technologies) and kept 12 hours at 4ºC.

$A\beta_{1-42}$ oligomeric preparations were then biochemically analyzed by BisTris/bicine western blotting (see section 4.3.3 materials and methods).

4. Molecular biology, cellular and biochemical methods

4.1. RNA extraction, cDNA synthesis and RT-qPCR

Total RNA was isolated using the RNeasy Mini kit (Qiagen) according to supplier's recommendations. Briefly, samples were lysed in RLT lysis buffer (12-well plates; 175 µL lysis buffer per well, 2 wells per condition or 350 µL per half mice hippocampus) and mixed with 1 volume of 70% ethanol. The mix was then transferred to a RNeasy Mini spin column, placed in a 2 ml collection tube and spun for 20 seconds at 9,300 x g. After discarding the flow-through, 350 µl of RW1 buffer were added to the spin column and spun for 20 seconds at 9,300 x g. Then, 80 µl of DNAse (RNase-Free DNase set; Qiagen) were added to the column and let it stand for 15 minutes. After that, 350 µl of RW1 buffer were added and spun for 20 seconds at 9,300 x g. Next, 500 µl of RPE buffer were added twice and spun for 20 seconds first and 2 minutes then at 15,700 x g. Then, RNeasy Mini spin columns were dried by an additional centrifugation of 1 minute at 15,700 x g. Finally, RNA was eluted by adding directly to the spin column membrane 40 µl of RNase-free water and centrifuguing it for 1 minute at 9,300 x g after waiting for 5 minutes to soak the membrane in order to achieve the maximal yield in the elution.

RNA concentration was determined using NanoDrop 2000 Spectrophotometer (Thermo Fisher Scientific), and RNA integrity was assessed by running the samples on an Agilent RNA 6000 Nano chip on an Agilent 2100 BioAnalyzer (Agilent Technologies). Samples with RNA integrity number (RIN) below 8 were excluded from further analysis.

For complementary DNA (cDNA) synthesis, 500 ng of RNA were reverse transcribed in a mix containing 2.5 µM oligo $d(T)_{18}$ primers, 2.5 µM random hexamers, 0.5 mM each dNTP, 5 mM DTT, 40 units of RNeaseOUT, 1X SSIV buffer and 200 units of SuperScript IV reverse transcriptase in a final volume of 20 µl. All reagents were from Thermo Fisher Scientific. First, a mix containing the RNA, oligo $d(T)_{18}$ primers, random hexamers and dNTPs was incubated at 65ºC for 5 minutes. Immediately after, the annealed RNA was incubated on ice and a mix containing DTT, RNeaseOUT and SSIV buffer was added. Then, reactions were incubated 2 minutes at 42ºC and 2 minutes at room temperature. Finally, SuperScript IV was added to the reaction mixture and incubated for 50 minutes at 42ºC and for 15 minutes at 70ºC. cDNA products were stored at -20ºC.

Quantitative real-time polymerase chain reaction (RT-qPCR) was performed in triplicate using 2.5 µl of 1:50 diluted cDNA and 7.5 µl of a mix containing custom designed primers (300 nM) and the Fast Sybr Green Master Mix (Thermo Fisher Scientific). Amplification was done in the 7500 Fast Real-Time PCR system (Applied Biosystems, v2.0.6) using the following program: 1 cycle of 20 seconds at 95ºC to activate the enzyme followed by 40 PCR amplification cycles consisting of denaturation at 95ºC for 3 seconds and annealing and extension at 60ºC for 30 seconds. Melting curve analysis was performed to corroborate the specificity of the amplified products.

Raw Ct data acquired with the 7500 Fast Real-Time PCR system were exported to LinRegPCR software to calculate the amplification efficiency for each reaction. Reactions with amplification efficiency below 1.6 were excluded from further analysis. mRNA fold change was calculated using the ΔΔCt-method (Pfaffl, 2001). The geometric mean of glyceraldehyde-3-phosphate dehydrogenase (*Gapdh*) and peptidylpolyl isomerase A (*Ppia*) gene expression was used to normalize data.

Sequences for the specific primers used are shown in **table 8.**

Table 8. List of sequences for the specific primers used for real time polymerase chain reaction (RT-qPCR).

Gene	Forward sequence	Reverse sequence
Bdnf	5'-CTT CTT TGC TGC AGA ACA GG-3'	5'-CTT CTC ACC TGG TGG AAC TT-3'
Gabra1	5'-AAA AGC GTG GTT CCA GAA AA-3'	5'-GCT GGT TGC TGT AGG AGC AT-3'
Gapdh	5'-AAT TCA ACG GCA CAG TCA AGG C-3'	5'-TAC TCA GCA CCG GCC TCA CC-3'
Gria1	5'-TCC CCA ACA ATA TCC AGA TAG GG-3'	5'-AGG CCG CAT GTT CCT GTG ATT-3'
Gria2	5'-AGT GCA TTT CGG GTA GGG ATG-3'	5'-CCT CCA AAT TGT CGA TAT GGG GT-3'
Grin1	5'- GCT CTG TGG ATA TCT ACT TCC G-3'	5'- CTC ATG GGA CTT GAG TAT GGA-3'
Grin2A	5'- GGA TAC AAC AGA AAC TTA GCC A-3'	5'- GTC TCT GGA ACT TCT TGT CAC-3'
Grin2B	5'- TCA GCA GAG GTA TCT ACA GC-3'	5'- AGG GTG GGT TAT TGT ACG AC-3'
Nr4a2	5'-GTG TTC AGG CGC AGT ATG G-3'	5'-TGG CGA TAA TTT CAG TGT TGG T-3'

Nr4a2-V5	5'-GAC TCC ATT GTT GAA TTC TCC TCC-3'	5'-ACC GAG GAG AGG GTT AGG GAT-3'
Ppia	5'-GAC TGA ATG GCT GGA TGG-3'	5'-GGA AAT GGT GAT CTT CTT GCT-3'

List in alphabetical order.

4.2. Chromatin immunoprecipitation

For chromatin immunoprecipitation (ChIP) we used two samples of 3 dishes of 60 mm of diameter per condition containing 1.5 million cells each dish. Mature cortical-cultured neurons were cross-linked by adding directly to the media 1% formaldehyde for 10 min at room temperature. The crosslinking was then quenched by adding 0.125 M glycine. Once fixed, cells were collected in 0.5 ml cold PBS 1X (box 1) supplemented with 1X protease and phosphatase inhibitors and centrifuged at 4ºC for 5 minutes at 400 x g, 5 minutes at 1,000 x g, 5 minutes at 2,000 x g, 3 minutes at 7,000 x g and 3 minutes at 14,000 x g. Pellets were homogenized and incubated 1 hour in 50 µl cold SDS-lysis buffer.

Solutions:

SDS-lysis buffer (in mM): 50 Tris-HCl pH 8.1, 100 NaCl, 5 EDTA, 1% SDS, 0.1% Na deoxycholate, 1X protease and phosphatase inhibitors.

ChIP dilution buffer (in mM): 16.7 Tris-HCl pH 8.1, 167 NaCl, 1.2 EDTA, 1.1% Triton X-100, 0.01% SDS, 0.1% Na deoxycholate.

Low-Salt wash buffer (in mM): 20 Tris-HCl pH 8.1, 150 NaCl, 2 EDTA, 1% Triton X-100, 0.1% SDS.

LiCl wash buffer (in mM): 10 Tris-HCl pH 8.1, 1 EDTA, 250 LiCl, 1% Nonidet P-40 (NP-40), 1% Na-deoxycholate.

NaCl elution buffer (in mM): 20 Tris-HCl pH 7.5, 5 EDTA, 70 NaCl, 5 DTT, 1% SDS.

TE buffer (in mM): 10 Tris-HCl, 1 EDTA, pH 8.

Box 4. Composition of solutions and reagents used for chromatin immunoprecipitation.

After cell lysis, two samples per condition were transferred to TPX microtubes (Diagenode) to improve sonication and shearing efficiency, and 180 µl of ChIP dilution buffer were added. Chromatin was sheared between 200 and 500 bp by sonication using a BioruptorPlus (Diagenode) (20 cycles of 30 seconds of sonication interleaved 30 seconds, and with a vortex every 5 cycles, at 4ºC). After chromatin fragmentation, 700 µl of ChIP dilution buffer were added and samples were centrifuged at 4ºC for 10 minutes at 12,000 x g. Supernatant (25 µl) was used as the input sample.

To avoid nonspecific unions, pre-cleared beads (Thermo Fisher Scientific) were added to each sample (50 µl/sample) and incubated during 2 hours at 4ºC in agitation. Next, samples were centrifuged for 2 minutes at 350 x g and the supernatant was transferred to

a DNA low-binding tube. ChIP was performed overnight at 4ºC by adding rabbit anti-CRTC1 (5 µl/sample) or rabbit anti-CREB (3 µl/sample) antibodies.

After antibody incubation, pre-cleared beads were added to each sample and incubated during 1 hour at 4ºC in agitation. Supernatant was discarded and beads with the immunoprecipitated DNA were rinsed twice with Low-Salt wash buffer, twice with LiCl wash buffer and twice with TE buffer (700 µl/sample each). To elute the immunoprecipitated DNA, 100 µl NaCl elution buffer were added to each sample and incubated at 65ºC for 15 minutes at 1,000 rpm in a thermomixer twice (immunoprecipitated samples).

100 µl of NaCl elution buffer without SDS were added to immunoprecipitated samples, and 282.5 µl of a mix containing ChIP Dilution Buffer supplemented with 177 mM NaCl, 4.42 mM DTT and 0.7% SDS were added to input samples. Input and immunoprecipitated DNA were decrosslinked during 4 hours at 65ºC at 600 rpm. Then, 10 mg/ml of proteinase K (Sigma) diluted in NaCl elution buffer was added and incubated during 4 hours at 65ºC at 600 rpm.

Next, samples were vigorously mixed with 500 µl of phenol:chloroform:isoamyl (Amresco) and centrifuged during 10 minutes at 16,000 x g. The superior phase (400 µl) was transferred to a DNA low-binding tube and a mix containing 1 ml absolute ethanol supplemented with 120 mM acetic sodium and 4 µg glycogen (stock 20 µg / µl) was added to each sample and kept at -20ºC overnight.

Samples were then centrifuged during 20 minutes at 2ºC at 20,000 x g. 1 ml of 70% ethanol was added to the supernatant and centrifuged during 20 minutes at 2ºC at 20,000 x g. Finally, supernatant was discarded and pellet was dried, resuspended in TE buffer and incubated for 20 minutes at 37ºC at 650 rpm.

Input and immunoprecipitated DNA were amplified by quantitative PCR using specific primers (400 nM) as previously explained (section 4.1 materials and methods), and the fold enrichment was calculated over an irrelevant region.

Sequences for the specific primers used are shown in **table 9.**

Table 9. Sequences for the specific primers used for ChIP-qPCR.

Gene	Forward sequence	Reverse sequence
Nr4a2	5'-TACCAAGGTGAACCGTTCC-3'	5'- GCCAACATGCACCTAAAGTC-3'
Irrelevant region – Nr4a3	5'- TCAGTCTTTGCCAGCAGGT-3'	5'- GCTCAGAAGCCAGTTGACAC-3'

4.3. Lysis, quantification and protein analysis

4.3.1. Tissue and cell lysis

Both primary neuronal cultures and tissue were homogenized in RIPA-lysis buffer containing (in mM): 50 Tris-HCl, pH 7.4, 150 NaCl, 2 mM EDTA, 0.5% Triton X-100, 1% NP-40, 0.1% SDS, 1 mM Na_3VO_4, 50mM NaF and 1 mM phenylmethylsulfonyl fluoride (PMSF) supplemented with protease and phosphatase inhibitors (Sigma).

Primary neuronal cultures were washed in PBS 1X (box 1) and then lysed in cold RIPA-lysis buffer (12-well plates; 40 µL lysis buffer per well, 2 wells per condition). Lysates were sonicated using 30% of power (relative output 0.5) for 3 seconds (Sonic Dismembrator model 300, Dynatech) and samples were kept at -20ºC until use.

For human and mice hippocampal tissue, 100 µL of cold RIPA-lysis buffer were used for each 10 mg of tissue. Samples were homogenated using a pestle homogenizer and solubilized 1h at 4ºC. Then, lysates were sonicated using 30% of power (relative output 0.5) three times for 15 seconds each interleaved with 30 seconds on ice. Next, they were centrifuged at 9,300 x g for 15 minutes at 4ºC and the supernatant was kept at -80ºC until use.

4.3.2. Protein quantification and Western blotting

Protein concentration was determined using the Pierce BCA protein assay kit (Thermo Fisher Scientific) following supplier's recommendations. Equal amounts of protein were diluted in sample loading buffer 4X and heated at 95ºC for 4 minutes.

Solutions and reagents:

Sample loading buffer (4X SDS-PAGE buffer): 278 mM Tris-HCl pH 6.8, 44% glycerol, 4.4% SDS, 0.008% bromophenol blue. β-mercaptoethanol 1.4 M added before use.

Acrylamide/Bis, 30%T/5%C Solution (Rio-Rad)

Running buffer 1X: 25mM Tris, 192 mM glycine, 0.1% SDS.

Transfer buffer 1X: 25mM Tris, 192 mM glycine, 20% methanol.

Ponceau S Staining Solution: 0.1% Ponceau S, 5% acetic acid.

Blocking buffer: 10% non-fat dried milk, 0.1% BSA pH 7.4 in PBS or Tris-HCl buffered saline (TBS).

TBS 1X (in mM): 136.89 NaCl, 20 Tris; pH 7.6.

PBS 1X (in mM): 136.89 NaCl, 2.68 KCl, 4.29 Na_2HPO_4 x $7H_2O$, 1.47 KH_2PO_4; pH 7.4.

PBS-Tween (PBS-T)/TBS-T: PBS or TBS supplemented with 0.05% tween-20.

Antibody dilution buffer: 0.1% BSA, 0.02% thimerosal in PBS or TBS 1X.

Box 5. Composition of solutions and reagents used for Western blotting.

Samples were loaded to polyacrylamide gels (7.5-12%) and separated by electrophoresis in running buffer 1X. Next, proteins were transferred to nitrocellulose membranes (GE Healthcare) in transfer buffer 1X. Membranes were stained with 0.1% Ponceau S solution (Sigma) to verify correct transference. Membranes were next washed and blocked 1 hour in blocking buffer, washed in PBS-Tween 20 (PBS-T) or TBS-T (2X 5 minutes, 2X 10 minutes) and incubated at 4ºC overnight with primary antibodies diluted in antibody dilution buffer if not otherwise stated **(table 10).** Membranes were washed in PBS-T or TBS-T (2X 5 minutes, 2X 10 minutes) and incubated for 1 hour at room temperature with appropriate horseradish peroxidase-conjugated secondary antibodies (HRP-linked anti-mouse or anti-rabbit IgG; BD Biosciences) diluted in blocking buffer. Blots were next washed in PBS-T or TBS-T (2X 5 minutes, 2X 10 minutes) and developed using ECL™ Western blotting Detection Reagents (GE Healthcare). Blots densitometry was performed using ImageJ (National Institutes of Health, Bethesda, MD), and protein levels were corrected for corresponding loading control (GAPDH, β-actin, β-tubulin or pancadherin).

Table 10. List of primary antibodies used for western blotting.

Antibodies	Source	Identifier	Dilution
Mouse monoclonal anti-β-actin (AC-15)	Sigma	A1978	1:20,000 (PBS)
Rabbit polyclonal anti-Akt	Cell Signaling	9272	1:1,000 (PBS)
Rabbit polyclonal anti-BDNF (N-20)	Santa Cruz Biotechnology	sc-546	1:500 (*)
Rabbit monoclonal anti-CREB (48H2)	Cell Signaling	9197	1:500 (PBS)
Rabbit monoclonal anti-CRTC1 (C71D11)	Cell Signaling	2587	1:10,000 (TBS)
Rabbit polyclonal anti-Erk1/2	Cell Signaling	9102	1:1,000 (PBS)
Mouse monoclonal anti-GABA-AR α1	Synaptic Systems	224-211	1:1,000 (TBS)
Mouse monoclonal anti-GAPDH (6C5)	Thermo Fisher Scientific	AM4300	1:10,000 (PBS)
Rabbit polyclonal anti-GFP	Santa Cruz Biotechnology	sc-8334	1:1000 (TBS)
Rabbit polyclonal anti-GluA1	Merck-Millipore	AB1504	1:1,000 (PBS)
Mouse monoclonal anti-GluA2 (6C4)	Merck-Millipore	MAB397	1:1,000 (PBS)
Mouse monoclonal GluN1 (54.1)	Merck-Millipore	MAB363	1:1,000 (TBS)
Rabbit polyclonal anti-GluN2A	Merck-Millipore	AB1555	1:1,000 (TBS)
Rabbit polyclonal anti-GluN2B	Merck-Millipore	AB1557	1:1,000 (TBS)
Mouse monoclonal anti-Nurr1 (N1404)	Abcam	ab41917	1:500 (blocking buffer)
Rabbit polyclonal anti-Nurr1	Millipore	ABN1675	1:2000
Rabbit polyclonal anti-pancadherin	Cell Signaling	4068S	1:1,000 (TBS)
Rabbit polyclonal anti-phospho-Akt(Ser473)	Cell Signaling	9271	1:1,000 (PBS)
Mouse monoclonal anti-phospho-CREB(Ser133) (1B6)	Cell Signaling	9196	1:500 (PBS)
Rabbit polyclonal anti-phospho-Erk1/2(Thr202/Tyr204)	Cell Signaling	9101	1:1,000 (PBS)
Rabbit monoclonal anti-phosphoGluA1(Ser845) (EPR2148)	Abcam	ab76321	1:1,000 (PBS)
Rabbit monoclonal anti-phospho-TrkB(Tyr706/Tyr707) (C50F3)	Cell Signaling	4621	1:1,000 (#)
Mouse monoclonal anti-PSD95 (6G6-1C9)	Abcam	ab2723	1:1,000 (PBS)

Mouse monoclonal anti-synaptophysin	Sigma	S5768	1:20,000 (PBS)
Rabbit monoclonal anti-TrkB (80E3)	Cell Signaling	4603	1:1,000 (#)
Mouse monoclonal anti-β-tubulin (5H1)	BD Biosciences	556321	1:20,000 (PBS)

List in alphabetical order. Source and final dilution used is indicated. Research resource identifiers (RRID) are shown in key resources table (see annex 2). TBS or PBS in parenthesis indicates whether antibody dilution buffer was prepared using PBS or TBS 1X. *BDNF primary antibody was prepared in a solution containing TBS 1X + 5% BSA + 0.1% tween-20 + 0.02% thimerosal. # TrkB and Tyr706/Tyr707pTrkB primary antibodies were prepared in a solution containing TBS 1X + 0.5% BSA + 0.2% tween-20 + 0.02% thimerosal

4.3.3. BisTris/Bicine Western blotting

To determine the aggregation state of $A\beta_{1-42}$ oligomeric preparations, we performed the classical western blotting with minor modifications.

Solutions and reagents:

Sample loading buffer: 0.72 M BisTris, 0.32 M Bicine, 2% SDS, 25% glycerol, 100mM dithiothreitol, 0.008% bromophenol blue.

Acrylamide/Bis, 30%T/2.7%C Solution (Rio-Rad)

Cathode Running buffer 1X: 0.2 M Bicine, 0.1 M NaOH, 0.25% SDS, pH 8.2

Anode Running buffer 1X: 0.2 M Tris, 0.05 M H_2SO_4, pH 8.1.

CAPS/Methanol transfer buffer: 10 mM N-cyclohexul-3-aminopropanesulfonic acid (CAPS) pH 11, 10% methanol.

Box 6. Composition of solutions and reagents used for BisTris/Bicine Western blotting.

Electrophoresis was performed in Cathode/Anode Running buffer and proteins were transferred to PVDF membranes (GE Healthcare), previously activated with methanol, in CAPS/methanol transfer buffer. Mouse monoclonal anti-APP 20.1 (generated by the 20.1 hydridoma cell line, a kind gift from Dr. W.E. Van Nostrand, University of Rhode Island) was used as primary antibody.

4.4. Biotynilation assay

Hippocampal-cultured neurons were washed in fresh prepared cold PBS 1X (box 1) supplemented with 1 mM $CaCl_2$ and 0.1 mM $MgCl_2$ pH 7.4 (PBS-Ca-Mg) and then incubated in PBS-Ca-Mg containing 1mg/ml EZ-link-sulfo-NHS-LC-biotin (Thermo Fisher) for 30 minutes on ice with shaking. Next, hippocampal neurons were rinsed 3X (10 minutes each) in PBS-Ca-Mg + 0.1 M glycine to quench free biotin and then scraped and lysed (6-well plates; 2 wells/condition; 500,000 neurons/well) in 300 µl cold lysis buffer containing (in mM) 50 HEPES pH 7.5, 50 NaCl, 10 EDTA, 10 ethylene glycol tetraacetic

acid (EGTA), 1 $NaVO_3$, 50 NaF, 25 NaPPi, 1 β-glycerophosphate, 1 PMSF, 1% Triton X-100 and supplemented with 1X protease and phosphate inhibitors.

Lysates were centrifuged for 20 minutes at 10,000 x g. Before pull-down of biotinylated proteins, 25% of the cell lysate was kept for total fraction. The remaining sample was combined with Neutravidin agarose beads (30 µl, Thermo Fisher) and incubated overnight at 4ºC. Beads were washed 3X with cold lysis buffer. To elute captured proteins, 2X SDS-PAGE buffer containing 125 mM Tris-HCl pH 6.8, 20% glycerol, 5% SDS and 0.004% bromophenol blue was added to the beads.

4.5. Subcellular fractionation

Hippocampal-cultured neurons were washed twice in cold PBS 1X (box 1) and lysed in 200 µl cold lysis buffer containing (in mM): 10 HEPES, 1.5 $MgCl_2$, 10 KCl and 0.1% Triton X-100 supplemented with 1X protease inhibitors for 10 minutes on ice (4 wells of 12-well plates per condition; 250,000 cells/well). Then, they were scraped, homogenized using a pestle homogenizer and incubated for 10 minutes more on ice. 10% of the cell lysate was kept for total fraction. The remaining sample was centrifuged for 10 minutes at 2,000 x g at 4ºC. Pellets were washed twice with 400 µl cold lysis buffer, homogenized and centrifuged before being resuspended in 50 µl cold lysis buffer to obtain the nuclear fraction. Supernatants were centrifuged for 10 minutes at 7,000 x g at 4ºC, and the remaining supernatants were centrifuged again for 1 hour at 100,000 x g at 4ºC. The supernatant obtained was the cytosolic fraction. Total and nuclear fractions were sonicated in an Ultrasonic Cleaner USC-T six times for 30 seconds each interleaved with 30 seconds on ice.

4.6. Post-synaptic density purification

Hippocampal-cultured neurons were washed in cold PBS 1X (box 1), scraped and homogenized using a pestle homogenizer in 600 µl HEPES-sucrose buffer (4 dishes of 60 mm of diameter per condition; 1.5 million cells/dish). A sample was taken for the homogenate fraction.

Solutions and reagents:

HEPES-sucrose buffer (in mM): 4 HEPES pH 7.4, 320 sucrose, 1 Na_3VO_4, 1 NaF, 0,5 NaPPi, 0.001 glycerophophate supplemented with 1X protease and phosphatase inhibitors.

HEPES buffer (in mM): 4 HEPES pH 7.4, 1 NaF, 0.5 NaPPi, 0.001 glycerophophate supplemented with 1X protease and phosphatase inhibitors.

HEPES-EDTA buffer (in mM): 50 HEPES, 2 EDTA, 0.5% Triton X-100 supplemented with 1X protease and phosphatase inhibitors.

Box 7. Composition of solutions and reagents used for subcellular fractionation.

The remaining homogenate was spun for 10 minutes at 1,000 x g. Then, the supernatant was spun twice for 15 minutes at 10,000 x g. The pellet containing the synaptosomal plasma membrane (SPM) was lysed in 300 µl HEPES buffer and centrifuged for 20 minutes at 25,000 x g. Next, the pellet was resuspended in 1 ml HEPES-sucrose buffer, loaded on a freshly prepared discontinuous sucrose gradient (from bottom to top: 1.25 ml 1.2 M sucrose, 1.25 ml 1 M sucrose, 1.25 ml 0.8 M sucrose) and centrifuged for 2 hours at 150,000 x g. The SPM fraction was diluted in 2.5 volumes of HEPES buffer and centrifuged for 30 minutes at 150,000 x g. The pellet was lysed in 200 µl HEPES-EDTA buffer with continuous vortex for 15 minutes and centrifuged for 20 minutes at 32,000 x g. Finally, the pellet containing the PSD fraction was resuspended in 60 µl HEPES-EDTA solution.

4.7. Luciferase reporter assay

pGL3-Nr4a2promoter was generated as previously described (Barneda-Zahonero et al., 2012). 17-19 DIV hippocampal neurons were transfected with the luciferase reporter plasmid pRL-TK, pGL3basic (Promega) and pGL3-Nr4a2promoter using the CalPhos Mammalian Transfection kit (Clontech) following supplier's recommendations.

The plasmid pGL3-Nr4a2promoter codifies for the protein luciferin under the control of the Nr4a2 promoter. Thus, luciferase expression depends on Nr4a2 activation. pRL-TK (renilla) is used as a control of transfection. Briefly, prior transfection, half of hippocampal culture cells medium was removed and mixed with the same amount of fresh medium (conditioned medium). A mixture containing 1 µg of specific plasmid, 0.15 µg of pRL-TK and $CaCl_2$ mixed drop wise with 2X HBS was prepared (final volume of 50 ul/well of 24-well plates containing 125,000 cells/ml; we used 3 wells/condition).

After 20 minutes at room temperature to allow calcium crystal formation, the DNA mixture was added drop wise to cultured neurons and incubated for 1 hour. Afterwards, medium was removed and replaced by 10% CO_2 pre-warmed medium (acidified medium) for 5 minutes to dissolve calcium precipitates. Next, acidified medium was replaced for conditioned medium for 24 hours before lysis.

After 24 hours of transfection, cells were lysed and assayed for luciferase activity using the Dual-Luciferase Reporter Assay System (Promega) according to supplier's recommendations. Luciferase and renilla activities were measured using the Wallac 1420 Victor 3 Multilabel Counter instrument (Servei de Cultius cel·lulars, producció d'anticossos i citometria, Institut de Biotecnologia i Biomedicina, Universitat Autònoma de Barcelona). Results were expressed as the ratio between luciferase and renilla luminescence.

4.8. Luminex assay

Release of BDNF protein from hippocampal-cultured neurons was assessed using a mouse pituitary magnetic bead panel (Milliplex map kit) according to supplier's recommendations. Briefly, cell culture medium (2 wells of 12-well plates, 250,000 cells/well, 1 ml medium/well) was centrifuged at 100 x g for 5 minutes to remove debris and supernatants were evaporated in a speed-vac at 800 x g at 4ºC and homogenized in 50 µl of distilled water.

Supplied assay buffer was added to the 96-well plate assay, sealed and mixed on a plate shaker at 500 rpm for 15 minutes at room temperature. Next, assay buffer was decanted and 25 µl of supplied standards or quality controls mixed with 25 µl of matrix solution (cell media) or 25 µl of samples mixed with 25 µl of assay buffer were added to the appropriate wells. Then, 25 µl of magnetic beads were added to each well, sealed and mixed on a plate shaker at 500 rpm overnight at 4ºC. Well content was decanted and washed twice with supplied washing buffer on a plate shaker at 500 rpm for 15 minutes. 50 µl of detection antibodies were added to each well and incubated at 500 rpm for one hour at room temperature. Next, 50 µl of streptavidin-phycoerythrin were added to each well and incubated at 500 rpm for 30 minutes at room temperature. Finally, well content was decanted and washed twice as previously. 100 µl of Drive Fluid were added to each well and incubated for at least 5 minutes before detection.

BDNF levels were detected using the MAGPIX with xPONENT software (MAGPIX 5.1.0.0). Median fluorescent intensity data were analyzed using a 5-parameter logistic or spline curve-fitting method for calculating BDNF concentration in each sample.

4.9. Immunofluorescence

Hippocampal neurons plated on 24-well plates containing coverslips (Thermo Electron corporation) were washed with 500 µl PBS 1X (box 1) and fixed in 400 µl of a solution containing 4% paraformaldehyde (PFA) and 4% sucrose in PBS 1X for 15 minutes at 4ºC. To label surface GluA1, prior fixation, hippocampal neurons were first incubated with primary antibody (Rabbit polyclonal anti-GluA1 N-term, Merck Millipore PC246) **(table 11)** diluted 1/5 in 200 µl PBS 1X (box 1) supplemented with 0.5 mM $CaCl_2$, 1 mM $MgCl_2$ and 4% sucrose for 15 minutes at 37ºC. Then, they were washed in cold supplemented PBS 1X and fixed as previously indicated.

After fixation, neurons were washed with cold PBS 1X (2X, 5 minutes each), permeabilized in 500 µl 0.1% Triton X-100 in PBS 1X for 20 minutes at room temperature and blocked in 500 µl 2-10% normal goat serum (Sigma) in PBS 1X (blocking buffer) for

45 minutes at 37ºC. After blocking, fixed neurons were incubated for 1 hour at 37ºC in soft agitation with primary antibodies diluted in 150 µl blocking buffer **(Table 11).** Cells were then washed with PBS 1X (2X, 5 minutes each) and incubated with appropriate secondary antibodies (1:500 goat anti-mouse, rabbit or chicken Alexa-405, 488 or 558; Thermo Fisher Scientific) diluted in 250 µl blocking buffer for 1 hour at 37ºC in soft agitation protected from light. Next, cells were washed with PBS 1X (2X, 5 minutes each) and incubated for 5 minutes with the nuclear marker Hoechst 33258 (1:10,000; Thermo Fisher Scientific) diluted in 500 µl PBS 1X. Finally, cells were washed again with PBS 1X (2X, 5 minutes each) before mounting in Fluoromont G mounting medium (SouthernBiotech).

Table 11. List of primary antibodies used for immunofluorescence analysis.

Antibodies	Source	Identifier	Dilution
Rabbit monoclonal anti-CRTC1 (C71D11)	Cell Signaling	2587	1:300
Rabbit polyclonal anti-GFP	Abcam	ab13970	1:1000
Rabbit polyclonal anti-GluA1	Merck-Millipore	AB1504	1:500
Rabbit polyclonal anti-GluA1 (N-term)	Merck-Millipore	PC246	1:5
Mouse monoclonal anti-Nurr1 (N1404)	Abcam	ab41917	1:100
Rabbit polyclonal anti-Nurr1/Nur77	Santa Cruz biotechnology	sc-990	1:50
Rabbit polyclonal anti-Nurr1	Sigma	N4663	1:200
Rabbit polyclonal anti-Nurr1	Abgent	AP6412a	1:50
Rabbit polyclonal anti-Nurr1	Millipore	AB5778	1:200
Mouse monoclonal anti-PSD95 (6G6-1C9)	Abcam	ab2723	1:500
Rabbit polyclonal anti-V5 tag	Abcam	ab9116	1:500

List in alphabetical order. Source and final dilution used is indicated. RRID is shown in key resources table (see annex 2).

5. Histological methods

5.1. Intracardial perfusion and tissue processing

Mice from E15 to P7 were decapitated and mice older than P15 were euthanized with an intraperitoneal injection of ketamine/xylazine (150mg/kg / 25mg/kg in 0.85% NaCl) and perfused intracardially with 4% PFA (pH 7 Histology grade, Casa Álvarez) at 6 ml/min during 6 minutes approximately. Brains were dissected out and placed in 4% PFA for 24 hours at 4ºC. Then, they were washed twice in PB 1X containing (in mM) 7.67 Na_2HPO_4 and 2.66 NaH_2PO_4 for 20 minutes at 4ºC in agitation. After washings, brains were kept in 70% ethanol until inclusion.

Paraffin embedding was done at the Histology Unit of Universitat Autònoma de Barcelona. Briefly, brains were dehydrated in a graded series of ethanol followed by xylene and then embedded in paraffin using a tissue processor (Leica TP 1020). The program used was the following: 70% ethanol for 30 minutes, 80% ethanol for 20 minutes, 96% ethanol (2X,

20 minutes), 100% ethanol (2X, 30 minutes; 1X, 40 minutes), 100% ethanol plus xylene for 30 minutes, xylene (2X, 40 minutes) and paraffin (2X, 60 minutes). Paraffin blocks were performed using a paraffin embedding station (Leica EG1150H) and kept at room temperature until sectioning.

Sagital sections (5 μm) were cut using a microtome (Leica RM 2255) and mounted on superfrost plus adhesion microscope slides (Thermo Fisher Scientific).

5.2. Immunohistochemistry

Sections were warmed at 60ºC for 2 hours. After that, they were deparaffinized and rehydrated in a graded series of ethanol following the next incubations: xylene (2X, 5 minutes), 100% ethanol (2X, 3 minutes), 96% ethanol for 3 minutes, 70% ethanol for 3 minutes, 50% ethanol for 3 minutes and distilled water for 3 minutes. Then, sections were microwave heated in Tris-EDTA antigen retrieval buffer (10 mM Tris, 0.1 mM EDTA with 0.05% tween-20, pH 9) for 25 minutes and kept in this same buffer for 30-40 minutes more until reaching room temperature (23-25ºC). Sections were then rinsed in PBS 1X (box 5) (3X; 10 minutes each) and blocked in 5% normal goat serum + 0.02% Triton X-100 in PBS 1X (blocking buffer) for 30 minutes in a humidity chamber at room temperature. Then, sections were incubated with primary antibodies (rabbit anti-Nr4a2, diluted 1:50 in blocking buffer) in a humidity chamber at 4ºC overnight and 30 minutes at room temperature. Afterwards, sections were rinsed in PBS 1X (3X; 10 minutes each) and incubated with goat anti-rabbit alexa 568 secondary antibody diluted in blocking buffer (1:300) in a humidity chamber for 90 minutes at room temperature. Next, sections were rinsed in PBS 1X (3X, 10 minutes each) and incubated for 5 minutes with the nuclear marker Hoechst 33258 (1:2,500-5,000) diluted in PBS 1X. Finally sections were rinsed again with PBS 1X (3X, 10 minutes each) and mounted using Fluoromont G mounting medium.

Slices from injected animals used for electrophysiological recordings were also fixed in 4% PFA for 24 hours and washed twice and kept in PBS 1X (box 1) until immunostaining. Slices were permeabilized with three washes of 5 minutes each of 1% Triton X-100 in TBS 1X containing 50 mM Tris and 150 mM NaCl pH 7.4 and then blocked in blocking solution containing 1% Triton X-100, 10% FBS and 0.3% BSA in TBS 1X for 1 hour in soft agitation. Afterwards, slices were incubated with primary antibodies (1:100 rabbit anti-Nr4a2 and 1:200 chicken anti-GFP antibodies, diluted in 200 µl blocking buffer) in eppendorfs softly agitated overnight at 4ºC and 1 hour at room temperature. Slices were then washed with 1% Triton X-100 in TBS 1X (3X, 5 minutes each) and incubated with appropriate secondary antibodies (1:500 goat anti-rabbit Alexa-568 or anti-chicken Alexa-

488) diluted in blocking buffer for 1 hour at room temperature in soft agitation protected from light. Next, cells were washed with 1% Triton X-100 in TBS 1X (“X, 5 minutes each) and incubated for 5 minutes with the nuclear marker Hoechst 33258 (1:10,000) diluted in TBS 1X. Finally, cells were washed again with TBS 1X for 5 minutes and with TB 1X containing 50 mM Tris pH 7.4 for 5 more minutes before mounting in Fluoromont G mounting medium.

6. Confocal image acquisition and analysis

Images were acquired using a Zeiss LSM700 Laser-Scanning microscope (Carl Zeiss Microscopy, Jena, Germany). They were taken using 20X, 40X or 60X immersion oil objectives, 16 bits and a minimum of 1024 x 1024 resolution. Settings for photomultiplier voltage, gain and offset were optically adjusted to minimize saturation and were maintained across conditions to allow proper comparisons.

Sequential frame acquisition was set to acquire an average of 10-15 stacks of 0.5 µm/stack for immofluorescence and 10-15 stacks of 1 µm/stack for immunohistochemistry.

Images were analyzed using ImageJ 2.0v or Imaris 8 software. For ImageJ analysis, staining intensity was measured using the maximal projection of all Z-stacked images. Integrated density values obtained were indicated as arbitrary units (A.U.).

7. AAV production and stereotaxic surgery

Adeno-associated viral vectors (AAV) were generated by the Vector Production Unit (Centre de Biotecnologia Animal i de Teràpia Gènica – CBATEG –, Universitat Autònoma de Barcelona). AAV2/10 to overexpress or silence Nr4a2 (containing either Nr4a2.V5 or shNr4a2.V5) under the CMV or histone 1 (H1) promoter, respectively, were generated.

For stereotaxic surgery, C57BL/6J P17 or 4.5 month-old mice were first anesthetized in a chamber with 3-5% isofluorane. They were placed in a stereotaxic frame (Kopf) with the head subjected by blunt ear bars and the nose placed into a ventilator and anesthesia system using continuous isofluorane (up to 3% for induction and 0.5-1.5% for maintenance in P17 mice, up to 5% for induction and 1.5-3% for maintenance in 4.5 month-old mice). Artificial tears ointment was applied in both eyes before surgery.

For electrophysisological recordings, P17 mice were used, and either AAV2/10.H1.scramble.RSV.GFP or AAV2/10.H1.shNr4a2.RSV.GFP were injected (1 uL; $6x10^{12}$ gc/ml; 0.15 µl/min). Injections were performed bilaterally into the dorsal CA1 region

(2.18 mm posterior to bregma, 1.75 lateral to bregma, 1.6 ventral from dural surface, according to Paxinos and Franklin mouse brain atlas) using a beveled needle (Hamilton). Both male and female mice were used with similar ratio for the two types of viruses. Slices for electrophysiology were prepared from NMDG-perfused injected animals 3-4 weeks after injection.

For behavioral experiments, we used 4.5 month-old male WT and $APP_{Sw,Ind}$ mice and either AAV2/10.CMV.scramble.RSV.GFP or AAV2/10.CMV.Nr4a2-V5.RSV.GFP were injected (3 uL; $6x10^{12}$ gc/ml; 0.5 µl/min). Injections were performed bilaterally into the dorsal CA1 region (2.18 mm posterior to bregma, 1.75 lateral to bregma, 1.6 ventral from dural surface, according to Paxinos and Franklin mouse brain atlas). Behavioral studies were performed at 6 and 12 months of age.

8. Electrophysiology

All experiments, except when indicated, were performed at 26.5 ± 1 ºC in a submersion-type recording chamber perfused at approximately 2 ml/min with ACSF (box 3) in presence or absence of the appropriate drug. Output signals from field and whole-cell recordings were acquired at 5 kHz, filtered at 2.4 kHz, and analyzed using custom-made software written in Igor Pro 4.09A (Wavemetrics Inc.). All experiments were performed using a Multiclamp 700A amplifier (Axon Instruments, Union City, CA, USA).

8.1. AMPA/NMDA and mEPSC recordings

Excitatory postsynaptic currents (EPSCs) and miniature EPSCs (mEPSCs) were recorded from CA1 pyramidal neurons voltage-clamped at -60 mV using patch-type pipettes (3-4 MΩ) containing the following (in mM): 131 Cs-gluconate, 8 NaCl, 1 $CaCl_2$, 10 EGTA, 10 glucose, 10 HEPES, pH 7.3, 292 mmol/kg osmolality. AMPA/NMDA ratios were analyzed by recording evoked AMPAR-mediated EPSCs at -60 mV and NMDAR-mediated EPSCs at +40 mV in the presence of 10 µM NBQX. mEPSCs were performed at 32 ºC with ACSF supplemented with 50 µM picrotoxin (PTX) and 0.5 µM tetrodotoxin (TTX), an antagonist of $GABA_A$ receptors and a sodium channel blocker, respectively, to block the formation and propagation of action potentials. The series resistance (range 8-16 MΩ) was monitored continuously. Neurons showing more than 15% change in series resistance were excluded from analysis.

8.2. LTD recordings

Field EPSPs (fEPSPs) were recorded with a patch-type pipette filled with 1M NaCl placed in the stratum radiatum (50-100 µm from CA1 pyramidal neurons somas).

Synaptic responses were evoked by stimulating Schaffer collaterals with a monopolar electrode filled with ACSF and positioned ≈100 µm away from the recording pipette elicited at 20 seconds interval. Stimulation was adjusted to obtain comparable magnitude synaptic responses across experiments (≈ 0.7 mV).

LTD was induced after 20 minutes of stable baseline by LFS of 900 pulses at 1 Hz. The magnitude of LTD was determined by comparing baseline-averaged responses before induction with responses 40-50 minutes after induction (10 minutes averaged-responses).

8.3. Paired-pulse ratio and Input/Output function

Paired-pulse ratio (PPR) was studied by delivering two stimuli at various inter-stimulus intervals (10-500 ms) and measuring the ratio of EPSP amplitudes of the second and first fEPSP. Input/Output function was measured by changing the stimulus intensity and measuring the fEPSP amplitude based on the fiber volley amplitude, representative of the number of axons firing an action potential.

9. Behavioral experiments

9.1. Experimental design

All mice were housed under standard laboratory conditions at the animal facility of the Universitat Autònoma de Barcelona, on a 12 hours light/dark cycle, 22 ± 2ºC, relative humidity 50-60% and with food and water available *ad libitum*. Littermates were housed together (maximum 5 mice per cage) until one week before starting the behavioral battery of tests, when they were separated in individual cages to avoid fighting.

A total number of 80 WT (non-transgenic) and $APP_{Sw,Ind}$ male mice were used (40 each genotype). Viral stereotaxic hippocampal injections to overexpress Nr4a2 were performed at 4.5 month-old mice and behavior and cognition were evaluated at 6 and 12 months of age (corresponding to an early and moderate stage of the disease, respectively). Experimental design is summarized in **figure 17.**

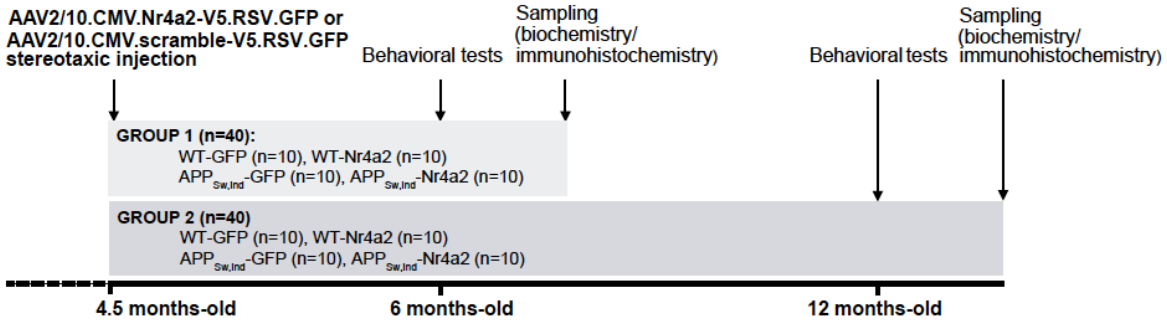

Figure 17. Experimental design for behavioral studies.

All behavioral experiments were performed during the light phase. Sensorimotor, emotional and cognitive mice status was evaluated by successive behavioral tests including: corner test (CT), open field test (OF), novel object recognition test (NOR), marble-burying test (MB), tail suspension test, Morris water maze (MWM), contextual fear conditioning (CFC) and nesting.

After completion of all behavioral tests, three animals per subgroup were processed for brain histologic analysis (see section 5.1 materials and methods). Remaining animals (5-7 mice per subgroup) were sacrificed and hippocampus, cortex, prefrontal cortex and cerebellum were dissected out and immediately stored at -80ºC for further analysis.

9.2. Corner test

Mice were placed individually in the center of a clean standard home-cage, filled with wood bedding, and the number of visited corners and rearings were counted during 30 seconds. Latency of the first rearing was also measured.

9.3. Open field test

Immediately after CT, mice were placed individually in the center of an open field (woodwork, white box, 50 x 50 x 20 cm height) and observed for 5 minutes. The following behavioral events were measured: latency to initiate movement, latency to leave the center of the field and that of entering the periphery, total time spend in the center and periphery, horizontal (total distance travelled and speed) and vertical (rearings) locomotor activities and latency, number and total duration of self-grooming behavior. Defecation boli and urination were also recorded (see **annex 3**).

9.4. Novel object recognition test

Twenty-four hours after the OF test, mice were placed individually in the center of the same OF for 1 minute (habituation to context). Afterwards, mice were exposed to two identical objects (sample) and allowed to explore them (defined as nose facing the oat 2 cm, sniffing or biting the objects) until reaching criteria (a total accumulated time of 20 seconds) during a period of a maximum of 10 minutes (training). After 4 hours, mice were subjected to a retention test in a 5 minutes session with two objects: one identical to those previously explored (familiar) and a new one (novel). The time that the mice spent exploring each of the objects was measured and preference for the novel object was expressed as a discrimination index (DI): DI = (time novel – time familiar) / (time novel + time familiar) x 100%. Mice that explored both objects for less than three seconds during training or two seconds during testing were not considered for the analysis.

9.5. Marble-burying test

One day after the NOR test, mice were placed individually in a standard home-cage facing the wall. In the cage there were nine marbles (1 x 1 x 1 cm) evenly spaced (three rows of three marbles) across the bedding surface in the opposite part of the cage from where the mouse was placed. Mice were left in the cage with marbles for a 30 minutes period. Time that mice took to turn and to initially touch marbles was measured. The number of marbles left “intact”, “changed of position or partially buried” and “buried”, were counted every 5 minutes.

9.6. Morris water maze

Mice were trained, four trials per day, spaced 30 minutes apart, to locate a hidden platform (11 cm diameter, 1 cm below the water surface) in a circular pool for mice (PanLab; 120 cm diameter, 84 cm height, 23ºC opaque water) located in an almost completely black room.

Mice were gently released facing the wall of the pool from one randomly selected point (one different in each of the four trials per day) and allowed to swim during 1 minute to find the platform. The first day (cue learning task), the platform was located in the middle of the N-E quadrant. It was visible 1 cm above the water surface and cued with a visible flag **(figure 18).** In the next five consecutive days (place learning task acquisition phase), the platform was hidden and located in a reversed position (in the middle of the S-W quadrant). We placed four geometric figures on each wall of the room that were used as external visual clues. The three next days, we added four internal visual clues located in

the wall of the pool, inaccessible for the mice. In all trials, mice reaching the platform were left there for 10 seconds, and mice failing to find the platform were placed on it for the same time. On the last day (probe), 2 hours after the last trial, mice were placed in the pool without platform and were allowed to swim for 1 minute.

For all learning days, variables regarding the time (escape latency), distance and speed were recorded by a computerized tracking system (ANY-maze). For the probe, the numbers of crossings over the removed platform position (annulus crossings), the time and distance travelled in each quadrant and the swimming speed, were also analyzed.

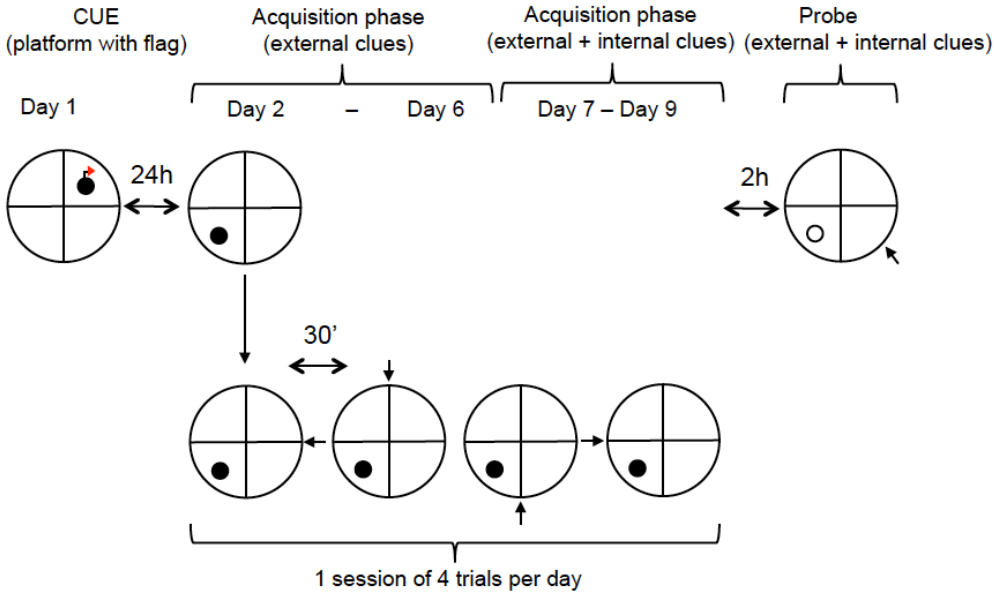

Figure 18. Schematic diagram of the Morris water maze (MWM) protocol used. Red triangle indicates the visible flag. Arrows indicate the entry position of the mice in the different sessions. Black circles indicate the hidden platform. Open circle indicates the location of the platform removed for the probe test.

9.7. Contextual fear conditioning

Mice were placed in a novel training chamber (15.9 cm x 14 cm x 12.7 cm) equipped with a bright light (1850 Lux) (Med Associates, St. Albans, Vermont). Spontaneous freezing response, which was defined as a complete cessation of all movement except for respiration, was measured during 3 minutes. Afterwards, mice received an electric foot shock (0.8 mA, 1sec) and freezing response was measured immediately after the shock for 2 minutes and 2 and 24 hours after the shock for 4 minutes. Freezing was analyzed automatically with a Video Freeze Software (Med Associates).

9.8. Nesting

Nesting behavior was evaluated by introducing a piece of paper tissue inside the mice home cage. The presence and quality of the nest were assessed 24, 48 and 72 hours later according to Torres-Lista & Giménez-Llort, 2013. Deacon score criteria (R. M. Deacon, 2006) 5-point scale from 1 to 5 being 1 when tissue was not noticeably touched, 2 partially torn up, 3 mostly shredded but with often no identifiable nest site, 4 with an identifiable but flat nest and 5 with a near perfect nest was used.

Bites in the paper were also evaluated following biting scale from 1 to 5, being 1 when there were no holes in the tissue, 2 a few bites, 3 many bites, 4 when the tissue was curly, but not completely and 5 completely curly.

Beddings were not changed during all the experiment to avoid manipulation of animals and/or introduction of other environmental context besides the nest material.

9.9. Tail suspension test

Mice were suspended by the base of the tail and recorded for 15 seconds as previously described (Lieu et al., 2013). Three separated trials spaced 30 minutes were performed. Hindlimb clasping was rated from 0 to 3 based on severity: 0 when hindlimbs spayed outwards and away from the abdomen, 1 when one hindlimb retracted inwards towards the abdomen for at least half of the observation period, 2 when both hindlimbs partially retracted inwards towards the abdomen for at least half of the observation period and 3 when both hindlimbs completely retracted inwards towards the abdomen for at least half of the observation period. Scores of 0.5 were used when appropriate. Hindlimb clasping severity scores were calculated by averaging the three separate trials.

10. Data and statistical analysis

Statistical analysis was performed using GraphPad Prism software v6.01 (GraphPad Software Inc., California, USA) and SPSS 17.0 software for behavioral studies.

We performed either unpaired Student's *t*-tests or analyses of variance (ANOVAs; one-, two- or three-way) followed by appropriate between-group comparisons according to each analysis requirements, Bonferroni or Tukey *post hoc* test for parametric samples or two-sided nonparametric Mann-Whitney test for nonparametric samples.

For behavioral analysis, differences between genotype, treatment and time interactions were analyzed by repeated-measures ANOVA, and correlation analysis was performed between different variables using nonparametric Spearman correlation coefficient.

Data is shown as the mean ± standard error of the mean (SEM) or standard deviation (SD). Statistically significant difference was set at *p*-value < 0.05, and is indicated as follows: *p < 0.05, **p < 0.01, ***p < 0.001, ****p < 0.0001.

VII. Results

CHAPTER I.

“Role of Nr4a2 in hippocampal synaptic plasticity”

CHAPTER I.

Role of Nr4a2 in hippocampal synaptic plasticity

1.1. Developmental profile of hippocampal Nr4a2 expression

A large body of evidence has suggested the role of the Nr4a family of transcription factors in a variety of physiological functions related to synaptic plasticity and cognition (Bridi & Abel, 2013; Hawk & Abel, 2011). However, no studies have addressed the expression of these factors during brain development. To specifically study the role of Nr4a2 in hippocampal synaptic plasticity and the molecular mechanisms involved, we first analyzed the expression pattern of this transcription factor in the hippocampus during its development.

Using hippocampal tissue of mice at different ages, ranging from E15 to P30, we observed that hippocampal Nr4a2 mRNA levels peaked between E18 and P3 stages **(figure 19A)**, whereas Nr4a2 protein levels reached its maximum during the first postnatal week and decreased afterwards to its lowest levels from P30 **(figure 19B)**. In order to characterize differential Nr4a2 expression through the hippocampus, we also analyzed Nr4a2 levels at distinct hippocampal regions by immunohistochemistry. Histological analysis showed a similar pattern in Nr4a2 immunoreactivity in CA1 compared to the whole hippocampal lysate analysis, dropping after P15 **(figure 19C)**. By contrast, Nr4a2 levels were fairly constant during development in CA3 and DG **(figure 20)**, observing only a significant reduction in Nr4a2 levels at P30 in CA3 when compared to P3 **(figure 20A)**. In the DG, it seems that Nr4a2 was preferentially expressed in the outer granule cell layer, and was more concentrated in the suprapyramidal blade, in line with previous results (Imura et al., 2019). Remarkably, we also found that Nr4a2 was highly expressed by hilar neurons in the polymorphic layer, mainly at P7-P15 stages, decreasing at P30.

We also checked Nr4a2 levels in primary cultures of hippocampal neurons at different DIV, observing that Nr4a2 levels significantly decreased through maturation. The highest Nr4a2 levels, both mRNA and protein, were observed at 3 DIV, whereas the lowest levels were found after more than two weeks in culture **(figure 19D,E)**, when hippocampal cultured-neurons reached their maturation. Thus, it seems that we can recapitulate the expression profile of Nr4a2 during hippocampal development, mainly in CA1, in hippocampal cultured-neurons. Altogether, these results show that Nr4a2 expression is higher in the immature hippocampus both *in vivo* and *in vitro.*

..

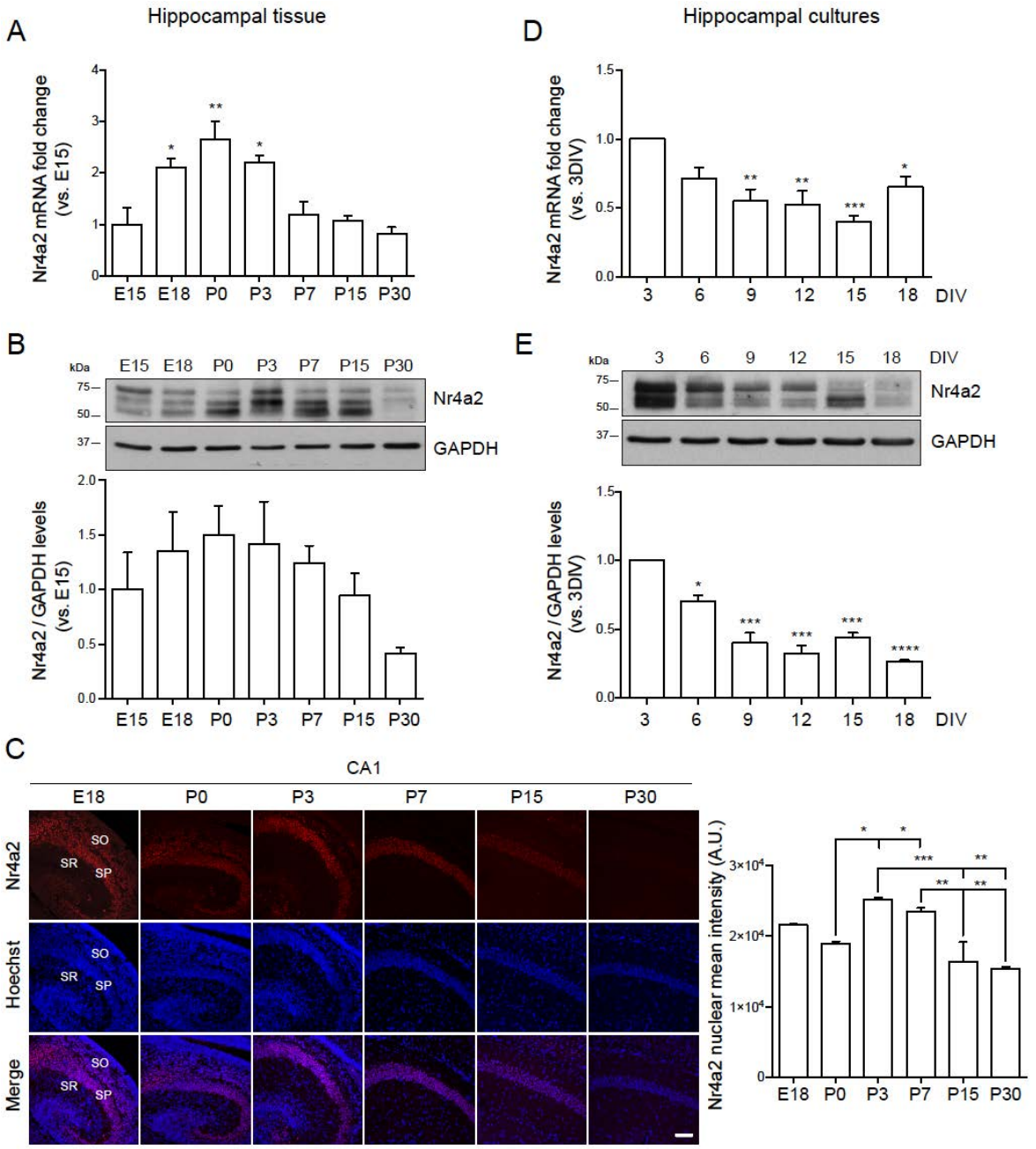

Figure 19. Nr4a2 mRNA and protein levels in hippocampal neurons.
(A) Nr4a2 mRNA and **(B)** protein levels at different developmental stages of mouse hippocampus. **(C)** Nr4a2 protein levels of hippocampal CA1 pyramidal neurons at different developmental stages of mouse hippocampus measured by immunohistochemistry. Magnification, 20x; scale bar, 100 µm. (**D)** Nr4a2 mRNA and **(E)** protein levels at different days *in vitro* (DIV) of mouse hippocampal-cultured neurons. n = 3 mice/stage (A, B); n= 3 mice/stage, 6 sections/mice (C) or n = 3 independent cultures (D,E). Data represent mean ± S.E.M. Statistical analysis was determined by one-way ANOVA followed by Bonferroni *post hoc* test. *p<0.05, **p<0.01, ***p<0.001, ****p<0.001. A.U., arbitrary units; SO, stratum oriens; SP, stratum pyramidale; SR, stratum radiatum.

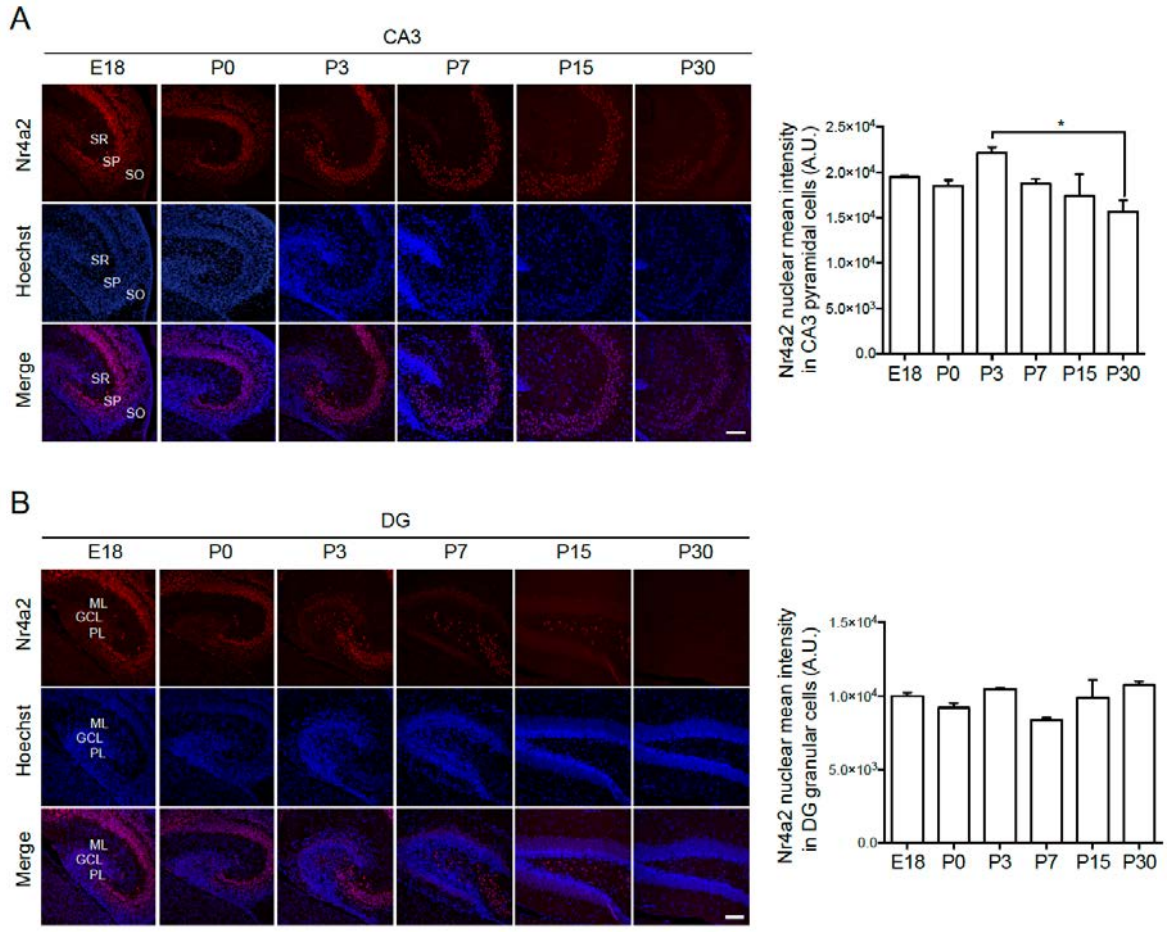

Figure 20. Nr4a2 protein levels in CA3 and DG of mouse hippocampus.
(A) Nr4a2 protein levels at CA3 and **(B)** DG at different developmental stages of mouse hippocampus assessed by immunohistochemistry. Magnification, 20x; scale bar, 100 µm. n = 3 mice/stage; 6 sections/mice. Data represent mean ± S.E.M. Statistical analysis was determined by one-way ANOVA followed by Bonferroni *post hoc* test. *p<0.05. A.U., arbitrary units; SO, stratum oriens; SP, stratum pyramidale; SR, stratum radiatum; ML, molecular layer; GCL, granule cell layer; PL, polymorphic layer.

Likewise, a significant decrease in Nr4a2 mRNA and protein levels was observed in cortical-cultured neurons through maturation **(figure 21)**, showing a similar pattern than hippocampal-cultured neurons **(figure 19D,E)**.

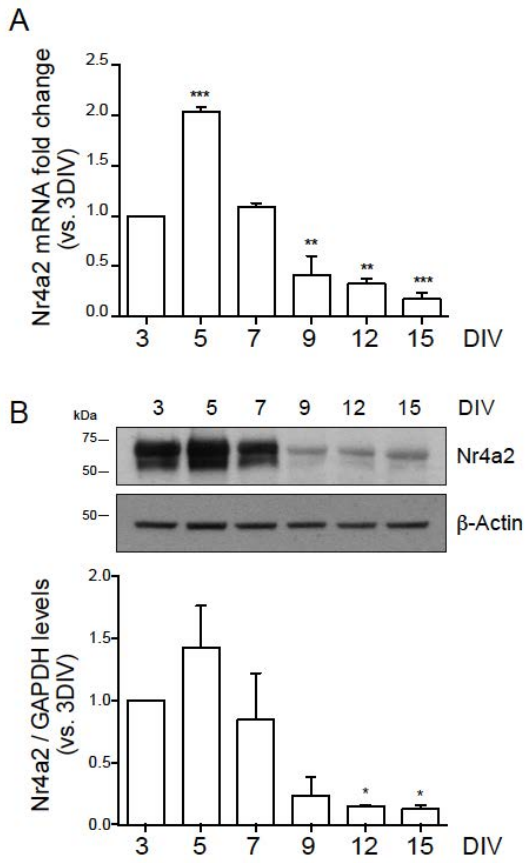

Figure 21. Nr4a2 mRNA and protein levels in cortical neurons.
(A) Nr4a2 mRNA and **(B)** protein levels at different days *in vitro* (DIV) of mouse cortical-cultured neurons. n = 2 independent cultures**.** Data represent mean ± S.D. Statistical analysis was determined by one-way ANOVA followed by Bonferroni *post hoc* test *p<0.05.

1.2 iGluR-Ca^{2+}/CREB/CRTC1 pathway mediates activity-dependent regulation of Nr4a2 in mature hippocampal neurons

Nr4a2, as the other members of the Nr4a family of orphan nuclear receptors, is activated in a ligand-independent manner (Maxwell & Muscat, 2006) and thus, Nr4a2 regulation is mainly dependent on its cellular levels. To address whether Nr4a2 protein levels in mature hippocampal and cortical-cultured neurons were modulated by neuronal activity, we used 4-aminopyridine (4-AP) or bicuculline as stimulus.

$GABA_A$ receptor antagonists have been widely used to increase neuronal activity in several *in vitro* hippocampal preparations (Arnold et al., 2005; Zhang et al., 2007). When the neuronal network activity of hippocampal-cultured neurons was disinhibited by bicuculline (bic; 50 µM) application, a $GABA_A$ receptor antagonist, there was a significant increase in Nr4a2 promoter activity within 15 minutes to 1 hour after treatment (15 minutes after bic treatment: 2.24 ± 0.48; 30 minutes: 1.99 ± 0.24; 1 hour: 1.96 ± 0.19 fold increase vs. basal) as determined by a luciferase assay **(figure 22A)**. The increase in Nr4a2 promoter activity resulted in a significant increase in Nr4a2 mRNA **(Figure 22B)** and protein levels **(figure 22C)**, reaching the highest expression after 2-4 hours of treatment (mRNA levels after 4 hours of bic treatment: 17.97 ± 1.4 fold increase vs.

basal; protein levels after 4 hours of bic treatment: 37.2 ± 1.2 fold increase vs. basal) and decreasing afterwards. The decrease in Nr4a2 protein levels observed after 24 hours of bicuculline treatment was completely reverted by the inhibition of the proteasome activity using MG-132 (10 μM). Proteasomal inhibition significantly increased Nr4a2 protein levels not only after long application of bicuculline but also in basal conditions (Nr4a2 protein levels after 24 hours of bic treatment: 7.65 ± 0.46, MG-132 + bic: 58 ± 9.42, MG-132: 41.7 ± 4.85 fold increase vs. basal) unraveling a highly specific regulation of Nr4a2 protein levels by the proteasome pathway in mature hippocampal-cultured neurons **(figure 22D)**.

Next, we explored the role of calcium on the activity-dependent increase in Nr4a2 levels by incubating hippocampal-cultured neurons with BAPTA-AM (20 μM) for 30 minutes before bicuculline treatment for 4 hours, time when the induction of Nr4a2 was maximal. BAPTA-AM is a calcium chelator that penetrates the plasma membrane and neutralizes the action of calcium released from intracellular stores. We found that activity-dependent increase of Nr4a2 was significantly reduced (around 60% vs. bic treatment) with the application of BAPTA-AM **(figure 22E)**, suggesting the requirement of calcium to trigger Nr4a2 induction. To decipher the source of calcium downstream of bicuculline application, we decided to block ionotropic glutamate receptors (iGluRs) and L-type VDCC as major routes for postsynaptic calcium influx. Blockade of L-type VDCC with nifedipine (10 μM) had no effect on bicuculline-mediated increase in Nr4a2 protein levels. By contrast, the antagonists of AMPAR and NMDAR-iGluRs, NBQX (10 μM) and MK-801 (10 μM), respectively, produced a significant decrease (around 60% and 45% vs. bic treatment, respectively) in Nr4a2 protein levels **(figure 22F)**, indicating that calcium influx through iGluRs contributes to activity-dependent Nr4a2 induction in mature hippocampal-cultured neurons.

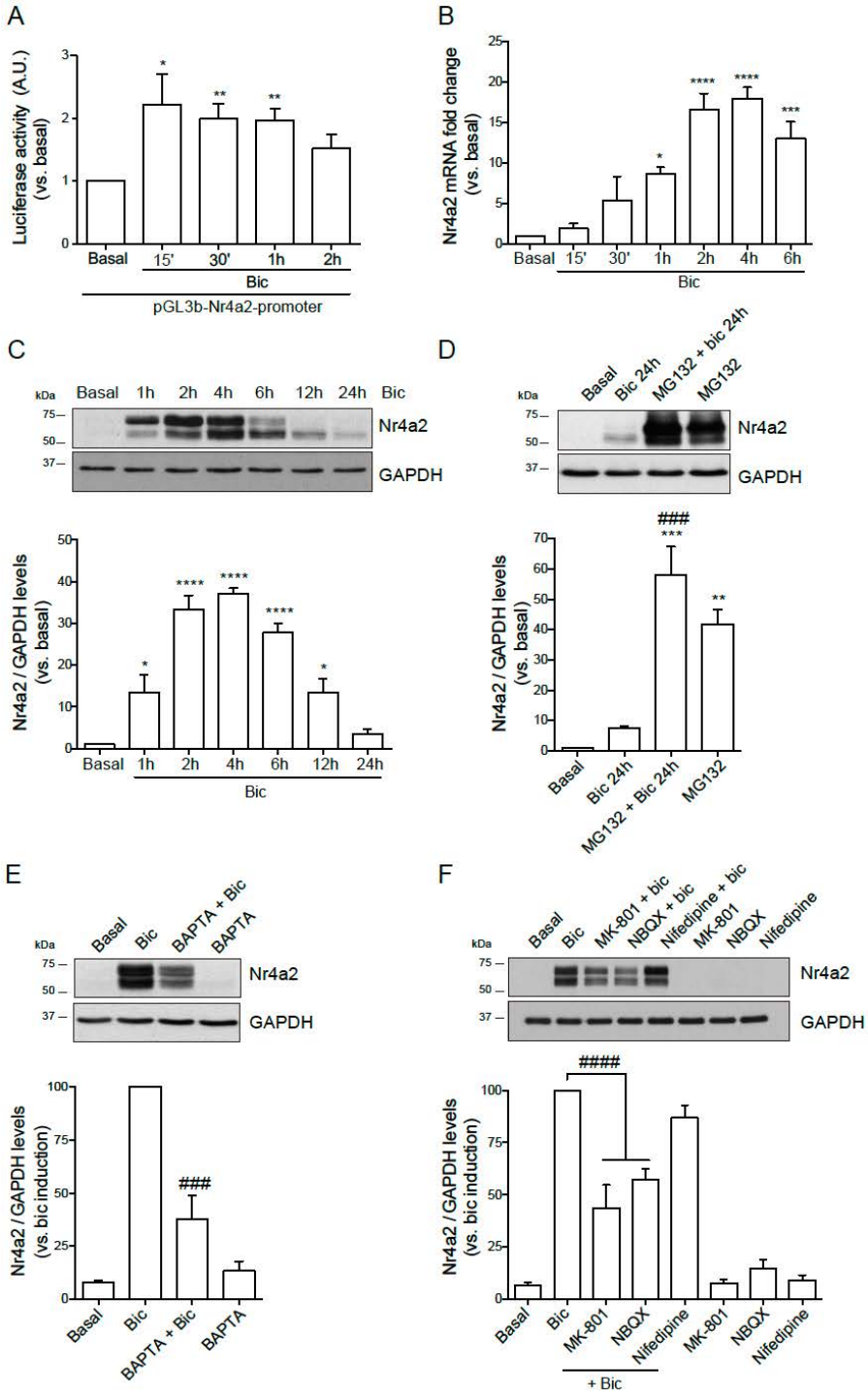

Figure 22. Activity-dependent transcriptional activation of Nr4a2 in mature hippocampal neurons is dependent on Ca^{2+} influx through iGluRs.

(A) Nr4a2 promoter activity measured by a luciferase assay after bicuculline (bic; 50 µM) treatment. **(B)** Time-course of Nr4a2 mRNA and **(C)** protein levels after bic treatment. **(D)** Nr4a2 protein levels after 24 hours stimulation with bic in presence of the proteosomal inhibitor MG-132 (10 µM). **(E)** Nr4a2 protein levels after bic treatment in presence of BAPTA-AM (20 µM), a cell-permeable calcium chelator. **(F)** Nr4a2 protein levels after bic treatment in presence of MK-801 (10 µM), a NMDAR antagonist, NBQX (10 µM), an AMPAR antagonist and nifedipine (10 µM), a L-type calcium channel blocker. n ≥ 3 independent hippocampal cultures. Data represent mean ± S.E.M. Statistical analysis was determined by one-way ANOVA followed by Bonferroni *post hoc* test. *p<0.05, **p<0.01, ***p<0.001, ****p<0.001 (*vs. basal, #vs. bic). A.U., arbitrary units.

The activity-dependent increase in Nr4a2 protein levels was not specific to bicuculline-mediated neuronal activity, as it also occurred following 4-AP treatment. 4-AP is a voltage-dependent K^+ channel blocker that increases neuronal activity by prolonging action potentials. We found that 4-AP (50 µM) treatment significantly increased Nr4a2 protein levels in both mature hippocampal and cortical-cultured neurons, reaching a pick of expression after 2-6 hours of treatment (6-fold increase after 4 hours of bic treatment in hippocampal neurons and almost 2-fold increase after 2 hours of bic treatment in cortical neurons) **(figure 23)**.

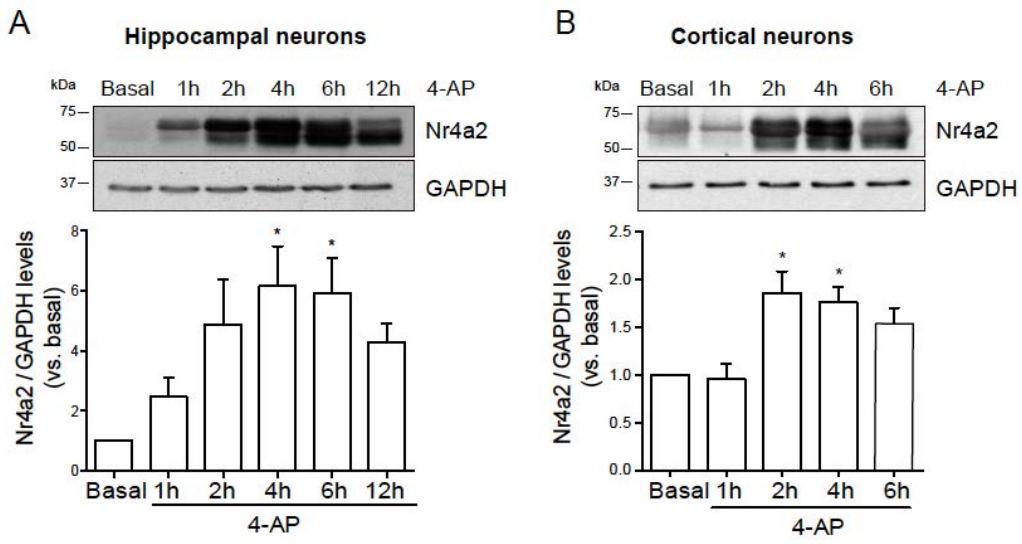

Figure 23. Activity-dependent induction of Nr4a2 by 4-aminopyridine.
(A) Time-course of Nr4a2 protein levels after 4-aminopyridine (4-AP; 50 µM) treatment in mature hippocampal and **(B)** cortical neurons. n = 3 independent cultures**.** Data represent mean ± S.E.M. Statistical analysis was determined by one-way ANOVA followed by Bonferroni *post hoc* test. *p<0.05.

We also observed that, in response to neuronal activity, Nr4a2 protein levels increased both in the cytosolic and nuclear fractions of hippocampal-cultured neurons **(figure 24A)**. Surprisingly, Nr4a2 transcription factor was also found in the PSD of both cultured-hippocampal neurons in response to neuronal activity induced by 4-AP and bicuculline treatment **(figure 24B,C)**, and also in adult hippocampal tissue **(figure 24D)**, opening the possibility to emerge as a synaptonuclear protein messenger.

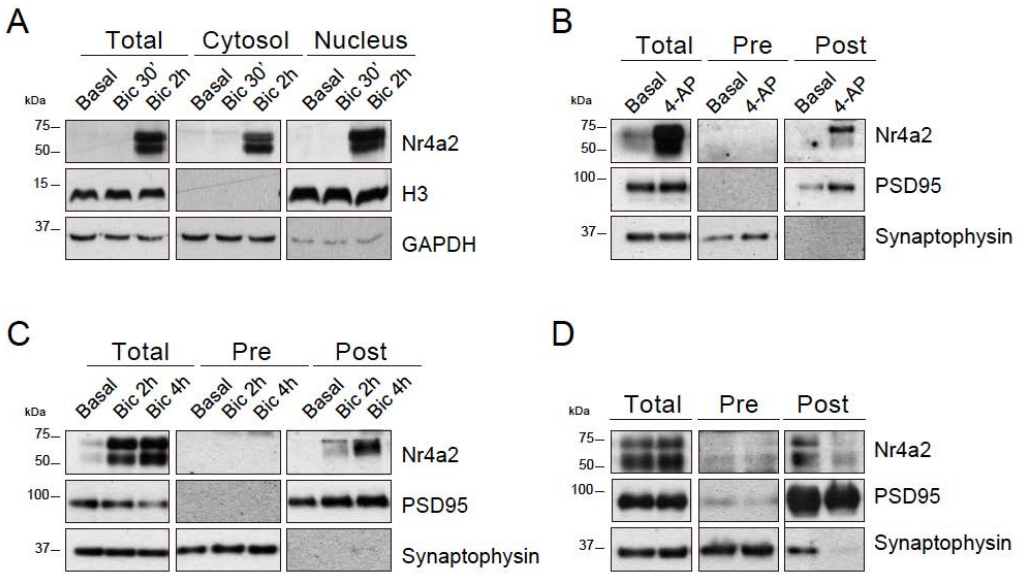

Figure 24. Nr4a2 transcription factor is present at the post-synaptic density both in mature hippocampal-cultured neurons and the adult mouse hippocampus.
(A) Cellular fractionation of mature hippocampal-cultured neurons after bicuculline (bic; 50 μM) treatment. **(B,C)** Synaptoneurosomes from mature hippocampal-cultured neurons after 4-aminopyridine (4-AP; 50 μM) or bic treatment, respectively. **(D)** Synaptoneurosomes of adult mouse hippocampus. All figures correspond to representative images from Western blotting analysis. n ≥ 3.

We further explored the molecular mechanisms involved in the activity-dependent Nr4a2 activation in hippocampal neurons downstream of calcium influx through iGluRs. We built-up our experiments based on previous studies reporting a NMDAR and CREB-dependent induction of Nr4a2 in cerebellar granule cells (Barneda-Zahonero et al., 2012) and the requirement of CRTC1 for an efficient CREB-mediated induction of Nr4a2 in cortical neurons (Parra-Damas et al., 2014). The presence of CRE sequences in Nr4a2 promoter region confers transcriptional responsiveness to both calcium and cAMP signals, which are mediated by CREB. However, CREB transcriptional activation depends not only on calcium- and cAMP-dependent phosphorylation at Ser133 (Mayr & Montminy, 2001), but also on the recruitment of specific coactivators like CRTC1. In response to neuronal activity, CRTC1 translocates from cytosol to nucleus to increase CREB binding to specific gene promoters (Ch'Ng et al., 2012; España et al., 2010b). Therefore, we firstly confirmed that neuronal activity induced by bicuculline treatment significantly increased CREB phosphorylation at Ser133 (almost 2-fold increase after 15 minutes of bic treatment) **(Figure 25A)** and promoted CRTC1 translocation from cytosol to nucleus **(Figure 25B)**, consistent with previous studies performed using other neuronal activity stimulus (Kovács et al., 2007; Parra-Damas et al., 2017b).

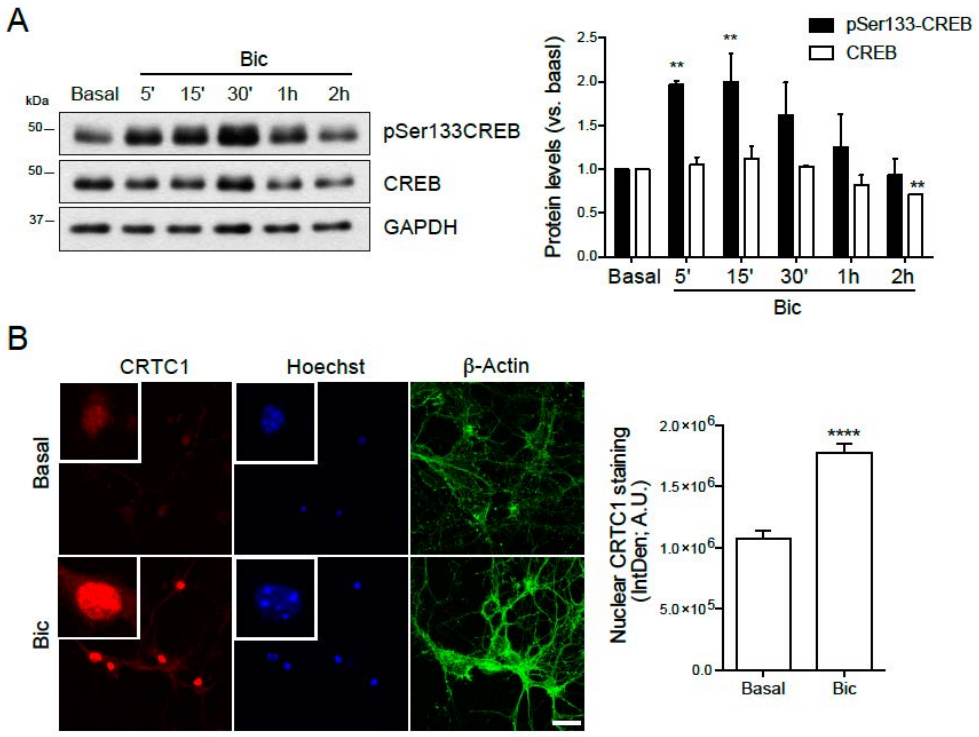

Figure 25. Bicuculline activates the CRTC1-CREB signaling pathway in mature hippocampal neurons.
(A) Time-course of total and Ser133-phosphorylated CREB levels in hippocampal-cultured neurons after bicuculline (bic; 50 μM) treatment. **(B)** CRTC1 nuclear staining after bic treatment. Magnification, 40x; scale bar, 25 μm. n = 3 independent cultures (A,B), n ≥ 25 neurons/culture (n ≥ 100 neurons/condition) (B). Data represent mean ± S.E.M. Statistical analysis was determined by one-way ANOVA followed by Bonferroni *post hoc* test (A) or Student's unpaired two-tailed t-test (B). **p<0.01, ****p<0.001. A.U., arbitrary units; IntDen, integrated density.

Previous work reported a constitutive binding of CREB to target gene promoters in the absence of neuronal activity, whereas recruitment of CRTC1 to proximal CRE/TATA promoters depended on neuronal activity (Parra-Damas et al., 2017b). Consistently, ChIP analysis confirmed the binding of CREB to Nr4a2 promoter under basal conditions and the recruitment of CRTC1 upon bicuculline treatment (more than two-fold increase vs. vehicle) **(Figure 26A)**. Furthermore, to confirm the involvement of CREB/CRTC1 signaling pathway in Nr4a2 regulation, we transduced hippocampal-cultured neurons with lentiviral vectors containing a shRNA against CREB and CRTC1, and we observed that both did significantly reduce the bicuculline-mediated increase in Nr4a2 mRNA and protein levels (75% and 60% vs. bic, respectively) **(Figure 26B,C)**.

CRTC1 activation involves its dephosphorylation at Ser151 by the calcium-dependent phosphatase PP2B/calcineurin and cAMP-mediated inhibition of salt-inducibles kinases 1/2 (SIK-1/2) (Li et al., 2009b). Accordingly, pharmacological inhibition of calcineurin with FK-506 (10 μM) significantly reduced the bicuculline-mediated increase of Nr4a2 protein

levels (around 70% decrease vs. bic treatment) **(Figure 26D)**. Surprisingly, Nr4a2 induction was even more strongly inhibited with the inhibition of calcineurin in neurons transduced with a shRNA against CRTC1, demonstrating that calcineurin is a primary mediator of Nr4a2 regulation a part from its role on CRTC1 dephosphorylation and consequent activation.

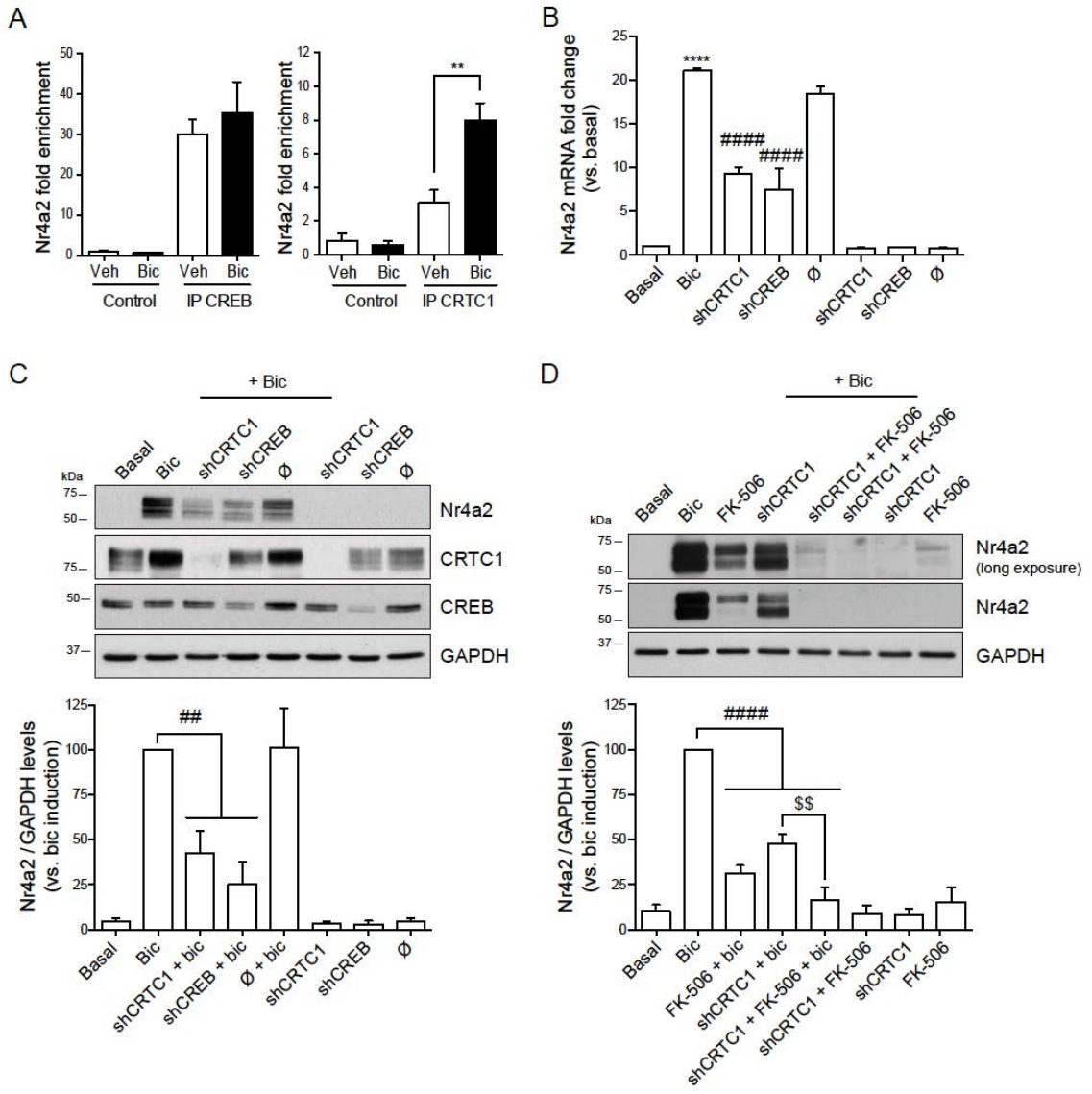

Figure 26. Activity-dependent increase of Nr4a2 mRNA and protein levels in mature hippocampal neurons requires CRTC1 and CREB.
(A) Nr4a2 promoter occupancy with CREB and CRTC1 proteins determined by ChIP analysis after bicuculline (bic; 50 µM) treatment. **(B)** Nr4a2 mRNA and **(C)** protein levels in Nr4a2, CREB and CRTC1 shRNA-transduced neurons. **(D)** Nr4a2 protein levels in CRTC1 shRNA-transduced neurons and/or calcineurin inhibition with FK-506 (10 µM). n = 4 independent cortical cultures (A) and n ≥ 3 independent hippocampal cultures (B-D). Data represent mean ± S.E.M. Statistical analysis was determined by one-way ANOVA followed by Bonferroni (or Tukey in D) *post hoc* test. *p<0.05, **p<0.01, ***p<0.001, ****p<0.0001 (vs. basal), (# vs. bic).

1.3. Nr4a2 mediates basal and activity-dependent BDNF production in mature hippocampal neurons

Nr4a2 transcriptional activity regulates BDNF levels in different systems. Volpicelli and colleagues have shown that Nr4a2 regulates *Bdnf* gene expression in rat midbrain neurons (Volpicelli et al., 2007) or Chen and colleagues have reported increased BDNF levels in activated rat microglia overexpressed with Nr4a2 (Chen et al., 2018). Moreover, BDNF was very early on implicated in modulating neuronal activity, and its own production and release have been shown to be activity-dependent (Kovács et al., 2007; Parra-Damas et al., 2014). However, relatively little is known about the mechanisms underlying the activity-dependent regulation of BDNF expression.

We firstly observed that neuronal activity induced by bicuculline treatment significantly increased BDNF mRNA and protein levels in mature hippocampal-cultured neurons **(Figure 27A,B)**. Interestingly, the time-course study revealed that BDNF levels peaked after Nr4a2 did. Moreover, neuronal activity not only raised BDNF levels but also elicited an increase of BDNF secretion to the culture medium of mature hippocampal-cultured neurons detected by a luminex assay (more than three-fold increase after 8 hours of bic treatment) **(Figure 27C)**. BDNF mRNA levels were decreased in Nr4a2 shRNA-transduced mature hippocampal neurons (around 50% vs. basal) **(figure 27D)**. In addition, basal and bicuculline-mediated raise in BDNF protein levels were also both significantly reduced in Nr4a2 shRNA-transduced neurons (BDNF protein levels after bic treatment: 1.56 ± 0.26, shNr4a2 + bic: 0.88 ± 0.28, shNr4a2: 0.52 ± 0.09 fold change vs. basal) **(Figure 27E-F)**. Moreover, Nr4a2 shRNA-transduction also significantly blocked BDNF secretion after neuronal activity in mature hippocampal neurons (BDNF secretion after bic treatment: 2.09 ± 0.34, shNr4a2 + bic: 1.09 ± 0.18 fold change vs. basal).

Further support for a role of Nr4a2 in the modulation of BDNF levels in hippocampal neurons was obtained with pharmacological activation of Nr4a2 using agonists previously described to physically interact with Nr4a2 and activate its transcriptional function (Nguyen et al., 2015) (see **table 4**). Nr4a2 activation by 8 hours of CQ treatment was able to significantly increase BDNF protein levels and secretion in a Nr4a2-dependent manner (BDNF protein levels after CQ treatment = 1.72 ± 0.08, shNr4a2 + CQ = 0.81 ± 0.21 fold change vs. basal; BDNF secretion after CQ treatment: 2.06 ± 0.56, shNr4a2 + CQ: 0.84 ± 0.24 fold change vs. basal) **(Figure 27G,H)**, opening the possibility to use Nr4a2 agonists to modulate BDNF, a crucial regulator of activity-dependent hippocampal synaptic plasticity and cognitive functions (Bekinschtein, Cammarota & Medina, 2014; Zagrebelsky & Korte, 2014).

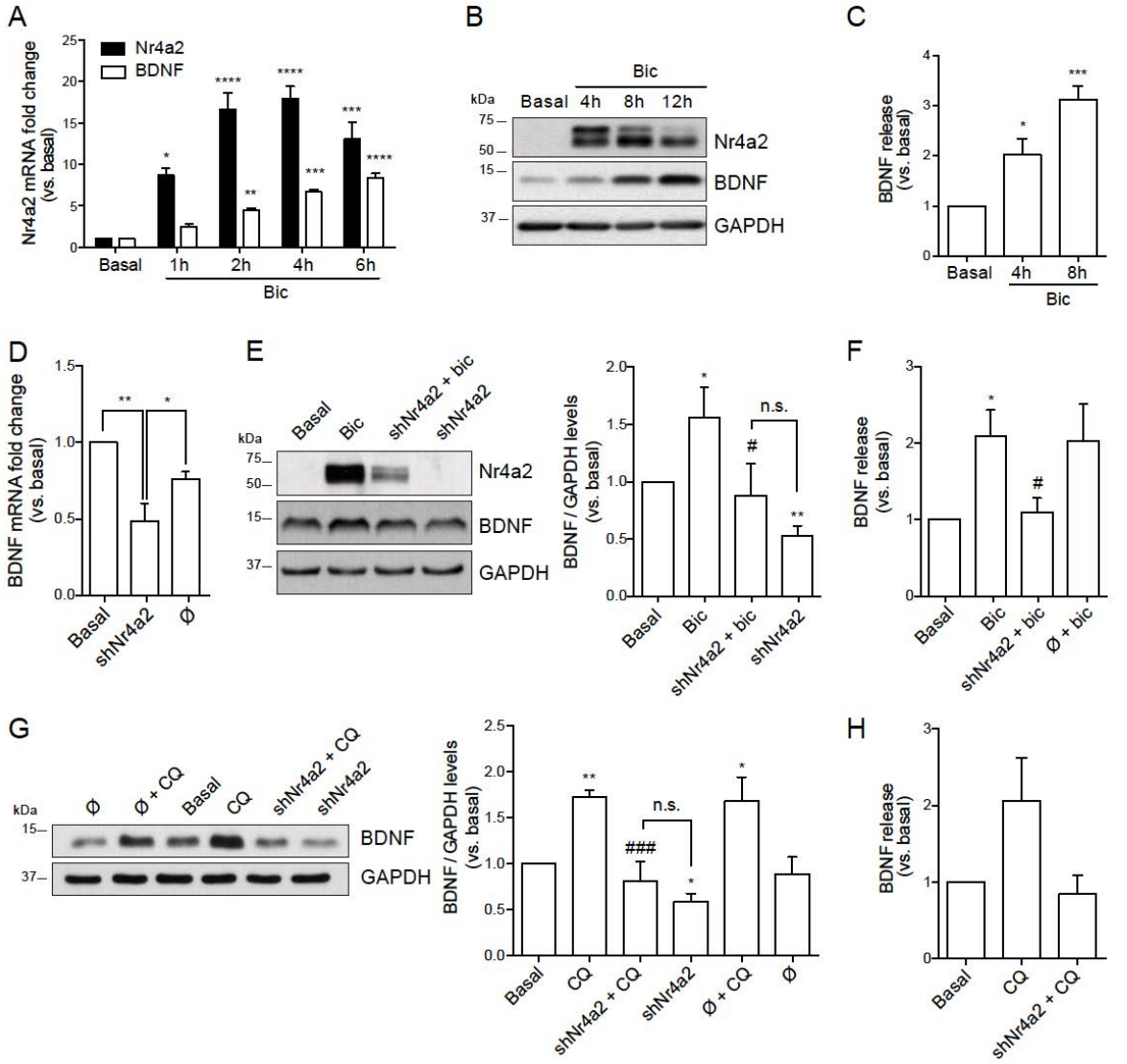

Figure 27. Nr4a2 is necessary for basal and activity-mediated BDNF production in mature hippocampal neurons.
(A) Time-course of Nr4a2 and BDNF mRNA and **(B)** protein levels after bicuculline (bic; 50 µM) treatment. **(C)** Extracellular BDNF secretion determined by Luminex bead assay after bic treatment. **(D)** BDNF mRNA levels in Nr4a2 shRNA-transduced neurons. **(E)** BDNF protein levels in Nr4a2 shRNA-transduced neurons in presence or absence of bic. **(F)** Extracellular BDNF secreted in Nr4a2 shRNA-transduced neurons in presence or absence of bic. **(G)** BDNF protein levels in the presence of the Nr4a2 agonist chloroquine (CQ; 10 µM) in Nr4a2 shRNA-transduced neurons. **(H)** Extracellular BDNF secreted after CQ treatment. n ≥ 3 independent hippocampal cultures. Data represent mean ± S.E.M. Statistical analysis was determined by one-way ANOVA followed by Bonferroni (or Tukey in D,F) *post hoc* test. *p<0.05, **p<0.01, ***p<0.001, ****p<0.0001 (*vs. basal, #vs. bic).

Since our results showed that Nr4a2 was regulated by the CREB/CRTC1 signaling pathway **(figure 26)**, we hypothesized that upstream of Nr4a2, the transcription factor CRTC1 would also modulate BDNF levels. In line with previous studies using cortical neurons (España et al., 2010b; Esvald et al., 2020; Fukuchi et al., 2014), we found that CRTC1 also modulated BDNF mRNA and protein levels in mature hippocampal-cultured

neurons. We observed that both CREB and CRTC1-shRNA transduced hippocampal neurons expressed less BDNF mRNA levels (around 70% of decrease vs. basal) **(figure 28A).** Accordingly, we observed that basal and bicuculline-mediated increase in BDNF protein levels were significantly reduced not only in Nr4a2-shRNA transduced hippocampal neurons, as it is shown in **figure 27D**, but also in CRTC1-shRNA transduced hippocampal neurons (BDNF protein levels after bic treatment: 1.56 ± 0.26, shCRTC1 + bic: 0.41 ± 0.05; shCRTC1: 0.3 ± 0.06 fold change vs. basal) **(figure 28B)**.

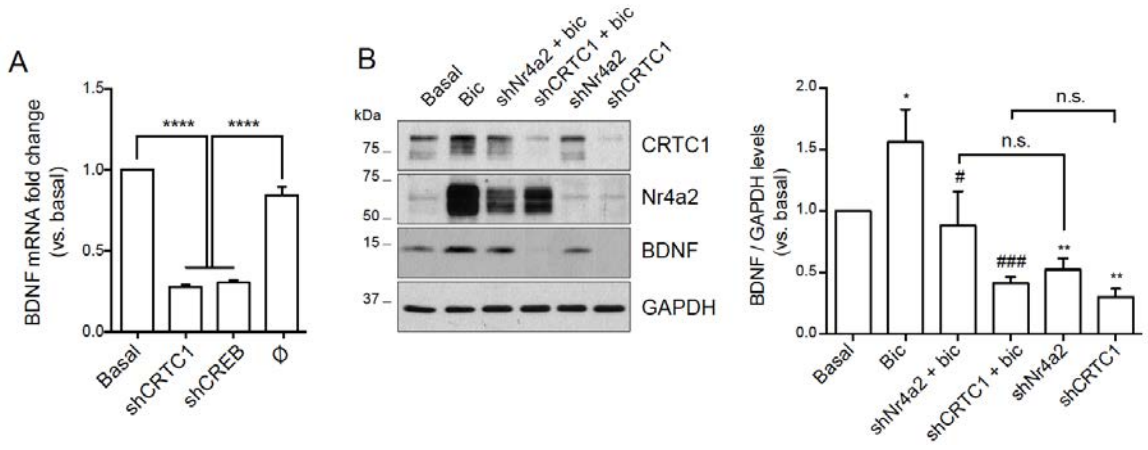

Figure 28. CRTC1 is necessary for basal and activity-mediated BDNF production in mature hippocampal neurons.
(A) BDNF mRNA levels in Nr4a2, CRTC1 and CREB shRNA-transduced neurons **(B)** BDNF protein levels in Nr4a2 and CRTC1 shRNA-transduced neurons in presence or absence of bicuculline (bic; 50 μM). n ≥ 3 independent hippocampal cultures. Data represent mean ± S.E.M. Statistical analysis was determined by one-way ANOVA followed by Tukey *post hoc* test. *p<0.05, **p<0.01, ***p<0.001 (*vs. basal, #vs. bic).

1.4. Nr4a2 modulates iGluRs levels in mature hippocampal neurons

Previous studies have shown that BDNF regulates the expression, trafficking and activity of iGluRs (Caldeira et al., 2007a,b; Zhang et al., 2018), but whether Nr4a2 could be upstream of this regulation in hippocampal neurons is still not known. Therefore, we wanted to address whether Nr4a2 was upstream of BDNF-dependent regulation of iGluRs expression. For that reason, we checked the levels of different subunits of excitatory (AMPA and NMDA) receptors in Nr4a2 shRNA-transduced mature hippocampal neurons, and we found a specific decrease in GuA1-AMPAR and GluN1-NMDAR protein subunits (around 30 and 40%, respectively) **(figure 29A)**. By contrast, no changes in protein levels were observed for GluA2, GluN2A and GluN2B subunits. In addition, we also addressed whether Nr4a2 modulated GABAergic transmission by checking the levels of $GABA_{A\text{-}\alpha1}$ subunit in Nr4a2 shRNA-transduced mature hippocampal neurons, but no changes were observed.

Consistent with the decrease in GuA1-AMPAR and GluN1-NMDAR protein subunits in Nr4a2 shRNA-transduced neurons, we observed that pharmacological activation of Nr4a2 with CQ incubation significantly increased both GuA1-AMPAR and GluN1-NMDAR protein subunits in mature hippocampal neurons. This increase was completely dependent on Nr4a2, since it was abolished in Nr4a2 shRNA-transduced neurons (GluA1-AMPAR protein levels after CQ treatment: 1.34 ± 0.13, shNr4a2 + CQ: 0.67 ± 0.08 fold change vs. basal; GluN1-NMDAR protein levels after CQ treatment: 1.24 ± 0.07, shNr4a2 ± CQ: 0.8 ± 0.12 fold change vs. basal) **(Figure 29B)**. Interestingly, CQ-mediated increase in GluA1-AMPAR protein levels was blunted by prior incubation during 30 minutes with the TrkB inhibitor ANA-12 (50 μM) (GluA1-AMPAR protein levels after CQ treatment: 1.35 ± 0.14, ANA-12 + CQ: 0.88 ± 0.04 fold change vs. basal), confirming the role of BDNF in GluA1-AMPAR protein levels **(Figure 29C)**. By contrast, CQ-mediated increase of GluN1-NMDAR protein levels was not disrupted with the inhibition of TrkB receptors **(Figure 29C)**, raising the possibility of a GluN1-NMDARs modulation by Nr4a2. Thus, although Nr4a2 is regulating both GluA1-AMPAR and GluN1-NMDAR protein subunits, only for GluA1 seemed to be BDNF-dependent.

TrkB receptor inhibition was confirmed by a reduction after 8 hours of different doses of ANA-12 treatment prior BDNF application (50 ng/ml for 5 minutes) of its autophosphorylation at Tyr706/Tyr707 and also a reduction in the phosphorylation of Akt and Erk downstream proteins **(Figure 29D)**.

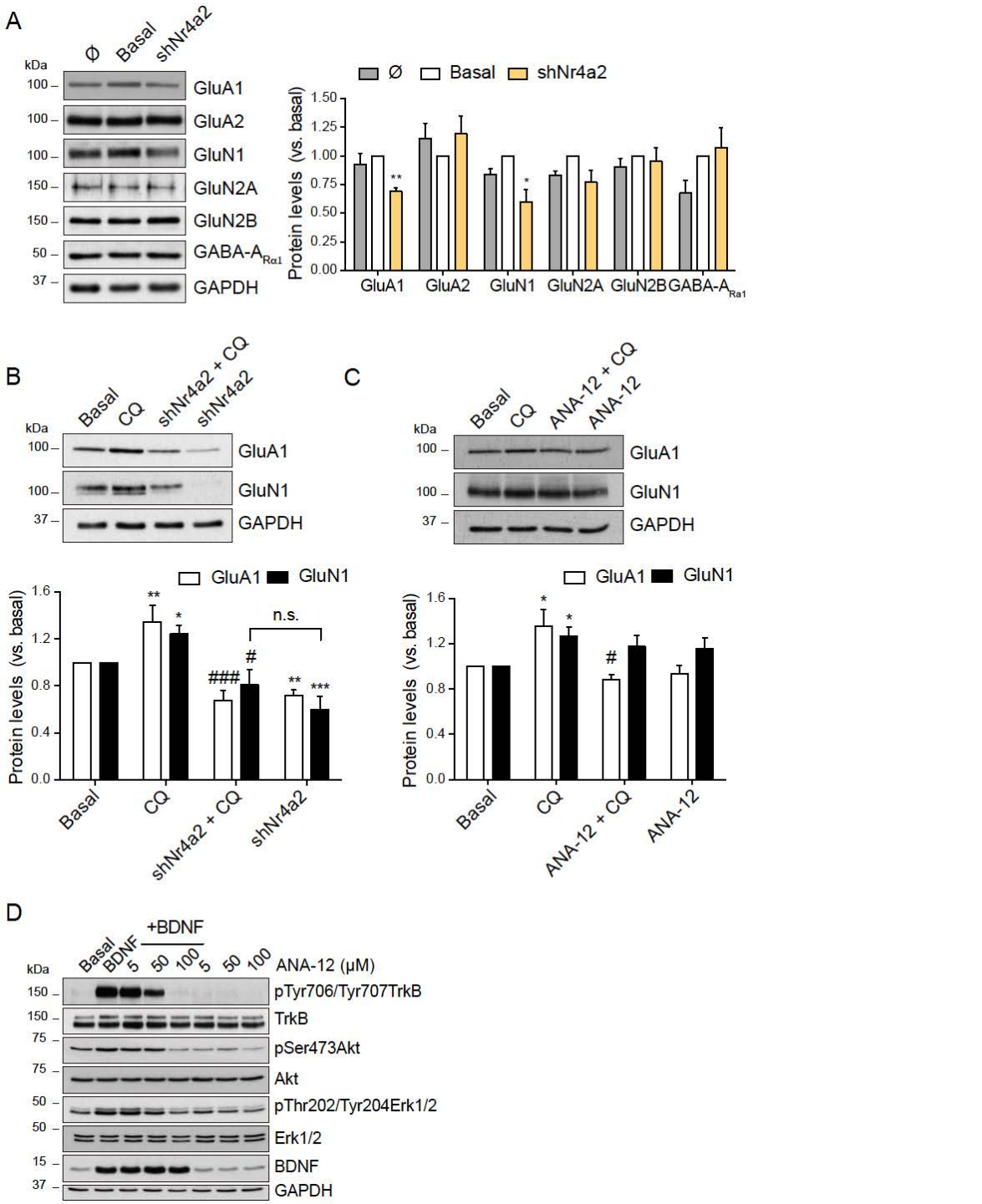

Figure 29. Nr4a2 modulates GluA1-AMPAR and GluN1-NMDAR protein levels in mature hippocampal neurons.

(A) Subunit expression levels of excitatory (AMPA and NMDA) and inhibitory (GABA-A) receptors in Nr4a2 shRNA-transduced neurons. **(B)** GluA1 and GluN1 protein levels in presence of the Nr4a2 agonist CQ (10 μM) in Nr4a2 shRNA-transduced neurons. **(C)** GluA1 and GluN1 protein levels in presence of the Nr4a2 agonist CQ in neurons treated with ANA-12 (50 μM), a TrkB inhibitor. **(D)** Protein levels of total and phosphorylated TrkB receptor and its two main downstream signaling pathways (Akt and Erk) in neurons treated with different doses of the TrkB inhibitor ANA-12 for 8 hours before BDNF application (50 ng/ml for 5 minutes). n ≥ 3 independent hippocampal cultures. Data represent mean ± S.E.M. Statistical analysis was determined by one-way ANOVA followed by Tukey *post hoc* test. *p<0.05, **p<0.01, ***p<0.001, ****p<0.0001 (vs. basal), (# vs. bic).

In contrast with the results obtained with Nr4a2 shRNA-transduced neurons in GluA1-AMPAR and GluN1-NMDAR protein levels, no changes were found in Gria1 and Grin1 mRNA levels **(Figure 30),** suggesting a possible role of Nr4a2 in post-transcriptional events.

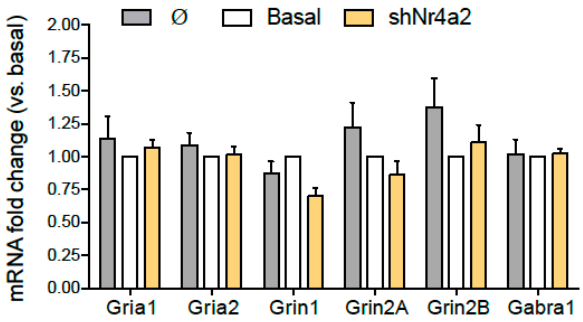

Figure 30. Nr4a2 does not seem to modulate Gria1 and Grin1 mRNA levels in mature hippocampal neurons. mRNA levels of different excitatory (AMPA and NMDA) and inhibitory ($GABA_A$) receptor subunits in Nr4a2 shRNA-transduced neurons. n = 3 independent hippocampal cultures. Data represent mean ± S.E.M. Statistical analysis was determined by one-way ANOVA followed by Tukey *post hoc* test (A,B)

Mature hippocampal neurons transduced with a shRNA against Nr4a2 showed a specific decrease in the amount of total GluA1-AMPAR and GluN1-NMDAR proteins, without affecting other synaptic proteins among the ones analyzed. Conversely, CRTC1 shRNA-transduced hippocampal-cultured neurons showed decreased levels of both pre-synaptic (synaptophysin) and post-synaptic (PSD-95) proteins (around 50% each) **(Figure 31A)**. A significant decrease in different excitatory and inhibitory receptor subunits was also found, including reduced levels of GluA1-AMPAR, GluN1-NMDAR, GluN2B-NMDAR and $GABA_AR\alpha1$, both at the transcriptional and translational level **(Figure 31B,C)**.

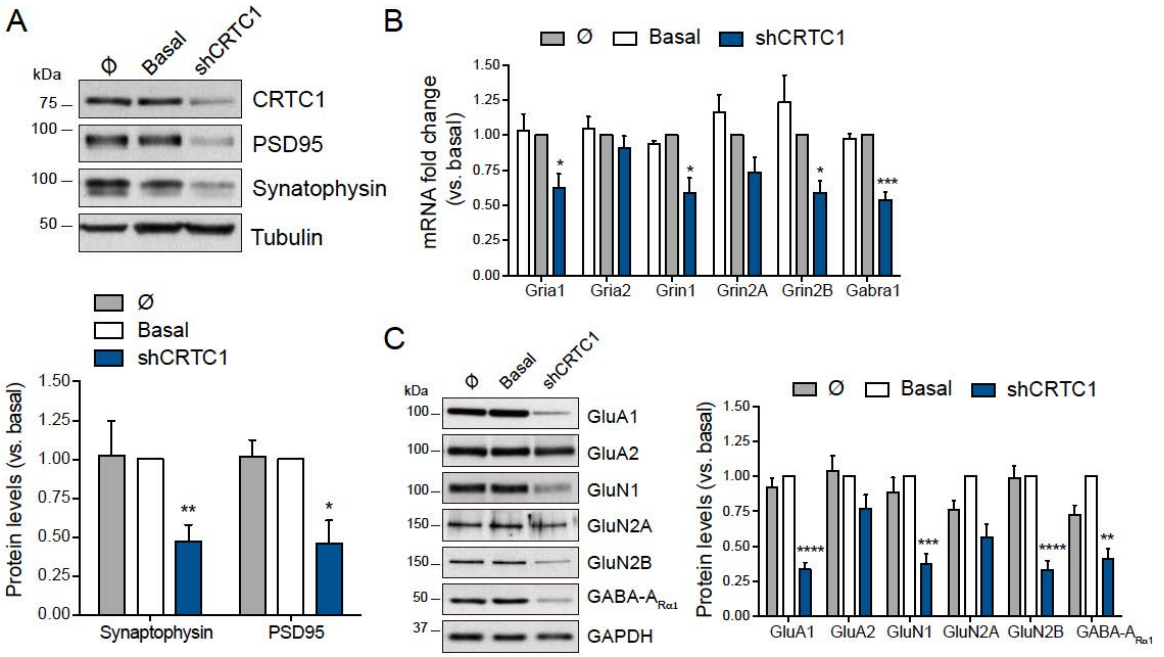

Figure 31. CRTC1 modulates both excitatory and inhibitory receptor subunits expression in mature hippocampal neurons.
(A) Levels of presynaptic and postsynaptic proteins in CRTC1 shRNA-transfected neurons. **(B,C)** mRNA and protein levels of different excitatory (AMPA and NMDA) and inhibitory ($GABA_A$) receptor subunits in CRTC1 shRNA-transduced neurons. n ≥ 3 independent hippocampal cultures. Data represent mean ± S.E.M. *p<0.05, **p<0.01, ***p<0.001. Statistical analysis was determined by one-way ANOVA followed by Tukey *post hoc* test.

In addition, to monitor whether changes in total receptor protein levels also imply changes in surface AMPAR and NMDAR levels, we analyzed the amount of surface GluA1-AMPARs and GluN1-NMDARs in Nr4a2 shRNA-transduced hippocampal neurons using a biotinylation assay. No changes were found at the surface **(figure 32A,C-E)**, even though GluA1-AMPAR levels were slightly reduced in Nr4a2 shRNA-transduced hippocampal-cultured neurons (shNr4a2: 0.65 ± 0.09 fold change vs. basal; p = 0.07 shNr4a2 vs. basal; p = 0.1 shNr4a2 vs. Ø) **(figure 32C)**. Next, to address whether we were not detecting significant changes in the surface because they were specifically occurring at the PSD, we isolated synaptoneurosomes of Nr4a2 shRNA-transduced hippocampal-cultured neurons, but no changes in the amount of synaptic GluA1-AMPAR neither GluN1-NMDAR were found **(figure 32B,F-H)**.

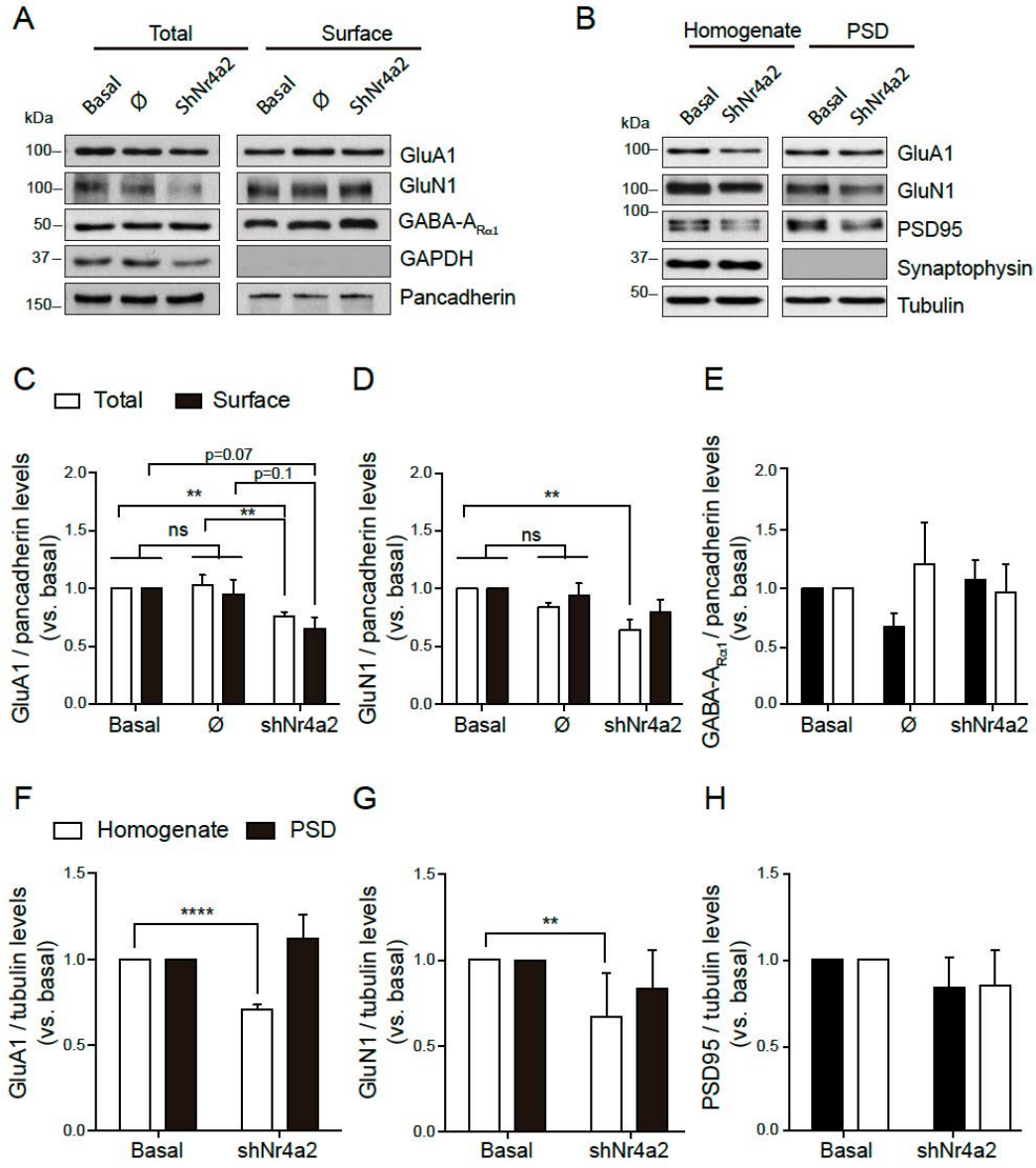

Figure 32. Absence of Nr4a2 does not seem to modify surface GluA1-AMPAR and GluN1-NMDAR protein levels in mature hippocampal neurons.
(A) Surface levels of GluA1 and GluN1 subunits in Nr4a2 shRNA-transduced neurons by a biotinylation assay. **(B)** Post-synaptic levels of GluA1 and GluN1 in synaptoneurosomes of Nr4a2 shRNA-transduced neurons. n ≥ 3 independent hippocampal cultures. Data represent mean ± S.E.M. *p<0.05, **p<0.01, ***p<0.001. Statistical analysis was determined by one-way ANOVA followed by Tukey *post hoc* test (A) or Student's unpaired two-tailed t-test (B).

In CRTC1 shRNA-transduced hippocampal neurons, biotynilation assays revealed decreased surface protein levels of GluA1-AMPAR, GluN1-NMDAR and also $GABA_AR\alpha1$ subunits (0.37 ± 0.07, 0.72 ± 0.12, 0.46 ± 0.18 fold change vs. basal, respectively) **(Figure 33A,C-E)**. Importantly, these changes were also found at the PSD. Synaptoneurosomes of CRTC1 shRNA-transduced hippocampal-cultured neurons had less synaptic GluA1-AMPAR, GluN1-NMDAR and PSD95 protein levels (0.57 ± 0.1, 0.6 ± 0.14, 0.64 ± 0.05 fold change vs. basal, respectively) **(Figure 33B,F-H)**.

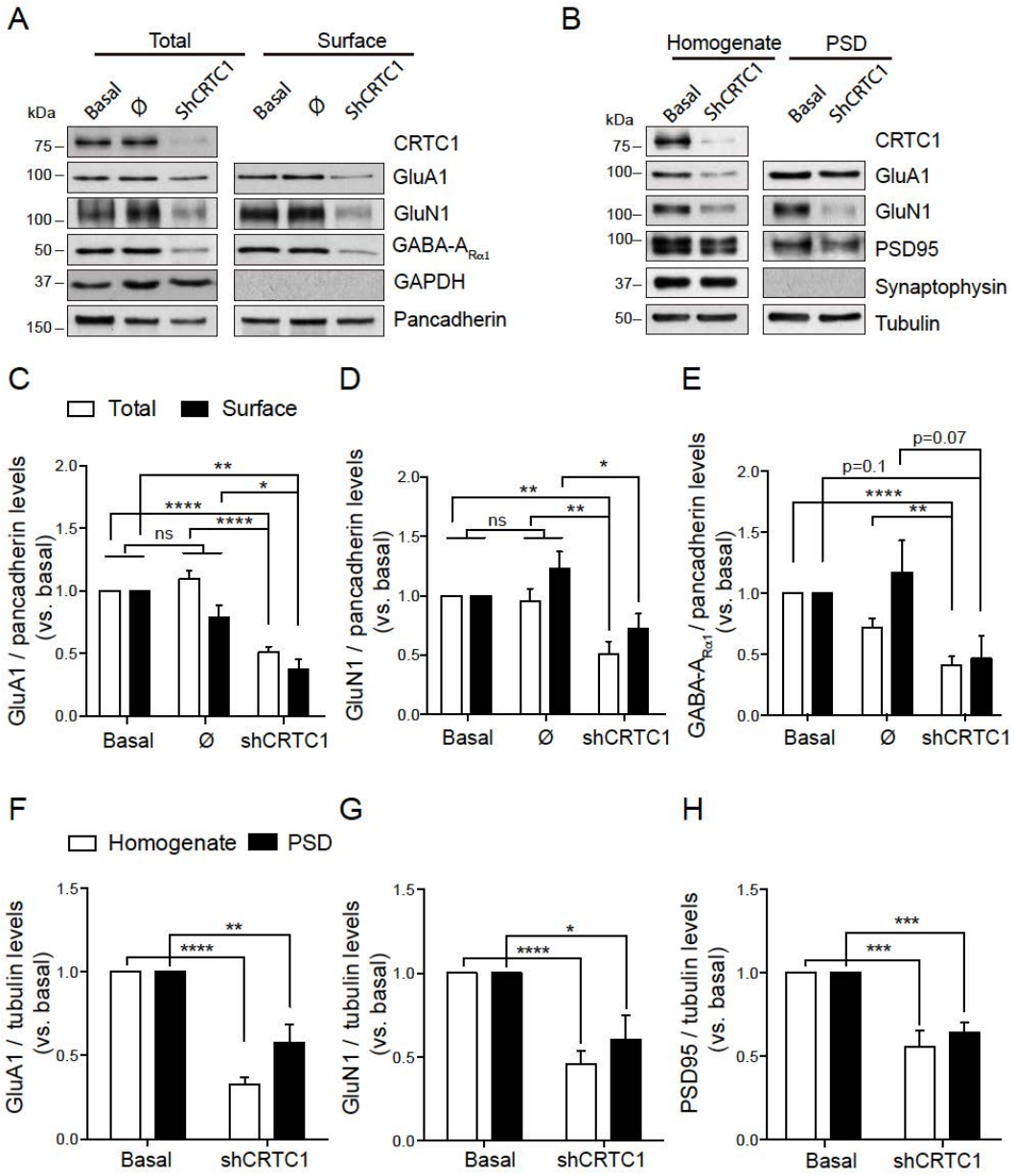

Figure 33. CRTC1 modulates synaptic GluA1-AMPAR and GluN1-NMDAR protein levels in mature hippocampal neurons.

(A) Surface levels of GluA1, GluN1 and GABA$_A$Rα1 subunits in CRTC1 shRNA-transduced neurons analyzed by a biotinylation assay. **(B)** Post-synaptic levels of GluA1, GluN1 and PSD95 in synaptoneurosomes of CRTC1 shRNA-transduced neurons. n ≥ 3 independent hippocampal cultures. Data represent mean ± S.E.M. *p<0.05, **p<0.01, ***p<0.001. Statistical analysis was determined by one-way ANOVA followed by Tukey *post hoc* test (A) or Students unpaired two-tailed t-test (B).

We also analyzed surface GluA1-AMPAR levels by confocal microscopy in Nr4a2 and CRTC1 shRNA-transduced hippocampal neurons. Consistent with the biotynilation assay data, no changes in surface GluA1-AMPAR levels were observed in Nr4a2 shRNA-transduced hippocampal neurons **(figure 34A)** meanwhile a significant decrease was found in CRTC1 shRNA-transduced hippocampal neurons **(figure 34B)**.

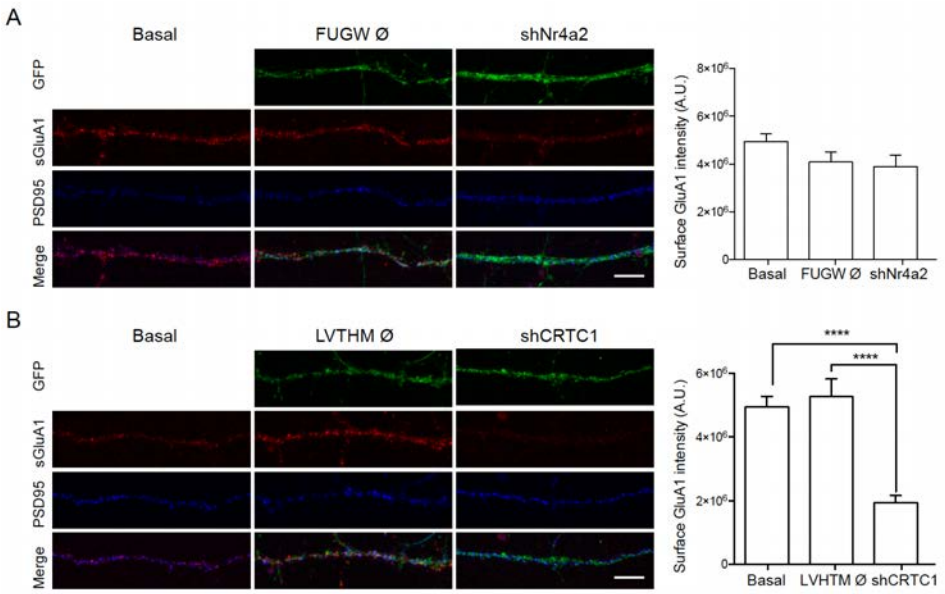

Figure 34. CRTC1 but not Nr4a2 is involved in surface expression of GluA1-AMPAR protein levels in mature hippocampal neurons.
Surface levels of GluA1-AMPAR in Nr4a2 **(A)** and CRTC1 **(B)** shRNA-transduced mature hippocampal neurons analyzed by confocal microscopy and Imaris software. Magnification, 63X; scale bar, 10 μm. n = 3 independent hippocampal cultures. n ≥ 20 dendrites/culture (n ≥ 60 dendrites/condition). Data represent mean ± S.E.M. ***p<0.001. Statistical analysis was determined by one-way ANOVA followed by Tukey *post hoc* test. A.U., arbitrary units; sGluA1, surface GluA1.

Since subtle changes in synaptic AMPARs levels between shRNA-transduced and control hippocampal neurons could be difficult to detect by biochemical methods or confocal imaging, we decided to analyze this issue using electrophysiological recordings in patched neurons (see next section).

1.5. Nr4a2 activation increases postsynaptic GluA1-AMPARs in CA1 pyramidal neurons

Synaptic AMPARs number and function largely determine excitatory neurotransmission and its activity-dependent plasticity. Therefore, to monitor whether Nr4a2 regulates not only total GluA1-AMPAR levels **(Figure 29)**, but also its levels at synapses, we explored in hippocampal slices the effects of Nr4a2 activation on AMPA/NMDA ratios and mEPSCs by whole-cell recordings in CA1 pyramidal neurons. Bath application of the Nr4a2 agonist AQ (30 μM) for 2-3 hours significantly increased AMPA/NMDA ratio and mEPSC amplitude, consistent with an increase in either the number and/or function of synaptic AMPARs **(Figure 35)**.

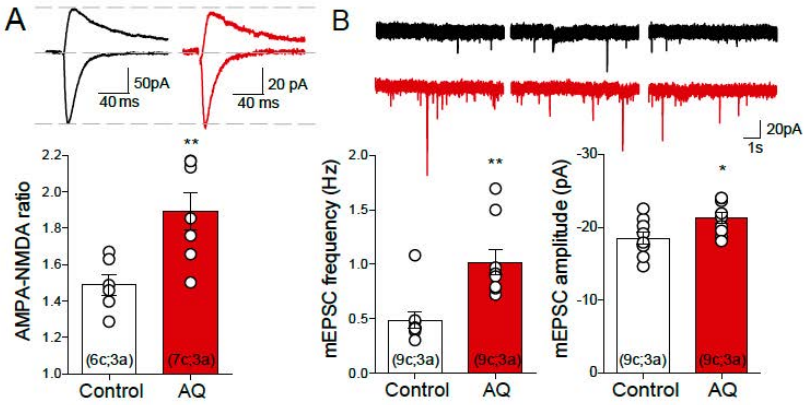

Figure 35. Nr4a2 activation increases post-synaptic GluA1-AMPARs in CA1 pyramidal neurons. **(A)** Representative AMPA/NMDA-EPSCs and **(B)** mEPSC *(top)* recorded from CA1 pyramidal cells in rat hippocampal slices in presence or absence of the Nr4a2 agonist amodiaquine (AQ; 30 µM); summary data *(bottom)*. Numbers in parenthesis indicate the number of animals (a) and cells (c). Data represent mean ± S.E.M. Statistical analysis was determined by Student's unpaired two-tailed t-test. *p<0.05, **p<0.01 (vs. basal).

Unexpectedly, CA1 pyramidal neurons incubated with AQ also showed an increase in mEPSC frequency. This could account for an increase in mEPSC detectability, by making small responses emerge from noise, or by unsilencing silent synapses. However, increased mEPSC frequency could also reflect changes in presynaptic properties as an increase in the probability of glutamate release. To study that, we analyzed the input-output function and the PPR of Schaffer collateral to CA1 neurons synapses. Both parameters were not altered in slices incubated with Nr4a2 agonists, ruling out any pre-synaptic effect that could account for the increase in the mEPSC frequency observed **(figure 36)**.

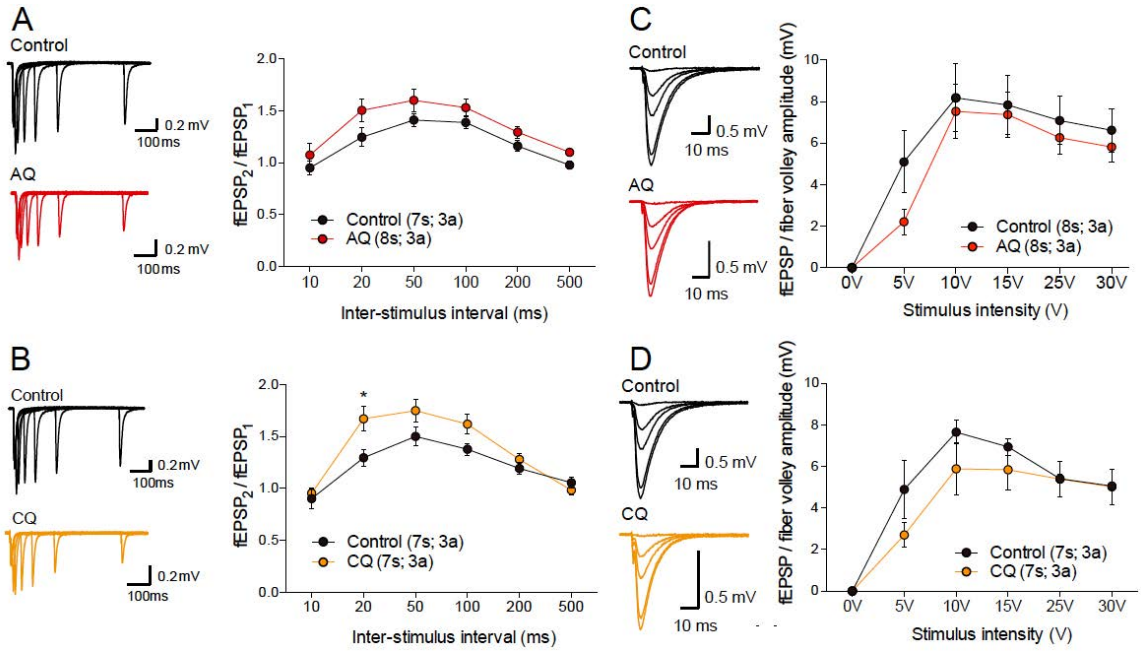

Figure 36. Nr4a2 activation does not alter either paired-pulse ratio nor Input-Output function in Schaffer collateral to CA1 synapses.
In all panels of this figure, representative traces *(left)*, quantification *(right)*. **(A,B)** Paired-pulse ratio (PPR) of Schaffer collateral to CA1 synapses after Nr4a2 agonists incubation measured at varying inter-stimulus intervals. **(C,D)** Input-Output function at Schaffer collateral to CA1 synapses after Nr4a2 agonists incubation. Numbers in parenthesis indicate the number of animals (a) and slices (s). Data represent mean ± S.E.M. Statistical analysis was determined by one-way ANOVA followed by Bonferroni *post hoc* test. *p<0.05.

1.6 Nr4a2 activation blocks and its absence increases stimuli-dependent synaptic depression in CA3-CA1 synapses

Next, we wonder whether Nr4a2 could be involved in the regulation of synaptic plasticity events dependent on synaptic AMPARs. Removal of AMPARs from the synapse is a key event for one of the major forms of long-lasting synaptic plasticity in the hippocampus, the LTD (Collingridge et al., 2010). Notably, bath application of Nr4a2 agonists, both AQ (30 μM) or CQ (60 μM) for 3-4 hours to rat hippocampal slices was able to completely block LTD elicited by low frequency stimulation (1 Hz, 900 pulses) at Schaffer collateral to CA1 synapses **(Figure 37)**.

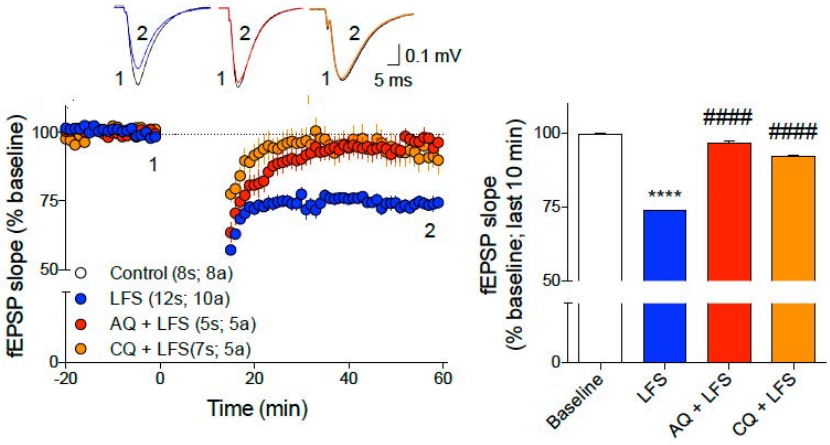

Figure 37. Nr4a2 activation blocks LTD at Schaffer collateral to CA1 synapses.
Field EPSP (fEPSP) responses from Schaffer-collateral synapses in rat slices before and after a LTD protocol (LFS; 900 pulses at 1 Hz) in presence or absence of AQ or CQ (60 μM). Illustrated traces are averages of 30 responses. Time course (left) and summary data (right). Numbers in parenthesis indicate the number of animals (a) or slices (s). Data represent mean ± S.E.M. Statistical analysis was determined by one-way ANOVA followed by Bonferroni *post hoc* test. ***p<0.001 (vs. basal), (# vs. LTD).

Then, we wanted to check whether we obtained a similar outcome inducing a chemical LTD (cLTD) in mature hippocampal-cultured neurons. Therefore, we applied 50 μM NMDA during 5 minutes in Mg^{2+} free-ACSF media to mature hippocampal-cultured neurons to study changes in cLTD (**figure 38A**; see materials and methods section 3.2). A

dephosphorylation of Ser845 GluA1-AMPAR subunit accompanied AMPARs endocytosis during cLTD as previously reported (Ehlers, 2000). We found that pre-incubation of AQ during 4 hours significantly restored the cLTD-induced dephosphorylation at Ser845-GluA1-AMPARs (phosphorylated Ser845-GluA1-AMPARs levels after cLTD: 0.25 ± 0.04, AQ + cLTD: 0.6 ± 0.13). Moreover, 4 hours of AQ incubation also increased Ser845-GluA1-AMPARs phosphorylation in basal conditions (1.44 ± 0.14 vs. basal) **(Figure 38B)**. These data suggest that Nr4a2 activation increases synaptic GluA1-AMPARs in basal and cLTD conditions, concordantly with the data obtained in AMPA/NMDA and mEPSC recordings in CA1 pyramidal neurons. Moreover, Nr4a2 activation is also able to block LTD both in acute hippocampal slices and mature hippocampal-cultured neurons.

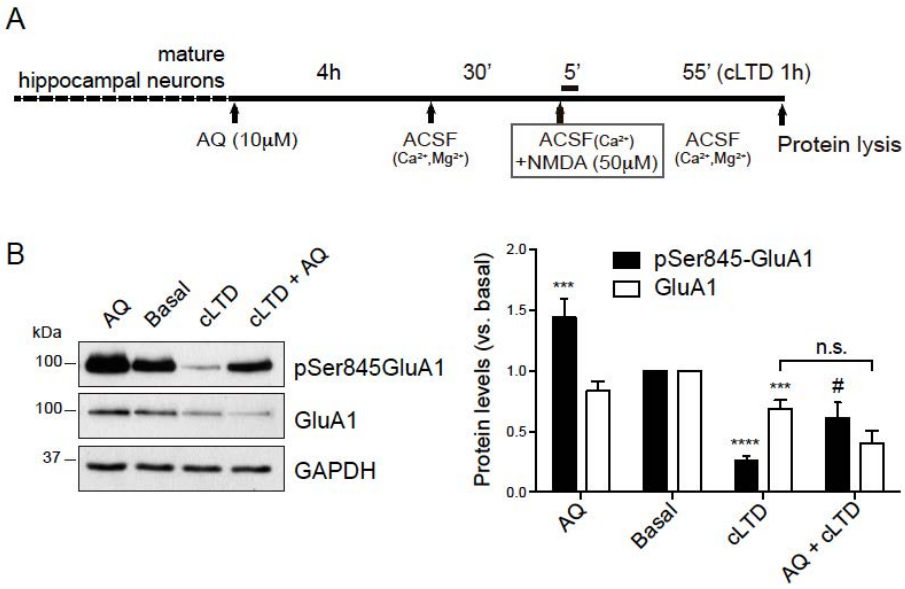

Figure 38. Nr4a2 activation using specific agonists blocks chemical LTD in mature hippocampal neurons.
(A) Experimental design scheme for the cLTD protocol. **(B)** Total and Ser845-phosporylated GluA1-AMPAR protein levels after a cLTD protocol (NMDA 50 µM during 5 min) in presence or absence of previous incubation during 4 hours with AQ (10 µM). n = 4 independent hippocampal cultures. Data represent mean ± S.E.M. *p<0.05, **p<0.01. Statistical analysis was determined by one-way ANOVA followed by Tukey *post hoc* test.

To confirm the role of Nr4a2 on the modulation of synaptic depression elicited by low frequency stimulation, P17-P19 mice were stereotaxically injected with AAV to silence Nr4a2 in dorsal CA1 **(figure 39A,B)**. Since our results showed that pharmacological activation of Nr4a2 did prevent LTD, we hypothesized that an increase in synaptic depression will be observed in absence of Nr4a2. Three to four weeks after injection, increased LTD at Schaffer collateral to CA1 synapses was effectively observed in Nr4a2 shRNA-injected animals **(figure 39C)**. The efficacy of the AAV2/10.H1.shNr4a2 construct

to silence Nr4a2 was checked by immunohistochemistry of the slices used for electrophysiological recordings **(figure 39D)**.

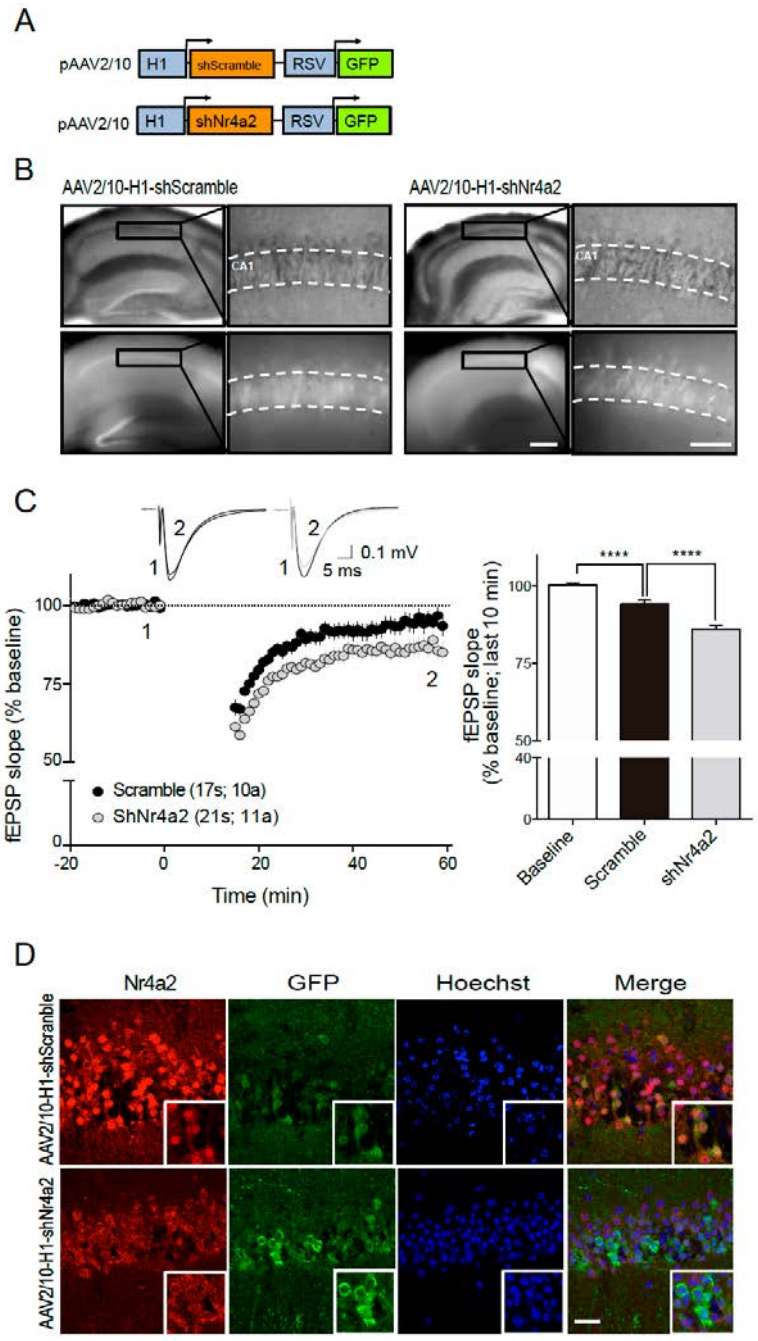

Figure 39. Absence of Nr4a2 increases stimuli-dependent synaptic depression at Schaffer collateral to CA1 synapses.

(A) Schematic representation of the AAV to silence Nr4a2. **(B)** Representative images of bright field *(top)* and fluorescent CA1 pyramidal cells *(bottom)* after 3-4 weeks of injection. Scale bar, 200 µm (left), 100 µm (right; zoom). **(C)** Schaffer-collateral fEPSP responses from hippocampal slices before and after LTD induction (LFS; 900 pulses at 1 Hz) in scramble or shNr4a2 injected mice. Time course (left) and summary data (right). Numbers in parenthesis indicate the number of animals (a) or slices (s). **(D)** Representative images of immunohistochemistry of hippocampal slices from injected mice used for LTD recordings (in C). Magnification, 40x; scale bar, 200 µm (B, right), 100 µm (B, left), 25 µm (D). Data represent mean ± S.E.M. Statistical analysis was determined by one-way ANOVA followed by Bonferroni *post hoc* test. ***p<0.001 (vs. basal), (# vs. LTD).

We also checked the effects of Nr4a2 overexpression in cLTD using a viral approach. We transduced hippocampal-cultured neurons with lentiviral vectors to overexpress Nr4a2 at 7 DIV and we induced a cLTD approximately ten days later, when neurons were mature. We observed that exogenous overexpression of Nr4a2 via lentiviral transduction failed to block the cLTD-mediated Ser845-GluA1-AMPARs dephosphorylation **(figure 40)**.

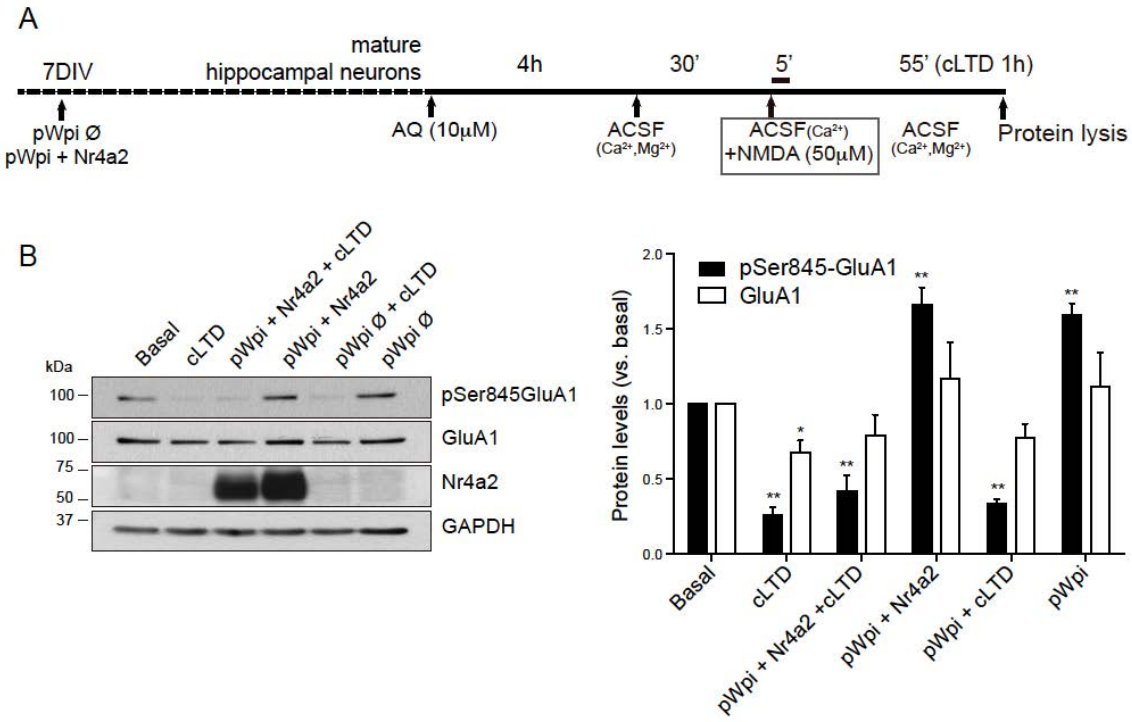

Figure 40. Nr4a2 overexpression failed to block chemical LTD in mature hippocampal neurons. **(A)** Experimental design scheme for the cLTD protocol. **(B)** Total and Ser845-phosporylated GluA1-AMPAR protein levels after a cLTD protocol (NMDA 50 μM during 5 min) in hippocampal neurons transduced with lentiviral vectors to overexpress Nr4a2 (pWpi+Nr4a2). n = 3 independent hippocampal cultures. Data represent mean ± S.E.M. *p<0.05, **p<0.01. Statistical analysis was determined by one-way ANOVA followed by Tukey *post hoc* test.

The efficacy to overexpress Nr4a2 of the FUGWshNr4a2+Nr4a2 and the pWpi+Nr4a2 lentiviral constructs was checked by western blotting against Nr4a2 and GFP antibodies **(figure 41A)**, and by immunofluorescence against GFP and V5-tag antibodies **(figure 41B)**. We were not able to check Nr4a2 by immunofluorescence because of the unspecificity of five different commercial antibodies analyzed **(figure 42)**.

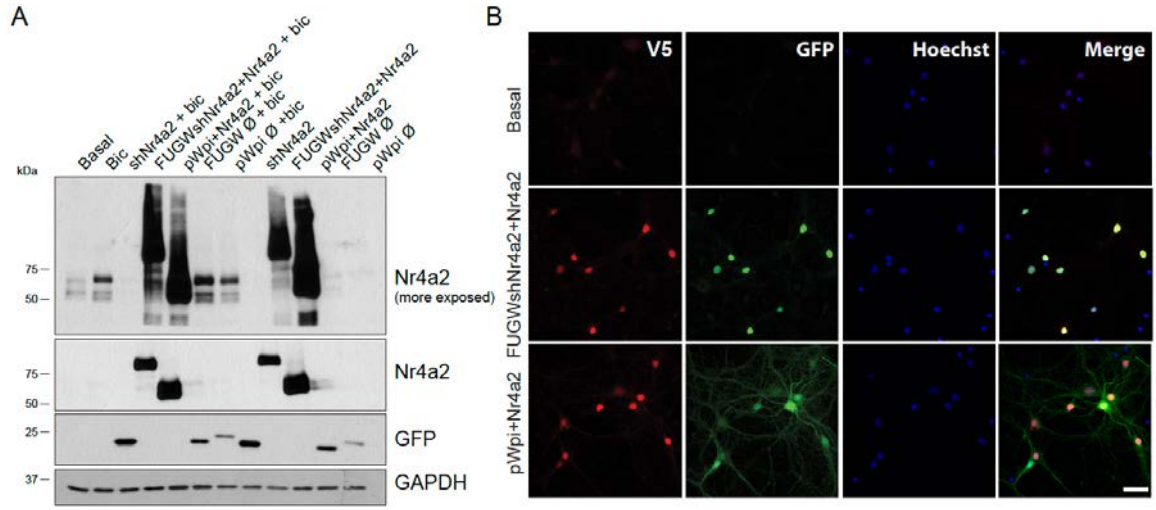

Figure 41. Lentiviral vectors efficiently overexpress Nr4a2.
Western Blot **(A)** and immunocytochemistry **(B)** of mature hippocampal-cultured neurons transduced with lentiviral vectors (FUGWshNr4a2+Nr4a2 and pWpi+Nr4a2). Magnification, 40x; scale bar, 25 µm.

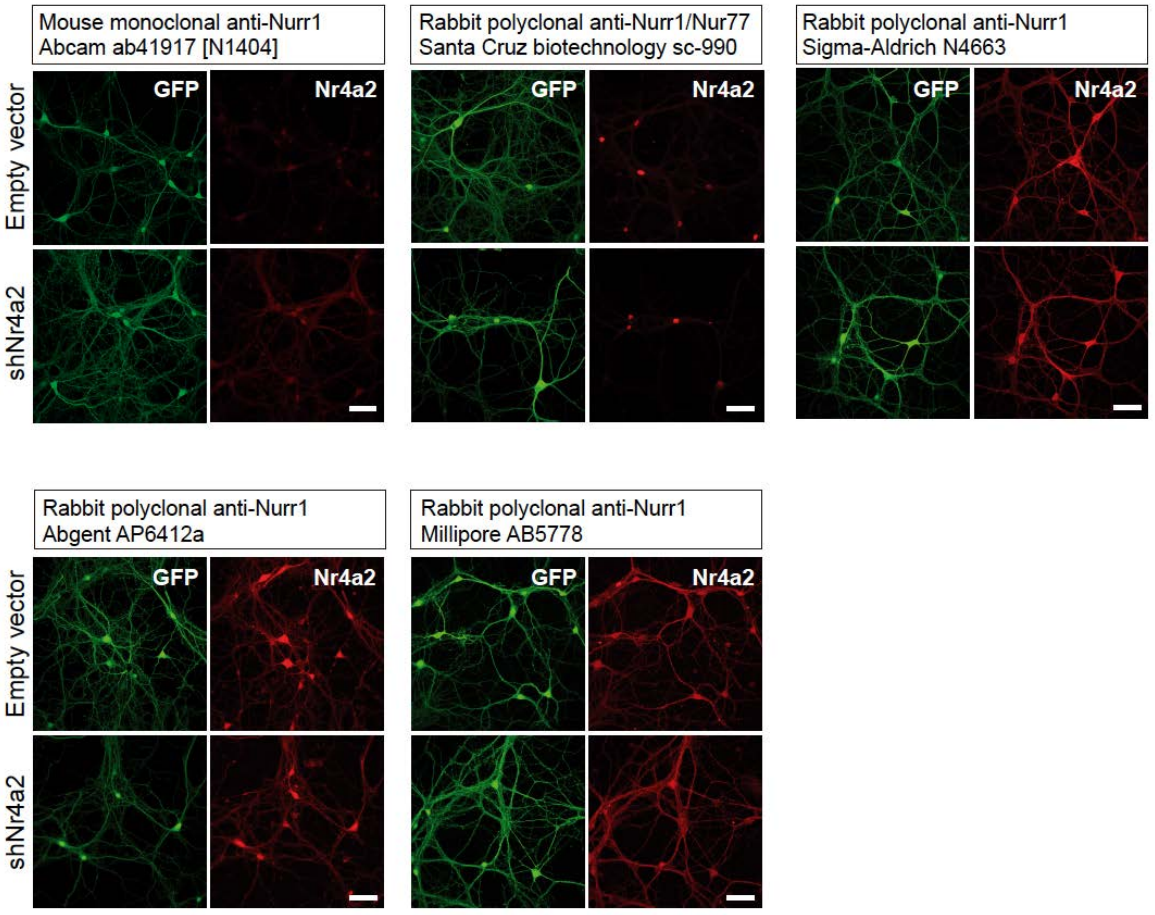

Figure 42. Nr4a2 antibodies specificity by immunocytochemistry.
Immunocytochemistry of mature hippocampal-cultured neurons transduced with lentiviral vectors to silence Nr4a2 (FUGW empty and FUGWshNr4a2) to check Nr4a2 antibodies specificity. Magnification, 40x; scale bar, 25 µm.

In summary, data presented in this first chapter show that Nr4a2 is an activity-inducible transcription factor that can be located at mouse hippocampal synapses. In mature hippocampal neurons, its activation relies on iGluRs-mediated calcium entry that activates the CREB/CRTC1 signaling pathway and calcineurin. Nr4a2 activation increases BDNF transcription, translation and secretion, and also leads to an increase in GluA1-AMPAR and GluN1-NMDAR total protein levels. Moreover, Nr4a2 activation also prompts to an increase of synaptic GluA1-AMPAR at CA1 pyramidal neurons, leading to increased AMPA/NMDA ratio, increased mEPSC amplitude and a blockade of LTD at Schaffer collateral to CA1 synapses **(figure 43)**.

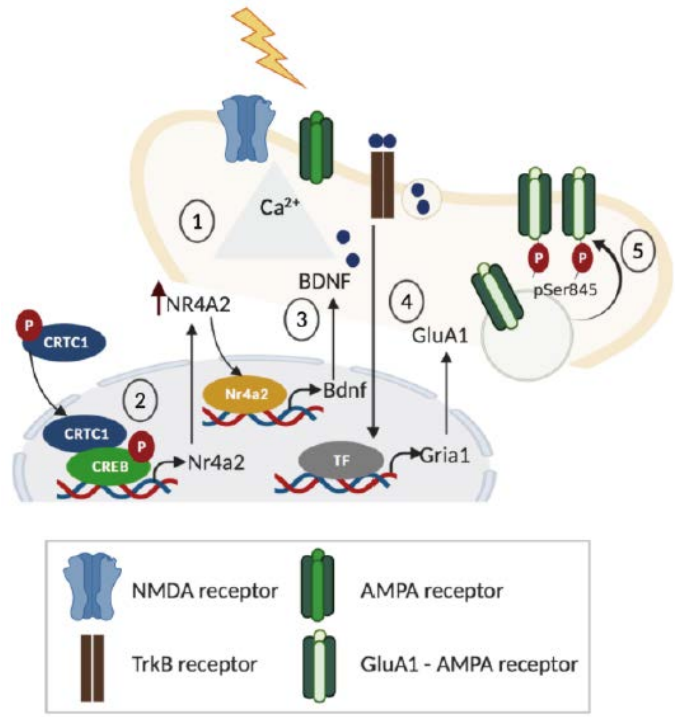

Figure 43. Proposed model for Nr4a2 function in hippocampal glutamatergic synaptic plasticity. Numbers depict the possible order of events leading to Nr4a2-mediated increase in synaptic AMPARs.

CHAPTER II

“Role of Nr4a2 in the synaptic failure occurring in early Alzheimer’s disease”

CHAPTER II

Role of Nr4a2 in the synaptic failure occurring in early Alzheimer's disease

2.1. Activity-dependent induction of Nr4a2 is impaired in presence of soluble forms of Aβ peptide

Hippocampal synaptic dysfunction is thought to underlie the initial development of AD (Masliah et al., 2001; Scheff et al., 2006, 2007) and to highly contribute to the cognitive deficits observed in AD patients. Indeed, synapse loss is one of the best neuroanatomical correlates of the cognitive impairment observed in AD (Bereczki et al., 2016; DeKosky & Scheff, 1990; Terry et al., 1991). Postulated by the oligomer hypothesis of AD more than 15 years ago, it is now widely accepted that oAβ could be the initial mediators leading to the synaptic dysfunction and eventual loss in AD **(figure 4)**. Importantly, we have previously demonstrated in chapter I that Nr4a2 transcription factor has a key role in hippocampal synaptic plasticity. Moreover, Nr4a2 mRNA has been found decreased in AD mouse models (España et al., 2010b; Moon et al., 2015; Parra-Damas et al., 2014). Therefore, to study the possible involvement of Nr4a2 in the synaptic failure occurring at early stages of AD, we firstly wanted to address whether oAβ could alter Nr4a2 levels in the hippocampus. For that reason, we treated mature hippocampal-cultured neurons with freshly prepared oAβ (5 μM) (see materials and methods, section 3.3). The presence of oAβ in fresh preparations was always checked biochemically by BisTris/bicine western blotting **(figure 44A)**. Notably, we observed a significant reduction in the activity-dependent increase of Nr4a2 protein levels in presence of oAβ (around 45% vs. 2 hours of bic treatment and 35% vs. 4 hours of bic treatment) **(figure 44B)**. These data is consistent with previous studies that reported decreased Nr4a2 mRNA levels in cell lines incubated with amyloid-$\beta_{1\text{-}42}$ (Terzioglu-Usak et al., 2017). Noteworthy, oAβ not only altered the activity-dependent increase in Nr4a2 protein levels, but also the Nr4a2 protein levels in hippocampal-cultured neurons transduced with pWpi-Nr4a2 lentiviral vector **(figure 44C)**. Moreover, we observed that Nr4a2 protein levels were also decreased in mature hippocampal-cultured neurons after a cLTD protocol **(figure 40)**, consistent with the similarities observed between LTD and oAβ-induced synaptic depression (Hsieh et al., 2006; Li et al., 2009a; Mucke & Selkoe, 2012).

In mouse models of AD, previous data also reported a decrease in CRTC1 levels (Wilson et al., 2016), which we also found reduced (around 30% of decrease vs. 4 hours of bic treatment) in presence of oAβ in mature hippocampal-cultured neurons **(figure 44D)**.

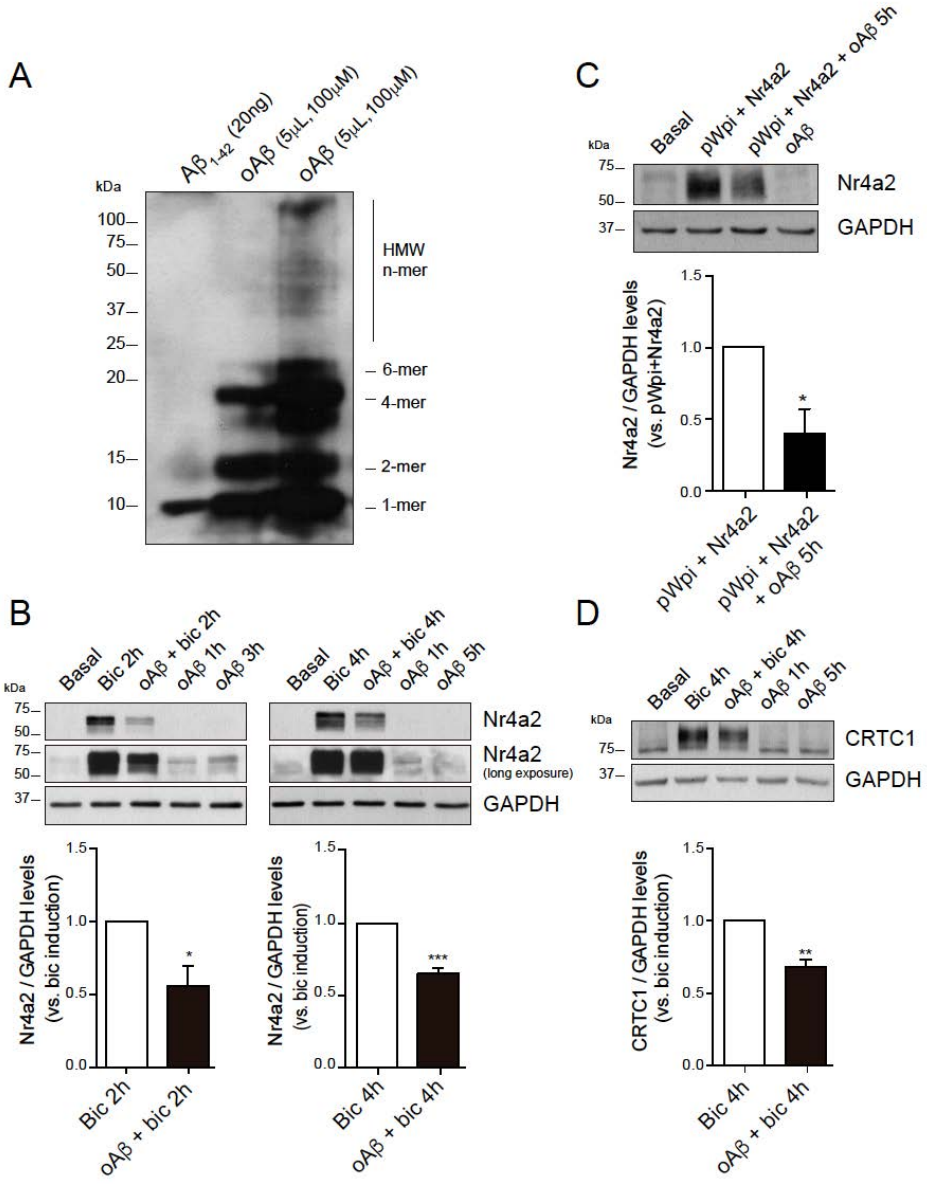

Figure 44. Amyloid-β oligomers (oAβ) reduce the activity-dependent increase in Nr4a2 protein levels in mature hippocampal neurons.
(A) Representative western blotting image of Aβ species present in soluble monomeric $Aβ_{1-42}$ and oligomeric preparations. **(B)** Nr4a2 protein levels after bicuculline (bic; 50 μM) treatment in presence or absence of oAβ (5 μM) applied 30 minutes before bic treatment. **(C)** Nr4a2 protein levels in pWpi+Nr4a2 transduced hippocampal neurons in presence or absence of oAβ during 5 hours. **(D)** CRTC1 protein levels after bic (50 μM) treatment in presence or absence of oAβ (5 μM) applied 30 minutes before bic treatment. n ≥ 3 independent hippocampal cultures. Data represent mean ± S.E.M. *p<0.05, **p<0.01 ***p<0.001. Statistical analysis was determined by Student's unpaired two-tailed t-test.

The decrease observed in Nr4a2 protein levels in presence of oAβ was not found in Nr4a2 mRNA. The bicuculline-mediated increase of Nr4a2 mRNA was not affected by oAβ **(figure 45A)** and basal levels of Nr4a2 mRNA were indeed increased by oAβ **(figure 45B)**. A possible explanation for these apparently contradictory findings could be the initial raise of intracellular calcium caused by oAβ, which could lead to Nr4a2 transcription (Berridge, 2011; Bezprozvanny & Mattson, 2008; Green & LaFerla, 2008).

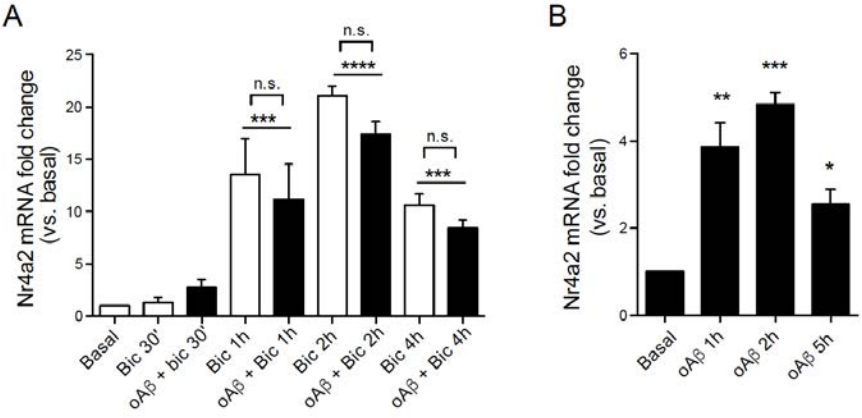

Figure 45. Amyloid-β oligomers (oAβ) do not disrupt the activity-dependent increase in Nr4a2 mRNA levels in mature hippocampal neurons.
(A) Nr4a2 mRNA levels after bicuculline (bic; 50 μM) treatment in presence or absence of oAβ (5 μM) applied 30 minutes before bic treatment. **(B)** Time course of Nr4a2 mRNA levels in presence of oAβ (5 μM). n = 3 independent hippocampal cultures. Data represent mean ± S.E.M. *p<0.05, *p<0.01, ***p<0.001, ****p<0.0001. Statistical analysis was determined by one-way ANOVA followed by Bonferroni *post hoc* test.

Altogether, these data demonstrate that oAβ alter hippocampal Nr4a2 protein levels, which can lead to synaptic dysfunction at early stages of AD.

2.2. Nr4a2 and BDNF protein levels are decreased in human postmortem hippocampal tissue

Nr4a2 expression has also been previously examined in AD patients, showing some discrepancies. Decreased levels of Nr4a2 mRNA at Braak III-IV and V-VI stages compared with control subjects were previously reported in postmortem human hippocampus (Parra-Damas et al., 2014). In line with these results, reduced levels of Nr4a2 protein were also found in the hippocampus and the superior frontal cortex of AD patients in another study (Moon et al., 2019a). Contrary, increased hippocampal Nr4a2 mRNA levels were reported in a cohort of late onset AD (LOAD) patients (Annese et al., 2018).

We checked Nr4a2 protein levels in postmortem hippocampal tissue samples from control subjects and AD patients, and we found a significant decrease in Nr4a2 protein levels specifically at Braak II stage, corresponding to a pre-symptomatic stage where synaptic deficits are already occurring, compared with healthy age-matched controls **(figure 46)**. By contrast, no changes were observed at Braak III-IV and Braak V-VI stages compared to controls. Demographic and clinical information about the cohort of patients used in this study is found in **table 6**.

We have previously demonstrated that Nr4a2 is involved in basal and activity-mediated BDNF production in hippocampal neurons **(figure 27)**. For that reason, we also analyzed BDNF protein levels in human postmortem hippocampal tissue. We observed a significant decrease in BDNF protein levels specifically at Braak III-IV stage, corresponding to MCI, compared to controls. We also found a significant reduction of BDNF at AD III-IV and AD V-VI compared to AD II, observing therefore lower BDNF protein expression as AD pathology progressed. A significant decrease at AD III-IV compared to AD II analyzing separately both isoforms of BDNF, 14 kilodaltons (KDa) and 18 KDa, was also present **(figure 46)**.

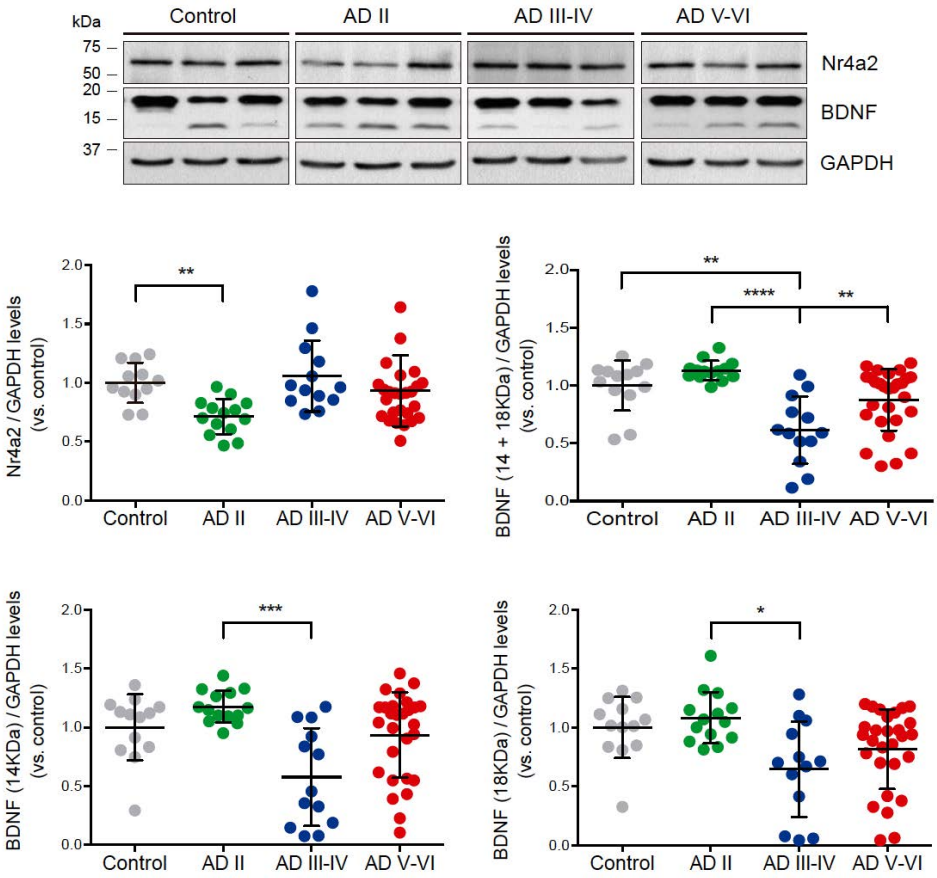

Figure 46. Analysis of Nr4a2 and BDNF levels in postmortem human hippocampus at different AD stages.
Representative western blotting images and quantification of Nr4a2 and BDNF (total, 14 KDa and 18KDa isoforms) protein levels in hippocampal human postmortem tissue samples of control subjects and AD patients classified as different Braak stages. n = 13-28/group. Data represent mean ± S.E.M. *p<0.05, **p<0.01, ***p<0.001, ****p<0.0001. Statistical analysis was determined by Kruskal-Wallis test.

2.3 Nr4a2 activation rescues the oAβ-mediated synaptic dysfunction in mature hippocampal neurons

As described in the introduction, oAβ disrupt hippocampal synaptic plasticity, impairing NMDA-dependent LTP (Barghorn et al., 2005; Jürgensen et al., 2011; Klyubin et al., 2008; Ma & Klann, 2012; Rammes et al., 2011; Shankar et al., 2008; Walsh et al., 2002) and promoting LTD (Hsieh et al., 2006; Kim et al., 2001; Li et al., 2009a; Ondrejcak et al., 2010; Shankar et al., 2008). oAβ also reduce S845-GluA1-AMPARs phosphorylation, leading to a decrease in surface expression of GluA1-AMPARs (Guntupalli, Widagdo & Anggono, 2016; Miñano-Molina et al., 2011). Importantly, in this doctoral thesis, we have shown that Nr4a2 activation is able to increase postsynaptic AMPARs **(figure 35)** and effectively block LTD at Schaffer collateral to CA1 synapses **(figure 37)**. In this regard, we also wanted to assess whether Nr4a2 activation was able to rescue the oAβ-mediated deficits in hippocampal synaptic plasticity. We firstly observed that Nr4a2 activation using AQ not only increased Ser845-GluA1-AMPARs phosphorylation in basal conditions, as we have previously seen in **figure 38**, but also completely rescued the oAβ-mediated dephosphorylation at Ser845-GluA1-AMPARs (phosphorylated levels of Ser845-GluA1-AMPARs after AQ treatment: 1.9 ± 0.21, oAβ + AQ: 1.66 ± 0.3, oAβ: 0.6 ± 0.07 fold change vs. basal) **(Figure 47).**

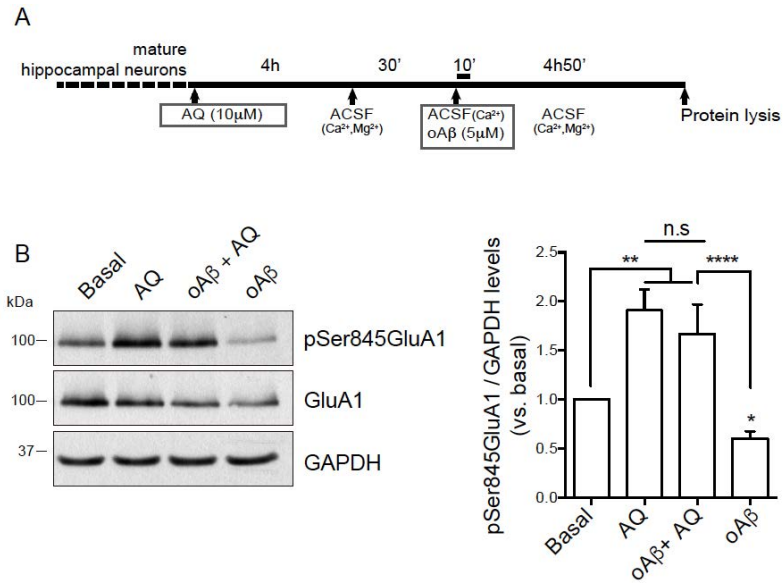

Figure 47. Nr4a2 activation rescues the oAβ-dependent reduction in Ser845-phosphorylated GluA1-AMPAR levels in mature hippocampal neurons.
(A) Experimental design scheme for the treatment of oAβ and Nr4a2 agonists. **(B)** Total and Ser845-phosporylated GluA1-AMPAR protein levels in oAβ (5 μM) treated hippocampal neurons during 5 hours in the presence or absence of previous incubation during 4 hours of AQ (10 μM). n = 4 independent hippocampal cultures. Data represent mean ± S.E.M. *p<0.05, **p<0.01, ****p<0.0001. Statistical analysis was determined by one-way ANOVA followed by Tukey *post hoc* test.

Moreover, Nr4a2 agonists were not only able to rescue the oAβ-mediated dephosphorylation at Ser845-GluA1-AMPARs in basal conditions, but also restored the oAβ-mediated cLTP impairment. As we have previously stated, it has been broadly studied that oAβ, both *in vitro* and *in vivo*, adversely affect LTP and block the increase in synaptic AMPARs mediated by cLTP. Accordingly, an increase in the phosphorylation at Ser845-GluA1-AMPARs was observed after a cLTP protocol, which consisted in applying FSK/Rol (50 μM / 0.1 μM) for 10 minutes in Mg^{2+} free-ACSF media to mature hippocampal-cultured neurons (**figure 48A**; see materials and methods section 3.2). This increase was significantly reduced in presence of oAβ, indicating a decrease in surface GluA1-AMPARs **(figure 48B)**, and significantly restored with the pre-incubation of Nr4a2 agonists, both CQ or AQ (phosphorylated levels of Ser845-GluA1-AMPARs after cLTP protocol: 7.1 ± 0.46, oAβ + cLTP: 4.4 ± 0.5, CQ + oAβ + cLTP: 7.2 ± 1.7, AQ + oAβ + cLTP: 7.8 ± 0.5 fold change vs. basal) **(figure 48C,D)**.

Importantly, Nr4a2 agonists were not only able to restore the oAβ-mediated impairment of cLTP, but also increased the Ser845-GluA1-AMPARs phosphorylation after a cLTP protocol (around 30%), indicating an increase of the cLTP magnitude **(figure 48C,D)**.

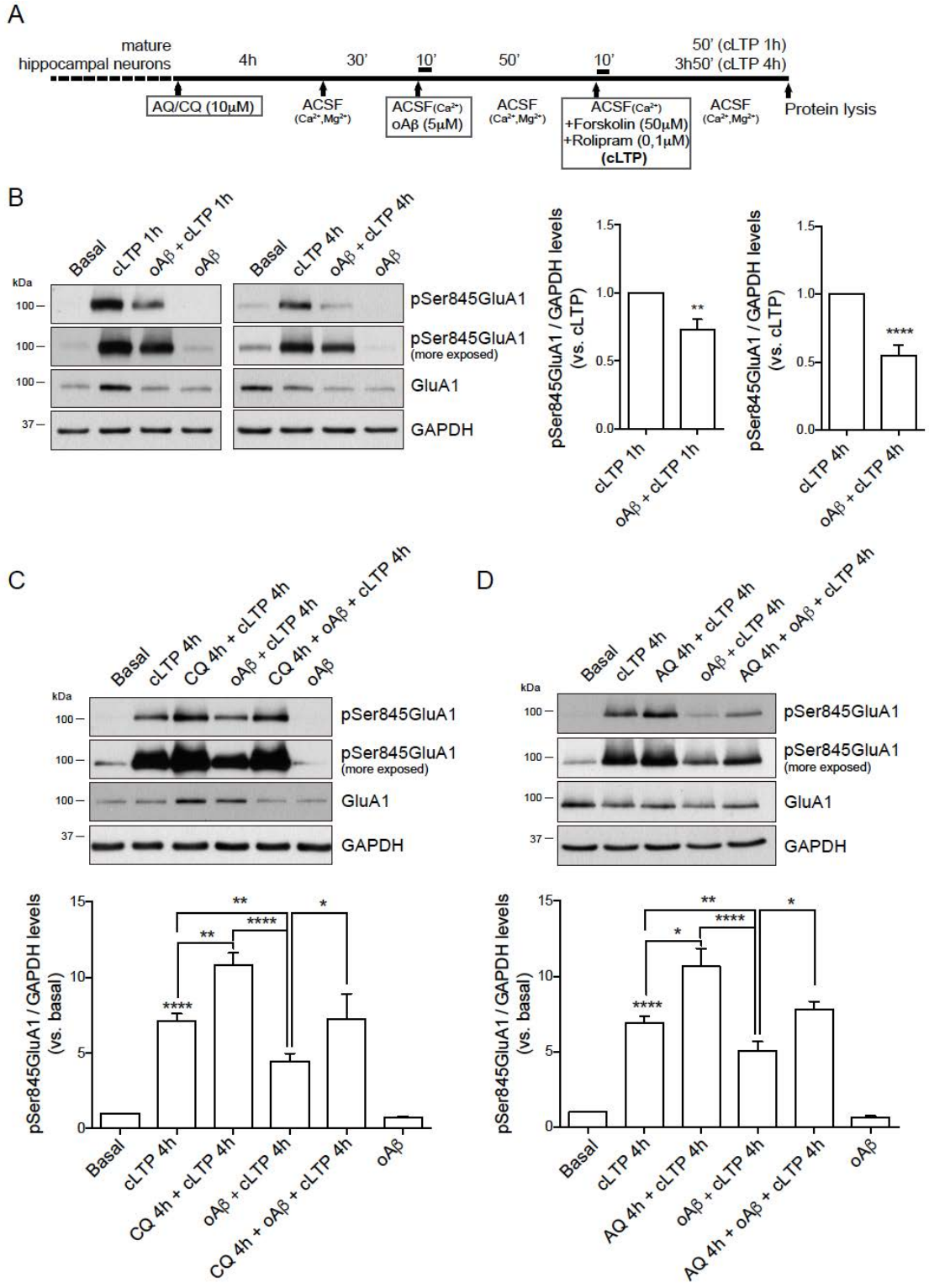

Figure 48. Nr4a2 agonists potentiate cLTP and partially rescue the oAβ-mediated cLTP impairment.

(A) Experimental design scheme for cLTP protocol. **(B)** Total and Ser845-phosporylated GluA1-AMPAR protein levels after a cLTP protocol (FSK/Rol; 50 µM/0.1 µM during 10 min) in presence or absence of oAβ (5 µM). **(C,D)** Total and Ser845-phosporylated GluA1-AMPAR protein levels after a cLTP protocol in presence or absence of the Nr4a2 agonist CQ (10 µM) or AQ (10 µM) and/or oAβ (5 µM). n ≥ 4 independent hippocampal cultures. Data represent mean ± S.E.M. *p<0.05, **p<0.01, ****p<0.0001. Statistical analysis was determined by one-way ANOVA followed by Tukey *post hoc* test.

Next, given the involvement of Nr4a2 in restoring the oAβ-mediated impairment of cLTP, we also checked whether the absence of Nr4a2 affected this plasticity in basal conditions. We found that hippocampal-cultured neurons transduced with Nr4a2-shRNA showed the same magnitude of cLTP compared with non-transduced neurons, indicating that decreased levels of Nr4a2 do not seem to impair cLTP in basal conditions **(figure 49)**.

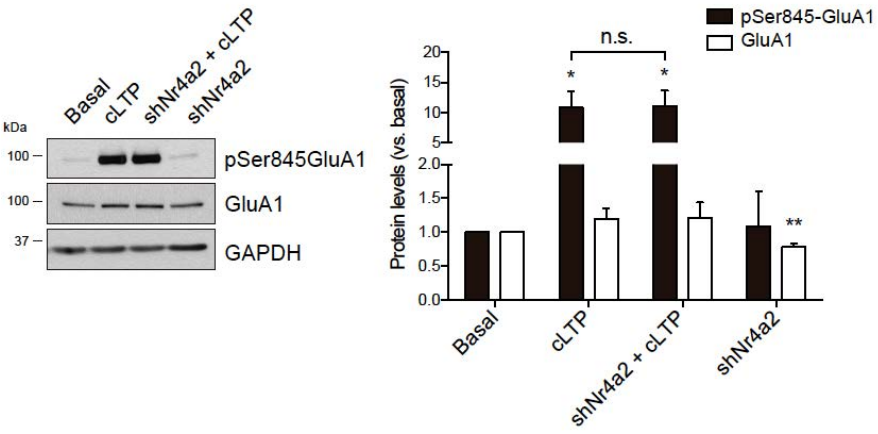

Figure 49. Absence of Nr4a2 using lentiviral vectors does not impair cLTP.
Total and Ser845-phosporylated GluA1-AMPAR protein levels after a cLTP protocol (FSK/Rol; 50 μM/0.1 μM during 10 min) in shNr4a2-transduced hippocampal neurons. n = 3 independent hippocampal cultures. Data represent mean ± S.E.M. *p<0.05, **p<0.01. Statistical analysis was determined by one-way ANOVA followed by Tukey *post hoc* test.

CHAPTER III

“Nr4a2 as a potential therapeutic target for Alzheimer’s disease”

CHAPTER III

Nr4a2 as a potential therapeutic target for Alzheimer's disease

3.1. Nr4a2 hippocampal overexpression ameliorates the cognitive deficits observed in the $APP_{Sw,Ind}$ mouse model of AD

We have shown that Nr4a2 activation blocks hippocampal LTD **(figure 37)** and the oAβ-mediated decrease in pSer845-GluA1-AMPAR protein levels **(figure 47)** as well as the oAβ-mediated impairment of cLTP **(Figure 48)**. These synaptic plasticity processes are thought to be the basis for particular types of learning and memory (Collingridge et al., 2010; Lynch, 2004; Malenka & Bear, 2004; Neves, Cooke & Bliss, 2008; Nicoll, 2017). Nevertheless, AD is characterized not only for cognitive deficits but also for behavioral disturbances that severely affect the progression of the pathology. Thus, our previous findings prompted us to study whether Nr4a2 hippocampal overexpression could ameliorate the three main behavioral features of AD, which are the cognitive loss, the Behavioral and Psychological Symptoms of Dementia (BPSD)-like behaviors and the abolishment of daily living activities, previously described to be altered in mouse models of AD (Baeta-Corral, Johansson & Giménez-Llort, 2018; España et al., 2010a; Torres-Lista & Giménez-Llort, 2013). To study that, we overexpressed the full length Nr4a2 construct with a V5 epitope tag by using stereotaxic AAV injections at 4.5 month-old WT and $APP_{Sw,Ind}$ mice, a murine model of AD that shows age dependent Aβ pathology (see materials and methods, **figure 15**). Behavior and cognition were evaluated at 6 and 12 months of age, mimicking an early and mild stage of AD pathology (see materials and methods**, figure 17**). We used the AAV2/10 serotype, which has been characterized by high and specific gene transduction in neurons of the adult mice brain (Cearley & Wolfe, 2006). To confirm the efficient Nr4a2-V5-GFP hippocampal overexpression, we firstly checked the levels of Nr4a2 and GFP proteins in hippocampal-cultured neurons transduced with the AAV10.CMV.Nr4a2 construct by western blotting **(figure 50A)** and the levels of GFP and V5-tag by immunofluorescence **(figure 50B)**.

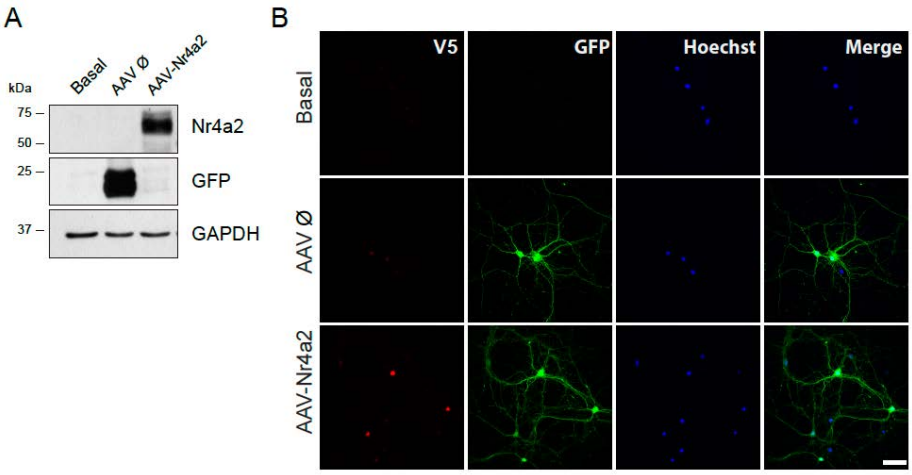

Figure 50. AAV efficiently overexpress Nr4a2.
Western Blot **(A)** and immunocytochemistry **(B)** of mature hippocampal-cultured neurons transduced with adenoassociate vectors (AAV2/10-Nr4a2.V5-GFP). Magnification, 40x; scale bar, 25 µm.

After completion of the behavior analysis, we also checked the levels of Nr4a2 and exogenous Nr4a2-V5 mRNA in the hippocampus of both WT and $APP_{Sw,Ind}$ mice at 6 and 12 months of age **(figure 51).**

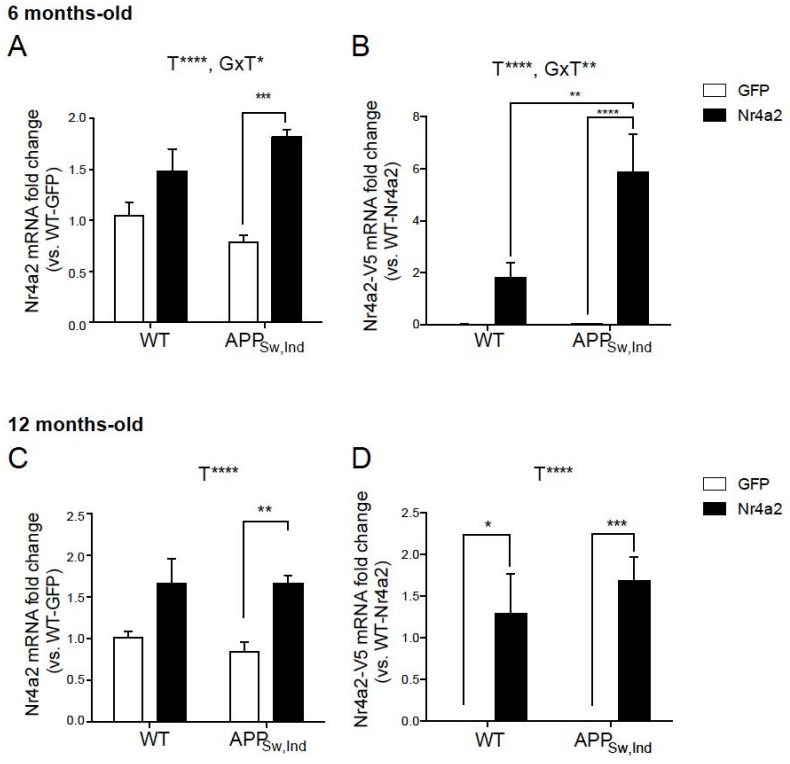

Figure 51. Verification of Nr4a2 overexpression in WT and $APP_{Sw,Ind}$ mice hippocampus at 6 and 12 months of age.
(A) Nr4a2 and Nr4a2-V5 mRNA levels in WT and $APP_{Sw,Ind}$ mice hippocampus at 6 months of age. **(B)** Nr4a2 and Nr4a2-V5 mRNA levels in WT and $APP_{Sw,Ind}$ mice hippocampus at 12 months of age. n = 5-7 mice/group. Data represent mean ± S.E.M. **p<0.01, ***p<0.001, ****p<0.001. Statistical analysis was determined by two-way ANOVA followed by Bonferroni *post hoc* test. The text at the top of each graph refers to the p-values of the two-way ANOVA. T, treatment effect; GxT, genotype x treatment interaction.

To examine the role of Nr4a2 in cognitive functions, specifically in spatial learning and memory, a key component of episodic memories that is hippocampus-dependent (Jeneson & Squire, 2011) and known to be affected in AD, mice were subjected to the MWM test (see materials and methods, **figure 18**). Distances covered to locate the platform in the cue learning task and the two first days of the acquisition phase are shown for both 6 and 12 months-old mice **(figure 52A,C)**. Learning acquisition was slower in $APP_{Sw,Ind}$ mice, covering more distance to reach the platform compared to WT mice, and was significantly restored by Nr4a2 overexpression, mimicking the same distance covered by the WT group to reach the platform the second day of the acquisition phase (distance in cm to reach the platform at PT2 of 6 months-old WT-GFP: 489.4 ± 56.6, WT-Nr4a2: 431.7 ± 65.7, $APP_{Sw,Ind}$-GFP: 661.9 ± 93, $APP_{Sw,Ind}$-Nr4a2: 431.89 ± 37; 12 months-old WT-GFP: 451 ± 66.1, WT-Nr4a2: 461.4 ± 95.3, $APP_{Sw,Ind}$-GFP: 629.5 ± 103, $APP_{Sw,Ind}$-Nr4a2: 487 ± 55.1).

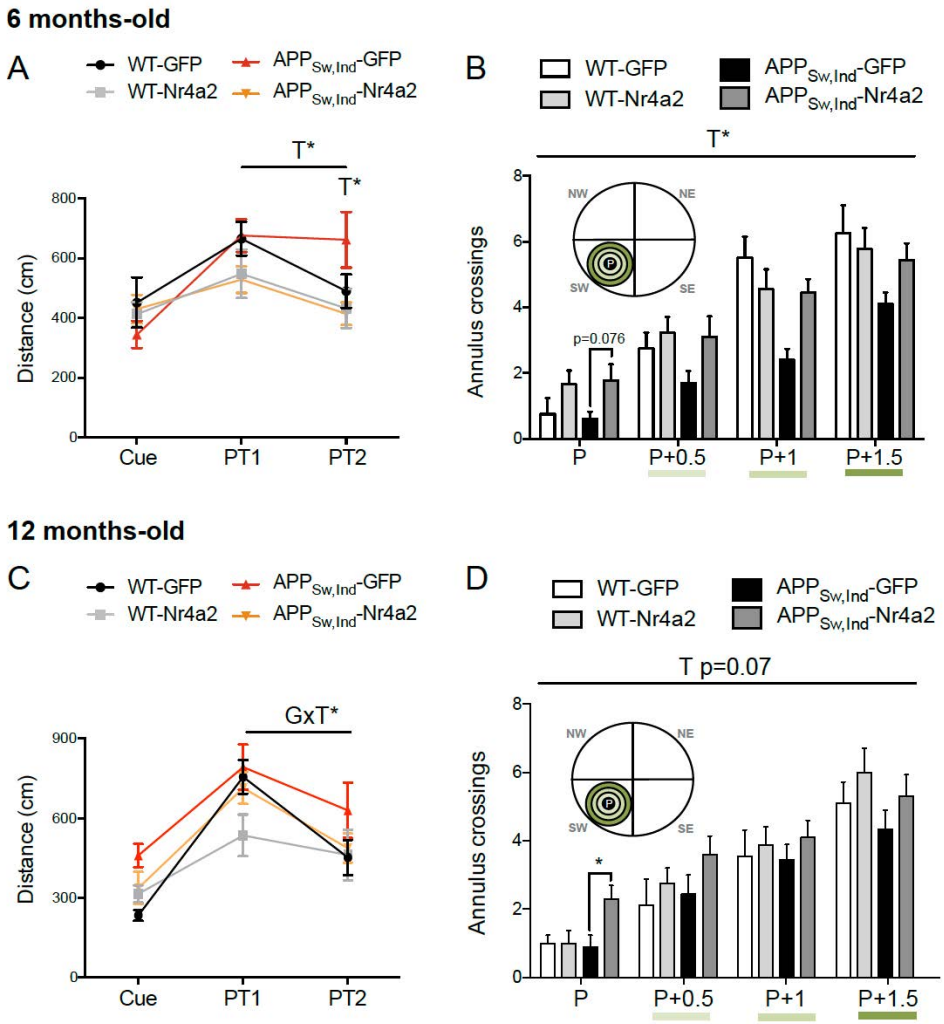

Figure 52. AAV-mediated Nr4a2 overexpression in the hippocampus ameliorates spatial learning and memory deficits in $APP_{Sw,Ind}$ mice assessed in the Morris water maze (MWM) test.
(A,C) Distance travelled to reach the platform in the cue and place learning tasks 1 and 2 (PT1, PT2) in 6 and 12 month-old WT and $APP_{Sw,Ind}$ mice with or without Nr4a2 overexpression. **(B,D)** Annulus crossings through the platform in the probe trial in 6 and 12 month-old WT and $APP_{Sw,Ind}$ mice with or without Nr4a2 overexpression. n = 8-10 mice/group. Data represent mean ± S.E.M. *p<0.05. Statistical analysis was determined by three-way ANOVA with repeated measures followed by Tukey *post hoc* test. The text at the top of each graph refers to the p-values of the three-way ANOVA. T, treatment effect; GxT, genotype x treatment interaction.

In the probe trial, $APP_{Sw,Ind}$ mice crossed less times the place where the platform was located, and $APP_{Sw,Ind}$-Nr4a2 mice crossed the same number of times as the WT group **(figure 52B,D)**, showing an effect of Nr4a2 overexpression not only in the learning, but also in the spatial memory.

To check that hippocampal overexpression of Nr4a2 was not affecting non-hippocampal dependent memories, mice were subjected to the NOR test, as the object recognition memory (ORM) does not require the dorsal hippocampus for retrieval (Vogel-Ciernia et al., 2013). This test is based in the spontaneous tendency of rodents to spend more time exploring a novel object than a familiar one. No significant differences in total exploration time were observed in the training at both ages **(figure 53A-C,F-G)**, meanwhile 6 month-old $APP_{Sw,Ind}$ mice showed a trend to explore more time the objects in the probe, even though it did not reach statistically significance **(figure 53D)**. However, preference for one object, although not significant, was observed in some experimental groups in the training phase at both ages, avoiding the correct interpretation of the results during the probe test. In the probe, at 6 months of age, the WT group showed poor memory for ORM, with no preference for the novel object **(figure 53E)**. This low performance of the WT group in the probe test impeded to take any conclusion about the effect of the Nr4a2 overexpression. Contrary, at 12 months of age, all four groups showed preference for the new object in the probe test, with no differences between genotype or Nr4a2 overexpression **(figure 53I)**, showing no ORM deficits in this cohort of $APP_{Sw,Ind}$ mice and no effect of Nr4a2 hippocampal overexpression.

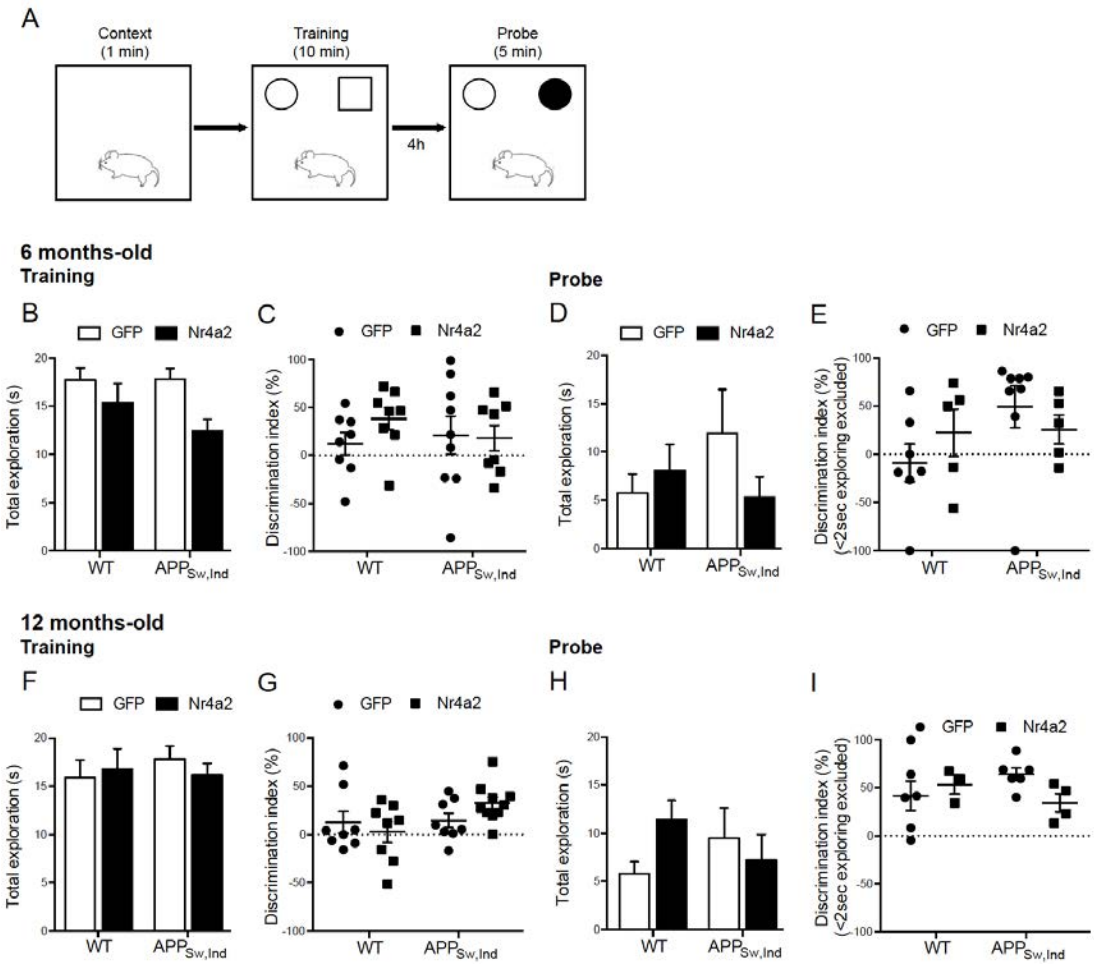

Figure 53. AAV-mediated Nr4a2 overexpression in the hippocampus does not change object recognition memory.
(A) Design of the novel object recognition (NOR) test used in this study. **(B-E)** Total exploration and discrimination index in the training and probe of the NOR test in 6 month-old WT and $APP_{Sw,Ind}$ mice with or without Nr4a2 overexpression. **(F-I)** Total exploration and discrimination index in the training and probe of the NOR test in 12 month-old WT and $APP_{Sw,Ind}$ mice with or without Nr4a2 overexpression. n = 8-10 mice/group. Data represent mean ± S.E.M. Statistical analysis was determined by two-way ANOVA followed by Bonferroni *post hoc* test.

The data presented so far indicate that Nr4a2 hippocampal overexpression is able to ameliorate hippocampus-dependent cognitive deficits such as spatial learning and memory impairments in the $APP_{Sw,Ind}$ mouse model of AD.

3.2. Nr4a2 hippocampal overexpression decreases the anxious profile and improves daily live activities in the $APP_{Sw,Ind}$ mouse model of AD

BPSDs such as anxiety are common clinical features of AD that significantly contribute to behavior disturbances. For that reason, we aimed to explore the effects of Nr4a2 hippocampal overexpression in the $APP_{Sw,Ind}$ mouse model of AD not only in cognition, but also in BPSD-like behaviors.

Firstly, neophobia to a new home-cage was analyzed by horizontal locomotor activity assessed by visited corners and vertical locomotor activity measured by rearings in the 30 seconds corner test, but no changes were observed **(annex 3)**. Then, anxiety-like behaviors and locomotion were evaluated in the open field (OF) test, a paradigm known to be a forced exploration test because the animals are confronted with an entirely new environment. Behavior in the central area was reduced in $APP_{Sw,Ind}$ mice both at 6 and 12 months of age, indicating an anxious profile, and completely restored by Nr4a2 hippocampal overexpression (time spent in the center of the open field, in seconds, of 6 months-old WT-GFP: 31.5 ± 4.4, WT-Nr4a2: 30.4 ± 5.1, $APP_{Sw,Ind}$-GFP: 13.2 ± 2.6, $APP_{Sw,Ind}$-Nr4a2: 35.1 ± 7.1; 12 months-old WT-GFP: 31.9 ± 4.4, WT-Nr4a2: 35.3 ± 5.1, $APP_{Sw,Ind}$-GFP: 19.9 ± 3.8, $APP_{Sw,Ind}$-Nr4a2: 47.9 ± 6.4) **(figure 54A-D)**. Importantly, overall exploratory behavior, shown as total distance travelled and mean speed, did not differ among groups, ruling out any locomotion deficit **(figure 54E-H)**.

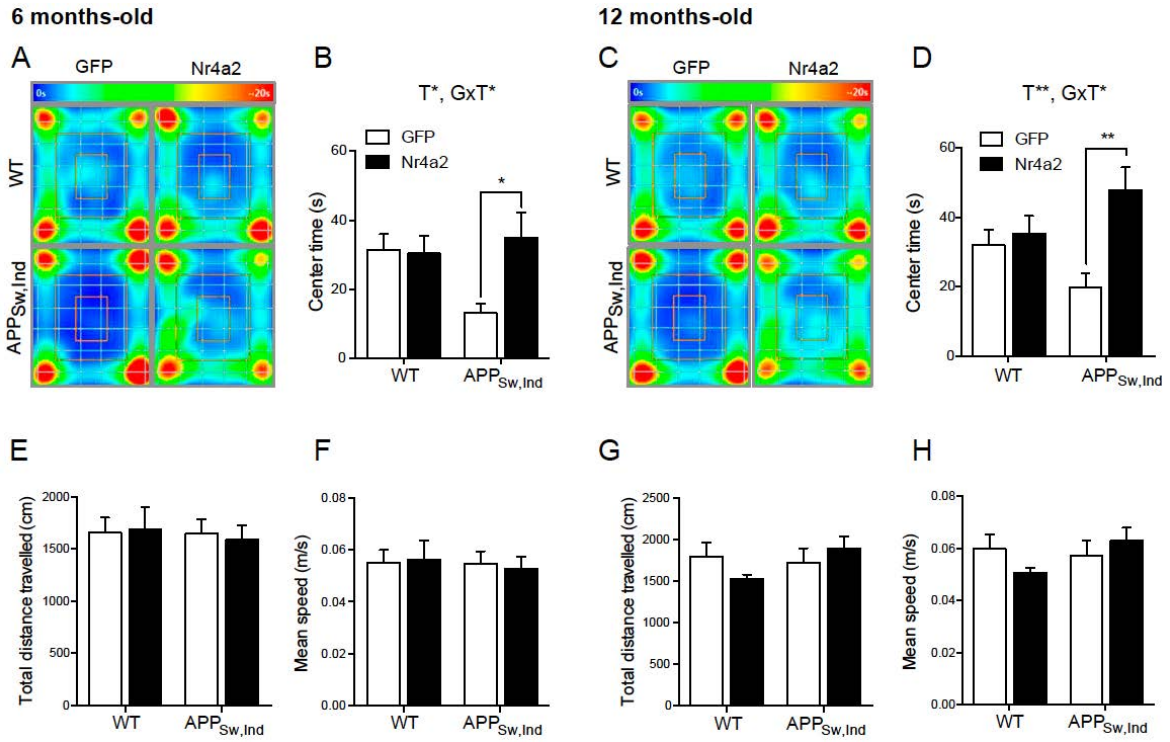

Figure 54. AAV-mediated Nr4a2 overexpression in the hippocampus decreases anxiety in $APP_{Sw,Ind}$ mice assessed in the open field test.
(A-D) Heat maps and time spent in the center of the field during the OF test of 6 and 12 month-old WT and $APP_{Sw,Ind}$ mice with or without Nr4a2 overexpression. **(E-H)** Total distance travelled and mean speed during the OF test. n = 8-10 mice/group. Data represent mean ± S.E.M. *p<0.05, **p<0.01. Statistical analysis was determined by two-way ANOVA followed by Bonferroni *post hoc* test. The text at the top of each graph refers to the p-values of the two-way ANOVA. T, treatment effect; GxT, genotype x treatment interaction.

Reduced anxiety-related behaviors of $APP_{Sw,Ind}$-Nr4a2 mice in the OF test were observed not only by more time spend in the center of the field compared to their age and genotype-matched $APP_{Sw,Ind}$ littermates, but also with less total wall rearings (WR) (total WR of 6 months-old WT-GFP: 32.5 ± 1.5, WT-Nr4a2: 33 ± 3.3, $APP_{Sw,Ind}$-GFP: 38 ± 3, $APP_{Sw,Ind}$-Nr4a2: 29.7 ± 3.3; 12 months-old WT-GFP: 35.2 ± 3.8, WT-Nr4a2: 27.8 ± 1.2, $APP_{Sw,Ind}$-GFP: 42.7 ± 4.4, $APP_{Sw,Ind}$-Nr4a2: 29.7 ± 2.1) **(figure 55A,D)** and WR per minute as function of time **(figure 55B,E)**, as well as less self-grooming behavior (time of self-grooming, in seconds, of 6 months-old WT-GFP: 3 ± 1, WT-Nr4a2: 2.9 ± 0.6, $APP_{Sw,Ind}$-GFP: 4.4 ± 1.2, $APP_{Sw,Ind}$-Nr4a2: 3 ± 0.7; 12 months-old WT-GFP: 3 ± 0.6, WT-Nr4a2: 3.5 ± 0.4, $APP_{Sw,Ind}$-GFP: 5.5 ± 1.2, $APP_{Sw,Ind}$-Nr4a2: 2.9 ± 0.5) **(figure 55C,F)**. Other parameters analyzed during the OF test are shown in **annex 3**.

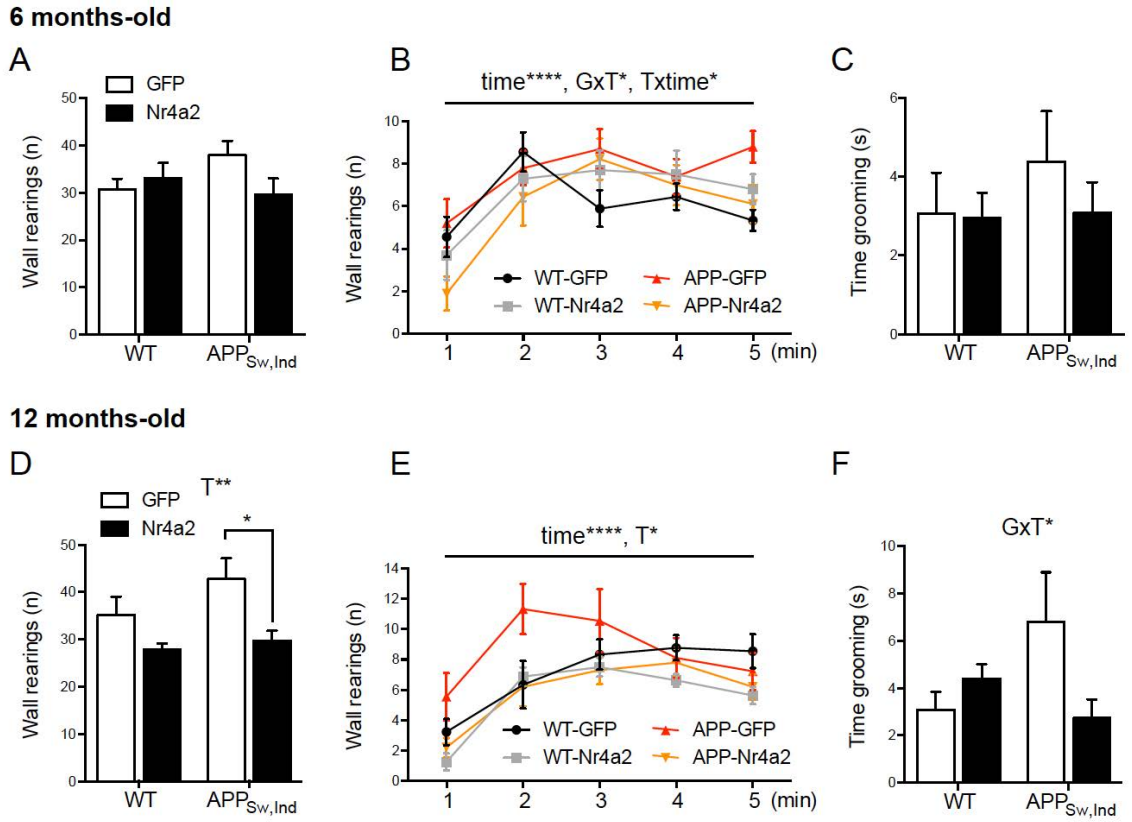

Figure 55. AAV-mediated Nr4a2 overexpression in the hippocampus reduces BPSD-like behaviors in $APP_{Sw,Ind}$ mice assessed in the open field test (OFT).
(A,B) Total and across time wall rearings (WR) and **(C)** time of self-grooming during the OFT of 6 month-old WT and $APP_{Sw,Ind}$ mice with or without Nr4a2 overexpression. **(D,E)** Total and across time wall rearings (WR) and **(F)** time of self-grooming during the OFT of 12 month-old WT and $APP_{Sw,Ind}$ mice with or without Nr4a2 overexpression. n = 8-10 mice/group. Data represent mean ± S.E.M. *p<0.05, **p<0.01, ****p<0.0001. Statistical analysis was determined by two-way ANOVA followed by Bonferroni *post hoc* test or three-way ANOVA with repeated measures followed by Tukey *post hoc* test (B,E). The text at the top of each graph refers to the p-values of the ANOVA test performed. T, treatment effect; GxT, genotype x treatment interaction; Txtime, treatment x time interaction.

Reduction of anxiety-related behaviors in the $APP_{Sw,Ind}$ mice after Nr4a2 overexpression was also denoted in some correlations found. A positive correlation between the number of visited corners in the CT and the WR performed in the first minute of the OF test was found both at 6 and 12 months-old mice (6 months-old mice Pearson's correlation r = 0.53, p = 0.001; 12 months-old mice Pearson's correlation r = 0.47, p = 0.004), being the $APP_{Sw,Ind}$ group the one visiting more corners in the CT and performing more WR in the first minute of the OF test and denoting, therefore, an anxious profile, completely restored by Nr4a2 overexpression. A negative correlation between the time to initiate movement and the WR performed in the first minute of the OF test was also found both at 6 and 12 months-old mice (6 months-old mice p = 0.016 r = -0.387; 12 months-old mice p = 0.001 r = -0.553), strengthening the anxious profile of the $APP_{Sw,Ind}$ group.

We also analyzed fear-related freezing responses in the contextual fear conditioning (CFC) test. Fear responses reflect neophobic and/or anxious behavior, overcoming deficits of conditioned memories in some mouse models of AD. Although it did not reach significance, $APP_{Sw,Ind}$ mice displayed increased freezing in comparison with age-matched WT mice both at 6 and 12 months of age at 2 and 24 hours post-shock, consistent with the increased unconditioned fear responses in the $APP_{Sw,Ind}$ mice previously reported (España et al., 2010a). Nr4a2 overexpression reduced freezing responses in $APP_{Sw,Ind}$ mice at 2 and 24 hours post-shock compared to their age and genotype-matched $APP_{Sw,Ind}$ littermates, reaching almost the freezing levels of the WT group (percentage of time freezing at 2 hours post-shock of 6 months-old WT-GFP: 12.38 ± 2.7, WT-Nr4a2: 22.15 ± 5.1, $APP_{Sw,Ind}$-GFP: 27.05 ± 7.5, $APP_{Sw,Ind}$-Nr4a2: 16.8 ± 4.01; and at 24 hours post-shock of WT-GFP: 23.3 ± 6.8, WT-Nr4a2: 38.8 ± 2.8, $APP_{Sw,Ind}$-GFP: 47.6 ± 10.1, $APP_{Sw,Ind}$-Nr4a2: 36.1 ± 11.6; at 2 hours post-shock of 12 months-old WT-GFP: 9.45 ± 1.8, WT-Nr4a2: 9.96 ± 2.3, $APP_{Sw,Ind}$-GFP: 14.25 ± 3, $APP_{Sw,Ind}$-Nr4a2: 7.65 ± 2.8; and at 24 hours post-shock of WT-GFP: 15.02 ± 3.4, WT-Nr4a2: 21.04 ± 3.7, $APP_{Sw,Ind}$-GFP: 20.8 ± 5.3, $APP_{Sw,Ind}$-Nr4a2: 13.8 ± 3.6) **(figure 56).** Noteworthy, a genotype x treatment significant interaction was found both at 2 and 24 hours post-shock when both ages were analyzed together since Nr4a2 overexpression increased the freezing response in WT mice.

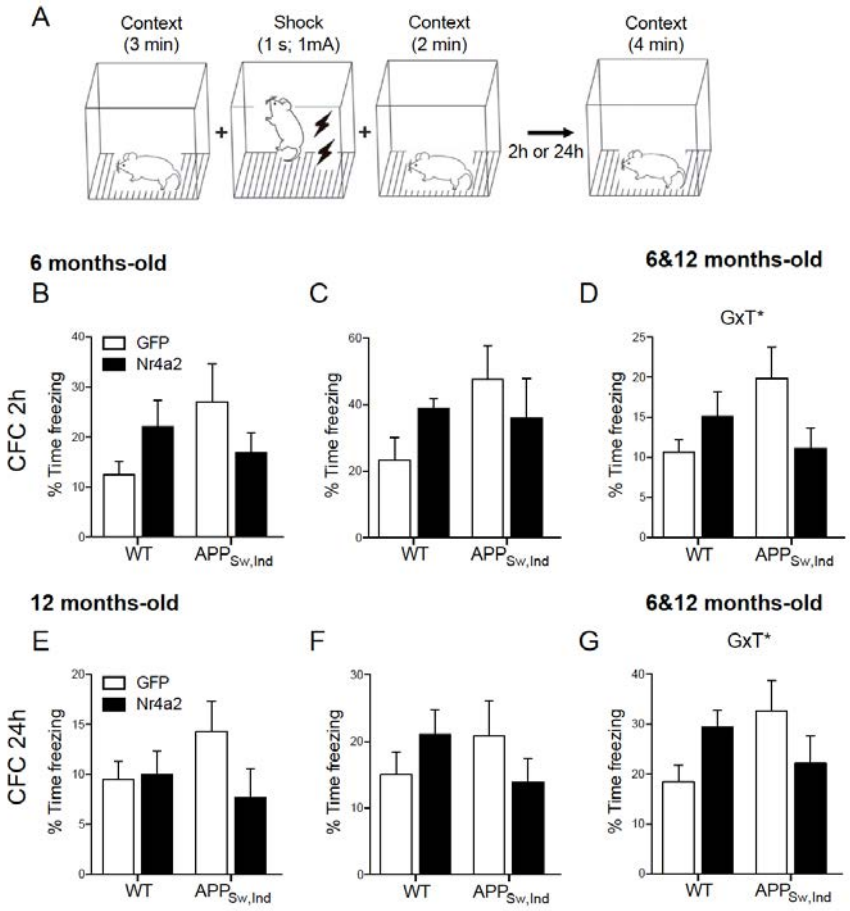

Figure 56. AAV-mediated Nr4a2 overexpression in the hippocampus reduces anxiety in $APP_{Sw,Ind}$ mice assessed in the contextual fear conditioning test (CFC).
(A) Design of the CFC test used in this study. **(B-D)** Freezing responses measured at 2 hours after training (context plus shock) of WT and $APP_{Sw,Ind}$ mice with or without Nr4a2 overexpression at 6, 12 and 6+12 months of age. **(E-G)** Freezing responses measured at 24 hours after training (context plus shock) of WT and $APP_{Sw,Ind}$ mice with or without Nr4a2 overexpression at 6, 12 and 6+12 months of age. n = 8-10 mice/group. Data represent mean ± S.E.M. *p<0.05. Statistical analysis was determined by two-way ANOVA followed by Bonferroni *post hoc* test. The text at the top of each graph refers to the p-values of the two-way ANOVA. T, treatment effect; GxT, genotype x treatment interaction.

Mice were also tested in the marble-burying test (MBT), considered to model the spectrum of anxiety, psychotic and obsessive-compulsive like symptoms (Angoa-Pérez et al., 2013). The burying of a marble is a natural defense mechanism in mice that occurs under conditions of stress or states of anxiety. The qualitative (three levels of interaction: intact, change of position and buried marbles) and quantitative analysis of the MBT showed that $APP_{Sw,Ind}$ mice buried a higher number of marbles compared to WT mice at 6 months, reproducing BPSD-like behaviors. Previous evidence of increase burying in the MBT in animal models of AD was shown in 3xTg-AD mice (Torres-Lista, López-Pousa & Giménez-Llort, 2015). Interestingly, we found that Nr4a2 overexpression reduced the number of buried marbles in $APP_{Sw,Ind}$ mice compared to their age and genotype-matched $APP_{Sw,Ind}$ littermates **(figure 57)**. In **figure 57A** we can see that $APP_{Sw,Ind}$ mice buried

around 40% of the marbles (the total number of marbles was 9), meanwhile $APP_{Sw,Ind}$-Nr4a2 mice only buried among 15% of the marbles after 15 minutes of test. However, Nr4a2 overexpression increased the number of buried marbles in WT mice (buried marbles after 15 minutes of test of 6 months-old WT-GFP: 1.8 ± 0.46, WT-Nr4a2: 3.2 ± 0.6, $APP_{Sw,Ind}$-GFP: 3.6 ± 0.8, $APP_{Sw,Ind}$-Nr4a2: 1.4 ± 0.5; 12 months-old WT-GFP: 2.7 ± 0.76, WT-Nr4a2: 3.7 ± 0.72, $APP_{Sw,Ind}$-GFP: 2.8 ± 0.9, $APP_{Sw,Ind}$-Nr4a2: 1.3 ± 0.5) **(Figure 57)**. By contrast, at 12 months of age, there were no differences in the number of buried marbles between WT and $APP_{Sw,Ind}$ mice even though Nr4a2 overexpression reduced the number of buried marbles in the $APP_{Sw,Ind}$ mice.

A positive correlation was found between the number of buried marbles in the MBT and the time freezing in the CFC test at 2 hours post-shock at 6 months of age (Pearson's correlation r = 0.44, p = 0.02).

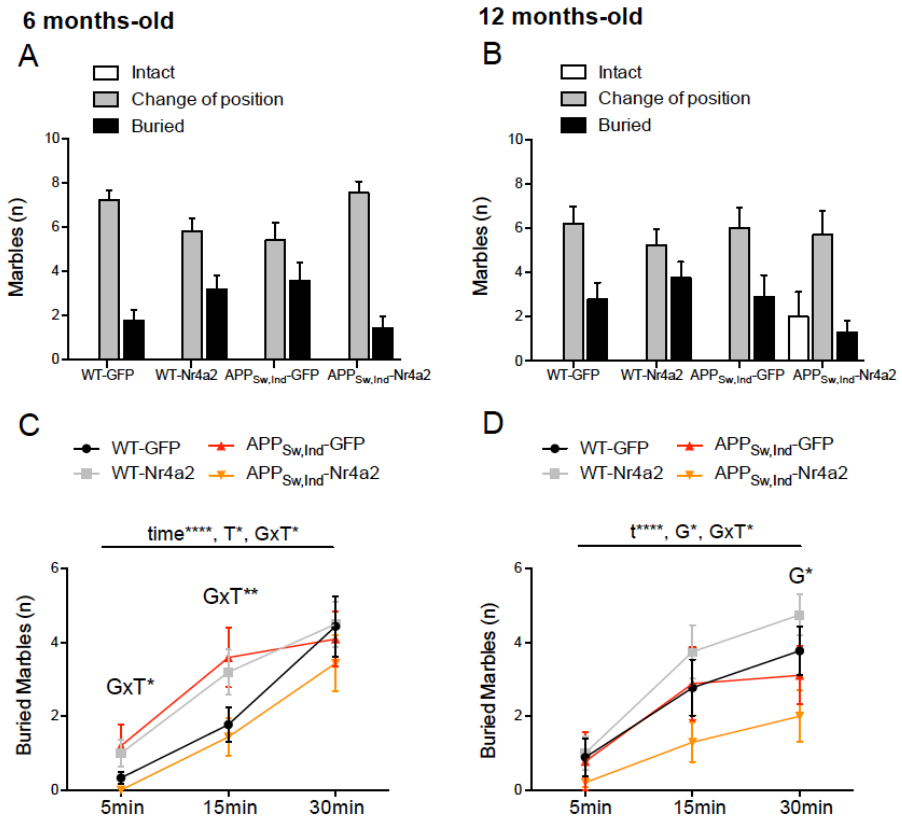

Figure 57. AAV-mediated Nr4a2 overexpression in the hippocampus reduces BPSD-like behaviors in $APP_{Sw,Ind}$ mice assessed in the marble burying test (MBT).
(A,B) Number of intact, change of position and buried marbles after 15 minutes in the MBT in 6 and 12 month-old WT and $APP_{Sw,Ind}$ mice with or without Nr4a2 overexpression. **(C,D)** Buried marbles across time in the MBT in 6 and 12 month-old WT and $APP_{Sw,Ind}$ mice with or without Nr4a2 overexpression. n = 8-10 mice/group. Data represent mean ± S.E.M. *p<0.05, **p<0.01. Statistical analysis was determined by two-way ANOVA followed by Bonferroni *post hoc* test (A,B) or three-way ANOVA with repeated measures followed by Tukey *post hoc* test (C,D). The text at the top of each graph refers to the p-values of the three-way ANOVA. G, genotype effect; GxT, genotype x treatment interaction.

We also examined executive functions and daily live activities, since typical natural behaviors are excellent ethological scenarios to reflect BPSD-like behaviors or cognitive disturbances. Therefore, to check whether Nr4a2 overexpression had any impact on naturally occurring daily life activities, we evaluated the nest building. Previous studies have reported impaired nest building in distinct mouse models of AD (Deacon et al., 2008; Filali & Lalonde, 2009; Torres-Lista & Giménez-Llort, 2013; Wesson & Wilson, 2011). When assessing well-being in the nest-building test, $APP_{Sw,Ind}$ mice at 12 months of age showed less nest-building ability compared to the WT group and less bitting score, and Nr4a2 overexpression increased both nesting and bitting activities in $APP_{Sw,Ind}$ mice, although it did not reach significance (nesting score after 72 hours of WT-GFP: 4 ± 0.33, WT-Nr4a2: 4 ± 0.26, $APP_{Sw,Ind}$-GFP: 3.5 ± 0.37, $APP_{Sw,Ind}$-Nr4a2: 4.4 ± 0.26; bitting score after 72 hours of WT-GFP: 4.1 ± 0.38, WT-Nr4a2: 4 ± 0.37, $APP_{Sw,Ind}$-GFP: 3 ± 0.4, $APP_{Sw,Ind}$-Nr4a2: 4.3 ± 0.3) **(figure 58)**.

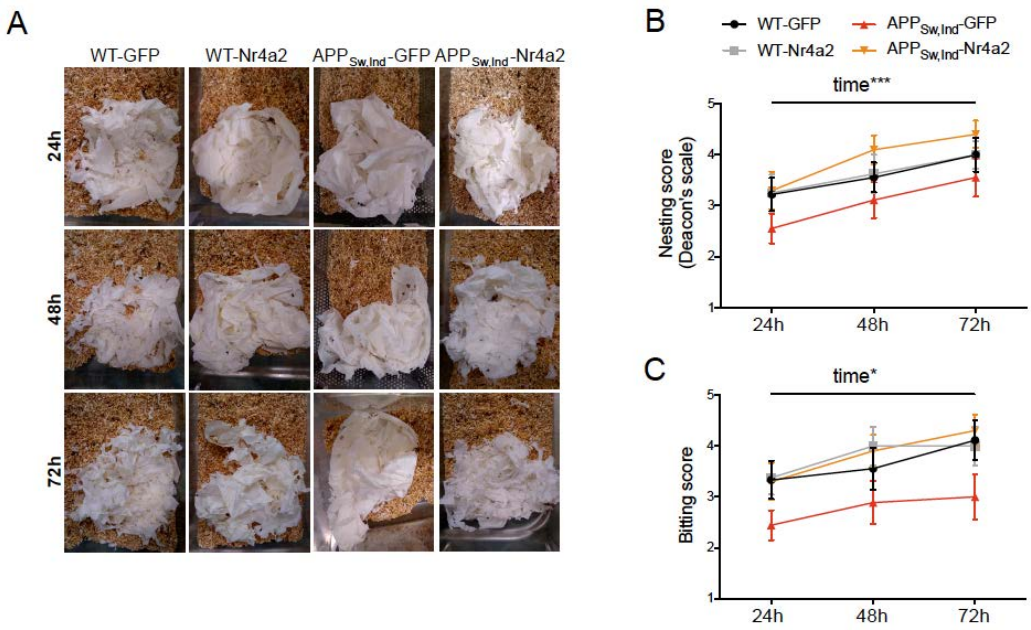

Figure 58. AAV-mediated Nr4a2 overexpression in the hippocampus improves the well-being in $APP_{Sw,Ind}$ mice assessed in the nest building test.
(A) Representative images of nest building at 24, 48 and 72h of 12 month-old WT and $APP_{Sw,Ind}$ mice with or without Nr4a2 overexpression. **(B,C)** Quantification of nest building and bitting according to Deacon's and bitting scale, respectively. n = 8-10 mice/group. Data represent mean ± S.E.M. *p<0.05, ***p<0.001. Statistical analysis was determined by three-way ANOVA with repeated measures followed by Tukey *post hoc* test.

Finally, mice also performed the tail suspension test. Hindlimb clasping has been shown to occur in various neurodegenerative mouse models (Lieu et al., 2013) as well as in various mouse models of AD (Lalonde & Strazielle, 2011). We found a significant difference between genotypes, were 12 months-old $APP_{Sw,Ind}$ mice were more prone to clasp but no effects of Nr4a2 overexpression were found **(figure 59).**

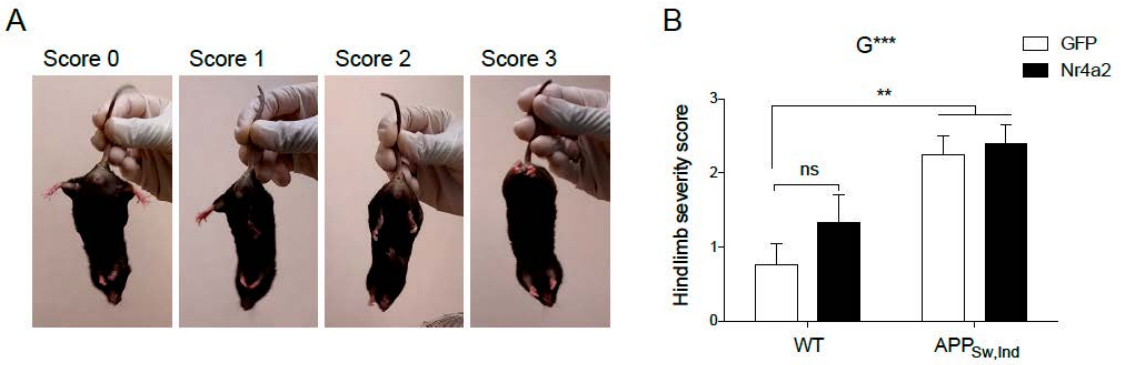

Figure 59. Hindlimb clasping in the $APP_{Sw,Ind}$ mice is not modified by AAV-mediated Nr4a2 overexpression in the hippocampus.
(A) Representative images of hindlimb clasping severity scores. **(B)** Quantification of hindlimb clasping behavior in 12 month-old WT and $APP_{Sw,Ind}$ mice with or without Nr4a2 overexpression. n = 8-10 mice/group. Data represent mean ± S.E.M. **p<0.01. Statistical analysis was determined by two-way ANOVA followed by Bonferroni *post hoc* test. T, treatment effect

A summary of the disturbances in daily life activities, BPSD-like behaviors and cognitive impairments observed in the $APP_{Sw,Ind}$ mice and the effect of the hippocampal Nr4a2 overexpression over them is shown in **figure 60**.

Behavioral domain	Behavioral test	Genotype	Nr4a2
Sensorimotor			
Reflexes	Hindlimb clasping	↑	
Locomotor			
Horizontal locomotor activity	Open field test		
Vertical locomotor activity	Open field test	↑	✓
Daily life activities	Nesting	↓	✓
Neuropshychiatric-like			
Neophobia	Corner test		
Anxiety	Open field test	↑	✓
	Contextual fear conditioning test	↑	✓
	Marble-burying test	↑	✓
Cognitive			
Recognition memory	Novel object recognition test		
Spatial learning	Morris Water maze	↓	✓
Spatial memory	Morris Water maze	↓	✓

Figure 60. Summary of hippocampal Nr4a2 overexpression effects at different behavioral domains on $APP_{Sw,Ind}$ mice.

3.3 Effects of Nr4a2 overexpression in the hippocampus of $APP_{Sw,Ind}$ mice

After behavioral analysis, we sought to determine changes in hippocampal protein levels that could explain the profiles observed in the cognitive abilities and BPSD-like behaviors after hippocampal Nr4a2 overexpression. As a preliminary approach, we analyzed protein levels of different subunits of both excitatory and inhibitory receptors and the neurotrophin

BDNF in whole hippocampal lysates of WT and $APP_{Sw,Ind}$ mice both at 6 and 12 months of age.

At 6 months-old, $APP_{Sw,Ind}$ mice presented decreased hippocampal protein levels of the neurotrophin BDNF, and also decreased protein levels of different subunits of iGluRs, both AMPARs and NMDARs, including GluA1, GluA2, GluN1 and GluN2B subunits, but Nr4a2 overexpression did not restore these levels. Moreover, Nr4a2 overexpression decreased GluN2A-NMDARs subunit and a genotype x treatment interaction was found in GluN1-NMDARs subunit **(figure 61)**.

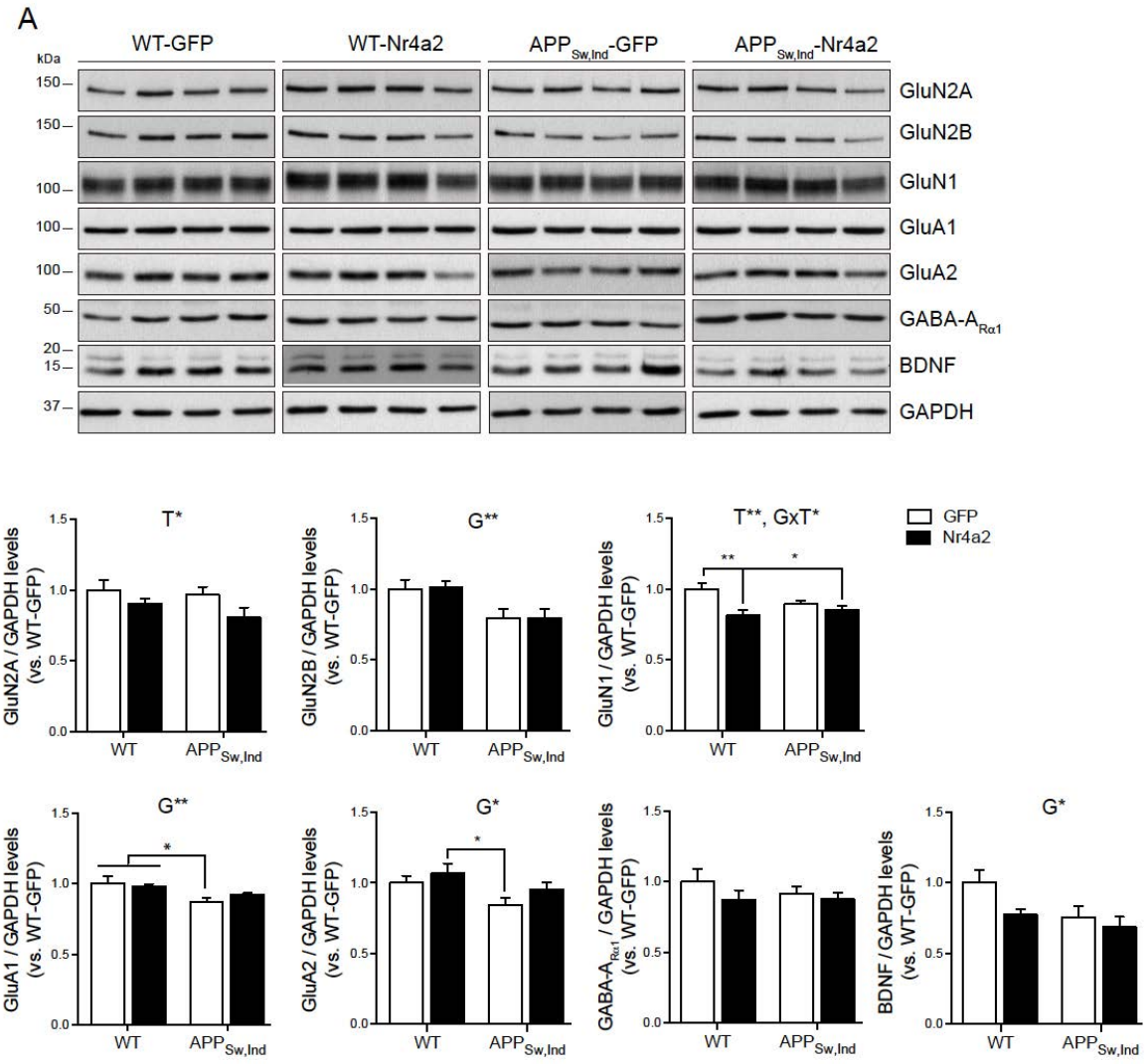

Figure 61. Analysis of the hippocampus of 6 month-old WT and $APP_{Sw,Ind}$ mice with or without Nr4a2 overexpression.
Representative image and protein levels quantification of different subunits of excitatory receptors (NMDAR: GluN2A, GluN2B, GluN1; AMPAR: GluA1, GluA2), inhibitory receptors (GABA-$_A$R) and neurotrpohins (BDNF) in the hippocampus of 6 month-old WT and $APP_{Sw,Ind}$ mice with or without Nr4a2 overexpression. n = 5-7 mice/group. Data represent mean ± S.E.M. **p<0.01. Statistical analysis was determined by two-way ANOVA followed by Bonferroni *post hoc* test. The text at the top of each graph refers to the p-values of the two-way ANOVA. G, genotype effect; T, treatment effect; GxT, genotype x treatment interaction.

At 12 months-old, $APP_{Sw,Ind}$ mice presented decreased hippocampal protein levels of both subunits of excitatory receptors, including GluA2, GluN1 and GluN2A subunits, and also inhibitory receptors such as the $GABA_AR\alpha1$ subunit. However, Nr4a2 overexpression failed to restore these levels. Moreover, Nr4a2 overexpression decreased GluN2B-NMDARs subunit and a genotype x treatment interaction was found in GluN1-NMDARs and GluA2-AMPARs subunits **(figure 62).**

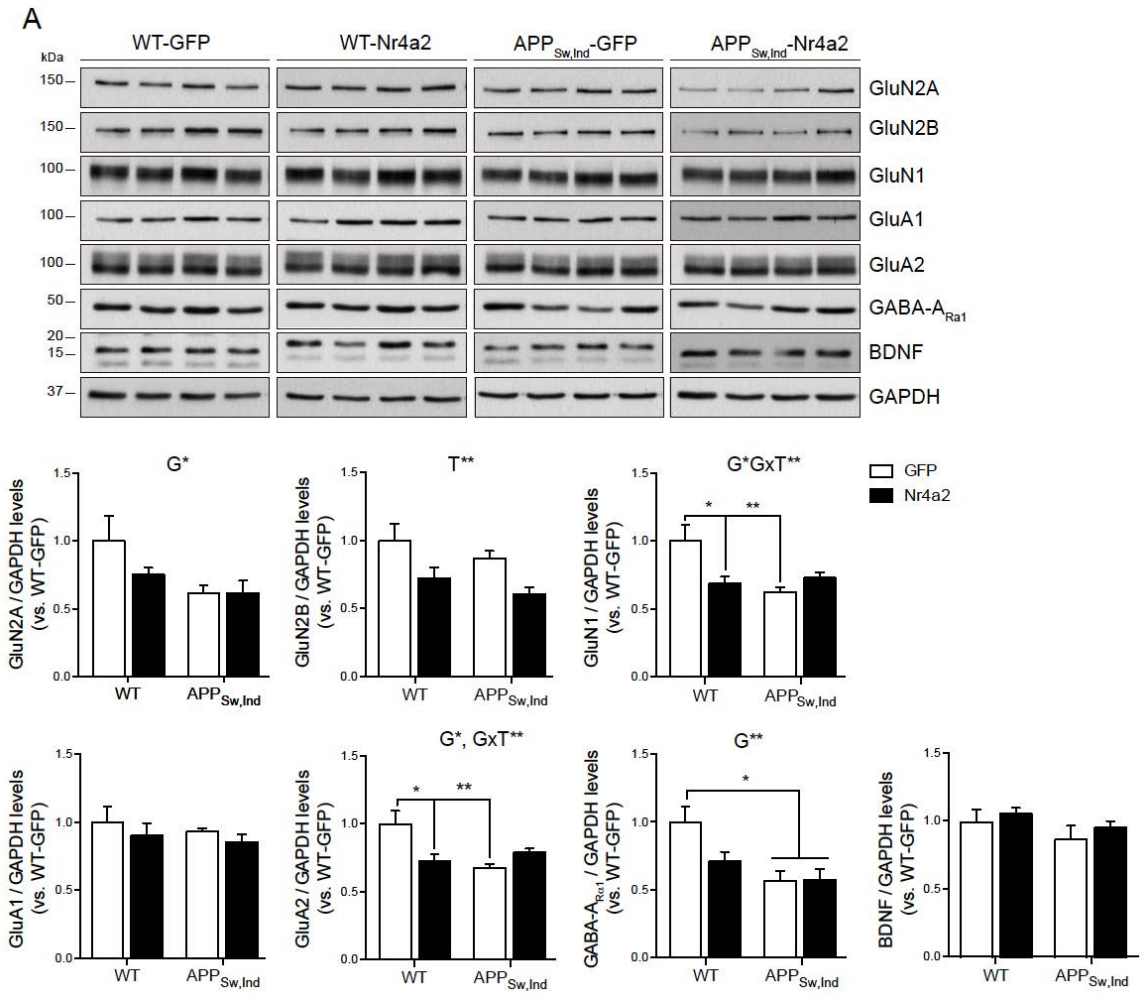

Figure 62. Analysis of the hippocampus of 12 month-old WT and $APP_{Sw,Ind}$ mice with or without Nr4a2 overexpression.

Representative image and protein levels quantification of different subunits of excitatory receptors (NMDAR: GluN2A, GluN2B, GluN1; AMPAR: GluA1, GluA2), inhibitory receptors ($GABA-_AR$) and neurotrpohins (BDNF) in the hippocampus of 12 month-old WT and $APP_{Sw,Ind}$ mice with or without Nr4a2 overexpression. n = 5-7 mice/group. Data represent mean ± S.E.M. **p<0.01. Statistical analysis was determined by two-way ANOVA followed by Bonferroni *post hoc* test. The text at the top of each graph refers to the p-values of the two-way ANOVA. G, genotype effect; T, treatment effect; GxT, genotype x treatment interaction.

VIII. Discussion

Despite several decades of research and investment, no disease-modifying therapy for Alzheimer's pathology has been found to date. AD is characterized by a long prodromal phase in which the pathophysiological process is already occurring but the clinical symptoms are still not present (Sperling, Mormino, & Johnson, 2014). The hippocampus, a brain area critical for learning and memory, is especially vulnerable to damage at early stages of AD (La Joie et al., 2013; Scheff et al., 2006, 2007) and seems to be the most severely affected brain area by the loss of synaptic proteins (Perez-Cruz et al., 2011). Indeed, hippocampal synaptic loss is currently established as the best neurobiological correlate of the cognitive decline observed in human AD patients and reflects the synaptic dysfunction that initiates the disease process (Bereczki et al., 2016; DeKosky & Scheff, 1990; Terry et al., 1991). Thus, interventions aimed to preserve or even restore synaptic plasticity will probably delay the onset or might even provide a cure for such devastating disorder.

Cognitive impairments, which begin early in the disease, have been attributed to oAβ-induced disruption of synaptic plasticity. Nevertheless, the underlying molecular mechanisms are yet to be fully understood. A substantial body of evidence indicates that activity-regulated transcriptional networks promote the refinement and plasticity of neuronal circuits, which are essential for cognitive functions. Likewise, downregulation of activity-dependent genes involved in synaptic plasticity and memory are associated with early learning and memory deficits in mouse models of AD (España et al., 2010b). Hence, it is becoming increasingly clear that understanding the transcriptional mechanisms that are disrupted at early stages of AD will provide novel therapeutic strategies targeting what is so far known to be the pathophysiological core of this pathology; the synaptic failure. In this sense, Nr4a transcription factors have emerged as promising candidates as they are involved in hippocampal synaptic plasticity and memory processes and are down-regulated at early stages in AD mouse models.

The present study has investigated the role of the activity-regulated Nr4a2 transcription factor in hippocampal synaptic plasticity and its involvement in the synaptic impairment that occurs at early stages of AD using a biochemical, electrophysiological and behavioral approach, with the goal to identify Nr4a2 as a potential therapeutic target for pre-clinical intervention in early AD.

1. Role of Nr4a2 in hippocampal synaptic plasticity

Previous reports have highlighted a role for the Nr4a family of transcription factors in hippocampal synaptic plasticity and cognitive functions (Bridi et al., 2017; Bridi & Abel,

2013; Hawk et al., 2012; McNulty et al., 2012; McQuown et al., 2011; Peña De Ortiz, Maldonado-Vlaar & Carrasquillo, 2000), but no data exist about the expression profile of Nr4a2 during hippocampal development. For that reason, we decided to start our studies by analyzing its expression in this brain area. We observed low levels of this transcription factor in mature hippocampal-cultured neurons and adult mice hippocampus, whereas much greater expression of Nr4a2 was found in immature hippocampal neurons. Although it is outside the scope of the present work, given the essential involvement of this transcription factor in the development of midbrain dopaminergic neurons (Jo et al., 2009; Saucedo-Cardenas et al., 1998; Sousa et al., 2007), it would be interesting to investigate a possible role of Nr4a2 in the development or maturation of other neuronal subpopulations such as hippocampal glutamatergic neurons. This possibility is reinforced by the fact that Nr4a2 is involved in hippocampal neurogenesis and it has been described to be preferentially expressed by early-born granule cells (Imura et al., 2019).

Moon and colleagues described that Nr4a2-positive cells were abundantly expressed in CA1 of the hippocampus. Hippocampal CA3 exhibited moderate numbers of Nr4a2-immunoreactive cells and the DG showed the weakest Nr4a2 immunoreactivity (Moon et al., 2015). Notably, we confirmed that Nr4a2 was mostly expressed in CA1 and CA3 rather than DG hippocampal subregion. In DG, Nr4a2 positive cells were sparsely distributed within the granule cell layer although high expression was found in hilar neurons of the DG polymorphic layer. Moreover, we described for the first time the expression profile of Nr4a2 in CA1 through development, a hippocampal subregion essential for synaptic plasticity and certain types of learning and memory (Tsien, Huerta & Tonegawa, 1996).

The induction of specific gene expression patterns in response to activity confers functional plasticity to neurons. In this regard, activity-dependent regulation of Nr4a2 mRNA expression was previously described in cortical neurons using pharmacological manipulations such as elevation of extracellular K^+ or increasing the intracellular concentration of cAMP using FSK (España et al., 2010b; Parra-Damas et al., 2014, 2017a). Importantly, we showed that both mRNA and also Nr4a2 protein levels in mature hippocampal-cultured neurons were regulated by neuronal activity using a better physiological-related stimulus such as the GABA-A receptor antagonist bicuculline.

Nr4a2, as an orphan nuclear receptor, is not regulated by classical endogenous ligands or transcriptional coactivators. Nr4a2 activity is mainly regulated at the level of gene expression and protein stability (Maxwell & Muscat, 2006). For that reason, Nr4a2 degradation emerged as one of the main regulators of Nr4a2 half-life, subcellular location and transcriptional activity. Nr4a2 can be both ubiquitinated and also sumoylated by

PIASγ, a SUMO-E3 ligase (Alvarez-Castelao, Losada, Ahicart, & Castaño, 2013; Arredondo et al., 2013). Moreover, previous data reported that the proteasome pathway was responsible for Nr4a2 degradation in PC12 cells, being this degradation dependent on its N-terminal region (aminoacids 1 to 31) (Alvarez-Castelao et al., 2013). In that sense, we found that not only neuronal activity, but also proteasomal inhibition significantly increased Nr4a2 protein levels in basal conditions and after a long-lasting (24 hours of bicuculline treatment) neuronal stimulation paradigm in mature hippocampal-cultured neurons. To fully confirm the involvement of the proteasome in the activity-dependent modulation of Nr4a2 in mature hippocampal-cultured neurons, it would be necessary to measure the levels of ubiquitinated and sumoylated Nr4a2 at different times of bicuculline treatment. Furthermore, it would be interesting to study whether synaptic activity is able to increase Nr4a2 protein levels in neurons transfected with a deleted N-terminal Nr4a2 construct, in order to elucidate whether the increase in Nr4a2 protein levels after activity is dependent on the induction-degradation balance.

Next, we wondered what mechanisms underlie the activity-dependent regulation of Nr4a2. Calcium-signaling pathways are essential for synaptic plasticity processes, such as hippocampal LTD and LTP, and also for activity-regulated transcription in neurons (Ghosh & Greenberg, 1995). Therefore, we hypothesized that it was also a requirement for Nr4a2 transcription in mature hippocampal-cultured neurons. Transcription of early genes normally occurs in response to calcium influx through VDCC (Ma et al., 2014), although other sources of calcium such as ligand-gated ion channels (AMPAR and NMDAR) or intracellular stores also participate (West & Greenberg, 2011). Contrary to previous data by Tokuoka and colleagues, who propose L-type VDCC and calcineurin as mediators of Nr4a2 induction after K^+/bicuculline stimulus (Tokuoka et al., 2014), we found that Nr4a2 induction after bicuculline treatment, without further depolarization using extracellular K^+, relies on iGluRs-mediated calcium entry, which activates calcineurin and the CREB/CRTC1 signaling pathway. This discrepancy could be caused by the use of extracellular K^+ as a neuronal stimulus, a long-established stimulation paradigm that fails to reproduce physiological conditions and thus engage different mechanisms.

Calcineurin activity is known to be required for CREB-mediated gene expression (Lam et al., 2009) since it is responsible for the dephosphorylation and consequent activation of the CREB coactivator CRTC1 (Bittinger et al., 2004). Notably, we found that calcineurin was not regulating Nr4a2 activity-dependent induction only through CRTC1 dephosphorylation. Therefore, a possible direct modulation of Nr4a2 through calcineurin activity or a secondary mediator could also be involved in the activity-dependent induction of Nr4a2. A possible candidate could be nuclear factor of activated T cells (NFAT), whose

activity is regulated by calcineurin and it has been involved in Nr4a2 induction in other cell types (Liu et al., 2003). Moreover, consistent with previous findings in cortical neurons (Parra-Damas et al., 2017b), we demonstrated that bicuculline-mediated neuronal activity induces a significant binding of CRTC1 to the proximal CRE/TATA promoter region of Nr4a2 meanwhile CREB binding was already observed in absence of neuronal stimulation.

Activity-dependent transcription collaborates with local dendritic translation to encode stimulus-specificity in the genome binding of some transcription factors (Brigidi et al., 2019). Transcription factors can localize at dendritic spines thereby regulating specific synaptic structural and molecular changes crucial for learning and memory functions. mRNA trafficking and translation are controlled by regulatory elements in the 5' and 3' UTRs of mRNAs. Interestingly, there are different mRNA splice variants of Nr4a2 that have different sizes for 3'-UTR (Pereira et al., 2017). Nevertheless, it remains to be explored whether they can be localized and translated at dendrites. Moreover, a key feature that distinguishes neurons from other cells is the degree to which they use spatial location to encode the meaning of intercellular communication. Therefore, it would be exciting to examine whether different stimuli could lead to different spatial dynamics in Nr4a2 translation.

In the last decade, several synaptonuclear protein messengers including Jacob, CRTC1, AIDA-1, ProSaP2/Shank3 and RNF10 have been identified and characterized as key players in synaptic plasticity processes (Marcello, Di Luca & Gardoni, 2018). Moreover, numerous recent studies have demonstrated that their modulation could represent a novel therapeutical approach in the pathogenesis of synaptopathies such as AD. For that reason, we wanted to address the subcellular localization of Nr4a2 in mature hippocampal-cultured neurons. Subcellular localization of Nr4a2 is controlled by specific nuclear import and export signals. As a transcription factor, Nr4a2 is mostly nuclear, but specific stimuli such as oxidative stress, promote Nr4a2 nuclear export in dopaminergic neuronal cell lines (García-Yague et al., 2013). We found that, in response to neuronal activity, Nr4a2 protein levels increased both in the cytosolic and nuclear fractions of mature hippocampal-cultured neurons. Furthermore, we demonstrated for the first time the presence of Nr4a2 in the PSD of both cultured-hippocampal neurons in response to neuronal activity and adult mice hippocampal tissue. These results suggest that Nr4a2 could emerge as a synaptonuclear protein messenger associated to hippocampal synaptic plasticity processes. Future experiments could address whether Nr4a2 protein levels in the PSD of cultured-hippocampal neurons in response to neuronal activity are affected by the presence of oAβ. Furthermore, it would be interesting to study whether

Nr4a2 protein levels could also increase in the hippocampal PSD after memory-inducing activities in mice, such as learning and other hippocampus-dependent tasks, and whether these levels are altered in mice models of AD, both at rest or after activity.

Nr4a2 transcription factor regulates several genes implicated in hippocampal synaptic plasticity and memory formation (Hawk et al., 2012; Volpicelli et al., 2007). Among them, BDNF emerges as a major candidate by which Nr4a2 influences synaptic plasticity and memory (Barneda-Zahonero et al., 2012). BDNF is a neurotrophic factor that has been widely described as a modulator of synaptic plasticity (Zagrebelsky & Korte, 2014) and the formation and long-term persistence of hippocampus-dependent memories (Bekinschtein, Cammarota & Medina, 2014; Miranda et al., 2019). We were able to confirm the requirement of Nr4a2 for basal and activity-mediated BDNF production in mature hippocampal-cultured neurons by loss and gain-of-function studies using lentiviral-mediated Nr4a2 knockdown and specific Nr4a2 agonists, respectively.

Previous studies have shown that BDNF regulates the expression, trafficking and activity of ionotropic glutamate receptors (Caldeira et al., 2007a,b; Zhang et al., 2018). Specifically, it has been reported that BDNF up-regulates the protein levels of AMPAR subunits in hippocampal neurons and induces the delivery of GluA1-AMPARs to the synapse by a protein synthesis-dependent mechanism (Caldeira et al., 2007a). It has also been described that BDNF increases the amount of GluN1, GluN2A and GluN2B subunits of NMDARs associated with the plasma membrane in cultured-hippocampal neurons (Caldeira et al., 2007b), although the current understanding of the regulation of NMDARs by BDNF is not as extensive as for AMPARs (Carvalho et al., 2008). We revealed for the first time that Nr4a2 regulated the levels of GluN1-NMDAR and GluA1-AMPAR subunits in mature hippocampal-cultured neurons. These regulation was specific, since no changes were observed in other subunits such as GluA2-AMPAR, GluN2A-NMDAR, GluN2B-NMDAR or $GABA_AR\alpha1$ subunits. Nonetheless, no data exist about the potential function of Nr4a2 in inhibitory neurotransmission, so it would be interesting to expand the study on the possible role of this transcription factor in inhibitory neurons.

Moreover, we observed that Nr4a2-mediated changes in GluA1-AMPAR protein levels were BDNF-dependent, describing the signaling pathway upstream of BDNF responsible for the increase in GluA1-AMPAR protein levels. By contrast, the blockade of BDNF receptor TrkB alone was not able to significantly blunt the Nr4a2-dependent increase in GluN1-NMDAR protein levels, suggesting that the regulation of NMDARs by Nr4a2 was BDNF-independent. However, Nr4a2 did not seem to affect Grin1 and Gria1 mRNA levels,

although both Grin1 and Gria1 promoters contain motifs for Nr4a2 binding. To fully explore the possible Nr4a2-mediated transcriptional regulation of these subunits, it would be necessary to check whether Nr4a2 agonists are able to increase GluN1-NMDAR and GluA1-AMPAR protein levels in presence of transcription and translation inhibitors.

Upstream of Nr4a2, CRTC1 has been previously involved in hippocampal synaptic plasticity processes (Kovács et al., 2007). Nevertheless, whether CRTC1 is able to modulate specific subunits of synaptic proteins has not been described yet. We found that CRTC1 shRNA-transduced hippocampal-cultured neurons showed decreased levels of both pre-synaptic and post-synaptic proteins such as synaptophysin and PSD-95, respectively. A significant decrease of different excitatory and inhibitory receptor subunits was also found, including reduced levels of GluA1-AMPAR, GluN1-NMDAR, GluN2B-NMDAR and $GABA_AR\alpha1$ subunits, both at the transcriptional and translational level. This general synaptic affectation caused by the absence of CRTC1 contrasts with the subtle changes mediated by Nr4a2, whose knocking-down alters critical subunits such as GluN1-NMDARs and GluA1-AMPARs. These results suggest that CRTC1 may act as a master synaptic regulator whereas Nr4a2 is controlling specific excitatory subunits.

In addition, we found reduced GluA1-AMPARs, GluN1-NMDARs and PSD95 protein levels at the PSD compartment of CRTC1 shRNA-transduced mature hippocampal neurons. By contrast, we detected no changes in either surface or synaptic GluA1-AMPARs and GluN1-NMDARs levels in Nr4a2 shRNA-transduced mature hippocampal neurons by biotynilation assays, PSD isolation or confocal microscopy analysis. A lack of resolution or specificity of the techniques used can mask subtle changes in the amount or localization of specific receptors. For that reason, we studied the mEPSC and the AMPA/NMDA ratio of CA1 pyramidal neurons of acute hippocampal slices by electrophysiological recordings to explore possible Nr4a2-mediated changes in synaptic AMPARs and/or NMDARs. Notably, we showed for the first time that Nr4a2 activation was able to increase synaptic AMPARs transmission reported by an increase in mEPSC amplitude and AMPA/NMDA ratio of CA1 pyramidal neurons of acute hippocampal slices. These outcomes can only be due to changes in post-synaptic AMPARs number.

Mechanistically, an increase in synaptic AMPARs results from recruitment of additional receptors from extra-synaptic sites and/or from fusion of AMPAR-containing vesicles with the postsynaptic sites (Huganir & Nicoll, 2013). Since the electrophysiological data point out a role for Nr4a2 in AMPARs synaptic delivery in the CA1 region of the hippocampus, it would be important to investigate whether this transcription factor might play a role in AMPARs diffusion and/or synaptic fusion in CA1 synapses using, for example, factors that inhibit SNARE-mediated membrane fusion. Another approach could be the use of

fluorescence recovery after photobleaching (FRAP) using an optical probe based on superecliptic pHluorin-GluA1, a pH-sensitive GFP variant, which is brightly fluorescent at neutral pH but is quenched in acidic endosomal lumen (Petrini et al., 2009) or an optical reporter for recycling endosome fusion based on transferrin receptor, as previously reported (Kennedy et al., 2010). These data would be tremendously valuable, since CA1-related memory deficits observed in aged or memory-impaired rodents are not associated with a loss of synapses from CA3 or EC inputs, but rather are believed to result from an increase in the number of silent synapses or synapses without excitatory glutamatergic AMPARs (Bie et al., 2018). Thus, the involvement of Nr4a2 in AMPARs synaptic delivery would provide mechanistic insights into the role of this transcription factor in hippocampal synaptic plasticity processes related to cognitive impairment.

Recent data have shown that hippocampal slices from Nr4a dominant negative mutant mice exhibit impairments in transcription-dependent hippocampal LTP maintenance (Bridi & Abel, 2013) while its pharmacological activation enhances hippocampal LTP (Bridi et al., 2017). Moreover, previous studies have also reported that training in different behavioral tasks increases the expression of Nr4a2 in the hippocampus (Hawk et al., 2012; McNulty et al., 2012; Oliveira et al., 2018; Peña De Ortiz, Maldonado-Vlaar & Carrasquillo, 2000). Similarly, memory enhancement by the genetic or pharmacological ablation of hippocampal HDAC3 further increases Nr4a2 (Vecsey et al., 2007), whereas the knock-down of Nr4a2 attenuates this memory enhancement (McQuown et al., 2011). In addition, several loss-of-function studies, including knockout (Rojas et al., 2007), siRNA knockdown (McNulty et al., 2012), antisense oligonucleotides (Colón-Cesario et al., 2006) or expression of a dominant-negative protein (Joshua D. Hawk et al., 2012) have concluded that Nr4a2 is required in specific forms of hippocampal-dependent learning and memory processes. However, specific effects of Nr4a2 in hippocampal synaptic plasticity and the underlying molecular determinants have not been examined yet. The oAβ-mediated synaptic depression shares several mechanisms with Hebbain LTD. For that reason, we wanted to examine the role of Nr4a2 in hippocampal synaptic plasticity by studying not only hippocampal LTP but also LTD. Importantly, we showed for the first time that the absence of Nr4a2 increased LTD at Schaffer collateral to CA1 synapses, while Nr4a2 activation was able to block both LTD at Schaffer collateral to CA1 synapses of acute hippocampal slices and NMDA-induced cLTD in mature hippocampal-cultured neurons. Nonetheless, it is important to mention that different outcomes in cLTD blockade were obtained after Nr4a2 activation using either agonists or exogenous Nr4a2 overexpression via lentiviral transduction. Whereas Nr4a2 activation using agonists significantly blocked cLTD in hippocampal-cultured neurons, exogenous Nr4a2

overexpression did not have any effect on cLTD. This discrepancy could arise from compensatory mechanisms that emerge due to the long-time overexpression of Nr4a2 in culture cells. To solve this issue, it would be valuable to deeply investigate the effects of Nr4a2 overexpression in cLTD using an inducible viral vector. Another interesting approach would be to specifically overexpress Nr4a2 at spines. This way we could examine whether cLTD affects Nr4a2 synaptic expression or localization, as well as check whether the absence of synaptic Nr4a2 is specifically involved in hippocampal LTD.

Overall, the data obtained place Nr4a2 as a pivotal modulator of hippocampal synaptic plasticity, opening the possibility to use its activation to restore the oAβ-mediated synaptic depression related to the cognitive dysfunction observed at early stages of AD.

2. Nr4a2 as a potential therapeutic target in AD

Compelling evidences have increasingly pointed out oAβ as the neurotoxic forms causing synaptic toxicity and leading to synaptic dysfunction and eventual loss. Among the synaptotoxic effects of oAβ, they impair hippocampal excitatory synaptic plasticity, weakening NMDAR-dependent LTP and promoting LTD (Shankar et al., 2008). Nevertheless, the molecular and cellular mechanisms underlying this synaptic impairment are still not fully understood. Importantly, sublethal concentrations of oAβ induce changes in expression of genes classified into several pathways important for neuronal physiology, including vesicle trafficking, cell adhesion, actin cytoskeleton dynamics, and insulin signaling (Sebollela et al., 2012). Evidences from studies using mice models of AD have shown that oAβ also deregulate genes necessary for cognitive processes such as *CRTC1* and CRTC1-dependent genes including *Arc*, *c-fos*, *Egr1* and *Bdnf* (Wilson et al., 2016). Our results are the first evidence showing that synthetic oAβ significantly decreased the activity-mediated induction of both CRTC1 and Nr4a2 protein levels in mature hippocampal-cultured neurons. Importantly, synthetic and brain-derived oAβ show biochemical identity (Gong et al., 2003), and the toxicology also appears parallel (De Felice et al., 2008), validating their use as an experimental tool.

Although the activity-mediated increase of Nr4a2 protein levels was clearly disrupted in presence of oAβ in mature hippocampal-cultured neurons, the activity-mediated increase of Nr4a2 mRNA levels was not altered. Indeed, basal levels of Nr4a2 mRNA were increased in presence of oAβ, probably due to the initial raise of intracellular calcium caused by oAβ (Berridge, 2011; Bezprozvanny & Mattson, 2008; Green & LaFerla, 2008). These data suggest that oAβ could affect activity-mediated induction of Nr4a2 protein levels either post-transcriptionally or by promoting Nr4a2 degradation. In mature

hippocampal-cultured neurons, Nr4a2 was highly degraded in basal conditions, since inhibiting the proteasome significantly increased its protein levels, suggesting that oAβ may interfere with this process.

Importantly, we demonstrated that oAβ significantly affected the activity-dependent Nr4a2 protein increase in mature hippocampal-cultured neurons. In addition, we showed that Nr4a2 was involved not only in basal and activity-mediated BDNF production in mature hippocampal neurons, but also regulated post-synaptic AMPARs in mature hippocampal neurons and acute hippocampal slices in a mechanism partially dependent on BDNF. Moreover, it is known that oAβ significantly disrupt hippocampal synaptic plasticity, leading to a dephosphorylation of Ser845-GluA1-AMPARs that accompanies their endocytosis (Hsieh et al., 2006; Miñano-Molina et al., 2011). Therefore, it is plausible to hypothesize that activating and/or restoring Nr4a2 levels could rescue the oAβ-mediated impairments in hippocampal synaptic plasticity. Indeed, we observed that Nr4a2 activation was able to completely restore the oAβ-mediated dephosphorylation of Ser845-GluA1-AMPARs that leads to their endocytosis and to significantly rescue the hippocampal oAβ-mediated cLTP impairment. Furthermore, although we found that the absence of Nr4a2 did not affect cLTP in mature hippocampal-cultured neurons, Nr4a2 activation significantly increased cLTP, suggesting that Nr4a2 could be involved not in LTP induction but maintenance. In general, these data allow us to speculate that Nr4a2 activating compounds may serve as powerful and selective enhancers of synaptic plasticity.

In fact, the potential role of Nr4a2 as a therapeutic target for AD has been recently suggested. In a study performed by Moon and colleagues, they found that knockdown of Nr4a2 significantly aggravated AD pathology while its overexpression alleviated it, including effects on Aβ accumulation, neuroinflammation and neurodegeneration (Moon et al., 2019). Importantly, the data provided in this doctoral thesis specifically point out the potential role of Nr4a2 as a therapeutic agent targeting the synaptic dysfunction that occurs at early stages of AD.

Genes directly implicated in synaptic plasticity, learning and memory seem to be upregulated in the hippocampus of environmental-enriched mice models of AD, such as *Egr1* or *arc* (Lazarov et al., 2005). Among them, an increase in BDNF has been extensively reported after environmental-enriched conditions (Dandi et al., 2018; Santoso, et al., 2020; Sun et al., 2010). Moreover, environmental enrichment has been recently proposed to prevent the oAβ-induced synaptic dysfunction blocking HDAC3 (Wei et al., 2020), known to negatively regulate Nr4a2 levels (McQuown et al., 2011). These findings open the possibility to explore whether Nr4a2 can be activated in environmental-enriched conditions being involved in its beneficial effects on synaptic function.

Decreased levels of plasticity-related genes, including Nr4a2, have been reported in some models of AD, including the hippocampus of trained $APP_{Sw,Ind}$ mice (Parra-Damas et al., 2017a). Nr4a2 expression has been also previously examined in AD human brains without achieving consistent results. Increased hippocampal Nr4a2 mRNA levels were previously reported in a cohort of LOAD patients (Annese et al., 2018). Conversely, decreased levels of Nr4a2 mRNA expression at Braak III-IV and V-VI stages compared to controls were found in postmortem human hippocampus (Parra-Damas et al., 2014). Likewise, reduced Nr4a2 protein levels were also reported in the hippocampus and the superior frontal cortex of AD patients (Moon et al., 2019b). These discrepancies between studies could arise from the distinct demographic and clinical features of the samples, including different gender, age, origin, social status or sample processing. Importantly, we found a significant decrease of Nr4a2 protein levels specifically at Braak II stage, corresponding to preclinical AD, where symptoms are still absent albeit synaptic deficits have already started. Concordantly, we also observed a significant decrease in BDNF protein levels at MCI stage, in line with previous studies reporting reduced hippocampal BDNF expression in AD human brains (Colangelo et al., 2002; Connor et al., 1997; Isidro Ferrer et al., 1999). It is also important to note that no differences were observed in Nr4a2 protein levels in Braak III-IV and Braak V-VI compared to controls because, although the vast majority of samples from these stages had less Nr4a2 protein levels compared to healthy control subjects, few expressed high amounts of Nr4a2. Therefore, to conclude whether Nr4a2 protein levels are indeed decreased at late stages of AD, more samples should be analyzed.

Noteworthy, a strong link between brain transcriptional profiles and blood in AD has also been pointed out (Naughton et al., 2014), opening the possibility to determine the levels of Nr4a2 or BDNF in cerebrospinal fluid and/or blood (plasma and blood cells) to evaluate whether they can emerge as potential biomarkers for preclinical AD. Analysis of genes in circulating fluids is a promising tool for early AD diagnosis, since their levels can be obtained using non-invasive procedures, with affordable techniques, and allowing patients follow-up over time. A recent meta-analysis showed a trend for decreased peripheral blood levels of BDNF that reach significance in AD patients compared with healthy control subjects (Ng et al., 2019). Disappointingly, no differences in Nr4a2 levels were found in whole peripheral blood of AD patients in another cohort of samples (Montarolo et al., 2016), although this negative result could probably be explained by the late AD stage of the patients enrolled in the study.

Altogether, these reported evidences prompted us to explore the effects of Nr4a2 hippocampal overexpression in the $APP_{Sw,Ind}$ mouse model of AD. $APP_{Sw,Ind}$ phenotype is

characterized by progressive Aβ pathology, showing increased $A\beta_{1-42}$/ $A\beta_{1-40}$ ratio as early as at 3 months of age (Mucke et al., 2000), coinciding with impaired hippocampal basal synaptic transmission and plasticity (Saganich et al., 2006). At 6 months-old, $APP_{Sw,Ind}$ mice have CRE-transcriptional deficits (España et al., 2010b), decreased pSer845-GluA1-AMPAR levels associated to early spatial memory deficits (Miñano-Molina et al., 2011) and increased anxiety (España et al., 2010a). At this age, hippocampal gliosis is also present (Wright et al., 2013), with diffusive Aβ plaques in the DG and neocortex, that become more evident from the age of 9 months (Mucke et al., 2000). We evaluated the effects of Nr4a2 hippocampal overexpression by using stereotaxic injections at CA1 hippocampal subregion of AAV containing the full length Nr4a2 construct in $APP_{Sw,Ind}$ mice at both 6 and 12 months of age, mimicking an early and moderate stage of the pathology.

We examined the potential role of Nr4a2 in hippocampus-dependent spatial learning and memory processes using the MWM test. Previous studies have implicated Nr4a2 in long-term spatial information storage in the hippocampus. It is known that Nr4a2 mRNA is increased in CA1 and CA3 hippocampal subregions after a spatial food search task (Peña De Ortiz et al., 2000). Likewise, hippocampal infusions of Nr4a2 antisense oligodeoxynucleotides impair learning and long-term memory in a holeboard spatial discrimination task in rats (Colón-Cesario et al., 2006). In agreement, we found that hippocampal Nr4a2 overexpression significantly ameliorated spatial learning and memory deficits in the MWM of both 6 and 12 months-old $APP_{Sw,Ind}$ mice.

It is worth to note that the MWM test, in spite of being one of the most widely established behavioral tests to evaluate spatial learning and memory in rodents, several logistical and theoretical issues limit its accurate interpretation (Gulinello et al., 2009). The trajectory covered to locate the platform is commonly considered the best variable to reflect the process of acquisition of a task, with the distance travelled leading to more reliable results than the escape latency (Gerlai, 2001). However, lack of sensitivity between treatment groups occurs when controls perform at low levels. For that reason, we presented only distances travelled in the MWM during the cue learning task and the two first days of the acquisition phase, since after that, the non-transgenic group (used as the control) exhibited a poor performance that difficulted a correct interpretation of the results. Indeed, Gulinello and colleagues validated a 2-day water maze protocol in mice which showed improved sensitivity compared to a typical probe trial, controlling non-cognitive factors that can lead to misinterpretation of the water maze assessment of memory (Gulinello et al., 2009). Other parameters that are worth to be considered in the MWM results are the distinct platform-searching and non-searching strategies used among the different groups analyzed. We observed that $APP_{Sw,Ind}$ mice showed thigmotaxis and circling behaviors the

firsts days of acquisition, denoting an anxious profile (Huang, Zhou & Zhang, 2012; Treit & Fundytus, 1988), whereas the WT group and the $APP_{Sw,Ind}$ mice with the Nr4a2 overexpression tend to float, showing lack of motivation or behavioral despair (Porsolt, Le Pichon & Jalfre, 1977).

Some discrepancies exist about the possible involvement of Nr4a2 in non-hippocampus dependent memories. A recent study has demonstrated that hippocampal overexpression of Nr4a2 did not ameliorate object recognition memory deficits, a hippocampus-independent task (Kwapis et al., 2019). On the other hand, Nr4a2 activation enhanced long-term memory in young mice as well as rescued memory decline in aged mice using a hippocampus-dependent spatial object recognition task (Chatterjee et al., 2020). Nevertheless, intraperitoneal injections of a Nr4a2 specific agonist enhanced long-term memory in the NOR test (Jin il Kim et al., 2016), suggesting that this transcription factor could also be enhancing non-hippocampus-dependent memories. Thus, we also aimed to evaluate the possible role of Nr4a2 in non-hippocampus dependent memories using the NOR test but, unexpectedly, the cohorts of $APP_{Sw,Ind}$ mice utilized in this study did not show deficits in object recognition memory, limiting our abilities to reach a conclusion on the potential effects of Nr4a2 hippocampal overexpression on this type of memory.

BPSD symptoms such as anxiety are common clinical features of AD that significantly contribute to behavior disturbances, although the underlying molecular mechanisms are not fully comprehended. In spite of being considered an important subject of interest in preclinical pharmacological screening, the number of experimental studies addressing BPSD-like behaviors is much inferior compared to the huge literature focused on cognition. For that reason, we aimed to explore not only the cognitive, but also the BPSD-effects of Nr4a2 hippocampal overexpression in the $APP_{Sw,Ind}$ mice model of AD. The anxious profile of $APP_{Sw,Ind}$ mice at both ages was observed in different behaviors such as the diminished time spent in the center of the open field in the OF test, the elevated number of buried marbles in the MB test or the increased freezing in the CFC. These distinct measures were previously validated as indicators of anxiety-like behaviors in mice (Baeta-Corral, Johansson & Giménez-Llort, 2018; España et al., 2010a). Importantly, the enhanced CFC response in cognitive impaired mice denotes the influence of BPSD on learning and memory tasks (España et al., 2010a). In all cases, Nr4a2 overexpression in $APP_{Sw,Ind}$ mice ameliorated these anxiety-like behaviors to levels compared to non-transgenic mice, showing for the first time the anxiolytic effects of hippocampal overexpression of Nr4a2 in an AD context. Other well-accepted tests to examine anxiety such as the dark-light box (Crawley & Goodwin, 1980), the elevated-plus maze (Rodgers

& Dalvi, 1997) or the social interaction test (File & Hyde, 1978) would be of great value to strengthen this finding.

It is plausible to speculate about the potential positive effects of Nr4a2 upregulation in psychiatric symptoms that may occur in patients with AD, since this transcription factor is robustly and specifically expressed in the medial habenula (Quina et al., 2009). The habenula is a brain area highly involved in depression, one of the most common psychiatric symptoms in AD. However, the downstream targets responsible for Nr4a2-mediated anxiolytic effects remain elusive. One possible effector could be BDNF, which we have demonstrated to be modulated by Nr4a2, and it has been previously reported to have a positive role in anxiety and depression-like behaviors (Ping et al., 2014; Rosa et al., 2016) and, importantly, to ameliorate these behaviors in Aβ-treated rats (X. Song et al., 2017).

Natural typical behaviors that represent active interaction with the environment are also excellent ethological scenarios to reflect both cognitive and non-cognitive disturbances in mice models of AD (Torres-Lista & Giménez-Llort, 2013). In agreement with this, we showed the first evidence of non-maternal nesting behavior in 12 months-old $APP_{Sw,Ind}$ mice, which was partially recovered by the hippocampal Nr4a2 overexpression in an attempt to model the beneficial role of this transcription factor on naturally occurring executive functions and daily life activities. These data correlate with previous findings in which the oral administration of the RXR agonist bexarotene, known to activate Nr4a2, to the APP/PS1 mice model of AD rescued the impaired non-maternal nesting behavior (Cramer et al., 2012).

We also reported for the first time hindlimb clasping in the $APP_{Sw,Ind}$ transgenic mouse. Hindlimb-flexion and paw-clasping have been previously described in various APP strains (Lalonde, Fukuchi & Strazielle, 2012), although Aβ pathology does not necessarily lead to this phenotype (Lalonde, Kim & Fukuchi, 2004). This behavior does not seem to be modulated by Nr4a2 hippocampal overexpression.

We have previously discussed the involvement of Nr4a2 in hippocampal activity-mediated BDNF production as well as in postsynaptic AMPARs recruitment. Furthermore, several recent reports have pointed out a beneficial role of both BDNF and AMPARs in cognitive deficits of various mice models of AD (Choi et al., 2018; De Pins et al., 2019; Hu et al., 2019; Mozafari et al., 2018). Nonetheless, the cohorts of animals used for the present study did not have an increase in either BDNF or different subunits of both excitatory and inhibitory receptors after Nr4a2 overexpression, at least at the time point analyzed. Further analysis at different time points after Nr4a2 overexpression, as well as the

examination of specific neuronal populations and/or neuronal compartments would help to clarify this unresolved question, since a broad analysis of whole hippocampal lysates limit us to find specific molecular changes.

Overall, the results presented so far show that restoring hippocampal Nr4a2 function has the ability to modulate not only cognitive functions, but also daily life activities and BPSD-like behaviors in the $APP_{Sw,Ind}$ mice model of AD. This agrees with the actual conception of the hippocampus as a structure not just concerned with the formation of memories, but also participating in information processing and the subsequent regulation of behavior (Bannerman et al., 2004). These results, along with the neuroprotective, anti-inflammatory and neurogenic properties of Nr4a2, make this transcription factor a great potential therapeutic target for AD. Therefore, it would be worth to explore the potential benefits of Nr4a2 upregulation in other models of AD as well as to examine whether these effects are modulated by gender, since only male mice were used for this study. Higher risk and severe progression of AD is found in women (Mazure & Swendsen, 2016), making it mandatory to include a gender perspective in the analysis whenever possible.

In addition, it would be necessary to recapitulate these findings not only with virally induced Nr4a2 overexpression, but also with Nr4a2 specific agonists. Notably, apart from the drug-induced Nr4a2 expression, research has focused on Nr4a2-based molecular therapy such as Nr4a2 gene- and cell-based therapy. One example is the significant recovery from neurological dysfunction after middle cerebral artery occlusion observed with the transplantation of Nr4a2-positive neuronal stem cells derived from wisdom teeth (Yang et al., 2009). In PD models, therapeutic effects have been also observed using different approaches such as intrastriatal transplantation of lentiviral vector-mediated Nr4a2 gene-modified mesenchymal stem cells (Wang et al., 2018), transplantation of Nr4a2-overexpressed olfactory ensheating cells (Liu et al., 2018), delivery of Nr4a2-polyethylene glycolylated liposomes-coupled microbubbles (Yue et al., 2018) or transference of Nr4a2 using non-pathogenic protein fragments derived from *Bacillus anthracis* along with endogenous nuclear import machinery (Paliga et al., 2019). Another outstanding and pioneer field of research is the miRNA-targeted therapy. Epigenetic factors, mainly small non-coding RNA such as miRNAs, have gained increasing attention in research on AD (Wang, Qin & Tang, 2019), and miRNAs targeting Nr4a2 have also been proposed as potential therapeutic agents. For instance, in a recent report, Xie and colleagues demonstrated that anti-miR-145-5p administration increased Nr4a2 expression and reduced infarct volume in acute cerebral ischemia (Xie et al., 2017).

In the face of such a devastating disease, it is a powerful reminder that research equals hope, and that effort to translate the advances in the cellular and molecular pathogenesis

of AD into early therapeutic strategies must continue. This doctoral thesis attempts to shed light into the molecular causes that lead to synaptic failure at preclinical AD stages in order to identify possible therapeutic targets. The results presented show for the first time mechanistic insights into the contribution of Nr4a2 transcription factor to hippocampal glutamatergic synaptic plasticity. Furthermore, we provide direct proof supporting a key role for Nr4a2 in the oAβ-mediated synaptic dysfunction that leads to learning and memory impairments at early stages of AD, emerging as a potential therapeutic candidate for delaying the onset or progression for such an insidious pathology.

No engineered animal model has yet reproduced the full spectrum of AD phenotypes in a manner closely similar to the human disease (Selkoe, 2011). Indeed, current knowledge of synaptic changes in AD is derived predominantly from preclinical work. These limitations pave the way to study the potential therapeutic actions of Nr4a2 in human engineered cultured neurons from AD patients such as human induced pluripotent stem cells (Ghatak et al., 2019; Majolo et al., 2019; Penney, Ralvenius & Tsai, 2020). Noteworthy, the beneficial roles of Nr4a2 treatment in AD patients are reinforced by the finding that memantine, one of the only four clinically approved drugs for the treatment of AD, indeed increases Nr4a2 expression in an *in vitro* PD model (Wei et al., 2016). We hope that the evidences provided herein allow further research aiming to translate to humans the potential beneficial effects of Nr4a2 activation in Alzheimer's pathology.

IX. Conclusions

The data obtained in this study identifies Nr4a2 transcription factor as a potential therapeutic agent targeting the synaptic failure occurring at early stages of Alzheimer's disease due to its involvement in the modulation of hippocampal synaptic plasticity.

This conclusion is drawn based on the following findings:

1. Nr4a2 modulates excitatory synaptic activity in the hippocampus by a mechanism dependent on CREB/CRTC1, BDNF and AMPARs.
2. Activity-dependent induction of Nr4a2 in mature hippocampal-cultured neurons is impaired in presence of oAβ. Moreover, in the cohort of subjects analyzed in this study, Nr4a2 protein levels were decreased in postmortem hippocampal tissue of AD patients diagnosed as Braak II stage.
3. Nr4a2 activation is able to restore synaptic dysfunction, rescuing the oAβ-dependent depression, the oAβ-mediated cLTP impairment and blocking hippocampal LTD.
4. Nr4a2 hippocampal overexpression partially ameliorates the cognitive deficits and significantly decreases the anxiety-related behaviors in the $APP_{Sw,Ind}$ mouse model of AD.

X. Annexes

Annex 1.

Vector maps.

pREV:

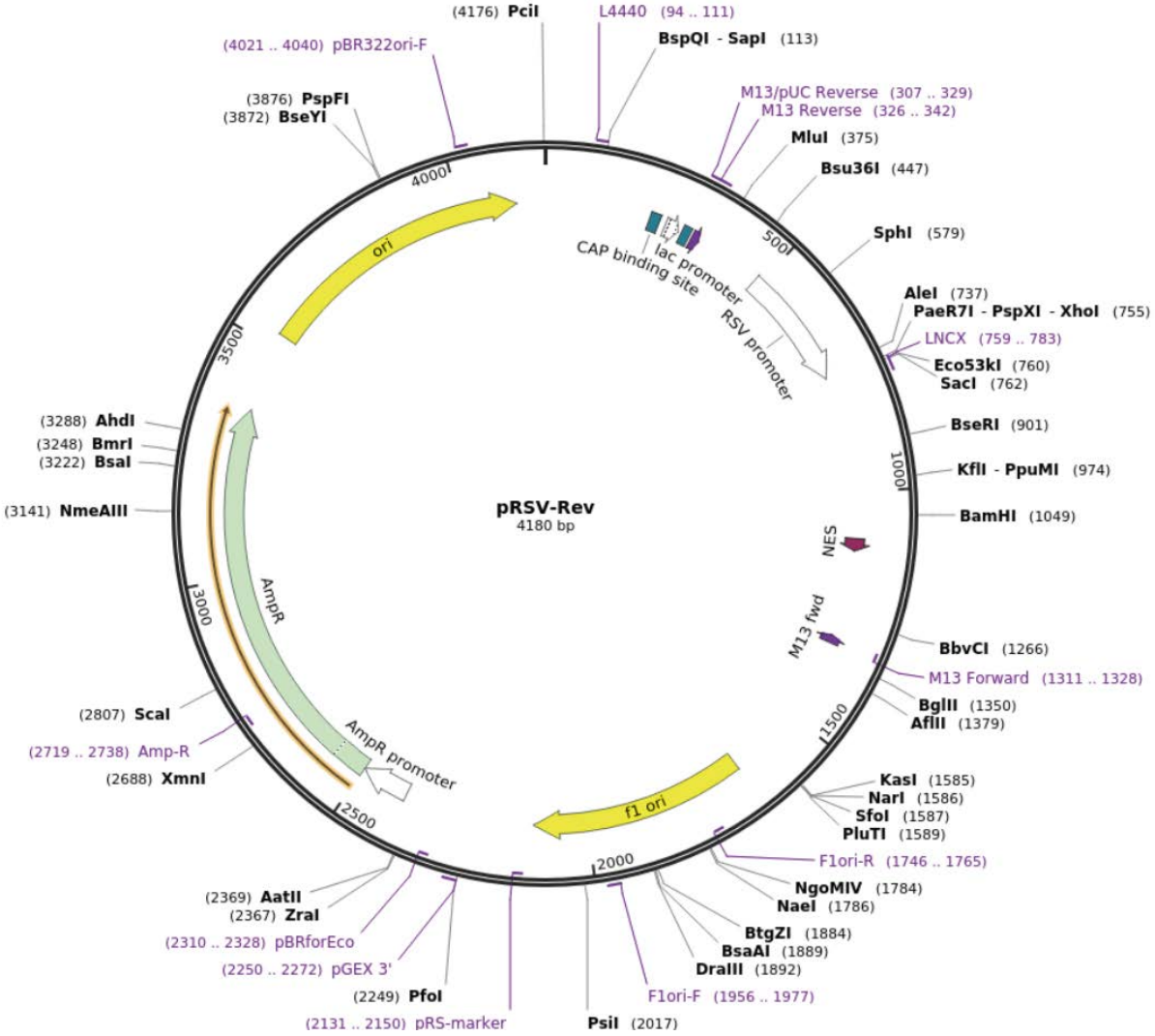
pRSV-Rev
4180 bp
(4176) PciI
L4440 (94 .. 111)
BspQI - SapI (113)
(4021 .. 4040) pBR322ori-F
M13/pUC Reverse (307 .. 329)
M13 Reverse (326 .. 342)
(3876) PspFI
(3872) BseYI
MluI (375)
Bsu36I (447)
SphI (579)
AleI (737)
PaeR7I - PspXI - XhoI (755)
LNCX (759 .. 783)
Eco53kI (760)
SacI (762)
BseRI (901)
KflI - PpuMI (974)
BamHI (1049)
(3288) AhdI
(3248) BmrI
(3222) BsaI
(3141) NmeAIII
BbvCI (1266)
M13 Forward (1311 .. 1328)
BglII (1350)
AflII (1379)
(2807) ScaI
(2719 .. 2738) Amp-R
(2688) XmnI
KasI (1585)
NarI (1586)
SfoI (1587)
PluTI (1589)
F1ori-R (1746 .. 1765)
NgoMIV (1784)
NaeI (1786)
BtgZI (1884)
BsaAI (1889)
DraIII (1892)
F1ori-F (1956 .. 1977)
PsiI (2017)
(2369) AatII
(2367) ZraI
(2310 .. 2328) pBRforEco
(2250 .. 2272) pGEX 3'
(2249) PfoI
(2131 .. 2150) pRS-marker
ori
CAP binding site
lac promoter
RSV promoter
NES
M13 fwd
AmpR
AmpR promoter
f1 ori
500
1000
1500
2000
2500
3000
3500
4000

pRRE:

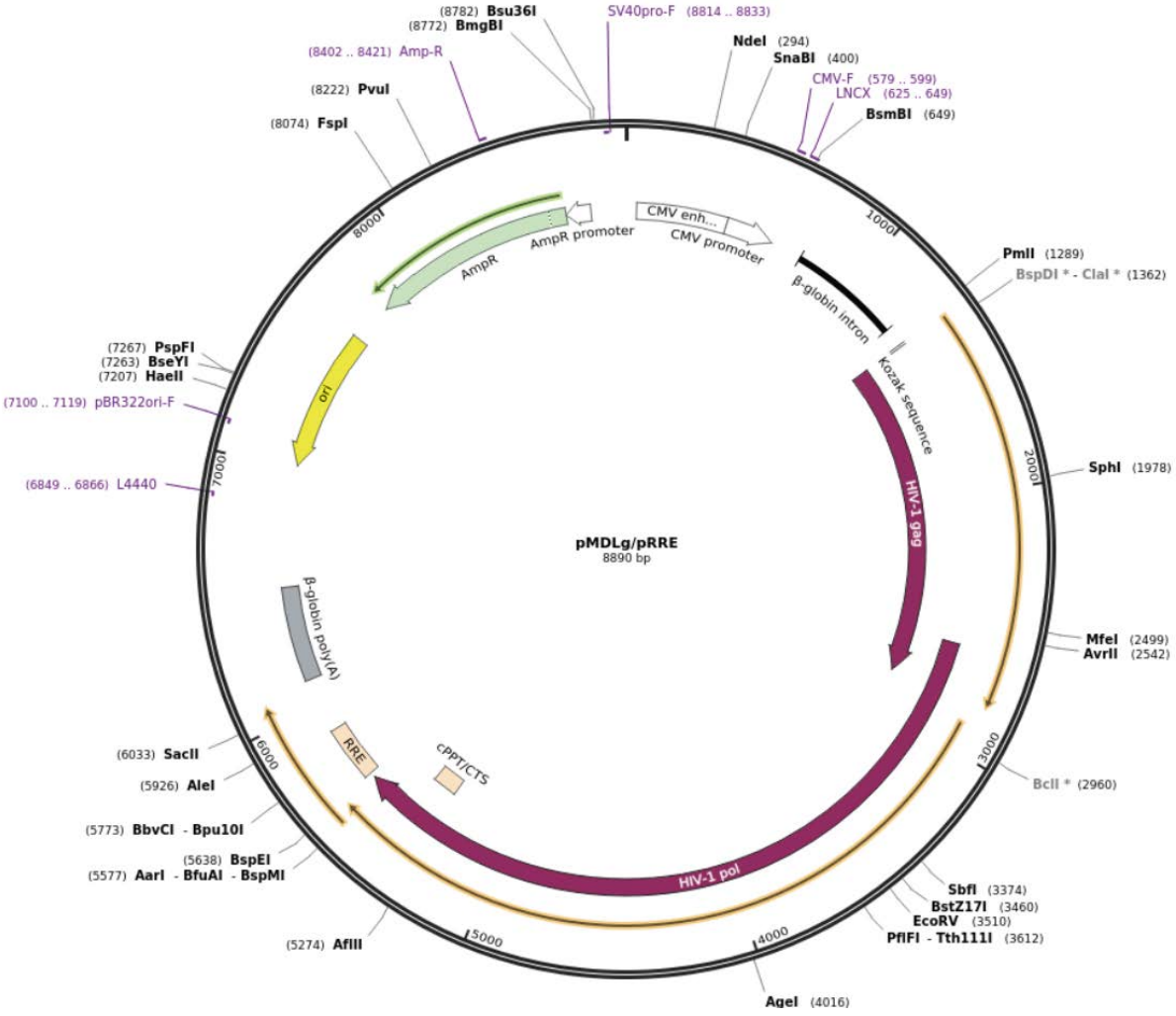
pMDLg/pRRE
8890 bp
(8782) Bsu36I
(8772) BmgBI
SV40pro-F (8814 .. 8833)
NdeI (294)
SnaBI (400)
(8402 .. 8421) Amp-R
CMV-F (579 .. 599)
LNCX (625 .. 649)
(8222) PvuI
BsmBI (649)
(8074) FspI
8000
1000
CMV enh...
CMV promoter
AmpR promoter
AmpR
β-globin intron
PmlI (1289)
BspDI * - ClaI * (1362)
(7267) PspFI
(7263) BseYI
(7207) HaeII
(7100 .. 7119) pBR322ori-F
ori
Kozak sequence
HIV-1 gag
7000
2000
SphI (1978)
(6849 .. 6866) L4440
β-globin poly(A)
MfeI (2499)
AvrII (2542)
RRE
cPPT/CTS
6000
3000
(6033) SacII
(5926) AleI
BclI * (2960)
(5773) BbvCI - Bpu10I
(5638) BspEI
(5577) AarI - BfuAI - BspMI
HIV-1 pol
SbfI (3374)
BstZ17I (3460)
EcoRV (3510)
PflFI - Tth111I (3612)
(5274) AflII
5000
4000
AgeI (4016)

pVSVG, pMD2.G:

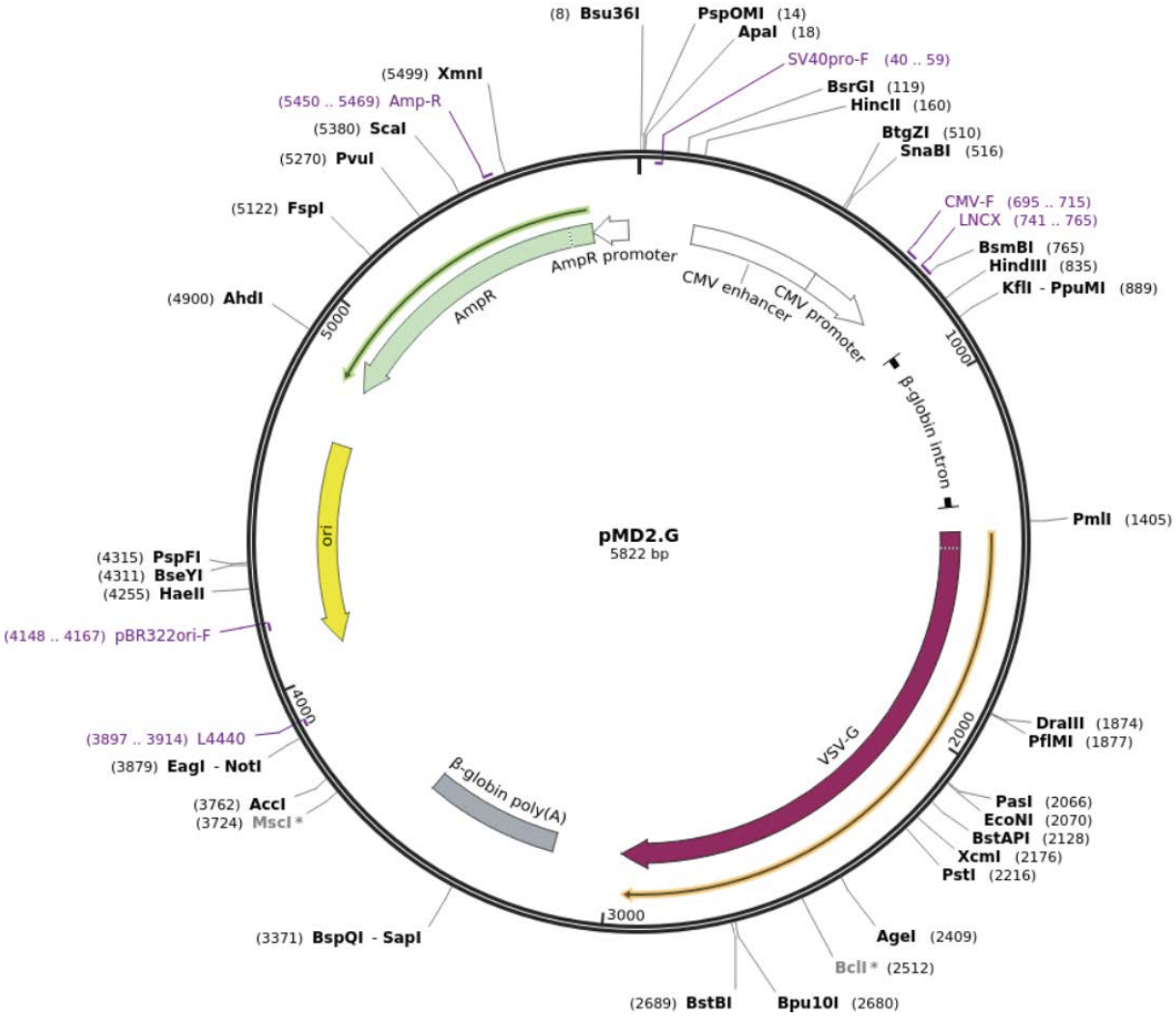
pMD2.G
5822 bp
(8) Bsu36I
PspOMI (14)
ApaI (18)
SV40pro-F (40 .. 59)
BsrGI (119)
HincII (160)
BtgZI (510)
SnaBI (516)
CMV-F (695 .. 715)
LNCX (741 .. 765)
BsmBI (765)
HindIII (835)
KflI - PpuMI (889)
PmlI (1405)
DraIII (1874)
PflMI (1877)
PasI (2066)
EcoNI (2070)
BstAPI (2128)
XcmI (2176)
PstI (2216)
AgeI (2409)
BclI * (2512)
Bpu10I (2680)
BstBI (2689)
(3371) BspQI - SapI
(3724) MscI *
(3762) AccI
(3879) EagI - NotI
(3897 .. 3914) L4440
(4148 .. 4167) pBR322ori-F
(4255) HaeII
(4311) BseYI
(4315) PspFI
(4900) AhdI
(5122) FspI
(5270) PvuI
(5380) ScaI
(5450 .. 5469) Amp-R
(5499) XmnI
AmpR promoter
AmpR
CMV enhancer
CMV promoter
β-globin intron
ori
β-globin poly(A)
VSV-G
1000
2000
3000
4000
5000

psPAX2:

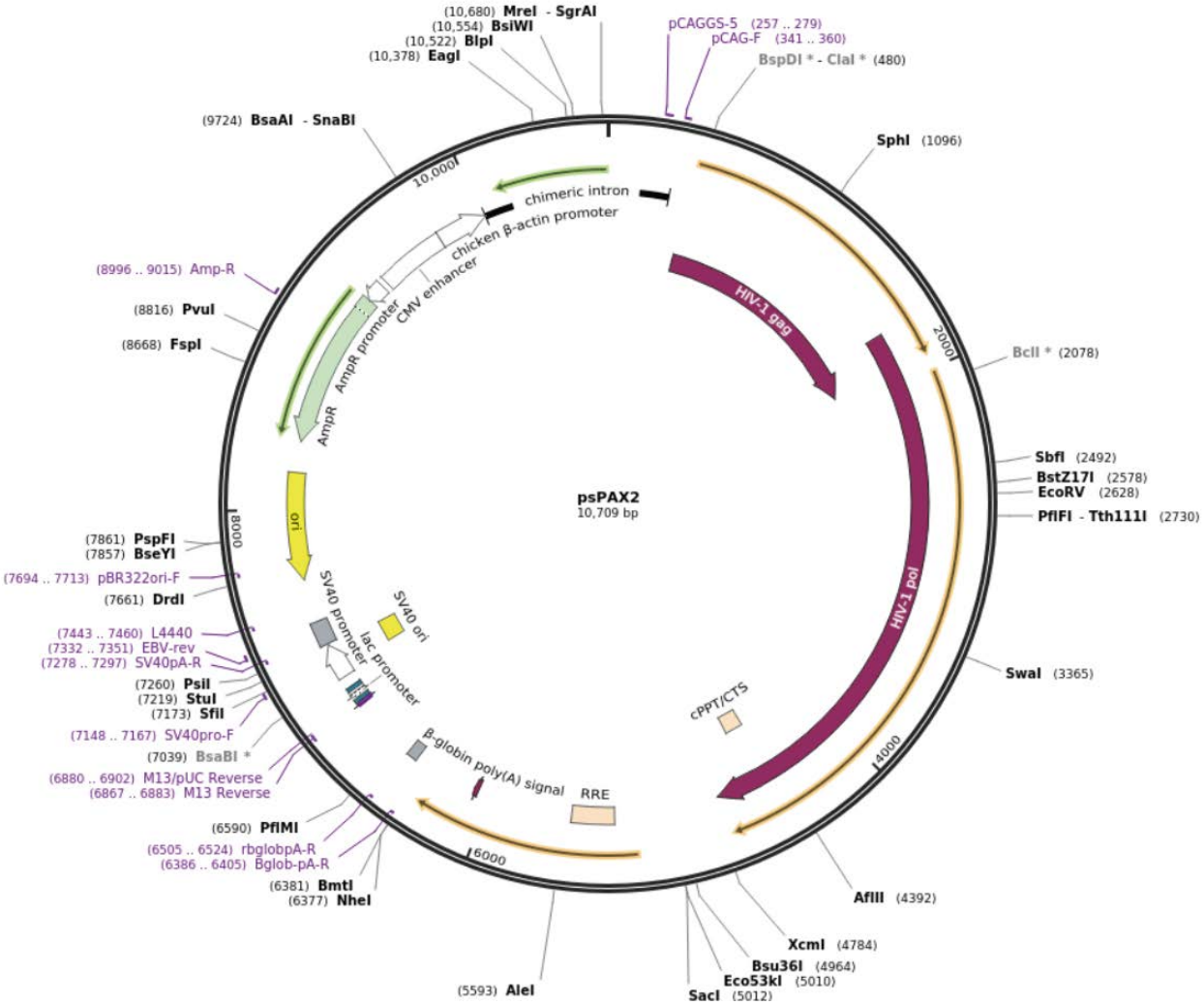
psPAX2
10,709 bp
(10,680) MreI - SgrAI
(10,554) BsiWI
(10,522) BlpI
(10,378) EagI
pCAGGS-5 (257 .. 279)
pCAG-F (341 .. 360)
BspDI * - ClaI * (480)
SphI (1096)
BclI * (2078)
SbfI (2492)
BstZ17I (2578)
EcoRV (2628)
PflFI - Tth111I (2730)
SwaI (3365)
AflII (4392)
XcmI (4784)
Bsu36I (4964)
Eco53kI (5010)
SacI (5012)
(5593) AleI
(6381) BmtI
(6377) NheI
(6590) PflMI
(6505 .. 6524) rbglobpA-R
(6386 .. 6405) Bglob-pA-R
(6880 .. 6902) M13/pUC Reverse
(6867 .. 6883) M13 Reverse
(7039) BsaBI *
(7148 .. 7167) SV40pro-F
(7260) PsiI
(7219) StuI
(7173) SfiI
(7443 .. 7460) L4440
(7332 .. 7351) EBV-rev
(7278 .. 7297) SV40pA-R
(7861) PspFI
(7857) BseYI
(7694 .. 7713) pBR322ori-F
(7661) DrdI
(8996 .. 9015) Amp-R
(8816) PvuI
(8668) FspI
(9724) BsaAI - SnaBI
chimeric intron
chicken β-actin promoter
CMV enhancer
AmpR promoter
AmpR
ori
SV40 promoter
SV40 ori
lac promoter
β-globin poly(A) signal
RRE
cPPT/CTS
HIV-1 gag
HIV-1 pol
2000
4000
6000
8000
10,000

pLVTHM:

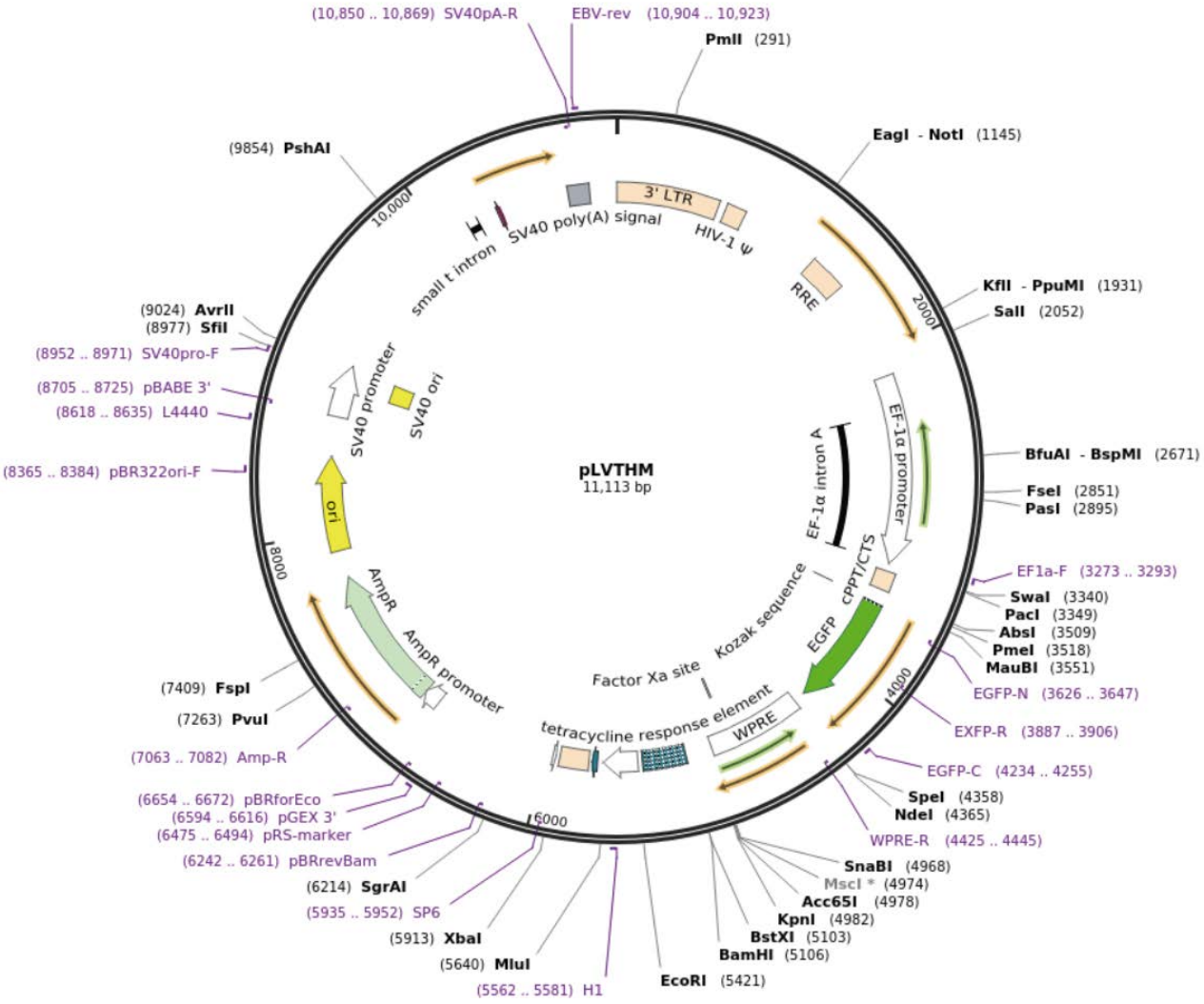
pLVTHM
11,113 bp
(10,850 .. 10,869) SV40pA-R
EBV-rev (10,904 .. 10,923)
PmlI (291)
EagI - NotI (1145)
KflI - PpuMI (1931)
SalI (2052)
BfuAI - BspMI (2671)
FseI (2851)
PasI (2895)
EF1a-F (3273 .. 3293)
SwaI (3340)
PacI (3349)
AbsI (3509)
PmeI (3518)
MauBI (3551)
EGFP-N (3626 .. 4647)
EXFP-R (3887 .. 3906)
EGFP-C (4234 .. 4255)
SpeI (4358)
NdeI (4365)
WPRE-R (4425 .. 4445)
SnaBI (4968)
MscI * (4974)
Acc65I (4978)
KpnI (4982)
BstXI (5103)
BamHI (5106)
EcoRI (5421)
(5562 .. 5581) H1
MluI (5640)
XbaI (5913)
(5935 .. 5952) SP6
SgrAI (6214)
(6242 .. 6261) pBRrevBam
(6475 .. 6494) pRS-marker
(6594 .. 6616) pGEX 3'
(6654 .. 6672) pBRforEco
(7063 .. 7082) Amp-R
PvuI (7263)
FspI (7409)
(8365 .. 8384) pBR322ori-F
(8618 .. 8635) L4440
(8705 .. 8725) pBABE 3'
(8952 .. 8971) SV40pro-F
SfiI (8977)
AvrII (9024)
PshAI (9854)
3' LTR
HIV-1 ψ
RRE
EF-1α promoter
EF-1α intron A
CPPT/CTS
EGFP
Kozak sequence
Factor Xa site
tetracycline response element
WPRE
AmpR promoter
AmpR
ori
SV40 ori
SV40 promoter
small t intron
SV40 poly(A) signal
2000
4000
6000
8000
10,000

pWPI:

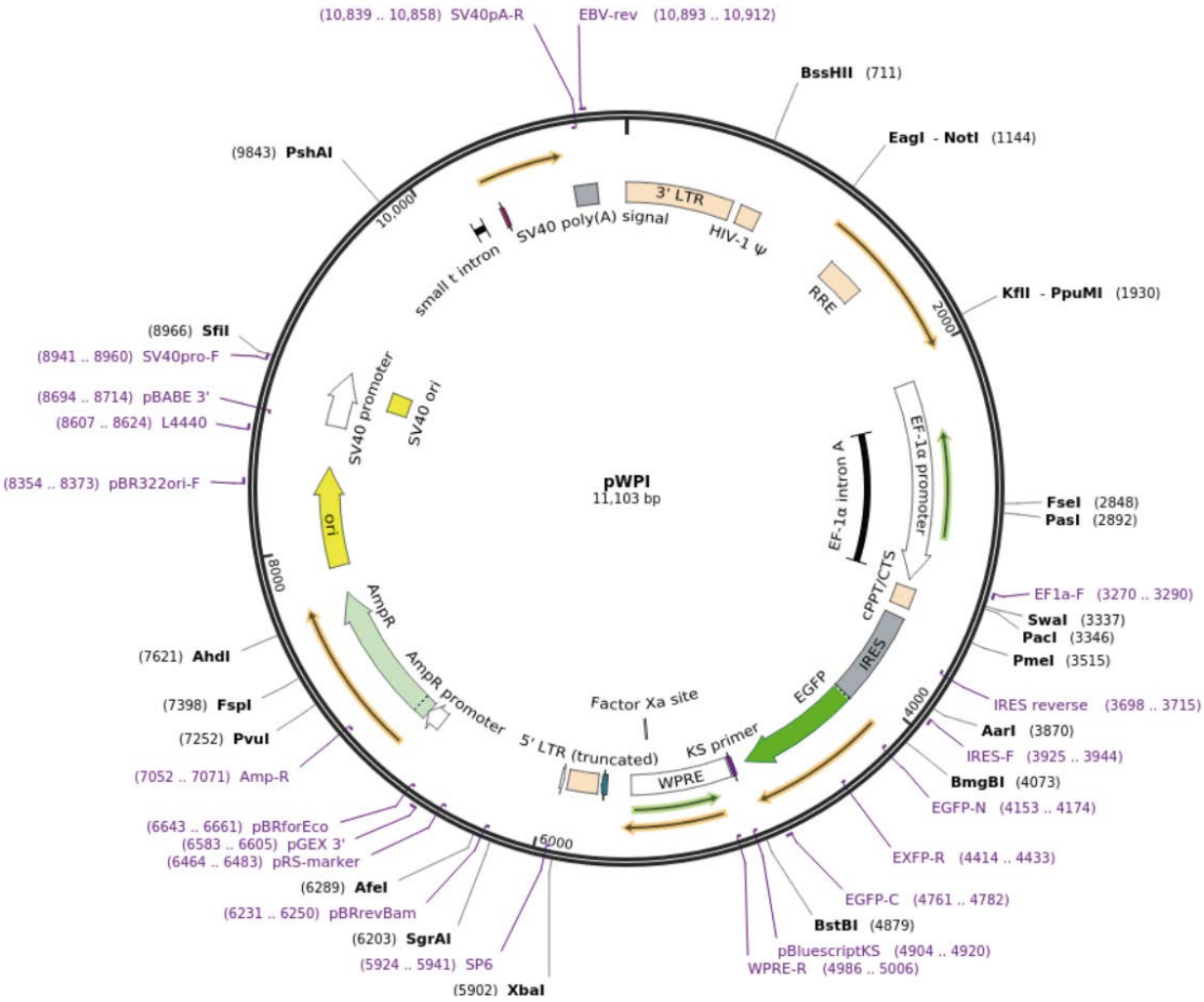
pWPI
11,103 bp
(10,839 .. 10,858) SV40pA-R
EBV-rev (10,893 .. 10,912)
BssHII (711)
EagI - NotI (1144)
KflI - PpuMI (1930)
FseI (2848)
PasI (2892)
EF1a-F (3270 .. 3290)
SwaI (3337)
PacI (3346)
PmeI (3515)
IRES reverse (3698 .. 3715)
AarI (3870)
IRES-F (3925 .. 3944)
BmgBI (4073)
EGFP-N (4153 .. 4174)
EXFP-R (4414 .. 4433)
EGFP-C (4761 .. 4782)
BstBI (4879)
pBluescriptKS (4904 .. 4920)
WPRE-R (4986 .. 5006)
(5902) XbaI
(5924 .. 5941) SP6
(6203) SgrAI
(6231 .. 6250) pBRrevBam
(6289) AfeI
(6464 .. 6483) pRS-marker
(6583 .. 6605) pGEX 3'
(6643 .. 6661) pBRforEco
(7052 .. 7071) Amp-R
(7252) PvuI
(7398) FspI
(7621) AhdI
(8354 .. 8373) pBR322ori-F
(8607 .. 8624) L4440
(8694 .. 8714) pBABE 3'
(8941 .. 8960) SV40pro-F
(8966) SfiI
(9843) PshAI
10,000
2000
4000
6000
8000
3' LTR
HIV-1 ψ
RRE
SV40 poly(A) signal
small t intron
SV40 promoter
SV40 ori
ori
AmpR
AmpR promoter
5' LTR (truncated)
Factor Xa site
KS primer
WPRE
EGFP
IRES
CPPT/CTS
EF-1α intron A
EF-1α promoter

pFUGW:

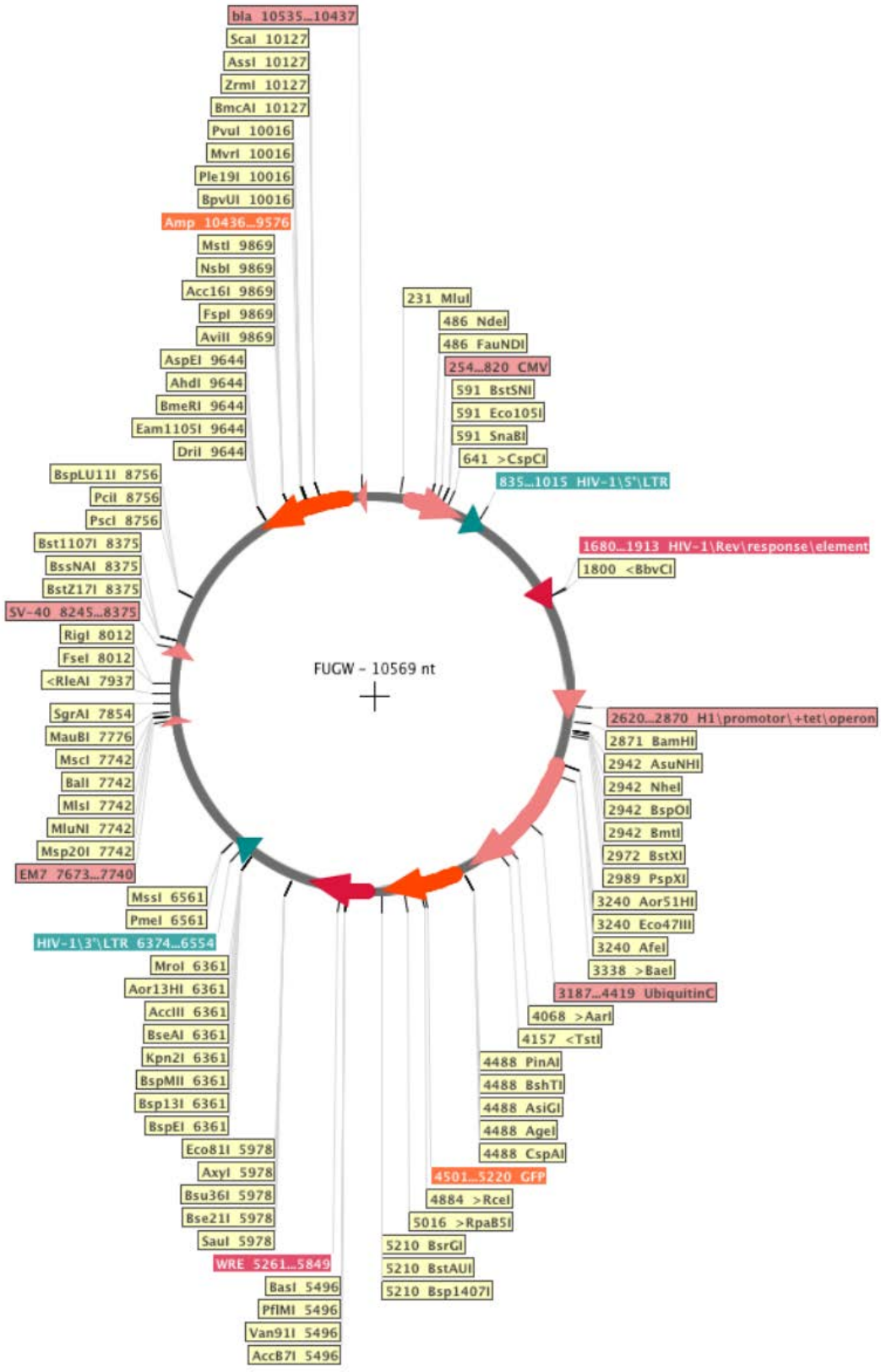
FUGW - 10569 nt
bla 10535...10437
ScaI 10127
AssI 10127
ZrmI 10127
BmcAI 10127
PvuI 10016
MvrI 10016
Ple19I 10016
BpvUI 10016
Amp 10436...9576
MstI 9869
NsbI 9869
Acc16I 9869
FspI 9869
AviII 9869
AspEI 9644
AhdI 9644
BmeRI 9644
Eam1105I 9644
DriI 9644
BspLU11I 8756
PciI 8756
PscI 8756
Bst1107I 8375
BssNAI 8375
BstZ17I 8375
SV-40 8245...8375
RigI 8012
FseI 8012
<RleAI 7937
SgrAI 7854
MauBI 7776
MscI 7742
BalI 7742
MlsI 7742
MluNI 7742
Msp20I 7742
EM7 7673...7740
MssI 6561
PmeI 6561
HIV-1\3'\LTR 6374...6554
MroI 6361
Aor13HI 6361
AccIII 6361
BseAI 6361
Kpn2I 6361
BspMII 6361
Bsp13I 6361
BspEI 6361
Eco81I 5978
AxyI 5978
Bsu36I 5978
Bse21I 5978
SauI 5978
WRE 5261...5849
BasI 5496
PflMI 5496
Van91I 5496
AccB7I 5496
231 MluI
486 NdeI
486 FauNDI
254...820 CMV
591 BstSNI
591 Eco105I
591 SnaBI
641 >CspCI
835...1015 HIV-1\5'\LTR
1680...1913 HIV-1\Rev\response\element
1800 <BbvCI
2620...2870 H1\promotor\+tet\operon
2871 BamHI
2942 AsuNHI
2942 NheI
2942 BspOI
2942 BmtI
2972 BstXI
2989 PspXI
3240 Aor51HI
3240 Eco47III
3240 AfeI
3338 >BaeI
3187...4419 UbiquitinC
4068 >AarI
4157 <TstI
4488 PinAI
4488 BshTI
4488 AsiGI
4488 AgeI
4488 CspAI
4501...5220 GFP
4884 >RceI
5016 >RpaBSI
5210 BsrGI
5210 BstAUI
5210 Bsp1407I

pcDNA3.1Nr4a2V5HisB:

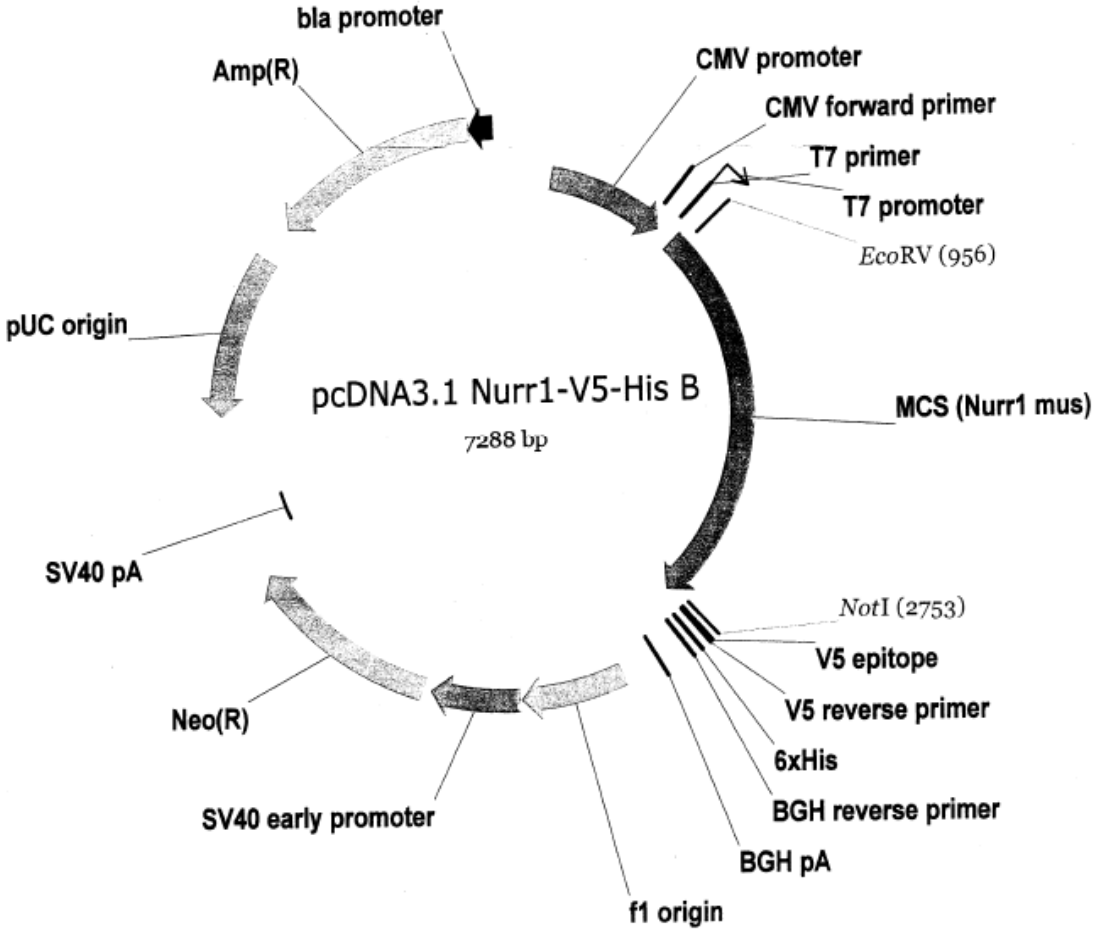

pRL-TK:

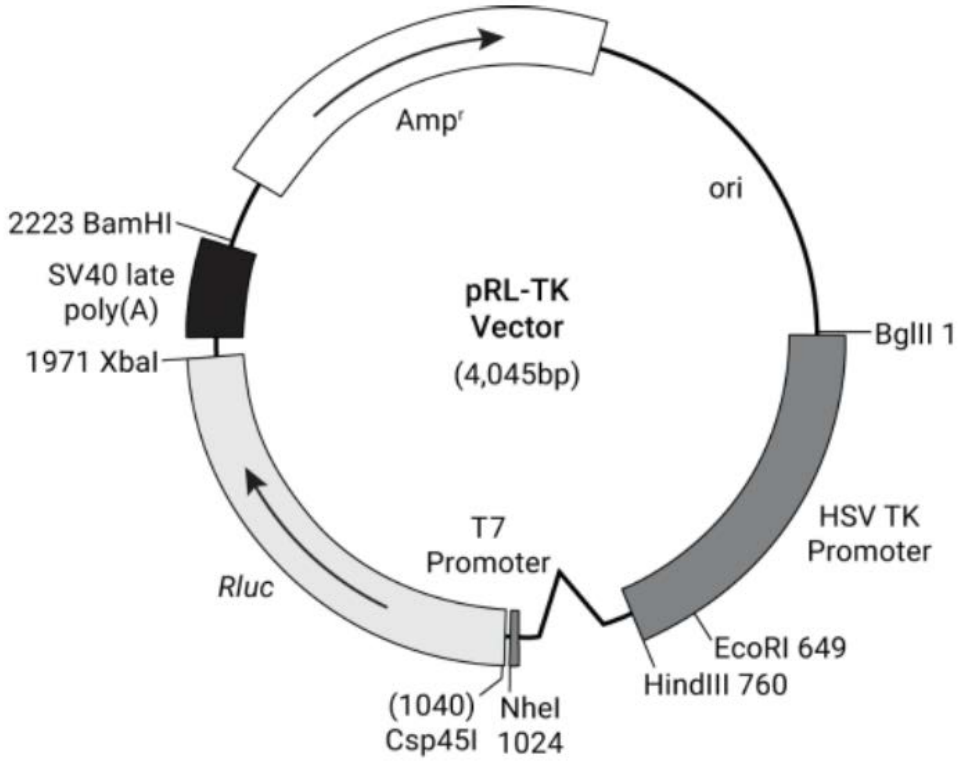
Amp^r
ori
2223 BamHI
SV40 late
poly(A)
1971 XbaI
pRL-TK
Vector
(4,045bp)
BglII 1
HSV TK
Promoter
T7
Promoter
Rluc
EcoRI 649
HindIII 760
(1040)
Csp45I
NheI
1024

pGL3b:

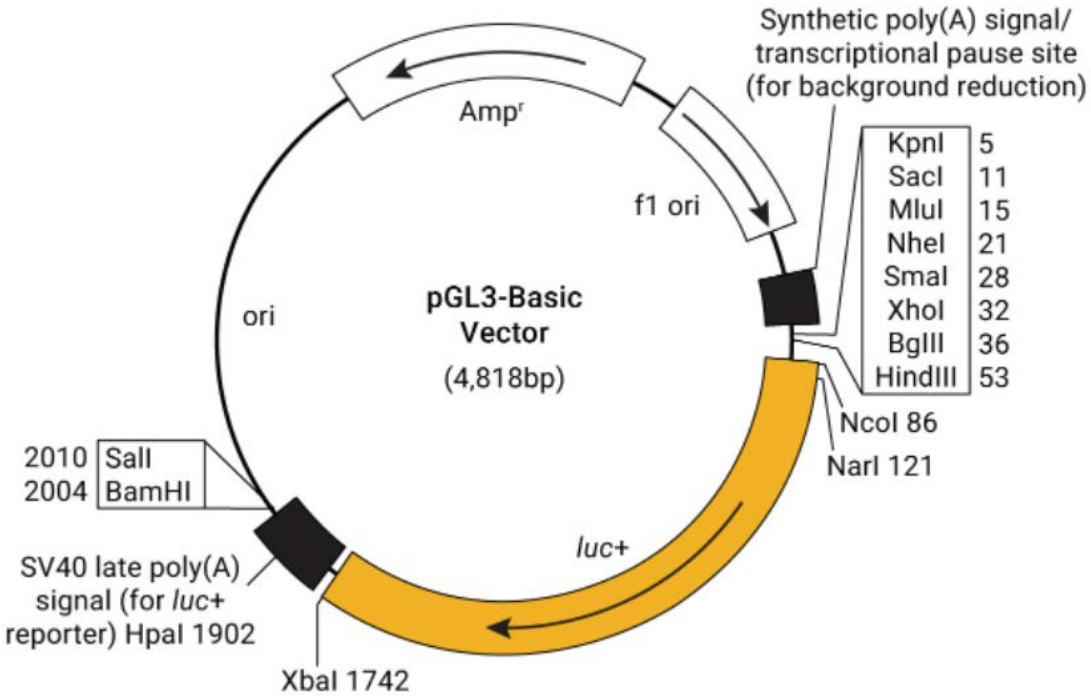
Synthetic poly(A) signal/
transcriptional pause site
(for background reduction)
Amp^r
f1 ori
ori
pGL3-Basic
Vector
(4,818bp)
KpnI 5
SacI 11
MluI 15
NheI 21
SmaI 28
XhoI 32
BglII 36
HindIII 53
NcoI 86
NarI 121
2010 SalI
2004 BamHI
luc+
SV40 late poly(A)
signal (for luc+
reporter) HpaI 1902
XbaI 1742

Annex 2.

Key resources table.

KEY RESOURCES TABLE

In alphabetical order

REAGENT or RESOURCE	SOURCE	IDENTIFIER
Antibodies		
ActinGreen 488 ReadyProbes reagent	Thermo Fisher Scientific	R37110
anti-Akt rabbit polyclonal	Cell Signaling	9272; RRID: AB_329827
anti-APP 20.1 mouse monoclonal	Dr. W.E. Van Nostrand	N/A
anti-β-actin (AC-15) mouse monoclonal	Sigma	A1978; RRID: AB_476692
anti-β-tubulin (5H1) mouse monoclonal	BD Biosciences	556321; RRID: AB_396360
anti-BDNF (N-20) rabbit polyclonal	Santa Cruz Biotechnology	sc-546; RRID: AB_630940
anti-CREB (48H2) rabbit monoclonal	Cell Signaling	9197; RRID: AB_331277
anti-CRTC1 (C71D11) rabbit monoclonal	Cell Signaling	2587; RRID: AB_2261091
anti-Erk1/2 rabbit polyclonal	Cell Signaling	9102; RRID: AB_330744
anti-GABA-AR α1 mouse monoclonal	Synaptic Systems	224-211; RRID: AB_2619928
anti-GAPDH (6C5) mouse monoclonal	Thermo Fisher Scientific	AM4300; RRID: AB_437392
anti-GFP rabbit polyclonal	Abcam	ab13970; RRID: AB_300798
anti-GFP rabbit polyclonal	Santa Cruz biotechnology	Sc-8334; RRID: AB_641123
anti-GluA1 rabbit polyclonal	Merck-Millipore	AB1504; RRID: AB_2113602
anti-GluA1 rabbit polyclonal	Merck-Millipore	PC246; RRID: AB_564636
anti-GluA2 (6C4) mouse monoclonal	Merck-Millipore	MAB397; RRID: AB_2113875
anti-GluN1 (54.1) mouse monoclonal	Merck-Millipore	MAB363; RRID: AB_94946
anti-GluN2A rabbit polyclonal	Merck-Millipore	AB1555; RRID: AB_2112325
anti-GluN2B rabbit polyclonal	Merck-Millipore	AB1557; RRID: AB_2112907
anti-Histone H3 rabbit polyclonal	Abcam	ab1791; RRID: AB_302613
anti-Nurr1 (N1404) mouse monclonal	Abcam	ab41917; RRID: AB_776887
anti-Nurr1 rabbit polyclonal	Sigma	N4663; RRID:AB_1841056
anti-Nurr1 rabbit polyclonal	Abgent	AP6412a; RRID:AB_2153902
anti-Nurr1 rabbit polyclonal	Millipore	AB5778; RRID:AB_92023
anti-Nurr1 rabbit polyclonal	Millipore	ABN1675
anti-Nurr1/Nur77 rabbit polyclonal	Santa Cruz biotechnology	sc-990; RRID: AB_2298676
anti-pancadherin rabbit polyclonal	Cell Signaling	4068S; RRID: AB_2158565
anti-phospho-Akt(Ser473) rabbit polyclonal	Cell Signaling	9271; RRID: AB_329825
anti-phospho-CREB(Ser133) (1B6) mouse monoclonal	Cell Signaling	9196; RRID: AB_331275
anti-phospho-Erk1/2(Thr202/Tyr204) rabbit polyclonal	Cell Signaling	9101; RRID: AB_331646
anti-phospho-GluA1(Ser845) (EPR2148) rabbit monoclonal	Abcam	ab76321; RRID: AB_1523688
anti-phospho-TrkB(Tyr706/Tyr707) (C50F3) rabbit monoclonal	Cell Signaling	4621; RRID: AB_916186
anti-PSD95 (6G6-1C9) mouse monoclonal	Abcam	ab2723; RRID: AB_303248
anti-synaptophysin mouse monoclonal	Sigma	S5768; RRID: AB_477523
anti-TrkB (80E3) rabbit monoclonal	Cell Signaling	4603; RRID: AB_2155125
anti-V5 tag rabbit polyclonal	Abcam	ab9116; RRID: AB_307024
Goat anti-chicken Alexa-488	Thermo Fisher Scientific	A11039; RRID: AB_142924
Goat anti-mouse Alexa-405	Life Technologies	A31553; RRID: AB_221604
Goat anti-mouse Alexa-568	Thermo Fisher Scientific	A11004; RRID: AB_141371
Goat anti-rabbit Alexa-488	Thermo Fisher Scientific	A11008; RRID: AB_143165

Goat anti-rabbit Alexa-568	Thermo Fisher Scientific	A11011; RRID: AB_143157
Hoechst 33258	Thermo Fisher Scientific	H3569, RRID: AB_2651133
HRP-linked anti-mouse IgG	BD Biosciences	554002; RRID: 395198
HRP-linked anti-rabbit IgG	BD Biosciences	554021; RRID: 395213
Media and supplements		
5-Fluoro-2'Deoxyuridine	Sigma	F0503
B-27 supplement	Thermo Fisher Scientific	17504
Deoxyribonuclease I from bovine pancreas (DNase I)	Sigma	D5025
DMEM	Thermo Fisher Scientific	41965039
DMEM F-12	Life technologies	11039-021
GlutaMAX	Thermo Fisher Scientific	35050-061
MEM	Thermo Fisher Scientific	51200-046
Mito+ serum extender	Corning	355006
Neurobasal	Thermo Fisher Scientific	21103049
Neurobasal-A	Thermo Fisher Scientific	10888022
Papain	Worthington	32K13664
Poly-D-lysine hydrobromide	Sigma	P6407
SOC Medium	Thermo Fisher Scientific	15544-034
Trypsin	Sigma	T9201
Trypsin inhibitor	Thermo Fisher Scientific	17075-029
Drugs		
4-aminopyridine (4-AP)	Tocris	0940
Amodiaquine dihydrochloride dehydrate (AQ)	Sigma	A2799
ANA-12	Sigma	SML0209
BAPTA-AM	Tocris	2787
BDNF; recombinant	R&D Systems	P23560
Bicuculline methiodide (Bic)	Tocris	2503
Chloroquine diphosphate salt (CQ)	Sigma	C6628
FK-506 monohydrate	Sigma	F4679
Forskolin (FSK)	Tocris	1099
Ketamine	Merial	Imalgene 100mg/ml
MK-801 maleate	Tocris	0924
MG-132	Tocris	1748
NBQX disodium salt	Tocris Alomone labs	1044 (electrophysiology) N-186 (biochemistry)
Nifedipine	Tocris	1075
N-Methyl-D-aspartate (NMDA)	Tocris	0114
Picrotoxin (PTX)	Hellobio	HB0506
Rolipram	Sigma	R6520
Tetrodotoxin citrate (TTX)	Tocis	1069
Xylazine	Bayer	Rompun 20 mg/ml
Chemicals and reagents		
Acrylamide/Bis 30%T/2.7C Solution	Bio-Rad	161-0158
Acrylamide/Bis 30%T/5%C Solution	Bio-Rad	161-0154
ECL^{IM} Western blotting Detection Reagents	GE Healthcare	RPN2106
Fluoromont G mounting medium	SouthernBiotech	0100-01
Formaldehid 4%	Casa Álvarez	FO090101.1221
Normal Goat Serum	Sigma	G9023
NP-40	Calbiochem	492016
Phosphatase Inhibitor Cocktail	Sigma	P2850
Ponceau S	Sigma	P-3504

Precision Plus Protein All Blue Standards	Bio-Rad	161-0373
Protease Inhibitor Cocktail	Sigma	P8340
Molecular biology reagents		
Calf intestinal alkaline phosphatase (CIAP)	New England BioLabs	M0290S
dNTP Set	Thermo Fisher Scientific	0181
Fast Sybr Green Master Mix	Thermo Fisher Scientific	4385612
GelRed Nucleic Acid Gel Stain	Biotium	41003
Oligo $d(T)_{18}$	Thermo Fisher Scientific	S0131
Phenol:chloroform isoamyl	Amresco	K169
Proteinase K	Sigma	3115879001
Random hexamer	Thermo Fisher Scientific	S0142
RNase-Free DNase Set	Qiagen	79254
RNaseOUT Recombinant Ribonuclease inhibitor	Thermo Fisher Scientific	10777019
T4 DNA ligase	New England BioLabs	M0202S
T4 polynucleotide kinase	New England BioLabs	M0201S
Taq polymerase Platinum-Pfx	Thermo Fisher Scientific	11708-013
SuperScript IV	Thermo Fisher Scientific	18090050
Ultrapure glycogen	Life Technologies	10814-010
Restriction enzymes		
AgeI	New England BioLabs	R0552S
BamHI	New England BioLabs	R0136S
NheI	New England BioLabs	R0131S
PmeI	New England BioLabs	R0560S
Commercial assays and material		
Agilent RNA 6000 Nano Kit	Agilent Technologies	5067-1511
CalPhos MammalianTransfection kit	Clontech	631312
Coverglasses	Paul Marienfeld Thermo Electron corporation	0111520 6776319
Dual-luciferase Reporter Assay System	Promega	E1910
EZ-link-sulfo-NHS-LC-biotin	Thermo Fisher Scientific	21335
In-Fusion HD Cloning	Clontech	639649
Microslides	Deltalab Thermo Fisher Scientific	D100003 J1800AMNZ
Milliplex map kit	Milliplex	MPTMAG-49K
Needle GA30, 13mm, PST 30º	Hamilton	HA-7803-07
Neutravidin Ultralink Resin	Thermo Fisher Scientific	53150
Nitrocellulose blotting membrane	GE Healthcare	10600001
Nucleobond Xtra Maxi EF	Macherey-Nagel	740424
NucleoSpin Gel and PCR clean-up	Macherey-Nagel	740609
NucleoSpin Plasmid (NoLid)	Macherey-Nagel	740499
Pierce BCA protein assay kit	Thermo Fisher Scientific	23225
Pierce Protein A Plus agarose	Thermo Fisher Scientific	22811
PVDF blotting membrane	GE Healthcare	10600029
RNeasy Mini-Kit	Qiagen	74104
Syringe Hamilton Gastight 1701	Hamilton	HA-7653-01
TPX microtube	Diagenode	C30010010-300
Biological samples		
Human brain tissue	Fundación CIEN (Instituto de Salud Carlos III, Madrid), Fundación Hospital Alcorcón (Madrid), Hospital Clínic - IDIBAPS (Barcelona), Hospital Bellvitge (Barcelona)	

Experimental models		
Human: HEK293T	Dharmacon	77HCL4517
Mouse: C57BL/6J	Charles River Labs	
Mouse: C57BL/6JRccHsd	Envigo	043
Rat: Sprague-Dawley	Charles River Labs	24109320
Bacterial strains		
Stellar Competent Cells	Clontech	636766
Subcloning efficiency DH5α competent cells	Thermo Fisher Scientific	18265017
Plasmids		
AAV2/10.CMV.Nr4a2.V5.IRES.GFP	Unitat Producció Viral (CBATEG, UAB)	N/A
AAV2/10.H1.shNr4a2.V5.IRES.GFP	Unitat Producció Viral (CBATEG, UAB)	N/A
pcDNA3.1Nr4a2V5HisB	Dr. Ángel Juan García Yagüe	N/A
pGl3basic	Promega	E1751
pFUGW	Dr. Robert C. Malenka	
pLVTHM	Dr. Didier Trono, Addgene	12247, RRID:Addgene_12247
pMD2.G, psPax2	Dr. Didier Trono, Addgene	12259, RRID:Addgene_12259 12260, RRID:Addgene_12260
pRL-TK vector	Promega	E2241
pVSVG, pRRE, pREV	Dr. Robert C. Malenka	
pWpi	Dr. Didier Trono, Addgene	12254; RRID:Addgene_12254
Software and Algorithms		
ANY-maze	Stoelting	http://sandiegoinstruments.com/any-maze-video-tracking/; RRID:SCR_014289
GraphPad Prism 6.01	GraphPad software	http://www.graphpad.com; RRID:SCR_002798
Igor Pro 4.09A	WaveMetrics	http://www.wavemetrics.com/products/igorpr/ogorpro.htm RRID:SCR_000325
ImageJ 2.0	NIH	https://imageJ.nih.gov/ij/; RRID:SCR_003070
Imaris 8	Bitplane, Oxford Instrument Company	http://www.bitplane.com/imaris; RRID:SCR_007370
LinRegPCR	University of Amsterdam	N/A
OriginPro 7.0	OriginLab corporation	http://www.originlab.com RRID:SCR_014212
SPSS 17.0	Ibm	http://www-01.ibm.com/software/uk/analytics/spss; RRID: SCR_002865
Video Freeze Software	Med associates inc.	SOF-843 www.med-associates.com

Annex 3.

Different behavioral markers for $APP_{Sw,Ind}$ mice and effects of Nr4a2 overexpression.

	6 months-old				12 months-old				Statistics (age)	Statistics
	WT-GFP	WT-Nr4a2	$APP_{Sw,Ind}$-GFP	$APP_{Sw,Ind}$-Nr4a2	WT-GFP	WT-Nr4a2	$APP_{Sw,Ind}$-GFP	$APP_{Sw,Ind}$-Nr4a2		
Corner test										
Latency of rearing	17,425 ± 3,256	20,188 ± 3,466	22,42 ± 2,611	23,796 ± 2,361	22,989 ± 2,768	22,52 ± 3,335	19,897 ± 2,357	20,684 ± 3,044		
Total number of rearings	2,75 ± 0,701	1,9 ± 0,96	1,5 ± 0,522	0,889 ± 0,423	1,222 ± 0,401	1,25 ± 0,526	2 ± 0,645	2,1 ± 0,674		GxA*
Total number of corners	5,5 ± 0,802	5,8 ± 0,696	5,7 ± 0,803	5,667 ± 0,764	4,444 ± 0,784	4,125 ± 0,934	6,778 ± 1,178	5 ± 0,856		
Open Field test										
Latency of an event (s)										
Initial movement	0,97 ± 0,075	1,231 ± 0,305	1,178 ± 0,171	1,174 ± 0,106	0,931 ± 0,098	1,038 ± 0,123	0,808 ± 0,132	0,927 ± 0,082		
Exit of the center	3,618 ± 0,846	4,246 ± 1,014	2,562 ± 0,46	5,347 ± 1,271	4,862 ± 0,961	7,103 ± 0,949	5,421 ± 1,462	7,657 ± 2,198		T*, A**
Entrance to periphery	7,198 ± 1,776	9,547 ± 2,512	5,316 ± 0,683	16,2 ± 3,301	17,214 ± 5,487	20,19 ± 2,802	17,919 ± 4,117	21,191 ± 5,671	T** (6M), APP-GFP vs APP-Nr4a2** (6M)	A****
Vertical activity	24,46 ± 3,697	32,327 ± 7,605	31,872 ± 6,985	54,668 ± 10,042	45,431 ± 8,426	54,655 ± 6,16	36,08 ± 6,883	52,431 ± 8,65	T p=0.052 (6M)	T*, A*
Self-grooming	223,65 ± 27,907	183,432 ± 22,89	228,234 ± 21,468	214,197 ± 19,6	210,678 ± 22,274	178,854 ± 17,082	234,36 ± 14,015	222,045 ± 26,707		G=0.055
Total number of an event										
Crossings	348,889 26,644±	347,778 ± 39,808	315,9 ± 19,921	334,556 ± 22,522	386,333 ± 30,437	333,625 ± 13,865	350,778 ± 35,822	399,7 ± 21,367		
Wall rearings	30,778 ± 2,172	33 ± 3,303	37,9 ± 3,024	29,667 ± 3,35	35,222 ± 3,8	27,875 ± 1,274	42,778 ± 4,403	29,7 ± 2,15	T** (12M)	T**
Rearings	2,75 ± 1,42	4 ± 1,38	2,6 ± 1,43	5,2 ± 1,61	3,11 ± 1,41	1,75 ± 0,59	1,11 ± 0,3	3,2 ± 1,34		
Time self-grooming	3.07 ± 1.03	2.95 ± 0.64	4.39 ± 1.27	3.09 ± 0.78	3,09 ± 0,75	4,39 ± 0,62	6,8 ± 2,09	2,73 ± 0,79		GxT*
Speed (m/s)	0,055 ± 0,005	0,056 ± 0,007	0,055 ± 0,005	0,053 ± 0,005	0,06 ± 0,006	0,051 ± 0,002	0,057 ± 0,006	0,063 ± 0,005		
Incidence										
Defecation	25	10	27.27	44.44	11,1	0	44,4	50		
Urination	12.5	30	36.36	11.11	22,2	25	11,1	50		
Marble test										
Latency to turn	4,578 ± 1,177	3,847 ± 0,906	2,03 ± 0,322	2,586 ± 0,544	3,347 ± 0,451	3,425 ± 0,641	3,416 ± 0,54	2,464 ± 0,312	G* (6M)	G*
Latency to marble touch	7,64 ± 2,514	5,402 ± 1,708	8,857 ± 2,602	5,523 ± 1,345	6,983 ± 1,021	7,645 ± 0,897	6,766 ± 0,995	7,518 ± 1,575		

Statistical analysis was determined by two-way ANOVA followed by Bonferroni *post hoc* test.
A, age effect; G, genotype effect; T, treatment effect; GxT, genotype x treatment interaction.

XI. References

Abdul, H. M., Sama, M. A., Furman, J. L., Mathis, D. M., Beckett, T. L., Weidner, A. M., … Norris, C. M. (2009). Cognitive decline in Alzheimer's disease is associated with selective changes in calcineurin/NFAT signaling. *Journal of Neuroscience*, *29*(41), 12957–12969. https://doi.org/10.1523/JNEUROSCI.1064-09.2009

Adesnik, H., Nicoll, R. A., & England, P. M. (2005). Photoinactivation of native AMPA receptors reveals their real-time trafficking. *Neuron*, *48*(6), 977–985. https://doi.org/10.1016/j.neuron.2005.11.030

Ahn, J. H., Lee, J. S., Cho, J. H., Park, J. H., Lee, T. K., Song, M., … Lee, C. H. (2018). Age-dependent decrease of Nurr1 protein expression in the gerbil hippocampus. *Biomedical Reports*, *8*(6), 517–522. https://doi.org/10.3892/br.2018.1094

Alberdi, E., Sánchez-Gómez, M. V., Cavaliere, F., Pérez-Samartín, A., Zugaza, J. L., Trullas, R., … Matute, C. (2010). Amyloid β oligomers induce Ca2+ dysregulation and neuronal death through activation of ionotropic glutamate receptors. *Cell Calcium*, *47*(3), 264–272. https://doi.org/10.1016/j.ceca.2009.12.010

Alberini, C. M. (2009). Transcription Factors in Long-Term Memory and Synaptic Plasticity. *Physiological Reviews*, *89*(1), 121–145. https://doi.org/10.1152/physrev.00017.2008

Aldavert-Vera, L., Huguet, G., Costa-Miserachs, D., Ortiz, S. P. de, Kádár, E., Morgado-Bernal, I., & Segura-Torres, P. (2013). Intracranial self-stimulation facilitates active-avoidance retention and induces expression of c-Fos and Nurr1 in rat brain memory systems. *Behavioural Brain Research*, *250*, 46–57. https://doi.org/10.1016/j.bbr.2013.04.025

Almeida, C. G., Tampellini, D., Takahashi, R. H., Greengard, P., Lin, M. T., Snyder, E. M., & Gouras, G. K. (2005). Beta-amyloid accumulation in APP mutant neurons reduces PSD-95 and GluR1 in synapses. *Neurobiology of Disease*, *20*(2), 187–198. https://doi.org/10.1016/j.nbd.2005.02.008

Alvarez-Castelao, B., Losada, F., Ahicart, P., & Castaño, J. G. (2013). The N-Terminal Region of Nurr1 (a.a 1-31) Is Essential for Its Efficient Degradation by the Ubiquitin Proteasome Pathway. *PLoS ONE*, *8*(2), 1–8. https://doi.org/10.1371/journal.pone.0055999

Ando, K., Uemura, K., Kuzuya, A., Maesako, M., Asada-Utsugi, M., Kubota, M., … Kinoshita, A. (2011). N-cadherin regulates p38 MAPK signaling via association with JNK-associated leucine zipper protein: Implications for neurodegeneration in Alzheimer disease. *Journal of Biological Chemistry*, *286*(9), 7619–7628. https://doi.org/10.1074/jbc.M110.158477

Angoa-Pérez, M., Kane, M. J., Briggs, D. I., Francescutti, D. M., & Kuhn, D. M. (2013). Marble Burying and Nestlet Shredding as Tests of Repetitive, Compulsive-like Behaviors in Mice. *Journal of Visualized Experiments*, (82). https://doi.org/10.3791/50978

Annese, A., Manzari, C., Lionetti, C., Picardi, E., Horner, D. S., Chiara, M., … D'Erchia, A. M. (2018). Whole transcriptome profiling of Late-Onset Alzheimer's Disease patients provides insights into the molecular changes involved in the disease. *Scientific Reports*, *8*(1), 4282. https://doi.org/10.1038/s41598-018-22701-2

Arai, H., Clark, C. M., Ewbank, D. C., Takase, S., Higuchi, S., Miura, M., … Sasaki, H. (1998). Cerebrospinal fluid tau protein as a potential diagnostic marker in Alzheimer's disease. *Neurobiology of Aging*, *19*(2), 125–126. https://doi.org/10.1016/S0197-4580(98)00018-9

Arnold, F. J. L., Hoffmann, F., Bengtson, C. P., Wittmann, M., Vanhoutte, P., & Bading, H. (2005). Microelectrode array recordings of cultured hippocampal networks reveal a simple model for transcription and protein synthesis-dependent plasticity. *Journal of Physiology*, *564*(1), 3–19. https://doi.org/10.1113/jphysiol.2004.077446

Arredondo, C., Orellana, M., Vecchiola, A., Pereira, L. A., Galdames, L., & Andrés, M. E. (2013). PIASγ Enhanced SUMO-2 Modification of Nurr1 Activation-Function-1 Domain Limits Nurr1 Transcriptional Synergy. *PLoS ONE*, *8*(1). https://doi.org/10.1371/journal.pone.0055035

Baazaoui, N., & Iqbal, K. (2018). A Novel Therapeutic Approach to Treat Alzheimer's Disease by Neurotrophic Support During the Period of Synaptic Compensation. *Journal of Alzheimer's Disease : JAD*, *62*(3), 1211–1218. https://doi.org/10.3233/JAD-170839

Baeta-Corral, R., Johansson, B., & Giménez-Llort, L. (2018). Long-term treatment with low-dose

caffeine worsens BPSD-Like profile in 3xTg-AD mice model of Alzheimer'S disease and affects mice with normal aging. *Frontiers in Pharmacology*, *9*(FEB), 1–17. https://doi.org/10.3389/fphar.2018.00079

Balducci, C., Mehdawy, B., Mare, L., Giuliani, A., Lorenzini, L., Sivilia, S., … Nistico, R. (2011). The gamma-secretase modulator CHF5074 restores memory and hippocampal synaptic plasticity in plaque-free Tg2576 mice. *Journal of Alzheimer's Disease : JAD*, *24*(4), 799–816. https://doi.org/10.3233/JAD-2011-101839

Banke, T. G., Bowie, D., Lee, H. K., Huganir, R. L., Schousboe, A., & Traynelis, S. F. (2000). Control of GluR1 AMPA receptor function by cAMP-dependent protein kinase. *Journal of Neuroscience*, *20*(1), 89–102. https://doi.org/10.1523/jneurosci.20-01-00089.2000

Bannerman, D. M., Rawlins, J. N., McHugh, S. B., Deacon, R. M., Yee, B. K., Bast, T., … Feldon, J. (2004). Regional dissociations within the hippocampus—memory and anxiety. *Neuroscience & Biobehavioral Reviews*, *28*(3), 273–283. https://doi.org/10.1016/j.neubiorev.2004.03.004

Barghorn, S., Nimmrich, V., Striebinger, A., Krantz, G., Keller, P., Janson, B., … Hillen, H. (2005). Globular amyloid β-peptide1-42 oligomer - A homogenous and stable neuropathological protein in Alzheimer's disease. *Journal of Neurochemistry*, *95*(3), 834–847. https://doi.org/10.1111/j.1471-4159.2005.03407.x

Barneda-Zahonero, B., Servitja, J. M., Badiola, N., Miñano-Molina, A. J., Fadó, R., Saura, C. A., & Rodríguez-Alvarez, J. (2012). Nurr1 protein is required for N-Methyl-D-aspartic Acid (NMDA) receptor-mediated neuronal survival. *Journal of Biological Chemistry*, *287*(14), 11351–11362. https://doi.org/10.1074/jbc.M111.272427

Baumgart, M., Snyder, H. M., Carrillo, M. C., Fazio, S., Kim, H., & Johns, H. (2015). Summary of the evidence on modifiable risk factors for cognitive decline and dementia: A population-based perspective. *Alzheimer's & Dementia*, *11*(6), 718–726. https://doi.org/10.1016/j.jalz.2015.05.016

Beckman, D., Ott, S., Donis-Cox, K., Janssen, W. G., Bliss-Moreau, E., Rudebeck, P. H., … Morrison, J. H. (2019). Oligomeric Aβ in the monkey brain impacts synaptic integrity and induces accelerated cortical aging. *Proceedings of the National Academy of Sciences of the United States of America*, *116*(52), 26239–26246. https://doi.org/10.1073/pnas.1902301116

Bejanin, A., Schonhaut, D. R., La Joie, R., Kramer, J. H., Baker, S. L., Sosa, N., … Rabinovici, G. D. (2017). Tau pathology and neurodegeneration contribute to cognitive impairment in Alzheimer's disease. *Brain*, *140*(12), 3286–3300. https://doi.org/10.1093/brain/awx243

Bekinschtein, P., Cammarota, M., & Medina, J. H. (2014). BDNF and memory processing. *Neuropharmacology*, *76*(PART C), 677–683. https://doi.org/10.1016/j.neuropharm.2013.04.024

Bekris, L. M., Yu, C.-E., Bird, T. D., & Tsuang, D. W. (2010). Review Article: Genetics of Alzheimer Disease. *Journal of Geriatric Psychiatry and Neurology*, *23*(4), 213–227. https://doi.org/10.1177/0891988710383571

Bensinger, S. J., & Tontonoz, P. (2009). A Nurr1 Pathway for Neuroprotection. *Cell*, *137*(1), 26–28. https://doi.org/10.1016/j.cell.2009.03.024

Berchtold, N. C., Sabbagh, M. N., Beach, T. G., Kim, R. C., Cribbs, D. H., & Cotman, C. W. (2014). Brain gene expression patterns differentiate mild cognitive impairment from normal aged and Alzheimer's disease. *Neurobiology of Aging*, *35*(9), 1961–1972. https://doi.org/10.1016/j.neurobiolaging.2014.03.031

Bereczki, E., Francis, P. T., Howlett, D., Pereira, J. B., Höglund, K., Bogstedt, A., … Aarsland, D. (2016). Synaptic proteins predict cognitive decline in Alzheimer's disease and Lewy body dementia. *Alzheimer's and Dementia*, *12*(11), 1149–1158. https://doi.org/10.1016/j.jalz.2016.04.005

Berridge, M. J. (2011). Calcium signalling and Alzheimer's disease. *Neurochemical Research*, *36*(7), 1149–1156. https://doi.org/10.1007/s11064-010-0371-4

Bezprozvanny, I., & Mattson, M. P. (2008). Neuronal calcium mishandling and the pathogenesis of Alzheimer's disease. *Trends in Neurosciences*, *31*(9), 454–463.

https://doi.org/10.1016/j.tins.2008.06.005

Bhaskar, K., Yen, S.-H., & Lee, G. (2005). Disease-related Modifications in Tau Affect the Interaction between Fyn and Tau. *Journal of Biological Chemistry*, *280*(42), 35119–35125. https://doi.org/10.1074/jbc.M505895200

Bie, B., Wu, J., Foss, J. F., & Naguib, M. (2018). Amyloid fibrils induce dysfunction of hippocampal glutamatergic silent synapses. *Hippocampus*, *28*(8), 549–556. https://doi.org/10.1002/hipo.22955

Bitel, C. L., Kasinathan, C., Kaswala, R. H., Klein, W. L., & Frederikse, P. H. (2012). Amyloid-β and Tau Pathology of Alzheimer's Disease Induced by Diabetes in a Rabbit Animal Model. *Journal of Alzheimer's Disease*, *32*(2), 291–305. https://doi.org/10.3233/JAD-2012-120571

Bittinger, M. A., McWhinnie, E., Meltzer, J., Iourgenko, V., Latario, B., Liu, X., … Labow, M. (2004). Activation of cAMP Response Element-Mediated Gene Expression by Regulated Nuclear Transport of TORC Proteins. *Current Biology*, *14*(23), 2156–2161. https://doi.org/10.1016/j.cub.2004.11.002

Bittner, T., Fuhrmann, M., Burgold, S., Ochs, S. M., Hoffmann, N., Mitteregger, G., … Herms, J. (2010). Multiple events lead to dendritic spine loss in triple transgenic Alzheimer's disease mice. *PLoS ONE*, *5*(11), 1–9. https://doi.org/10.1371/journal.pone.0015477

Blalock, E. M., Geddes, J. W., Chen, K. C., Porter, N. M., Markesbery, W. R., & Landfield, P. W. (2004). Incipient Alzheimer's disease: Microarray correlation analyses reveal major transcriptional and tumor suppressor responses. *Proceedings of the National Academy of Sciences of the United States of America*, *101*(7), 2173–2178. https://doi.org/10.1073/pnas.0308512100

Blennow, K., Leon, M. J. De, & Zetterberg, H. (2006). *Alzheimer ' s disease*. *368*, 387–403. https://doi.org/10.1016/S0140-6736(06)69113-7

Bliss, T. V. P., & Lomo, T. (1973). Long-lasting potentiation of synaptic transmission in the dentate area of the anaesthetized rabbit following stimulation of the perforant path. *J. Physiol*, *232*, 331–356. http://doi.org/10.1113/jphsiol.1973.sp010273

Bliss, T. V. P., & Collingridge, G. L. (2013). Expression of NMDA receptor-dependent LTP in the hippocampus: bridging the divide. *Molecular Brain*, *6*, 1–14. https://doi.org/10.1186/1756-6606-6-5. http://doi.org/10.1186/1756-6606-6-5

Boakye, C. H. A., Doddapaneni, R., Shah, P. P., Patel, A. R., Godugu, C., Safe, S., … Singh, M. (2013). Chemoprevention of Skin Cancer with 1,1-Bis (3′-Indolyl)-1-(Aromatic) Methane Analog through Induction of the Orphan Nuclear Receptor, NR4A2 (Nurr1). *PLoS ONE*, *8*(8), 1–10. https://doi.org/10.1371/journal.pone.0069519

Braak, H., & Braak, E. (1991). Neuropathological stageing of Alzheimer-related changes. *Acta Neuropathologica*, *82*(4), 239–259. https://doi.org/10.1007/BF00308809

Bramham, C. R. (2008). Local protein synthesis, actin dynamics, and LTP consolidation. *Current Opinion in Neurobiology*, *18*(5), 524–531. https://doi.org/10.1016/j.conb.2008.09.013

Bredt, D. S., & Nicoll, R. A. (2003). AMPA receptor trafficking at excitatory synapses. *Neuron*, *40*(2), 361–379. https://doi.org/10.1016/S0896-6273(03)00640-8

Bridi, M. S., & Abel, T. (2013). The NR4A orphan nuclear receptors mediate transcription-dependent hippocampal synaptic plasticity. *Neurobiology of Learning and Memory*, *105*, 151–158. https://doi.org/10.1016/j.nlm.2013.06.020

Bridi, M. S., Hawk, J. D., Chatterjee, S., Safe, S., & Abel, T. (2017). Pharmacological Activators of the NR4A Nuclear Receptors Enhance LTP in a CREB/CBP-Dependent Manner. *Neuropsychopharmacology*, *42*(6), 1243–1253. https://doi.org/10.1038/npp.2016.253

Brigidi, G. S., Hayes, M. G. B., Delos Santos, N. P., Hartzell, A. L., Texari, L., Lin, P. A., … Bloodgood, B. L. (2019). Genomic Decoding of Neuronal Depolarization by Stimulus-Specific NPAS4 Heterodimers. *Cell*, *179*(2), 373-391.e27. https://doi.org/10.1016/j.cell.2019.09.004

Buonarati, O. R., Hammes, E. A., Watson, J. F., Greger, I. H., & Hell, J. W. (2019). Mechanisms of postsynaptic localization of AMPA-type glutamate receptors and their regulation during long-term potentiation. *Science Signaling*, *12*(562), 1–10. https://doi.org/10.1126/scisignal.aar6889

Caetano, F. A., Beraldo, F. H., Hajj, G. N. M., Guimaraes, A. L., Jürgensen, S., Wasilewska-Sampaio, A. P., … Prado, M. A. M. (2011). Amyloid-beta oligomers increase the localization of prion protein at the cell surface. *Journal of Neurochemistry*, *117*(3), 538–553. https://doi.org/10.1111/j.1471-4159.2011.07225.x

Calabrese, B., Shaked, G. M., Tabarean, I. V., Braga, J., Koo, E. H., & Halpain, S. (2007). Rapid, concurrent alterations in pre- and postsynaptic structure induced by naturally-secreted amyloid-β protein. *Molecular and Cellular Neuroscience*, *35*(2), 183–193. https://doi.org/10.1016/j.mcn.2007.02.006

Caldeira, M. V., Melo, C. V., Pereira, D. B., Carvalho, R., Correia, S. S., Backos, D. S., … Duarte, C. B. (2007a). Brain-derived neurotrophic factor regulates the expression and synaptic delivery of α-amino-3-hydroxy-5-methyl-4-isoxazole propionic acid receptor subunits in hippocampal neurons. *Journal of Biological Chemistry*, *282*(17), 12619–12628. https://doi.org/10.1074/jbc.M700607200

Caldeira, M. V., Melo, C. V., Pereira, D. B., Carvalho, R. F., Carvalho, A. L., & Duarte, C. B. (2007b). BDNF regulates the expression and traffic of NMDA receptors in cultured hippocampal neurons. *Molecular and Cellular Neuroscience*, *35*(2), 208–219. https://doi.org/10.1016/j.mcn.2007.02.019

Cantanelli, P., Sperduti, S., Ciavardelli, D., Stuppia, L., Gatta, V., & Sensi, S. L. (2014). Age-dependent modifications of AMPA receptor subunit expression levels and related cognitive effects in 3xTg-AD mice. *Frontiers in Aging Neuroscience*, *6*(AUG), 1–11. https://doi.org/10.3389/fnagi.2014.00200

Carvalho, A. L., Caldeira, M. V., Santos, S. D., & Duarte, C. B. (2008). Role of the brain-derived neurotrophic factor at glutamatergic synapses. *British Journal of Pharmacology*, *153*(MAR), suppl 1, 310–324. https://doi.org/10.1038/sj.bjp.0707509

Castellano, J. M., Kim, J., Stewart, F. R., Jiang, H., DeMattos, R. B., Patterson, B. W., … Holtzman, D. M. (2011). Human apoE Isoforms Differentially Regulate Brain Amyloid- Peptide Clearance. *Science Translational Medicine*, *3*(89), 89ra57-89ra57. https://doi.org/10.1126/scitranslmed.3002156

Cavallucci, V., Berretta, N., Nobili, A., Nisticò, R., Mercuri, N. B., & D'Amelio, M. (2013). Calcineurin inhibition rescues early synaptic plasticity deficits in a mouse model of Alzheimer's disease. *NeuroMolecular Medicine*, *15*(3), 541–548. https://doi.org/10.1007/s12017-013-8241-2

Cearley, C. N., & Wolfe, J. H. (2006). Transduction characteristics of adeno-associated virus vectors expressing cap serotypes 7, 8, 9, and Rh10 in the mouse brain. *Molecular Therapy*, *13*(3), 528–537. https://doi.org/10.1016/j.ymthe.2005.11.015

Celsi, F., Svedberg, M., Unger, C., Cotman, C. W., Carrì, M. T., Ottersen, O. P., … Torp, R. (2007). Beta-amyloid causes downregulation of calcineurin in neurons through induction of oxidative stress. *Neurobiology of Disease*, *26*(2), 342–352. https://doi.org/10.1016/j.nbd.2006.12.022

Ch'Ng, T. H., Uzgil, B., Lin, P., Avliyakulov, N. K., O'Dell, T. J., & Martin, K. C. (2012). Activity-dependent transport of the transcriptional coactivator CRTC1 from synapse to nucleus. *Cell*, *150*(1), 207–221. https://doi.org/10.1016/j.cell.2012.05.027

Chang, C. Z., Kwan, A. L., & Howng, S. L. (2010). 6-Mercaptopurine exerts an immunomodulatory and neuroprotective effect on permanent focal cerebral occlusion in rats. *Acta Neurochirurgica*, *152*(8), 1383–1390. https://doi.org/10.1007/s00701-010-0608-7

Chater, T. E., & Goda, Y. (2014). The role of AMPA receptors in postsynaptic mechanisms of synaptic plasticity. *Frontiers in Cellular Neuroscience*, *8*(NOV), 1–14. https://doi.org/10.3389/fncel.2014.00401

Chatterjee, S., Walsh, E. N., Yan, A. L., Giese, K. P., Safe, S., & Abel, T. (2020). Pharmacological activation of Nr4a rescues age-associated memory decline. *Neurobiology of Aging*, *85*, 140–144. https://doi.org/10.1016/j.neurobiolaging.2019.10.001

Chen, X., Lin, R., Chang, L., Xu, S., Wei, X., Zhang, J., … Wang, Q. (2013). Enhancement of long-term depression by soluble amyloid beta protein in rat hippocampus is mediated by metabotropic glutamate receptor and involves activation of p38MAPK, STEP and caspase-3.

Neuroscience, *253*, 435–443. https://doi.org/10.1016/j.neuroscience.2013.08.054

Chen, X. X., Qian, Y., Wang, X. P., Tang, Z. W., Xu, J. T., Lin, H., … Deng, X. L. (2018). Nurr1 promots neurogenesis of dopaminergic neuron and represses inflammatory factors in the transwell coculture system of neural stem cells and microglia. *CNS Neuroscience and Therapeutics*, *24*(9), 790–800. https://doi.org/10.1111/cns.12825

Chen, Y., Wang, Y., Ertürk, A., Kallop, D., Jiang, Z., Weimer, R. M., … Sheng, M. (2014). Activity-induced Nr4a1 regulates spine density and distribution pattern of excitatory synapses in pyramidal neurons. *Neuron*, *83*(2), 431–443. https://doi.org/10.1016/j.neuron.2014.05.027

Cheng, I. H., Scearce-Levie, K., Legleiter, J., Palop, J. J., Gerstein, H., Bien-Ly, N., … Mucke, L. (2007). Accelerating Amyloid-β Fibrillization Reduces Oligomer Levels and Functional Deficits in Alzheimer Disease Mouse Models. *Journal of Biological Chemistry*, *282*(33), 23818–23828. https://doi.org/10.1074/jbc.M701078200

Chetelat, G. (2013). Alzheimer disease: Abeta-independent processes-rethinking preclinical AD. *Nature Reviews. Neurology*, *9*(3), 123–124. https://doi.org/10.1038/nrneurol.2013.21

Choi, S. H., Bylykbashi, E., Chatila, Z. K., Lee, S. W., Pulli, B., Clemenson, G. D., … Tanzi, R. E. (2018). Combined adult neurogenesis and BDNF mimic exercise effects on cognition in an Alzheimer's mouse model. *Science*, *361*(6406), eaan8821. https://doi.org/10.1126/science.aan8821

Chu, Y., Le, W., Kompoliti, K., Jankovic, J., Mufson, E. J., & Kordower, J. H. (2006). Nurr1 in Parkinson's disease and related disorders. *The Journal of Comparative Neurology*, *494*(3), 495–514. https://doi.org/10.1002/cne.20828

Cirrito, J. R., Kang, J.-E., Lee, J., Stewart, F. R., Verges, D. K., Silverio, L. M., … Holtzman, D. M. (2008). Endocytosis Is Required for Synaptic Activity-Dependent Release of Amyloid-β In Vivo. *Neuron*, *58*(1), 42–51. https://doi.org/10.1016/j.neuron.2008.02.003

Cissé, M., Duplan, E., Lorivel, T., Dunys, J., Bauer, C., Meckler, X., … Checler, F. (2017). The transcription factor XBP1s restores hippocampal synaptic plasticity and memory by control of the Kalirin-7 pathway in Alzheimer model. *Molecular Psychiatry*, *22*(11), 1562–1575. https://doi.org/10.1038/mp.2016.152

Cissé, Moustapha, Halabisky, B., Harris, J., Devidze, N., Dubal, D. B., Sun, B., … Mucke, L. (2011). Reversing EphB2 depletion rescues cognitive functions in Alzheimer model. *Nature*, *469*(7328), 47–52. https://doi.org/10.1038/nature09635

Cleary, J. P., Walsh, D. M., Hofmeister, J. J., Shankar, G. M., Kuskowski, M. A., Selkoe, D. J., & Ashe, K. H. (2005). Natural oligomers of the amyloid-β protein specifically disrupt cognitive function. *Nature Neuroscience*, *8*(1), 79–84. https://doi.org/10.1038/nn1372

Cline, E. N., Bicca, M. A., Viola, K. L., & Klein, W. L. (2018). The Amyloid-β Oligomer Hypothesis: Beginning of the Third Decade. *Journal of Alzheimer's Disease*, *64*(s1), S567–S610. https://doi.org/10.3233/JAD-179941

Colangelo, V., Schurr, J., Ball, M. J., Pelaez, R. P., Bazan, N. G., & Lukiw, W. J. (2002). Gene expression profiling of 12633 genes in Alzheimer hippocampal CA1: Transcription and neurotrophic factor down-regulation and up-regulation of apoptotic and pro-inflammatory signaling. *Journal of Neuroscience Research*, *70*(3), 462–473. https://doi.org/10.1002/jnr.10351

Coleman, P. D., & Yao, P. J. (2003). Synaptic slaughter in Alzheimer's disease. *Neurobiology of Aging*, *24*(8), 1023–1027. https://doi.org/10.1016/j.neurobiolaging.2003.09.001

Colgin, L. L. (2013). Mechanisms and Functions of Theta Rhythms. *Annual Review of Neuroscience*, *36*(1), 295–312. https://doi.org/10.1146/annurev-neuro-062012-170330

Collingridge, G. L., Peineau, S., Howland, J. G., & Wang, Y. T. (2010). Long-term depression in the CNS. *Nature Reviews Neuroscience*, *11*(7), 459–473. https://doi.org/10.1038/nrn2867

Colón-Cesario, W. I., Martínez-Montemayor, M. M., Morales, S., Félix, J., Cruz, J., Adorno, M., … Peña De Ortiz, S. (2006). Knockdown of Nurr1 in the rat hippocampus: Implications to spatial discrimination learning and memory. *Learning and Memory*, *13*(6), 734–744. https://doi.org/10.1101/lm.407706

Connor, B., Young, D., Yan, Q., Faull, R. L. M., Synek, B., & Dragunow, M. (1997). Brain-derived neurotrophic factor is reduced in Alzheimer's disease. *Molecular Brain Research*, *49*(1–2), 71–81. https://doi.org/10.1016/S0169-328X(97)00125-3

Corder, E. H., Saunders, A. M., Strittmatter, W. J., Schmechel, D. E., Gaskell, P. C., Small, G. W., … Pericak-Vance, M. A. (1993). Gene dose of apolipoprotein E type 4 allele and the risk of Alzheimer's disease in late onset families. *Science*, *261*(5123), 921–923. https://doi.org/10.1126/science.8346443

Corder, E., Lannfelt, L., & Mulder, M. (1998). Apolipoprotein E and herpes simplex virus 1 in Alzheimer's disease [4]. *Lancet*, *352*(9136), 1312–1313. https://doi.org/10.1016/S0140-6736(05)70525-0

Counts, S. E., Alldred, M. J., Che, S., Ginsberg, S. D., & Mufson, E. J. (2014). Synaptic gene dysregulation within hippocampal CA1 pyramidal neurons in mild cognitive impairment. *Neuropharmacology*, *79*, 172–179. https://doi.org/10.1016/j.neuropharm.2013.10.018

Cramer, P. E., Cirrito, J. R., Wesson, D. W., Lee, C. Y. D., Karlo, J. C., Zinn, A. E., … Landreth, G. E. (2012). ApoE-Directed Therapeutics Rapidly Clear -Amyloid and Reverse Deficits in AD Mouse Models. *Science*, *335*(6075), 1503–1506. https://doi.org/10.1126/science.1217697

Crawley, J., & Goodwin, F. K. (1980). Preliminary report of a simple animal behavior model for the anxiolytic effects of benzodiazepines. *Pharmacology, Biochemistry, and Behavior*, *13*(2), 167–170. https://doi.org/10.1016/0091-3057(80)90067-2

Crouzin, N., Baranger, K., Cavalier, M., Marchalant, Y., Cohen-Solal, C., Roman, F. S., … Vignes, M. (2013). Area-Specific Alterations of Synaptic Plasticity in the 5XFAD Mouse Model of Alzheimer's Disease: Dissociation between Somatosensory Cortex and Hippocampus. *PLoS ONE*, *8*(9), 4–12. https://doi.org/10.1371/journal.pone.0074667

Cummings, J. L., Morstorf, T., & Zhong, K. (2014). Alzheimer's disease drug-development pipeline: Few candidates, frequent failures. *Alzheimer's Research and Therapy*, *6*(4), 1–7. https://doi.org/10.1186/alzrt269

D'Amelio, M., Cavallucci, V., Middei, S., Marchetti, C., Pacioni, S., Ferri, A., … Cecconi, F. (2011). Caspase-3 triggers early synaptic dysfunction in a mouse model of Alzheimer's disease. *Nature Neuroscience*, *14*(1), 69–79. https://doi.org/10.1038/nn.2709

Dandi, E., Kalamari, A., Touloumi, O., Lagoudaki, R., Nousiopoulou, E., Simeonidou, C., … Tata, D. A. (2018). Beneficial effects of environmental enrichment on behavior, stress reactivity and synaptophysin/BDNF expression in hippocampus following early life stress. *International Journal of Developmental Neuroscience : The Official Journal of the International Society for Developmental Neuroscience*, *67*, 19–32. https://doi.org/10.1016/j.ijdevneu.2018.03.003

Davies, C. A., Mann, D. M. A., Sumpter, P. Q., & Yates, P. O. (1987). A quantitative morphometric analysis of the neuronal and synaptic content of the frontal and temporal cortex in patients with Alzheimer's disease. *Journal of the Neurological Sciences*, *78*(2), 151–164. https://doi.org/10.1016/0022-510X(87)90057-8

Davies, M. R., Harding, C. J., Raines, S., Tolley, K., Parker, A. E., Downey-Jones, M., & Needham, M. R. C. (2005). Nurr1 dependent regulation of pro-inflammatory mediators in immortalised synovial fibroblasts. *Journal of Inflammation*, *2*, 1–8. https://doi.org/10.1186/1476-9255-2-15

de Calignon, A., Polydoro, M., Suárez-Calvet, M., William, C., Adamowicz, D. H., Kopeikina, K. J., … Hyman, B. T. (2012). Propagation of Tau Pathology in a Model of Early Alzheimer's Disease. *Neuron*, *73*(4), 685–697. https://doi.org/10.1016/j.neuron.2011.11.033

De Felice, F. G., Velasco, P. T., Lambert, M. P., Viola, K., Fernandez, S. J., Ferreira, S. T., & Klein, W. L. (2007). Aβ oligomers induce neuronal oxidative stress through an N-methyl-D-aspartate receptor-dependent mechanism that is blocked by the Alzheimer drug memantine. *Journal of Biological Chemistry*, *282*(15), 11590–11601. https://doi.org/10.1074/jbc.M607483200

De Felice, F. G., Wu, D., Lambert, M. P., Fernandez, S. J., Velasco, P. T., Lacor, P. N., … Klein, W. L. (2008). Alzheimer's disease-type neuronal tau hyperphosphorylation induced by A beta oligomers. *Neurobiology of Aging*, *29*(9), 1334–1347. https://doi.org/10.1016/j.neurobiolaging.2007.02.029

de la Monte, S. M., & Wands, J. R. (2006). Molecular indices of oxidative stress and mitochondrial

dysfunction occur early and often progress with severity of Alzheimer's disease. *Journal of Alzheimer's Disease : JAD*, *9*(2), 167–181. https://doi.org/10.3233/jad-2006-9209

de la Monte, S. M., & Wands, J. R. (2008). Alzheimer's Disease is Type 3 Diabetes—Evidence Reviewed. *Journal of Diabetes Science and Technology*, *2*(6), 1101–1113. https://doi.org/10.1177/193229680800200619

De Miranda, B. R., Popichak, K. A., Hammond, S. L., Jorgensen, B. A., Phillips, A. T., Safe, S., & Tjalkens, R. B. (2015). The Nurr1 activator 1,1-bis(3′-indolyl)-1-(p-chlorophenyl) methane blocks inflammatory gene expression in BV-2 microglial cells by inhibiting nuclear factor κB. *Molecular Pharmacology*, *87*(6), 1021–1034. https://doi.org/10.1124/mol.114.095398

De Miranda, B. R., Popichak, K. A., Hammond, S. L., Miller, J. A., Safe, S., & Tjalkens, R. B. (2015). Novel para-phenyl substituted diindolylmethanes protect against MPTP neurotoxicity and suppress glial activation in a mouse model of Parkinson's disease. *Toxicological Sciences*, *143*(2), 360–373. https://doi.org/10.1093/toxsci/kfu236

De Pins, B., Cifuentes-Díaz, C., Thamila Farah, A., López-Molina, L., Montalban, E., Sancho-Balsells, A., … Giralt, A. (2019). Conditional BDNF delivery from astrocytes rescues memory deficits, spine density, and synaptic properties in the 5xFAD mouse model of alzheimer disease. *Journal of Neuroscience*, *39*(13), 2441–2458. https://doi.org/10.1523/JNEUROSCI.2121-18.2019

De Strooper, B., & Karran, E. (2016). The Cellular Phase of Alzheimer's Disease. *Cell*, *164*(4), 603–615. https://doi.org/10.1016/j.cell.2015.12.056

Deacon, R. M. (2006). Assessing nest building in mice. *Nature Protocols*, *1*(3), 1117–1119. https://doi.org/10.1038/nprot.2006.170

Deacon, R. M. J., Cholerton, L. L., Talbot, K., Nair-Roberts, R. G., Sanderson, D. J., Romberg, C., … Rawlins, J. N. P. (2008). Age-dependent and -independent behavioral deficits in Tg2576 mice. *Behavioural Brain Research*, *189*(1), 126–138. https://doi.org/10.1016/j.bbr.2007.12.024

Decker, H., Jürgensen, S., Adrover, M. F., Brito-Moreira, J., Bomfim, T. R., Klein, W. L., … Ferreira, S. T. (2010). N-Methyl-d-aspartate receptors are required for synaptic targeting of Alzheimer's toxic amyloid-β peptide oligomers. *Journal of Neurochemistry*, *115*(6), 1520–1529. https://doi.org/10.1111/j.1471-4159.2010.07058.x

Decker, H., Lo, K. Y., Unger, S. M., Ferreira, S. T., & Silverman, M. A. (2010). Amyloid-β peptide oligomers disrupt axonal transport through an NMDA receptor-dependent mechanism that is mediated by glycogen synthase kinase 3β in primary cultured hippocampal neurons. *Journal of Neuroscience*, *30*(27), 9166–9171. https://doi.org/10.1523/JNEUROSCI.1074-10.2010

Decressac, M., Volakakis, N., Björklund, A., & Perlmann, T. (2013). NURR1 in Parkinson disease - From pathogenesis to therapeutic potential. *Nature Reviews Neurology*, *9*(11), 629–636. https://doi.org/10.1038/nrneurol.2013.209

DeKosky, S. T., & Scheff, S. W. (1990). Synapse loss in frontal cortex biopsies in Alzheimer's disease: correlation with cognitive severity. *Annals of Neurology*, *27*(5), 457–464. https://doi.org/10.1002/ana.410270502

Demuro, A., Mina, E., Kayed, R., Milton, S. C., Parker, I., & Glabe, C. G. (2005). Calcium dysregulation and membrane disruption as a ubiquitous neurotoxic mechanism of soluble amyloid oligomers. *Journal of Biological Chemistry*, *280*(17), 17294–17300. https://doi.org/10.1074/jbc.M500997200

Devi, L., & Ohno, M. (2014). PERK mediates eIF2α phosphorylation responsible for BACE1 elevation, CREB dysfunction and neurodegeneration in a mouse model of Alzheimer's disease. *Neurobiology of Aging*, *35*(10), 2272–2281. https://doi.org/10.1016/j.neurobiolaging.2014.04.031

Dickerson, B. C., & Sperling, R. A. (2009). Large-scale functional brain network abnormalities in alzheimer's disease: Insights from functional neuroimaging. *Behavioural Neurology*, *21*(1–2), 63–75. https://doi.org/10.3233/BEN-2009-0227

Dickey, C. A., Loring, J. F., Montgomery, J., Gordon, M. N., Eastman, P. S., & Morgan, D. (2003). Selectively reduced expression of synaptic plasticity-related genes in amyloid precursor

protein + presenilin-1 transgenic mice. *Journal of Neuroscience*, *23*(12), 5219–5226. https://doi.org/10.1523/jneurosci.23-12-05219.2003

Diering, G. H., & Huganir, R. L. (2018). The AMPA Receptor Code of Synaptic Plasticity. *Neuron*, *100*(2), 314–329. https://doi.org/10.1016/j.neuron.2018.10.018

Ding, Y., Zhao, J., Zhang, X., Wang, S., Viola, K. L., Chow, F. E., … Gong, Y. (2019). Amyloid Beta Oligomers Target to Extracellular and Intracellular Neuronal Synaptic Proteins in Alzheimer's Disease. *Frontiers in Neurology*, *10*. https://doi.org/10.3389/fneur.2019.01140

Dong, J., Li, S., Mo, J. L., Cai, H. Bin, & Le, W. D. (2016). Nurr1-Based Therapies for Parkinson's Disease. *CNS Neuroscience and Therapeutics*, *22*(5), 351–359. https://doi.org/10.1111/cns.12536

Doody, R. S., Thomas, R. G., Farlow, M., Iwatsubo, T., Vellas, B., Joffe, S., … Mohs, R. (2014). Phase 3 trials of solanezumab for mild-to-moderate alzheimer's disease. *New England Journal of Medicine*, *370*(4), 311–321. https://doi.org/10.1056/NEJMoa1312889

Drolle, E., Hane, F., Lee, B., & Leonenko, Z. (2014). Atomic force microscopy to study molecular mechanisms of amyloid fibril formation and toxicity in Alzheimer's disease. *Drug Metabolism Reviews*, *46*(2), 207–223. https://doi.org/10.3109/03602532.2014.882354

Dubois, C., Hengerer, B., & Mattes, H. (2006). Identification of a potent agonist of the orphan nuclear receptor Nurr1. *ChemMedChem*, *1*(9), 955–958. https://doi.org/10.1002/cmdc.200600078

Dunah, A. W., Hueske, E., Wyszynski, M., Hoogenraad, C. C., Jaworski, J., Pak, D. T., … Sheng, M. (2005). LAR receptor protein tyrosine phosphatases in the development and maintenance of excitatory synapses. *Nature Neuroscience*, *8*(4), 458–467. https://doi.org/10.1038/nn1416

Eckert, A., Nisbet, R., Grimm, A., & Götz, J. (2014). March separate, strike together - Role of phosphorylated TAU in mitochondrial dysfunction in Alzheimer's disease. *Biochimica et Biophysica Acta - Molecular Basis of Disease*, *1842*(8), 1258–1266. https://doi.org/10.1016/j.bbadis.2013.08.013

Ehlers, M. D. (2000). Reinsertion or degradation of AMPA receptors determined by activity-dependent endocytic sorting. *Neuron*, *28*(2), 511–525. https://doi.org/10.1016/S0896-6273(00)00129-X

España, J., Giménez-Llort, L., Valero, J., Miñano, A., Rábano, A., Rodriguez-Alvarez, J., … Saura, C. A. (2010a). Intraneuronal β-Amyloid Accumulation in the Amygdala Enhances Fear and Anxiety in Alzheimer's Disease Transgenic Mice. *Biological Psychiatry*, *67*(6), 513–521. https://doi.org/10.1016/j.biopsych.2009.06.015

España, J., Valero, J., Miñano-Molina, A. J., Masgrau, R., Martín, E., Guardia-Laguarta, C., … Saura, C. A. (2010b). β-amyloid disrupts activity-dependent gene transcription required for memory through the CREB coactivator CRTC1. *Journal of Neuroscience*, *30*(28), 9402–9410. https://doi.org/10.1523/JNEUROSCI.2154-10.2010

Esteban, J. A., Shi, S. H., Wilson, C., Nuriya, M., Huganir, R. L., & Malinow, R. (2003). PKA phosphorylation of AMPA receptor subunits controls synaptic trafficking underlying plasticity. *Nature Neuroscience*, *6*(2), 136–143. https://doi.org/10.1038/nn997

Esvald, E.-E., Tuvikene, J., Sirp, A., Patil, S., Bramham, C. R., & Timmusk, T. (2020). CREB family transcription factors are major mediators of BDNF transcriptional autoregulation in cortical neurons. *The Journal of Neuroscience*, 0367–19. https://doi.org/10.1523/JNEUROSCI.0367-19.2019

Evans, N. A., Facci, L., Owen, D. E., Soden, P. E., Burbidge, S. A., Prinjha, R. K., … Skaper, S. D. (2008). Aβ1–42 reduces synapse number and inhibits neurite outgrowth in primary cortical and hippocampal neurons: A quantitative analysis. *Journal of Neuroscience Methods*, *175*(1), 96–103. https://doi.org/10.1016/j.jneumeth.2008.08.001

Fahnestock, M., Garzon, D., Holsinger, R. M. D., & Michalski, B. (2002). *Neurotrophic factors and Alzheimer's disease: are we focusing on the wrong molecule?* https://doi.org/10.1007/978-3-7091-6139-5_22

Fahnestock, M. (2011). Brain-derived neurotrophic factor: the link between amyloid-β and memory

loss. *Future Neurology*, *6*(5), 627–639. https://doi.org/10.2217/fnl.11.44

Fahnestock, M., & Shekari, A. (2019). ProNGF and neurodegeneration in Alzheimer's disease. *Frontiers in Neuroscience*, *13*(FEB), 1–11. https://doi.org/10.3389/fnins.2019.00129

Fan, X., Luo, G., Ming, M., Pu, P., Li, L., Yang, D., & Le, W. (2009). Nurr1 expression and its modulation in microglia. *Neuroimmunomodulation*, *16*(3), 162–170. https://doi.org/10.1159/000204229

Fein, J. A., Sokolow, S., Miller, C. A., Vinters, H. V., Yang, F., Cole, G. M., & Gylys, K. H. (2008). Co-localization of amyloid beta and tau pathology in Alzheimer's disease synaptosomes. *American Journal of Pathology*, *172*(6), 1683–1692. https://doi.org/10.2353/ajpath.2008.070829

Ferreira, S. T., & Klein, W. L. (2011). The Aβ oligomer hypothesis for synapse failure and memory loss in Alzheimer's disease. *Neurobiology of Learning and Memory*, *96*(4), 529–543. https://doi.org/10.1016/j.nlm.2011.08.003

Ferrer, I., Blanco, R., Carmona, M., & Puig, B. (2001). Phosphorylated c-Myc expression in Alzheimer disease, pick's disease, progressive supranuclear palsy and corticobasal degeneration. *Neuropathology and Applied Neurobiology*, *27*(5), 343–351. https://doi.org/10.1046/j.1365-2990.2001.00348.x

Ferrer, I., Marín, C., Rey, M. J., Ribalta, T., Goutan, E., Blanco, R., … Martí, E. (1999). BDNF and Full-length and Truncated TrkB Expression in Alzheimer Disease. Implications in Therapeutic Strategies. *Journal of Neuropathology and Experimental Neurology*, *58*(7), 729–739. https://doi.org/10.1097/00005072-199907000-00007

Filali, M., & Lalonde, R. (2009). Age-related cognitive decline and nesting behavior in an APPswe/PS1 bigenic model of Alzheimer's disease. *Brain Research*, *1292*, 93–99. https://doi.org/10.1016/j.brainres.2009.07.066

File, S. E., & Hyde, J. R. G. (1978). Can Social Interaction Be Used To Measure Anxiety? *British Journal of Pharmacology*, *62*(1), 19–24. https://doi.org/10.1111/j.14765381.1978.tb07001.x

Fleischmann, A., Hvalby, O., Jensen, V., Strekalova, T., Zacher, C., Layer, L. E., … Gass, P. (2003). Impaired long-term memory and NR2A-type NMDA receptor-dependent synaptic plasticity in mice lacking c-fos in the CNS. *Journal of Neuroscience*, *23*(27), 9116–9122. https://doi.org/10.1523/jneurosci.23-27-09116.2003

Forlenza, O. V., Diniz, B. S., & Gattaz, W. F. (2010). Diagnosis and biomarkers of predementia in Alzheimer's disease. *BMC Medicine*, *8*(1), 89. https://doi.org/10.1186/1741-7015-8-89

Forny-Germano, L., Lyra E Silva, N. M., Batista, A. F., Brito-Moreira, J., Gralle, M., Boehnke, S. E., … De Felice, F. G. (2014). Alzheimer's disease-like pathology induced by amyloid-β oligomers in nonhuman primates. *Journal of Neuroscience*, *34*(41), 13629–13643. https://doi.org/10.1523/JNEUROSCI.1353-14.2014

Francis, P. T. (2005). The Interplay of Neurotransmitters in Alzheimer's Disease. *CNS Spectrums*, *10*(S18), 6–9. https://doi.org/10.1017/S1092852900014164

Freir, D. B., Fedriani, R., Scully, D., Smith, I. M., Selkoe, D. J., Walsh, D. M., & Regan, C. M. (2011). Aβ oligomers inhibit synapse remodelling necessary for memory consolidation. *Neurobiology of Aging*, *32*(12), 2211–2218. https://doi.org/10.1016/j.neurobiolaging.2010.01.001

Frey, U., Krug, M., Reymann, K. G., & Matthies, H. (1988). Anisomycin, an inhibitor of protein synthesis, blocks late phases of LTP phenomena in the hippocampal CA1 region in vitro. *Brain Research*, *452*(1–2), 57–65. https://doi.org/10.1016/0006-8993(88)90008-X

Fukuchi, M., Kirikoshi, Y., Mori, A., Eda, R., Ihara, D., Takasaki, I., … Tsuda, M. (2014). Excitatory GABA induces BDNF transcription via CRTC1 and phosphorylated CREB-related pathways in immature cortical cells. *Journal of Neurochemistry*, *131*(2), 134–146. https://doi.org/10.1111/jnc.12801

Furukawa, K., Sopher, B. L., Rydel, R. E., Begley, J. G., Pham, D. G., Martin, G. M., … Mattson, M. P. (1996). Increased activity-regulating and neuroprotective efficacy of alpha-secretase-derived secreted amyloid precursor protein conferred by a C-terminal heparin-binding

domain. *Journal of Neurochemistry*, *67*(5), 1882–1896. https://doi.org/10.1046/j.1471-4159.1996.67051882.x

García-Yague, A. J., Rada, P., Rojo, A. I., Lastres-Becker, I., & Cuadrado, A. (2013). Nuclear import and export signals control the subcellular localization of nurr1 protein in response to oxidative stress. *Journal of Biological Chemistry*, *288*(8), 5506–5517. https://doi.org/10.1074/jbc.M112.439190

Gatta, V., D'Aurora, M., Granzotto, A., Stuppia, L., & Sensi, S. L. (2014). Early and sustained altered expression of aging-related genes in young 3xTg-AD mice. *Cell Death and Disease*, *5*(2), 1–10. https://doi.org/10.1038/cddis.2014.11

Gatz, M., Reynolds, C. A., Fratiglioni, L., Johansson, B., Mortimer, J. A., Berg, S., … Pedersen, N. L. (2006). Role of Genes and Environments for Explaining Alzheimer Disease. *Archives of General Psychiatry*, *63*(2), 168. https://doi.org/10.1001/archpsyc.63.2.168

Gerlai, R. (2001). Behavioral tests of hippocampal function: Simple paradigms complex problems. *Behavioural Brain Research*, *125*(1–2), 269–277. https://doi.org/10.1016/S0166-4328(01)00296-0

Ghatak, S., Dolatabadi, N., Trudler, D., Zhang, X. T., Wu, Y., Mohata, M., … Lipton, S. A. (2019). Mechanisms of hyperexcitability in Alzheimer's disease hiPSC-derived neurons and cerebral organoids vs isogenic controls. *ELife*, *8*, 1–22. https://doi.org/10.7554/eLife.50333

Ghosh, A., & Greenberg, M. E. (1995). Calcium signaling in neurons: molecular mechanisms and cellular consequences. *Science (New York, N.Y.)*, *268*(5208), 239–247. https://doi.org/10.1126/science.7716515

Giacobini, E., & Gold, G. (2013). Alzheimer disease therapy--moving from amyloid-beta to tau. *Nature Reviews. Neurology*, *9*(12), 677–686. https://doi.org/10.1038/nrneurol.2013.223

Ginsberg, S. D., Alldred, M. J., & Che, S. (2012). Gene expression levels assessed by CA1 pyramidal neuron and regional hippocampal dissections in Alzheimer's disease. *Neurobiology of Disease*, *45*(1), 99–107. https://doi.org/10.1016/j.nbd.2011.07.013

Ginsberg, S. D., Alldred, M. J., Counts, S. E., Cataldo, A. M., Neve, R. L., Jiang, Y., … Che, S. (2010). Microarray analysis of hippocampal CA1 neurons implicates early endosomal dysfunction during Alzheimer's disease progression. *Biological Psychiatry*, *68*(10), 885–893. https://doi.org/10.1016/j.biopsych.2010.05.030

Glenner, G. G., & Wong, C. W. (1984). Alzheimer's disease: initial report of the purification and characterization of a novel cerebrovascular amyloid protein. *Biochemical and Biophysical Research Communications*, *120*(3), 885–890. https://doi.org/10.1016/s0006-291x(84)80190-4

Goedert, M. (1993). Tau protein and the neurofibrillary pathology of Alzheimer's disease. *Trends in Neurosciences*, *16*(11), 460–465. https://doi.org/10.1016/0166-2236(93)90078-Z

Gómez Ravetti, M., Rosso, O. A., Berretta, R., & Moscato, P. (2010). Uncovering molecular biomarkers that correlate cognitive decline with the changes of hippocampus' gene expression profiles in Alzheimer's disease. *PLoS ONE*, *5*(4). https://doi.org/10.1371/journal.pone.0010153

Gong, Y., Chang, L., Viola, K. L., Lacor, P. N., Lambert, M. P., Finch, C. E., … Klein, W. L. (2003). Alzheimer's disease-affected brain: presence of oligomeric A beta ligands (ADDLs) suggests a molecular basis for reversible memory loss. *Proceedings of the National Academy of Sciences of the United States of America*, *100*(18), 10417–10422. https://doi.org/10.1073/pnas.1834302100

Govindarajulu, M., Pinky, P. D., Bloemer, J., Ghanei, N., Suppiramaniam, V., & Amin, R. (2018). Signaling Mechanisms of Selective PPAR γ Modulators in Alzheimer's Disease. *PPAR Research*, *2018*. https://doi.org/10.1155/2018/2010675

Graham, W. V., Bonito-Oliva, A., & Sakmar, T. P. (2017). Update on Alzheimer's Disease Therapy and Prevention Strategies. *Annual Review of Medicine*, *68*(1), 413–430. https://doi.org/10.1146/annurev-med-042915-103753

Green, K. N., & LaFerla, F. M. (2008). Linking Calcium to Aβ and Alzheimer's Disease. *Neuron*, *59*(2), 190–194. https://doi.org/10.1016/j.neuron.2008.07.013

Greger, I. H., Watson, J. F., & Cull-Candy, S. G. (2017). Structural and Functional Architecture of AMPA-Type Glutamate Receptors and Their Auxiliary Proteins. *Neuron*, *94*(4), 713–730. https://doi.org/10.1016/j.neuron.2017.04.009

Grimes, D. A., Han, F., Panisset, M., Racacho, L., Xiao, F., Zou, R., … Bulman, D. E. (2006). Translated mutation in the Nurr1 gene as a cause for Parkinson's disease. *Movement Disorders : Official Journal of the Movement Disorder Society*, *21*(7), 906–909. https://doi.org/10.1002/mds.20820

Grochowska, K. M., Yuanxiang, P., Bär, J., Raman, R., Brugal, G., Sahu, G., … Kreutz, M. R. (2017). Posttranslational modification impact on the mechanism by which amyloid-β induces synaptic dysfunction. *EMBO Reports*, *18*(6), 962–981. https://doi.org/10.15252/embr.201643519

Grooms, S. Y., Noh, K. M., Regis, R., Bassell, G. J., Bryan, M. K., Carroll, R. C., & Zukin, R. S. (2006). Activity bidirectionally regulates AMPA receptor mRNA abundance in dendrites of hippocampal neurons. *Journal of Neuroscience*, *26*(32), 8339–8351. https://doi.org/10.1523/JNEUROSCI.0472-06.2006

Groot, C., Hooghiemstra, A. M., Raijmakers, P. G. H. M., van Berckel, B. N. M., Scheltens, P., Scherder, E. J. A., … Ossenkoppele, R. (2016). The effect of physical activity on cognitive function in patients with dementia: A meta-analysis of randomized control trials. *Ageing Research Reviews*, *25*, 13–23. https://doi.org/10.1016/j.arr.2015.11.005

Gruart, A., López-Ramos, J. C., Muñoz, M. D., & Delgado-García, J. M. (2008). Aged wild-type and APP, PS1, and APP + PS1 mice present similar deficits in associative learning and synaptic plasticity independent of amyloid load. *Neurobiology of Disease*, *30*(3), 439–450. https://doi.org/10.1016/j.nbd.2008.03.001

Gu, Z., Liu, W., & Yan, Z. (2009). B-amyloid impairs AMPA receptor trafficking and function by reducing Ca2+/calmodulin-dependent protein kinase II synaptic distribution. *Journal of Biological Chemistry*, *284*(16), 10639–10649. https://doi.org/10.1074/jbc.M806508200

Gulinello, M., Gertner, M., Mendoza, G., Schoenfeld, B. P., Oddo, S., LaFerla, F., … Faber, D. S. (2009). Validation of a 2-day water maze protocol in mice. *Behavioural Brain Research*, *196*(2), 220–227. https://doi.org/10.1016/j.bbr.2008.09.002

Gulisano, W., Melone, M., Ripoli, C., Tropea, M. R., Li Puma, D. D., Giunta, S., … Puzzo, D. (2019). Neuromodulatory action of picomolar extracellular Aβ42 oligomers on presynaptic and postsynaptic mechanisms underlying synaptic function and memory. *Journal of Neuroscience*, *39*(30), 5986–6000. https://doi.org/10.1523/JNEUROSCI.0163-19.2019

Guntupalli, S., Jang, S. E., Zhu, T., Huganir, R. L., Widagdo, J., & Anggono, V. (2017). GluA1 subunit ubiquitination mediates amyloid-β-induced loss of surface α-amino-3-hydroxy-5-methyl-4-isoxazolepropionic acid (AMPA) receptors. *Journal of Biological Chemistry*, *292*(20), 8186–8194. https://doi.org/10.1074/jbc.M116.774554

Guntupalli, S., Widagdo, J., & Anggono, V. (2016). Amyloid- β -Induced Dysregulation of AMPA Receptor Trafficking. *Neural Plasticity*, *2016*. https://doi.org/10.1155/2016/3204519

Guzowski, J. F., Lyford, G. L., Stevenson, G. D., Houston, F. P., McGaugh, J. L., Worley, P. F., & Barnes, C. A. (2000). Inhibition of activity-dependent arc protein expression in the rat hippocampus impairs the maintenance of long-term potentiation and the consolidation of long-term memory. *Journal of Neuroscience*, *20*(11), 3993–4001. https://doi.org/10.1523/jneurosci.20-11-03993.2000

Haass, C., & Selkoe, D. J. (2007). Soluble protein oligomers in neurodegeneration: lessons from the Alzheimer's amyloid β-peptide. *Nature Reviews Molecular Cell Biology*, *8*(2), 101–112. https://doi.org/10.1038/nrm2101

Hammond, S. L., Popichak, K. A., Li, X., Hunt, L. G., Richman, E. H., Damale, P. U., … Tjalkens, R. B. (2018). The nurr1 ligand,1,1-bis(39-Indolyl)-1-(p-Chlorophenyl)methane, modulates glial reactivity and is neuroprotective in mptp-induced parkinsonisms. *Journal of Pharmacology and Experimental Therapeutics*, *365*(3), 636–651. https://doi.org/10.1124/jpet.117.246389

Hammond, S. L., Safe, S., & Tjalkens, R. B. (2015). A novel synthetic activator of Nurr1 induces dopaminergic gene expression and protects against 6-hydroxydopamine neurotoxicity in vitro.

Neuroscience Letters, *607*, 83–89. https://doi.org/10.1016/j.neulet.2015.09.015

Han, B.-S., Minh, N. Van, Choi, H.-Y., Byun, J.-S., & Kim, W.-G. (2017). Daphnane and Phorbol Diterpenes, Anti-neuroinflammatory Compounds with Nurr1 Activation from the Roots and Stems of Daphne genkwa. *Biological & Pharmaceutical Bulletin*, *40*(12), 2205–2211. https://doi.org/10.1248/bpb.b17-00641

Hansen, K. B., Yi, F., Perszyk, R. E., Furukawa, H., Wollmuth, L. P., Gibb, A. J., & Traynelis, S. F. (2018). Structure, function, and allosteric modulation of NMDA receptors. *Journal of General Physiology*, *150*(8), 1081–1105. https://doi.org/10.1085/jgp.201812032

Hardy, J. A., & Higgins, G. A. (1992). Alzheimer's disease: The amyloid cascade hypothesis. *Science*, *256*(5054), 184–185. https://doi.org/10.1126/science.1566067

Hardy, J, & Allsop, D. (1991). Amyloid deposition as the central event in the aetiology of Alzheimer's disease. *Trends in Pharmacological Sciences*, *12*(10), 383–388. https://doi.org/10.1016/0165-6147(91)90609-v

Hardy, John, & Selkoe, D. J. (2002). The amyloid hypothesis of Alzheimer's disease: Progress and problems on the road to therapeutics. *Science*, *297*(5580), 353–356. https://doi.org/10.1126/science.1072994

Harris, J. A., Devidze, N., Verret, L., Ho, K., Halabisky, B., Thwin, M. T., … Mucke, L. (2010). Transsynaptic Progression of Amyloid-β-Induced Neuronal Dysfunction within the Entorhinal-Hippocampal Network. *Neuron*, *68*(3), 428–441. https://doi.org/10.1016/j.neuron.2010.10.020

Harris, S. A., & Harris, E. A. (2015). Herpes Simplex Virus Type 1 and Other Pathogens are Key Causative Factors in Sporadic Alzheimer's Disease. *Journal of Alzheimer's Disease*, *48*(2), 319–353. https://doi.org/10.3233/JAD-142853

Hawk, Josh D., & Abel, T. (2011). The role of NR4A transcription factors in memory formation. *Brain Research Bulletin*, *85*(1–2), 21–29. https://doi.org/10.1016/j.brainresbull.2011.02.001

Hawk, Joshua D., Bookout, A. L., Poplawski, S. G., Bridi, M., Rao, A. J., Sulewski, M. E., … Abel, T. (2012). NR4A nuclear receptors support memory enhancement by histone deacetylase inhibitors. *Journal of Clinical Investigation*, *122*(10), 3593–3602. https://doi.org/10.1172/JCI64145

Hill, N. T. M., Mowszowski, L., Naismith, S. L., Chadwick, V. L., Valenzuela, M., & Lampit, A. (2017). Computerized cognitive training in older adults with mild cognitive impairment or dementia: A systematic review and meta-analysis. *American Journal of Psychiatry*, *174*(4), 329–340. https://doi.org/10.1176/appi.ajp.2016.16030360

Hoover, B. R., Reed, M. N., Su, J., Penrod, R. D., Kotilinek, L. A., Grant, M. K., … Liao, D. (2010). Tau Mislocalization to Dendritic Spines Mediates Synaptic Dysfunction Independently of Neurodegeneration. *Neuron*, *68*(6), 1067–1081. https://doi.org/10.1016/j.neuron.2010.11.030

Hoozemans, J. J. M., Veerhuis, R., Van Haastert, E. S., Rozemuller, J. M., Baas, F., Eikelenboom, P., & Scheper, W. (2005). The unfolded protein response is activated in Alzheimer's disease. *Acta Neuropathologica*, *110*(2), 165–172. https://doi.org/10.1007/s00401-005-1038-0

Hsia, A. Y., Masliah, E., McConlogue, L., Yu, G.-Q., Tatsuno, G., Hu, K., … Mucke, L. (1999). Plaque-independent disruption of neural circuits in Alzheimer's disease mouse models. *Proceedings of the National Academy of Sciences*, *96*(6), 3228–3233. https://doi.org/10.1073/pnas.96.6.3228

Hsieh, H., Boehm, J., Sato, C., Iwatsubo, T., Tomita, T., Sisodia, S., & Malinow, R. (2006). AMPAR Removal Underlies Aβ-Induced Synaptic Depression and Dendritic Spine Loss. *Neuron*, *52*(5), 831–843. https://doi.org/10.1016/j.neuron.2006.10.035

Hu, W., Feng, Z., Xu, J., Jiang, Z., & Feng, M. (2019). Brain-derived neurotrophic factor modified human umbilical cord mesenchymal stem cells-derived cholinergic-like neurons improve spatial learning and memory ability in Alzheimer's disease rats. *Brain Research*, *1710*, 61–73. https://doi.org/10.1016/j.brainres.2018.12.034

Huang, Y., Zhou, W., & Zhang, Y. (2012). Bright lighting conditions during testing increase thigmotaxis and impair water maze performance in BALB/c mice. *Behavioural Brain Research*, *226*(1), 26–31. https://doi.org/10.1016/j.bbr.2011.08.043

Huganir, R. L., & Nicoll, R. A. (2013). AMPARs and synaptic plasticity: The last 25 years. *Neuron*, *80*(3), 704–717. https://doi.org/10.1016/j.neuron.2013.10.025

Huifang, M., Lesné, S., Kotilinek, L., Steidl-Nichols, J. V., Sherman, M., Younkin, L., … Ashe, K. H. (2007). Involvement of β-site APP cleaving enzyme 1 (BACE1) in amyloid precursor protein-mediated enhancement of memory and activity-dependent synaptic plasticity. *Proceedings of the National Academy of Sciences of the United States of America*, *104*(19), 8167–8172. https://doi.org/10.1073/pnas.0609521104

Hutton, M., Lendon, C. L., Rizzu, P., Baker, M., Froelich, S., Houlden, H., … Owen, F. (1998). Association of missense and 5'-splice-site mutations in tau with the inherited dementia FTDP-17. *Nature, 393*(6686), 702-705. http://doi.org/10.1038/31508

Hyman, B. T., Phelps, C. H., Beach, T. G., Bigio, E. H., Cairns, N. J., Carrillo, M. C., … Montine, T. J. (2012). National Institute on Aging-Alzheimer's Association guidelines for the neuropathologic assessment of Alzheimer's disease. *Alzheimer's & Dementia*, *8*(1), 1–13. https://doi.org/10.1016/j.jalz.2011.10.007

Hyman, B., Van Hoesen, G., Damasio, A., & Barnes, C. (1984). Alzheimer's disease: cell-specific pathology isolates the hippocampal formation. *Science*, *225*(4667), 1168–1170. https://doi.org/10.1126/science.6474172

Ichinose, H., Ohye, T., Suzuki, T., Sumi-Ichinose, C., Nomura, T., Hagino, Y., & Nagatsu, T. (1999). Molecular cloning of the human Nurr1 gene: Characterization of the human gene and cDNAs. *Gene*, *230*(2), 233–239. https://doi.org/10.1016/S0378-1119(99)00065-7

Imura, T., Kobayashi, Y., Suzutani, K., Ichikawa-Tomikawa, N., & Chiba, H. (2019). Differential expression of a stress-regulated gene Nr4a2 characterizes early- and late-born hippocampal granule cells. *Hippocampus*, *29*(6), 539–549. https://doi.org/10.1002/hipo.23045

Iqbal, K., Del C. Alonso, A., Chen, S., Chohan, M. O., El-Akkad, E., Gong, C. X., … Grundke-Iqbal, I. (2005). Tau pathology in Alzheimer disease and other tauopathies. *Biochimica et Biophysica Acta - Molecular Basis of Disease*, *1739*(2), 198–210. https://doi.org/10.1016/j.bbadis.2004.09.008

Ittner, L. M., Ke, Y. D., Delerue, F., Bi, M., Gladbach, A., van Eersel, J., … Götz, J. (2010). Dendritic function of tau mediates amyloid-β toxicity in alzheimer's disease mouse models. *Cell*, *142*(3), 387–397. https://doi.org/10.1016/j.cell.2010.06.036

Itzhaki, R. F. (2014). Herpes simplex virus type 1 and Alzheimer's disease: Increasing evidence for a major role of the virus. *Frontiers in Aging Neuroscience*, *6*(AUG), 1–9. https://doi.org/10.3389/fnagi.2014.00202

Iulita, M. F., Allard, S., Richter, L., Munter, L. M., Ducatenzeiler, A., Weise, C., … Cuello, A. C. (2014). Intracellular Aβ pathology and early cognitive impairments in a transgenic rat overexpressing human amyloid precursor protein: A multidimensional study. *Acta Neuropathologica Communications*, *2*(1), 1–17. https://doi.org/10.1186/2051-5960-2-61

Jackson, J., Jambrina, E., Li, J., Marston, H., Menzies, F., Phillips, K., & Gilmour, G. (2019). Targeting the synapse in Alzheimer's disease. *Frontiers in Neuroscience*, *13*(JUL), 1–8. https://doi.org/10.3389/fnins.2019.00735

Jacob, C. P., Koutsilieri, E., Bartl, J., Neuen-Jacob, E., Arzberger, T., Zander, N., … Grunblatt, E. (2007). Alterations in expression of glutamatergic transporters and receptors in sporadic Alzheimer's disease. *Journal of Alzheimer's Disease : JAD*, *11*(1), 97–116. https://doi.org/10.3233/jad-2007-11113

Jacobi, E., & von Engelhardt, J. (2017). Diversity in AMPAR complexes in the brain. *Current Opinion in Neurobiology*, *45*, 32–38. https://doi.org/10.1016/j.conb.2017.03.001

Jacobsen, J. S., Wu, C. C., Redwine, J. M., Comery, T. A., Arias, R., Bowlby, M., … Bloom, F. E. (2006). Early-onset behavioral and synaptic deficits in a mouse model of Alzheimer's disease. *Proceedings of the National Academy of Sciences of the United States of America*, *103*(13), 5161–5166. https://doi.org/10.1073/pnas.0600948103

Jakaria, M., Haque, M. E., Cho, D. Y., Azam, S., Kim, I. S., & Choi, D. K. (2019). Molecular Insights into NR4A2(Nurr1): an Emerging Target for Neuroprotective Therapy Against Neuroinflammation and Neuronal Cell Death. *Molecular Neurobiology*, *56*(8), 5799–5814.

https://doi.org/10.1007/s12035-019-1487-4

James, B. D., & Bennett, D. A. (2019). Causes and Patterns of Dementia: An Update in the Era of Redefining Alzheimer's Disease. *Annual Review of Public Health*, *40*(1), 65–84. https://doi.org/10.1146/annurev-publhealth-040218-043758

Jeneson, A., & Squire, L. R. (2011). and Medial Temporal Lobe Function. *Learning and Memory*, *19*(1), 15–25. https://doi.org/10.1101/lm.024018.111.19

Ji, L., Gong, C., Ge, L., Song, L., Chen, F., Jin, C., … Zhou, G. (2017). Orphan nuclear receptor Nurr1 as a potential novel marker for progression in human pancreatic ductal adenocarcinoma. *Experimental and Therapeutic Medicine*, *13*(2), 551–559. https://doi.org/10.3892/etm.2016.3968

Jiang, L., Dai, S., Li, J., Liang, X., Qu, L., Chen, X., … Chen, Y. (2019). Structural basis of binding of homodimers of the nuclear receptor NR4A2 to selective Nur-responsive DNA elements. *Journal of Biological Chemistry*, *294*(51), 19795–19803. https://doi.org/10.1074/jbc.RA119.010730

Jo, A. Y., Kim, M. Y., Lee, H. S., Rhee, Y. H., Lee, J. E., Baek, K. H., … Lee, S. H. (2009). Generation of dopamine neurons with improved cell survival and phenotype maintenance using a degradation-resistant Nurr1 mutant. *Stem Cells*, *27*(9), 2238–2246. https://doi.org/10.1002/stem.146

Joiner, M. L. A., Lisé, M. F., Yuen, E. Y., Kam, A. Y. F., Zhang, M., Hall, D. D., … Hell, J. W. (2010). Assembly of a B 2-adrenergic receptorGluR1 signalling complex for localized cAMP signalling. *EMBO Journal*, *29*(2), 482–495. https://doi.org/10.1038/emboj.2009.344

Jones, L., Holmans, P. A., Hamshere, M. L., Harold, D., Moskvina, V., Ivanov, D., … Williams, J. (2010). Genetic evidence implicates the immune system and cholesterol metabolism in the aetiology of Alzheimer's disease. *PLoS ONE*, *5*(11). https://doi.org/10.1371/journal.pone.0013950

Jurado, S. (2018). AMPA receptor trafficking in natural and pathological aging. *Frontiers in Molecular Neuroscience*, *10*(JAN), 1–14. https://doi.org/10.3389/fnmol.2017.00446

Jurado, S., Goswami, D., Zhang, Y., Molina, A. J. M., Südhof, T. C., & Malenka, R. C. (2013). LTP Requires a Unique Postsynaptic SNARE Fusion Machinery. *Neuron*, *77*(3), 542–558. https://doi.org/10.1016/j.neuron.2012.11.029

Jürgensen, S., Antonio, L. L., Mussi, G. E. A., Brito-Moreira, J., Bomfim, T. R., De Felice, F. G., … Ferreira, S. T. (2011). Activation of D1/D5 dopamine receptors protects neurons from synapse dysfunction induced by amyloid-β oligomers. *Journal of Biological Chemistry*, *286*(5), 3270–3276. https://doi.org/10.1074/jbc.M110.177790

Kadkhodaei, B., Alvarsson, A., Schintu, N., Ramsköld, D., Volakakis, N., Joodmardi, E., … Perlmanna, T. (2013). Transcription factor Nurr1 maintains fiber integrity and nuclear-encoded mitochondrial gene expression in dopamine neurons. *Proceedings of the National Academy of Sciences of the United States of America*, *110*(6), 2360–2365. https://doi.org/10.1073/pnas.1221077110

Kamenetz, F., Tomita, T., Hsieh, H., Seabrook, G., Borchelt, D., Iwatsubo, T., … Point, W. (2003). APP Processing and Synaptic Function. *Neuron*, *37(6)*, 925–937. https://doi.org/10.1016/S0896-6273(03)00124-7

Kametani, F., & Hasegawa, M. (2018). Reconsideration of amyloid hypothesis and tau hypothesis in Alzheimer's disease. *Frontiers in Neuroscience*, *12*(JAN). https://doi.org/10.3389/fnins.2018.00025

Kandimalla, R., Thirumala, V., & Reddy, P. H. (2017). Is Alzheimer's disease a Type 3 Diabetes? A critical appraisal. *Biochimica et Biophysica Acta - Molecular Basis of Disease*, *1863*(5), 1078–1089. https://doi.org/10.1016/j.bbadis.2016.08.018

Kane, M. D., Lipinski, W. J., Callahan, M. J., Bian, F., Durham, R. A., Schwarz, R. D., … Walker, L. C. (2000). Evidence for seeding of β-amyloid by intracerebral infusion of Alzheimer brain extracts in β-amyloid precursor protein-transgenic mice. *Journal of Neuroscience*, *20*(10), 3606–3611. https://doi.org/10.1523/jneurosci.20-10-03606.2000

Kang, J., Lemaire, H. G., Unterbeck, A., Salbaum, J. M., Masters, C. L., Grzeschik, K. H., … Müller-Hill, B. (1987). The precursor of Alzheimer's disease amyloid A4 protein resembles a cell-surface receptor. *Nature*, *325*(6106), 733–736. https://doi.org/10.1038/325733a0

Kasai, H., Fukuda, M., Watanabe, S., Hayashi-Takagi, A., & Noguchi, J. (2010). Structural dynamics of dendritic spines in memory and cognition. *Trends in Neurosciences*, *33*(3), 121–129. https://doi.org/10.1016/j.tins.2010.01.001

Katzman, R. (2004). A neurologist's view of Alzheimer's disease and dementia. *International Psychogeriatrics*, *16*(3), 259–273. https://doi.org/10.1017/S1041610204000456

Kedia, N., Almisry, M., & Bieschke, J. (2017). Glucose directs amyloid-beta into membrane-active oligomers. *Physical Chemistry Chemical Physics*, *19*(27), 18036–18046. https://doi.org/10.1039/C7CP02849K

Kennedy, M. J., Davison, I. G., Robinson, C. G., & Ehlers, M. D. (2010). Syntaxin-4 Defines a Domain for Activity-Dependent Exocytosis in Dendritic Spines. *Cell*, *141*(3), 524–535. https://doi.org/10.1016/j.cell.2010.02.042

Kim, Jin il, Jeon, S. G., Kim, K. A., Kim, Y. J., Song, E. J., Choi, J., … Chung, H. (2016). The pharmacological stimulation of Nurr1 improves cognitive functions via enhancement of adult hippocampal neurogenesis. *Stem Cell Research*, *17*(3), 534–543. https://doi.org/10.1016/j.scr.2016.09.027

Kim, J. H., Anwyl, R., Suh, Y. H., Djamgoz, M. B. A., & Rowan, M. J. (2001). Use-dependent effects of amyloidogenic fragments of β-amyloid precursor protein on synaptic plasticity in rat hippocampus in vivo. *Journal of Neuroscience*, *21*(4), 1327–1333. https://doi.org/10.1523/jneurosci.21-04-01327.2001

Kim, Jungsu, Basak, J. M., & Holtzman, D. M. (2009). The Role of Apolipoprotein E in Alzheimer's Disease. *Neuron*, *63*(3), 287–303. https://doi.org/10.1016/j.neuron.2009.06.026

Kim, Jungsu, Chakrabarty, P., Hanna, A., March, A., Dickson, D. W., Borchelt, D. R., … Janus, C. (2013). Normal cognition in transgenic BRI2-Aβ mice. *Molecular Neurodegeneration*, *8*(1), 1–12. https://doi.org/10.1186/1750-1326-8-15

Kim, Jungsu, & Holtzman, D. M. (2010). Medicine. Prion-like behavior of amyloid-beta. *Science (New York, N.Y.)*, *330*(6006), 918–919. https://doi.org/10.1126/science.1198314

Klein, W. L., Krafft, G. A., & Finch, C. E. (2001). Targeting small Abeta oligomers: the solution to an Alzheimer's disease conundrum? *Trends in Neurosciences*, *24*(4), 219–224. https://doi.org/10.1016/s0166-2236(00)01749-5

Klyubin, I., Betts, V., Welzel, A. T., Blennow, K., Zetterberg, H., Wallin, A., … Rowan, M. J. (2008). Amyloid β protein dimer-containing human CSF disrupts synaptic plasticity: Prevention by systemic passive immunization. *Journal of Neuroscience*, *28*(16), 4231–4237. https://doi.org/10.1523/JNEUROSCI.5161-07.2008

Knowles, J. K., Rajadas, J., Nguyen, T. V. V., Yang, T., LeMieux, M. C., Vander Griend, L., … Longo, F. M. (2009). The p75 neurotrophin receptor promotes amyloid-β(1-42)-induced neuritic dystrophy in vitro and in vivo. *Journal of Neuroscience*, *29*(34), 10627–10637. https://doi.org/10.1523/JNEUROSCI.0620-09.2009

Koffie, R. M., Meyer-Luehmann, M., Hashimoto, T., Adams, K. W., Mielke, M. L., Garcia-Alloza, M., … Spires-Jones, T. L. (2009). Oligomeric amyloid β associates with postsynaptic densities and correlates with excitatory synapse loss near senile plaques. *Proceedings of the National Academy of Sciences of the United States of America*, *106*(10), 4012–4017. https://doi.org/10.1073/pnas.0811698106

Koistinaho, M., Ort, M., Cimadevilla, J. M., Vondrous, R., Cordell, B., Koistinaho, J., … Higgins, L. S. (2001). Specific spatial learning deficits become severe with age in β-amyloid precursor protein transgenic mice that harbor diffuse β-amyloid deposits but do not form plaques. *Proceedings of the National Academy of Sciences of the United States of America*, *98*(25), 14675–14680. https://doi.org/10.1073/pnas.261562998

Kolata, G. Down syndrome--Alzheimer's linked. *Science.* 230 (4730), 1152–1153. https://doi.org/10.1126/science.2933807

Kopeikina, K. J., Polydoro, M., Tai, H. C., Yaeger, E., Carlson, G. A., Pitstick, R., … Spires-Jones, T. L. (2013). Synaptic alterations in the rTg4510 mouse model of tauopathy. *Journal of Comparative Neurology*, *521*(6), 1334–1353. https://doi.org/10.1002/cne.23234

Kovács, K. A., Steullet, P., Steinmann, M., Do, K. Q., Magistretti, P. J., Halfon, O., & Cardinaux, J. R. (2007). TORC1 is a calcium- and cAMP-sensitive coincidence detector involved in hippocampal long-term synaptic plasticity. *Proceedings of the National Academy of Sciences of the United States of America*, *104*(11), 4700–4705. https://doi.org/10.1073/pnas.0607524104

Kuhn, P. H., Wang, H., Dislich, B., Colombo, A., Zeitschel, U., Ellwart, J. W., … Lichtenthaler, S. F. (2010). ADAM10 is the physiologically relevant, constitutive α-secretase of the amyloid precursor protein in primary neurons. *EMBO Journal*, *29*(17), 3020–3032. https://doi.org/10.1038/emboj.2010.167

Kumar, A. (2011). Long-term potentiation at CA3-CA1 hippocampal synapses with special emphasis on aging, disease, and stress. *Frontiers in Aging Neuroscience*, *3*(MAY), 1–20. https://doi.org/10.3389/fnagi.2011.00007

Kwapis, J. L., Alaghband, Y., López, A. J., Long, J. M., Li, X., Shu, G., … Wood, M. A. (2019). HDAC3-mediated repression of the Nr4a family contributes to age-related impairments in long-term memory. *Journal of Neuroscience*, *39*(25), 4999–5009. https://doi.org/10.1523/JNEUROSCI.2799-18.2019

La Joie, R., Perrotin, A., De La Sayette, V., Egret, S., Doeuvre, L., Belliard, S., … Chetelat, G. (2013). Hippocampal subfield volumetry in mild cognitive impairment, Alzheimer's disease and semantic dementia. *NeuroImage: Clinical*, *3*, 155–162. http://doi.org/10.1016/j.nicl.2013.08.007

Lacor, P. N., Buniel, M. C., Chang, L., Fernandez, S. J., Gong, Y., Viola, K. L., … Klein, W. L. (2004). Synaptic targeting by Alzheimer's-related amyloid β oligomers. *Journal of Neuroscience*, *24*(45), 10191–10200. https://doi.org/10.1523/JNEUROSCI.3432-04.2004

Lacor, P. N., Buniel, M. C., Furlow, P. W., Clemente, A. S., Velasco, P. T., Wood, M., … Klein, W. L. (2007). Aβ oligomer-induced aberrations in synapse composition, shape, and density provide a molecular basis for loss of connectivity in Alzheimer's disease. *Journal of Neuroscience*, *27*(4), 796–807. https://doi.org/10.1523/JNEUROSCI.3501-06.2007

Lalonde, R., Kim, H. D., & Fukuchi, K. (2004). Exploratory activity, anxiety, and motor coordination in bigenic APPswe + PS1/ΔE9 mice. *Neuroscience Letters*, *369*(2), 156–161. https://doi.org/10.1016/j.neulet.2004.07.069

Lalonde, R., & Strazielle, C. (2011). Brain regions and genes affecting limb-clasping responses. *Brain Research Reviews*, *67*(1–2), 252–259. https://doi.org/10.1016/j.brainresrev.2011.02.005

Lalonde, Robert, Fukuchi, K., & Strazielle, C. (2012). Neurologic and motor dysfunctions in APP transgenic mice. *Reviews in the Neurosciences*, *23*(4). https://doi.org/10.1515/revneuro-2012-0041

Lam, B. Y. H., Zhang, W., Enticknap, N., Haggis, E., Cader, M. Z., & Chawla, S. (2009). Inverse regulation of plasticity-related immediate early genes by calcineurin in hippocampal neurons. *Journal of Biological Chemistry*, *284*(18), 12562–12571. https://doi.org/10.1074/jbc.M901121200

Lammich, S., Kojro, E., Postina, R., Gilbert, S., Pfeiffer, R., Jasionowski, M., … Fahrenholz, F. (1999). Constitutive and regulated α-secretase cleavage of Alzheimer's amyloid precursor protein by a disintegrin metalloprotease. *Proceedings of the National Academy of Sciences of the United States of America*, *96*(7), 3922–3927. https://doi.org/10.1073/pnas.96.7.3922

Lazarov, O., Robinson, J., Tang, Y. P., Hairston, I. S., Korade-Mirnics, Z., Lee, V. M. Y., … Sisodia, S. S. (2005). Environmental enrichment reduces Aβ levels and amyloid deposition in transgenic mice. *Cell*, *120*(5), 701–713. https://doi.org/10.1016/j.cell.2005.01.015

Le, W, Conneely, O. M., He, Y., Jankovic, J., & Appel, S. H. (1999). Reduced Nurr1 expression increases the vulnerability of mesencephalic dopamine neurons to MPTP-induced injury. *Journal of Neurochemistry*, *73*(5), 2218–2221.

Le, Weidong, Pan, T., Huang, M., Xu, P., Xie, W., Zhu, W., … Jankovic, J. (2008). Decreased NURR1 gene expression in patients with Parkinson's disease. *Journal of the Neurological Sciences*, *273*(1–2), 29–33. https://doi.org/10.1016/j.jns.2008.06.007

Lee, H. K., Kameyama, K., Huganir, R. L., & Bear, M. F. (1998). NMDA induces long-term synaptic depression and dephosphorylation of the GluR1 subunit of AMPA receptors in hippocampus. *Neuron*, *21*(5), 1151–1162. https://doi.org/10.1016/S0896-6273(00)80632-7

Lee, H. K., Takamiya, K., Han, J. S., Man, H., Kim, C. H., Rumbaugh, G., … Huganir, R. L. (2003). Phosphorylation of the AMPA receptor GluR1 subunit is required for synaptic plasticity and retention of spatial memory. *Cell*, *112*(5), 631–643. https://doi.org/10.1016/S0092-8674(03)00122-3

Lee, H. K., Takamiya, K., He, K., Song, L., & Huganir, R. L. (2010). Specific roles of AMPA receptor subunit GluR1 (GluA1) phosphorylation sites in regulating synaptic plasticity in the CA1 region of hippocampus. *Journal of Neurophysiology*, *103*(1), 479–489. https://doi.org/10.1152/jn.00835.2009

Lesne, S., Koh, M. T., Kotilinek, L., Kayed, R., Glabe, C. G., Yang, A., … Ashe, K. H. (2006). A specific amyloid-beta protein assembly in the brain impairs memory. *Nature*, *440*(7082), 352–357. https://doi.org/10.1038/nature04533

Letenneur, L., Pérès, K., Fleury, H., Garrigue, I., Barberger-Gateau, P., Helmer, C., … Dartigues, J. F. (2008). Seropositivity to Herpes Simplex Virus antibodies and risk of Alzheimer's disease: A population-based cohort study. *PLoS ONE*, *3*(11), 1–5. https://doi.org/10.1371/journal.pone.0003637

Levenson, J. M., Roth, T. L., Lubin, F. D., Miller, C. A., Huang, I. C., Desai, P., … Sweatt, J. D. (2006). Evidence that DNA (cytosine-5) methyltransferase regulates synaptic plasticity in the hippocampus. *Journal of Biological Chemistry*, *281*(23), 15763–15773. https://doi.org/10.1074/jbc.M511767200

Lévy, J., Grotto, S., Mignot, C., Maruani, A., Delahaye-Duriez, A., Benzacken, B., … Tabet, A. C. (2018). NR4A2 haploinsufficiency is associated with intellectual disability and autism spectrum disorder. *Clinical Genetics*, *94*(2), 264–268. https://doi.org/10.1111/cge.13383

Lewerenz, J., & Maher, P. (2009). Basal levels of eIF2α phosphorylation determine cellular antioxidant status by regulating ATF4 and xCT expression. *Journal of Biological Chemistry*, *284*(2), 1106–1115. https://doi.org/10.1074/jbc.M807325200

Li, S., Hong, S., Shepardson, N. E., Walsh, D. M., Shankar, G. M., & Selkoe, D. (2009a). Soluble Oligomers of Amyloid β Protein Facilitate Hippocampal Long-Term Depression by Disrupting Neuronal Glutamate Uptake. *Neuron*, *62*(6), 788–801. https://doi.org/10.1016/j.neuron.2009.05.012

Li, S., Jin, M., Koeglsperger, T., Shepardson, N. E., Shankar, G. M., & Selkoe, D. J. (2011b). Soluble a β oligomers inhibit long-term potentiation through a mechanism involving excessive activation of extrasynaptic NR2B-containing NMDA receptors. *Journal of Neuroscience*, *31*(18), 6627–6638. https://doi.org/10.1523/JNEUROSCI.0203-11.2011

Li, S., Zhang, C., Takemori, H., Zhou, Y., & Xiong, Z. Q. (2009). TORC1 regulates activity-dependent CREB-target gene transcription and dendritic growth of developing cortical neurons. *Journal of Neuroscience*, *29*(8), 2334–2343. https://doi.org/10.1523/JNEUROSCI.2296-08.2009

Li, T., Yang, Z., Li, S., Cheng, C., Shen, B., & Le, W. (2018). Alterations of NURR1 and Cytokines in the Peripheral Blood Mononuclear Cells: Combined Biomarkers for Parkinson's Disease. *Frontiers in Aging Neuroscience*, *10*(NOV). https://doi.org/10.3389/fnagi.2018.00392

Lian, Q., Ladner, C. J., Magnuson, D., & Lee, J. M. (2001). Selective Changes of Calcineurin (Protein Phosphatase 2B) Activity in Alzheimer's Disease Cerebral Cortex. *Experimental Neurology*, *167*(1), 158–165. https://doi.org/10.1006/exnr.2000.7534

Liang, W. S., Dunckley, T., Beach, T. G., Grover, A., Mastroeni, D., Ramsey, K., … Stephan, D. A. (2010). Neuronal gene expression in non-demented individuals with intermediate Alzheimer's Disease neuropathology. *Neurobiology of Aging*, *31*(4), 549–566. https://doi.org/10.1016/j.neurobiolaging.2008.05.013

Liang, W. S., Reiman, E. M., Valla, J., Dunckley, T., Beach, T. G., Grover, A., … Stephan, D. A. (2008). Alzheimer's disease is associated with reduced expression of energy metabolism genes in posterior cingulate neurons. *Proceedings of the National Academy of Sciences of the United States of America*, *105*(11), 4441–4446. https://doi.org/10.1073/pnas.0709259105

Liao, D., Miller, E. C., & Teravskis, P. J. (2014). Tau acts as a mediator for Alzheimer's disease-related synaptic deficits. *European Journal of Neuroscience*, *39*(7), 1202–1213. https://doi.org/10.1111/ejn.12504

Lieu, C. A., Chinta, S. J., Rane, A., & Andersen, J. K. (2013). Age-Related Behavioral Phenotype of an Astrocytic Monoamine Oxidase-B Transgenic Mouse Model of Parkinson's Disease. *PLoS ONE*, *8*(1). https://doi.org/10.1371/journal.pone.0054200

Limon, A., Reyes-Ruiz, J. M., & Miledi, R. (2012). Loss of functional GABA A receptors in the Alzheimer diseased brain. *Proceedings of the National Academy of Sciences of the United States of America*, *109*(25), 10071–10076. https://doi.org/10.1073/pnas.1204606109

Lisman, J., Yasuda, R., & Raghavachari, S. (2012). Mechanisms of CaMKII action in long-term potentiation. *Nature Reviews Neuroscience*, *13*(3), 169–182. https://doi.org/10.1038/nrn3192

Liu, D., Jia, H., Holmes, D. I. R., Stannard, A., & Zachary, I. (2003). Vascular Endothelial Growth Factor-Regulated Gene Expression in Endothelial Cells: KDR-Mediated Induction of Egr3 and the Related Nuclear Receptors Nur77, Nurr1, and Nor1. *Arteriosclerosis, Thrombosis, and Vascular Biology*, *23*(11), 2002–2007. https://doi.org/10.1161/01.ATV.0000098644.03153.6F

Liu, L., Drouet, V., Wu, J. W., Witter, M. P., Small, S. A., Clelland, C., & Duff, K. (2012). Trans-synaptic spread of tau pathology in vivo. *PLoS ONE*, *7*(2), 1–9. https://doi.org/10.1371/journal.pone.0031302

Liu, Q., Qin, Q., Sun, H., Zhong, D., An, R., Tian, Y., … Li, G. (2018). Neuroprotective effect of olfactory ensheathing cells co-transfected with Nurr1 and Ngn2 in both in vitro and in vivo models of Parkinson's disease. *Life Sciences*, *194*(July 2017), 168–176. https://doi.org/10.1016/j.lfs.2017.12.038

Llopis, S., Singleton, B., Duplessis, T., Carrier, L., Rowan, B., & Williams, C. (2013). Dichotomous roles for the orphan nuclear receptor NURR1 in breast cancer. *BMC Cancer*, *13*(1), 1. https://doi.org/10.1186/1471-2407-13-139

López, A. J., Hemstedt, T. J., Jia, Y., Hwang, P. H., Campbell, R. R., Kwapis, J. L., … Wood, M. A. (2019). Epigenetic regulation of immediate-early gene Nr4a2/Nurr1 in the medial habenula during reinstatement of cocaine-associated behavior. *Neuropharmacology*, *153*(DEC), 13–19. https://doi.org/10.1016/j.neuropharm.2019.04.016

Lu, W., & Roche, K. W. (2012). Posttranslational regulation of AMPA receptor trafficking and function. *Current Opinion in Neurobiology*, *22*(3), 470–479. https://doi.org/10.1016/j.conb.2011.09.008

Lu, W., Shi, Y., Jackson, A. C., Bjorgan, K., During, M. J., Sprengel, R., … Nicoll, R. A. (2009). Subunit Composition of Synaptic AMPA Receptors Revealed by a Single-Cell Genetic Approach. *Neuron*, *62*(2), 254–268. https://doi.org/10.1016/j.neuron.2009.02.027

Lu, Y., Christian, K., & Lu, B. (2008). BDNF: A key regulator for protein synthesis-dependent LTP and long-term memory? *Neurobiology of Learning and Memory*, *89*(3), 312–323. https://doi.org/10.1016/j.nlm.2007.08.018

Lue, L. F., Kuo, Y. M., Roher, A. E., Brachova, L., Shen, Y., Sue, L., … Rogers, J. (1999). Soluble amyloid β peptide concentration as a predictor of synaptic change in Alzheimer's disease. *American Journal of Pathology*, *155*(3), 853–862. https://doi.org/10.1016/S0002-9440(10)65184-X

Luscher, C., & Malenka, R. C. (2012). NMDA Receptor-Dependent Long-Term Potentiation and Long-Term Depression (LTP/LTD). *Cold Spring Harbor Perspectives in Biology*, *4*(6), a005710–a005710. https://doi.org/10.1101/cshperspect.a005710

Lynch, M. A. (2004). Long-Term Potentiation and Memory. *Physiological Reviews*, *84*(1), 87–136. https://doi.org/10.1152/physrev.00014.2003

Ma, H., Groth, R. D., Cohen, S. M., Emery, J. F., Li, B., Hoedt, E., … Tsien, R. W. (2014). γcaMKII

shuttles Ca2+/CaM to the nucleus to trigger CREB phosphorylation and gene expression. *Cell*, *159*(2), 281–294. https://doi.org/10.1016/j.cell.2014.09.019

Ma, T., & Klann, E. (2012). Amyloid β: linking synaptic plasticity failure to memory disruption in Alzheimer's disease. *Journal of Neurochemistry*, *120*(SUPPL. 1), 140–148. https://doi.org/10.1111/j.1471-4159.2011.07506.x

Maezawa, I., Zimin, P. I., Wulff, H., & Jin, L. W. (2011). Amyloid-β protein oligomer at low nanomolar concentrations activates microglia and induces microglial neurotoxicity. *Journal of Biological Chemistry*, *286*(5), 3693–3706. https://doi.org/10.1074/jbc.M110.135244

Magdesian, M. H., Carvalho, M. M. V. F., Mendes, F. A., Saraiva, L. M., Juliano, M. A., Juliano, L., … Ferreira, S. T. (2008). Amyloid-β binds to the extracellular cysteine-rich domain of frizzled and inhibits Wnt/β-catenin signaling. *Journal of Biological Chemistry*, *283*(14), 9359–9368. https://doi.org/10.1074/jbc.M707108200

Majolo, F., Marinowic, D. R., MacHado, D. C., & Da Costa, J. C. (2019). Important advances in Alzheimer's disease from the use of induced pluripotent stem cells. *Journal of Biomedical Science*, *26*(1), 1–19. https://doi.org/10.1186/s12929-019-0501-5

Malenka, R. C., & Bear, M. F. (2004). LTP and LTD: An embarrassment of riches. *Neuron*, *44*(1), 5–21. https://doi.org/10.1016/j.neuron.2004.09.012

Malewicz, M., Kadkhodaei, B., Kee, N., Volakakis, N., Hellman, U., Viktorsson, K., … Perlmann, T. (2011). Essential role for DNA-PK-mediated phosphorylation of NR4A nuclear orphan receptors in DNA double-strand break repair. *Genes and Development*, *25*(19), 2031–2040. https://doi.org/10.1101/gad.16872411

Malinow, R., & Malenka, R. C. (2002). AMPA Receptor Trafficking and Synaptic Plasticity. *Annual Review of Neuroscience*, *25*(1), 103–126. https://doi.org/10.1146/annurev.neuro.25.112701.142758

Man, H. Y., Sekine-Aizawa, Y., & Huganir, R. L. (2007). Regulation of α-amino-3-hydroxy-5-methyl-4-isoxazolepropionic acid receptor trafficking through PKA phosphorylation of the Glu receptor 1 subunit. *Proceedings of the National Academy of Sciences of the United States of America*, *104*(9), 3579–3584. https://doi.org/10.1073/pnas.0611698104

Mandrekar-Colucci, S., & Landreth, G. E. (2011). Nuclear receptors as therapeutic targets for Alzheimer's disease. *Expert Opinion on Therapeutic Targets*, *15*(9), 1085–1097. https://doi.org/10.1517/14728222.2011.594043

Mango, D., Saidi, A., Cisale, G. Y., Feligioni, M., Corbo, M., & Nisticò, R. (2019). Targeting synaptic plasticity in experimental models of Alzheimer's disease. *Frontiers in Pharmacology*, *10*(JUL), 1–8. https://doi.org/10.3389/fphar.2019.00778

Marcello, E., Di Luca, M., & Gardoni, F. (2018). Synapse-to-nucleus communication: from developmental disorders to Alzheimer's disease. *Current Opinion in Neurobiology*, *48*, 160–166. https://doi.org/10.1016/j.conb.2017.12.017

Marchetti, M., & Marie, H. (2011). Hippocampal synaptic plasticity in Alzheimer's disease: What have we learned so far from transgenic models? *Reviews in the Neurosciences*, *22*(4), 373–402. https://doi.org/10.1515/RNS.2011.035

Mariani, M. M., Malm, T., Lamb, R., Jay, T. R., Neilson, L., Casali, B., … Landreth, G. E. (2017). Neuronally-directed effects of RXR activation in a mouse model of Alzheimer's disease. *Scientific Reports*, *7*(FEB), 1–12. https://doi.org/10.1038/srep42270

Marksteiner, J., Kaufmann, W. A., Gurka, P., & Humpel, C. (2002). Synaptic proteins in alzheimer's disease. *Journal of Molecular Neuroscience*, *18*(1–2), 53–63. https://doi.org/10.1385/JMN:18:1-2:53

Martin, K. C., Barad, M., & Kandel, E. R. (2000). Local protein synthesis and its role in synapse-specific plasticity. *Current Opinion in Neurobiology*, *10*(5), 587–592. https://doi.org/10.1016/S0959-4388(00)00128-8

Martin, S. J., Grimwood, P. D., & Morris, R. G. M. (2000). Synaptic Plasticity and Memory: An Evaluation of the Hypothesis. *Annual Review of Neuroscience*, *23*(1), 649–711. https://doi.org/10.1146/annurev.neuro.23.1.649

Masliah, E., Mallory, M., Alford, M., DeTeresa, R., Hansen, L. A., McKeel, D. W., & Morris, J. C. (2001). Altered expression of synaptic proteins occurs early during progression of Alzheimer's disease. *Neurology*, *56*(1), 127–129. https://doi.org/10.1212/WNL.56.1.127

Matsuzaki, M., Honkura, N., Ellis-Davies, G. C. R., & Kasai, H. (2004). Structural basis of long-term potentiation in single dendritic spines. *Nature*, *429*(6993), 761–766. https://doi.org/10.1038/nature02617

Maxwell, M. A., & Muscat, G. E. O. (2006). The NR4A Subgroup: Immediate Early Response Genes with Pleiotropic Physiological Roles. *Nuclear Receptor Signaling*, *4*(1), nrs.04002. https://doi.org/10.1621/nrs.04002

Mayr, B., & Montminy, M. (2001). Transcriptional regulation by the phosphorylation-dependent factor CREB. *Nature Reviews Molecular Cell Biology*, *2*(8), 599–609. https://doi.org/10.1038/35085068

Mazure, C. M., & Swendsen, J. (2016). Sex differences in Alzheimer's disease and other dementias. *The Lancet Neurology*, *15*(5), 451–452. https://doi.org/10.1016/S1474-4422(16)00067-3

Mc Donald, J. M., Savva, G. M., Brayne, C., Welzel, A. T., Forster, G., Shankar, G. M., … Walsh, D. M. (2010). The presence of sodium dodecyl sulphate-stable Aβ dimers is strongly associated with Alzheimer-type dementia. *Brain*, *133*(5), 1328–1341. https://doi.org/10.1093/brain/awq065

McFarland, K., Spalding, T. A., Hubbard, D., Ma, J. N., Olsson, R., & Burstein, E. S. (2013). Low dose bexarotene treatment rescues dopamine neurons and restores behavioral function in models of Parkinson's disease. *ACS Chemical Neuroscience*, *4*(11), 1430–1438. https://doi.org/10.1021/cn400100f

McLean, C. A., Cherny, R. A., Fraser, F. W., Fuller, S. J., Smith, M. J., Beyreuther, K., … Masters, C. L. (1999). Soluble pool of Aβ amyloid as a determinant of severity of neurodegeneration in Alzheimer's disease. *Annals of Neurology*, *46*(6), 860–866. https://doi.org/10.1002/1531-8249(199912)46:6<860::AID-ANA8>3.0.CO;2-M

McNamara, R. K., Hussain, R. J., Simon, E. J., Stumpo, D. J., Blackshear, P. J., Abel, T., & Lenox, R. H. (2005). Effect of myristoylated alanine-rich C kinase substrate (MARCKS) overexpression on hippocampus-dependent learning and hippocampal synaptic plasticity MARCKS transgenic mice. *Hippocampus*, *15*(5), 675–683. https://doi.org/10.1002/hipo.20089

McNulty, S. E., Barrett, R. M., Vogel-Ciernia, A., Malvaez, M., Hernandez, N., Davatolhagh, M. F., … Wood, M. A. (2012). Differential roles for Nr4a1 and Nr4a2 in object location vs. object recognition long-term memory. *Learning and Memory*, *19*(12), 588–592. https://doi.org/10.1101/lm.026385.112

McQuown, S. C., Barrett, R. M., Matheos, D. P., Post, R. J., Rogge, G. A., Alenghat, T., … Wood, M. A. (2011). HDAC3 is a critical negative regulator of long-term memory formation. *Journal of Neuroscience*, *31*(2), 764–774. https://doi.org/10.1523/JNEUROSCI.5052-10.2011

Mei, F., Nagappan, G., Ke, Y., Sacktor, T. C., & Lu, B. (2011). BDNF facilitates L-LTP maintenance in the absence of protein synthesis through PKMζ. *PLoS ONE*, *6*(6). https://doi.org/10.1371/journal.pone.0021568

Mendes, N. D., Fernandes, A., Almeida, G. M., Santos, L. E., Selles, M. C., Lyra e Silva, N. M., … Sebollela, A. (2018). Free-floating adult human brain-derived slice cultures as a model to study the neuronal impact of Alzheimer's disease-associated Aβ oligomers. *Journal of Neuroscience Methods*, *307*(May), 203–209. https://doi.org/10.1016/j.jneumeth.2018.05.021

Miller, E. C., Teravskis, P. J., Dummer, B. W., Zhao, X., Huganir, R. L., & Liao, D. (2014). Tau phosphorylation and tau mislocalization mediate soluble Aβ oligomer-induced AMPA glutamate receptor signaling deficits. *European Journal of Neuroscience*, *39*(7), 1214–1224. https://doi.org/10.1111/ejn.12507

Miller, J. A., Oldham, M. C., & Geschwind, D. H. (2008). A systems level analysis of transcriptional changes in Alzheimer's disease and normal aging. *Journal of Neuroscience*, *28*(6), 1410–1420. https://doi.org/10.1523/JNEUROSCI.4098-07.2008

Miñano-Molina, A. J., España, J., Martín, E., Barneda-Zahonero, B., Fadó, R., Solé, M., …

Rodríguez-Alvarez, J. (2011). Soluble oligomers of amyloid-β peptide disrupt membrane trafficking of α-amino-3-hydroxy-5-methylisoxazole-4-propionic acid receptor contributing to early synapse dysfunction. *Journal of Biological Chemistry*, *286*(31), 27311–27321. https://doi.org/10.1074/jbc.M111.227504

Miranda, M., Morici, J. F., Zanoni, M. B., & Bekinschtein, P. (2019). Brain-Derived Neurotrophic Factor: A Key Molecule for Memory in the Healthy and the Pathological Brain. *Frontiers in Cellular Neuroscience*, *13*(AUG), 1–25. https://doi.org/10.3389/fncel.2019.00363

Molnár, E. (2011). Long-term potentiation in cultured hippocampal neurons. *Seminars in Cell and Developmental Biology*, *22*(5), 506–513. https://doi.org/10.1016/j.semcdb.2011.07.017

Montarolo, F., Martire, S., Perga, S., & Bertolotto, A. (2019). Nurr1 impairment in multiple sclerosis. *International Journal of Molecular Sciences*, *20*(19), 1–9. https://doi.org/10.3390/ijms20194858

Montarolo, F., Perga, S., Martire, S., Navone, D. N., Marchet, A., Leotta, D., & Bertolotto, A. (2016). Altered NR4A Subfamily Gene Expression Level in Peripheral Blood of Parkinson's and Alzheimer's Disease Patients. *Neurotoxicity Research*, *30*(3), 338–344. https://doi.org/10.1007/s12640-016-9626-4

Montarolo, F., Raffaele, C., Perga, S., Martire, S., Finardi, A., Furlan, R., … Bertolotto, A. (2014). Effects of isoxazolo-pyridinone 7e, a potent activator of the nurr1 signaling pathway, on experimental autoimmune encephalomyelitis in mice. *PLoS ONE*, *9*(9), 1–9. https://doi.org/10.1371/journal.pone.0108791

Moon, M., Jeong, I., Kim, C. H., Kim, J., Lee, P. K. J., Mook-Jung, I., … Kim, K. S. (2015). Correlation between orphan nuclear receptor Nurr1 expression and amyloid deposition in 5XFAD mice, an animal model of Alzheimer's disease. *Journal of Neurochemistry*, *132*(2), 254–262. https://doi.org/10.1111/jnc.12935

Moon, M., Jung, E. S., Jeon, S. G., Cha, M.-Y., Jang, Y., Kim, W., … Kim, K.-S. (2019). Nurr1 (NR4A2) regulates Alzheimer's disease-related pathogenesis and cognitive function in the 5XFAD mouse model. *Aging Cell*, *18*(1), e12866. https://doi.org/10.1111/acel.12866

Morise, J., Suzuki, K. G. N., Kitagawa, A., Wakazono, Y., Takamiya, K., Tsunoyama, T. A., … Oka, S. (2019). AMPA receptors in the synapse turnover by monomer diffusion. *Nature Communications*, *10*(1), 5245. https://doi.org/10.1038/s41467-019-13229-8

Morley, J. E., & Farr, S. A. (2014). The role of amyloid-beta in the regulation of memory. *Biochemical Pharmacology*, *88*(4), 479–485. https://doi.org/10.1016/j.bcp.2013.12.018

Morris, R. G. M. (1999). *D . O . Hebb : The Organization of Behavior , Wiley : New York ; 1949*. *50*(99), 9230. http://doi.org/10.1016/s0361-9230(99)00182-3

Mosconi, L., Tsui, W.-H., De Santi, S., Li, J., Rusinek, H., Convit, A., … de Leon, M. J. (2005). Reduced hippocampal metabolism in MCI and AD: automated FDG-PET image analysis. *Neurology*, *64*(11), 1860–1867. https://doi.org/10.1212/01.WNL.0000163856.13524.08

Mozafari, N., Shamsizadeh, A., Fatemi, I., Allahtavakoli, M., Moghadam-Ahmadi, A., Kaviani, E., & Kaeidi, A. (2018). CX691 as an AMPA receptor positive modulator, improves the learning and memory in a rat model of Alzheimer's disease. *Iranian Journal of Basic Medical Sciences*, *21*(7), 724–730. https://doi.org/10.22038/ijbms.2018.28544.6934

Mucke, L., Masliah, E., Yu, G. Q., Mallory, M., Rockenstein, E. M., Tatsuno, G., … McConlogue, L. (2000). High-level neuronal expression of Aβ(1-42) in wild-type human amyloid protein precursor transgenic mice: Synaptotoxicity without plaque formation. *Journal of Neuroscience*, *20*(11), 4050–4058. https://doi.org/10.1523/jneurosci.20-11-04050.2000

Mucke, L., & Selkoe, D. J. (2012). Neurotoxicity of Amyloid-β Protein: Synaptic and Network Dysfunction. *Cold Spring Harbor Perspectives in Medicine*, *2*(7), 1–17. http://doi.org/10.1101/cshperspect.a006338

Munnur, D., Somers, J., Skalka, G., Weston, R., Jukes-Jones, R., Bhogadia, M., … Malewicz, M. (2019). NR4A Nuclear Receptors Target Poly-ADP-Ribosylated DNA-PKcs Protein to Promote DNA Repair. *Cell Reports*, *26*(8), 2028-2036.e6. https://doi.org/10.1016/j.celrep.2019.01.083

Nagahara, A. H., Mateling, M., Kovacs, I., Wang, L., Eggert, S., Rockenstein, E., … Tuszynski, M. H. (2013). Early BDNF treatment ameliorates cell loss in the entorhinal cortex of APP transgenic mice. *Journal of Neuroscience*, *33*(39), 15596–15602. https://doi.org/10.1523/JNEUROSCI.5195-12.2013

Nagahara, A. H., Merrill, D. A., Coppola, G., Tsukada, S., Schroeder, B. E., Shaked, G. M., … Tuszynski, M. H. (2009). Neuroprotective effects of brain-derived neurotrophic factor in rodent and primate models of Alzheimer's disease. *Nature Medicine*, *15*(3), 331–337. https://doi.org/10.1038/nm.1912

Naughton, B. J., Duncan, F. J., Murrey, D. A., Meadows, A. S., Newsom, D. E., Stoicea, N., … Fu, H. (2014). Blood Genome-Wide Transcriptional Profiles Reflect Broad Molecular Impairments and Strong Blood-Brain Links in Alzheimer's Disease. *Journal of Alzheimer's Disease*, *43*(1), 93–108. https://doi.org/10.3233/JAD-140606

Nelson, P. T., & Schmitt, F. A. (2011). Age Number One Factor of Alzheimer'S Disease. *Acta Neuropathol*, *121*(5), 571–587. https://doi.org/10.1007/s00401-011-0826-y.Alzheimer

Nery, A. A., Magdesian, M. H., Trujillo, C. A., Sathler, L. B., Juliano, M. A., Juliano, L., … Ferreira, S. T. (2013). Rescue of Amyloid-Beta-Induced Inhibition of Nicotinic Acetylcholine Receptors by a Peptide Homologous to the Nicotine Binding Domain of the Alpha 7 Subtype. *PLoS ONE*, *8*(7). https://doi.org/10.1371/journal.pone.0067194

Neves, G., Cooke, S. F., & Bliss, T. V. P. (2008). Synaptic plasticity, memory and the hippocampus: A neural network approach to causality. *Nature Reviews Neuroscience*, *9*(1), 65–75. https://doi.org/10.1038/nrn2303

Ng, T., Ho, C., Tam, W., Kua, E., & Ho, R. (2019). Decreased Serum Brain-Derived Neurotrophic Factor (BDNF) Levels in Patients with Alzheimer's Disease (AD): A Systematic Review and Meta-Analysis. *International Journal of Molecular Sciences*, *20*(2), 257. https://doi.org/10.3390/ijms20020257

Nguyen, Q. T., Han, M., Moon, J., Kim, K.-S., Jeong, I., Shin, J., … Ringe, D. (2015). Nuclear receptor Nurr1 agonists enhance its dual functions and improve behavioral deficits in an animal model of Parkinson's disease. In *Proceedings of the National Academy of Sciences, 112*(28), 8756-8761. https://doi.org/10.1073/pnas.1509742112

Nicoll, R. A. (2017). Review A Brief History of Long-Term Potentiation. *Neuron, 93*(2), 281–290. http://doi.org/10.1016/j.neuron.2016.12.015

Nicoll, R. A., & Schmitz, D. (2005). Synaptic plasticity at hippocampal mossy fibre synapses. *Nature Reviews Neuroscience*, *6*(11), 863–876. https://doi.org/10.1038/nrn1786

Nikolaev, A., McLaughlin, T., O'Leary, D. D. M., & Tessier-Lavigne, M. (2009). APP binds DR6 to trigger axon pruning and neuron death via distinct caspases. *Nature*, *457*(7232), 981–989. https://doi.org/10.1038/nature07767

Novak, P., Prcina, M., & Kontsekova, E. (2011). Tauons and prions: infamous cousins? *Journal of Alzheimer's Disease : JAD*, *26*(3), 413–430. https://doi.org/10.3233/JAD-2011-110194

Nussbaum, J. M., Seward, M. E., & Bloom, G. S. (2013). Alzheimer disease: A tale of two prions. *Prion*, *7*(1), 14–19. https://doi.org/10.4161/pri.22118

Oakley, H., Cole, S. L., Logan, S., Maus, E., Shao, P., Craft, J., … Vassar, R. (2006). Intraneuronal β-amyloid aggregates, neurodegeneration, and neuron loss in transgenic mice with five familial Alzheimer's disease mutations: Potential factors in amyloid plaque formation. *Journal of Neuroscience*, *26*(40), 10129–10140. https://doi.org/10.1523/JNEUROSCI.1202-06.2006

Oddo, S., Caccamo, A., Shepherd, J. D., Murphy, M. P., Golde, T. E., Kayed, R., … LaFerla, F. M. (2003). Triple-transgenic model of Alzheimer's Disease with plaques and tangles: Intracellular Aβ and synaptic dysfunction. *Neuron*, *39*(3), 409–421. https://doi.org/10.1016/S0896-6273(03)00434-3

Oliveira, A., Martinho, R., Serrão, P., & Moreira-Rodrigues, M. (2018). Epinephrine Released During Traumatic Events May Strengthen Contextual Fear Memory Through Increased Hippocampus mRNA Expression of Nr4a Transcription Factors. *Frontiers in Molecular Neuroscience*, *11*(SEP), 1–11. https://doi.org/10.3389/fnmol.2018.00334

Ondrejcak, T., Klyubin, I., Hu, N. W., Barry, A. E., Cullen, W. K., & Rowan, M. J. (2010). Alzheimer's disease amyloid β-protein and synaptic function. *NeuroMolecular Medicine*, *12*(1), 13–26. https://doi.org/10.1007/s12017-009-8091-0

Ordentlich, P., Yan, Y., Zhou, S., & Heyman, R. A. (2003). Identification of the Antineoplastic Agent 6-Mercaptopurine as an Activator of the Orphan Nuclear Hormone Receptor Nurr1. *Journal of Biological Chemistry*, *278*(27), 24791–24799. https://doi.org/10.1074/jbc.M302167200

Paliga, D., Raudzus, F., Leppla, S. H., Heumann, R., & Neumann, S. (2019). Lethal Factor Domain-Mediated Delivery of Nurr1 Transcription Factor Enhances Tyrosine Hydroxylase Activity and Protects from Neurotoxin-Induced Degeneration of Dopaminergic Cells. *Molecular Neurobiology*, *56*(5), 3393–3403. https://doi.org/10.1007/s12035-018-1311-6

Palop, J. J., Chin, J., Roberson, E. D., Wang, J., Thwin, M. T., Bien-Ly, N., … Mucke, L. (2007). Aberrant Excitatory Neuronal Activity and Compensatory Remodeling of Inhibitory Hippocampal Circuits in Mouse Models of Alzheimer's Disease. *Neuron*, *55*(5), 697–711. https://doi.org/10.1016/j.neuron.2007.07.025

Parra-Damas, A., Valero, J., Ferrer, I., Saura, C. A., Espana, J., Martin, E., … Rodriguez-Alvarez, J. (2014). Crtc1 Activates a Transcriptional Program Deregulated at Early Alzheimer's Disease-Related Stages. *Journal of Neuroscience*, *34*(17), 5776–5787. https://doi.org/10.1523/jneurosci.5288-13.2014

Parra-Damas, Arnaldo, Chen, M., Enriquez-Barreto, L., Ortega, L., Acosta, S., Perna, J. C., … Saura, C. A. (2017a). CRTC1 Function During Memory Encoding Is Disrupted in Neurodegeneration. *Biological Psychiatry*, *81*(2), 111–123. https://doi.org/10.1016/j.biopsych.2016.06.025

Parra-Damas, Arnaldo, Rubió-Ferrarons, L., Shen, J., & Saura, C. A. (2017b). CRTC1 mediates preferential transcription at neuronal activity-regulated CRE/TATA promoters. *Scientific Reports*, *7*(1), 1–13. https://doi.org/10.1038/s41598-017-18215-y

Pastalkova, E., Serrano, P., Pinkhasova, D., Wallace, E., Fenton, A. A., & Sacktor, T. C. (2006). Storage of spatial information by the maintenance mechanism of LTP. *Science*, *313*(5790), 1141–1444. https://doi.org/10.1126/science.1128657

Paula-Lima, A. C., Adasme, T., Sanmartín, C., Sebollela, A., Hetz, C., Carrasco, M. A., … Hidalgo, C. (2011). Amyloid β-peptide oligomers stimulate RyR-mediated Ca2+ release inducing mitochondrial fragmentation in hippocampal neurons and prevent RyR-mediated dendritic spine remodeling produced by BDNF. *Antioxidants and Redox Signaling*, *14*(7), 1209–1223. https://doi.org/10.1089/ars.2010.3287

Pegoraro, S., Broccard, F. D., Ruaro, M. E., Bianchini, D., Avossa, D., Pastore, G., … Torre, V. (2010). Sequential steps underlying neuronal plasticity induced by a transient exposure to gabazine. *Journal of Cellular Physiology*, *222*(3), 713–728. https://doi.org/10.1002/jcp.21998

Peña De Ortiz, S., Maldonado-Vlaar, C. S., & Carrasquillo, Y. (2000). Hippocampal expression of the orphan nuclear receptor gene hzf-3/nurr1 during spatial discrimination learning. *Neurobiology of Learning and Memory*, *74*(2), 161–178. https://doi.org/10.1006/nlme.1999.3952

Peng, S., Garzon, D. J., Marchese, M., Klein, W., Ginsberg, S. D., Francis, B. M., … Fahnestock, M. (2009). Decreased brain-derived neurotrophic factor depends on amyloid aggregation state in transgenic mouse models of Alzheimer's disease. *Journal of Neuroscience*, *29*(29), 9321–9329. https://doi.org/10.1523/JNEUROSCI.4736-08.2009

Peng, S., Wuu, J., Mufson, E. J., & Fahnestock, M. (2005). Precursor form of brain-derived neurotrophic factor and mature brain-derived neurotrophic factor are decreased in the pre-clinical stages of Alzheimer's disease. *Journal of Neurochemistry*, *93*(6), 1412–1421. https://doi.org/10.1111/j.1471-4159.2005.03135.x

Penn, A. C., Zhang, C. L., Georges, F., Royer, L., Breillat, C., Hosy, E., … Choquet, D. (2017). Hippocampal LTP and contextual learning require surface diffusion of AMPA receptors. *Nature*, *549*(7672), 384–388. https://doi.org/10.1038/nature23658

Penney, J., Ralvenius, W. T., & Tsai, L. H. (2020). Modeling Alzheimer's disease with iPSC-derived brain cells. *Molecular Psychiatry*, *25*(1), 148–167. https://doi.org/10.1038/s41380-019-0468-3

Pereira, L. A., Munita, R., González, M. P., & Andrés, M. E. (2017). Long 3'UTR of Nurr1 mRNAs is targeted by miRNAs in mesencephalic dopamine neurons. *PLoS ONE*, *12*(11), 1–15. https://doi.org/10.1371/journal.pone.0188177

Perez-Cruz, C., Nolte, M. W., Van Gaalen, M. M., Rustay, N. R., Termont, A., Tanghe, A., … Ebert, U. (2011). Reduced spine density in specific regions of CA1 pyramidal neurons in two transgenic mouse models of Alzheimer's disease. *Journal of Neuroscience*, *31*(10), 3926–3934. https://doi.org/10.1523/JNEUROSCI.6142-10.2011

Petrini, E. M., Lu, J., Cognet, L., Lounis, B., Ehlers, M. D., & Choquet, D. (2009). Endocytic Trafficking and Recycling Maintain a Pool of Mobile Surface AMPA Receptors Required for Synaptic Potentiation. *Neuron*, *63*(1), 92–105. https://doi.org/10.1016/j.neuron.2009.05.025

Pfaffl, M. W. (2001). A new mathematical model for relative quantification in real-time RT-PCR. *Nucleic Acids Research*, *29*(9), 45e – 45. https://doi.org/10.1093/nar/29.9.e45

Pham, E., Crews, L., Ubhi, K., Hansen, L., Adame, A., Salmon, D., … John, R. (2011). *Alterations in Synaptic Scaffold Proteins*. *277*(14), 3051–3067. https://doi.org/10.1111/j.1742-4658.2010.07719.x.Progressive

Pigino, G., Morfini, G., Atagi, Y., Deshpande, A., Yu, C., Jungbauer, L., … Brady, S. (2009). Disruption of fast axonal transport is a pathogenic mechanism for intraneuronal amyloid beta. *Proceedings of the National Academy of Sciences of the United States of America*, *106*(14), 5907–5912. https://doi.org/10.1073/pnas.0901229106

Pimplikar, S. W., Nixon, R. A., Robakis, N. K., Shen, J., & Tsai, L. H. (2010). Amyloid-independent mechanisms in Alzheimer's disease pathogenesis. *Journal of Neuroscience*, *30*(45), 14946–14954. https://doi.org/10.1523/JNEUROSCI.4305-10.2010

Ping, G., Qian, W., Song, G., & Zhaochun, S. (2014). Valsartan reverses depressive/anxiety-like behavior and induces hippocampal neurogenesis and expression of BDNF protein in unpredictable chronic mild stress mice. *Pharmacology Biochemistry and Behavior*, *124*, 5–12. https://doi.org/10.1016/j.pbb.2014.05.006

Pooler, A. M., & Hanger, D. P. (2010). Functional implications of the association of tau with the plasma membrane. *Biochemical Society Transactions*, *38*(4), 1012–1015. https://doi.org/10.1042/BST0381012

Poon, W. W., Blurton-Jones, M., Tu, C. H., Feinberg, L. M., Chabrier, M. A., Harris, J. W., … Cotman, C. W. (2011). β-Amyloid impairs axonal BDNF retrograde trafficking. *Neurobiology of Aging*, *32*(5), 821–833. https://doi.org/10.1016/j.neurobiolaging.2009.05.012

Porsolt, R. D., Le Pichon, M., & Jalfre, M. (1977). Depression: a new animal model sensitive to antidepressant treatments. *Nature*, *266*(5604), 730–732. https://doi.org/10.1038/266730a0

Potashkin, J. A., Bottero, V., Santiago, J. A., & Quinn, J. P. (2019). Computational identification of key genes that may regulate gene expression reprogramming in Alzheimer's patients. *PLoS ONE*, *14*(9), 1–21. https://doi.org/10.1371/journal.pone.0222921

Proctor, D. T., Coulson, E. J., & Dodd, P. R. (2011). Post-synaptic scaffolding protein interactions with glutamate receptors in synaptic dysfunction and Alzheimer's disease. *Progress in Neurobiology*, *93*(4), 509–521. https://doi.org/10.1016/j.pneurobio.2011.02.002

Prusiner, S. B. (1984). Some speculations about prions, amyloid, and Alzheimer's disease. *The New England Journal of Medicine*, *310*(10), 661–663. https://doi.org/10.1056/NEJM198403083101021

Puzzo, D., Privitera, L., Leznik, E., Fà, M., Staniszewski, A., Palmeri, A., & Arancio, O. (2008). Picomolar amyloid-β positively modulates synaptic plasticity and memory in hippocampus. *Journal of Neuroscience*, *28*(53), 14537–14545. https://doi.org/10.1523/JNEUROSCI.2692-08.2008

Qian, Y., Chen, X. X., Wang, W., Li, J. J., Wang, X. P., Tang, Z. W., … Deng, X. L. (2020). Transplantation of Nurr1-overexpressing neural stem cells and microglia for treating parkinsonian rats. *CNS Neuroscience and Therapeutics*, *26*(1), 55–65. https://doi.org/10.1111/cns.13149

Qiao, S., Tao, S., Rojo De La Vega, M., Park, S. L., Vonderfecht, A. A., Jacobs, S. L., … Wondrak,

G. T. (2013). The antimalarial amodiaquine causes autophagic-lysosomal and proliferative blockade sensitizing human melanoma cells to starvation- And chemotherapy-induced cell death. *Autophagy*, *9*(12), 2087–2102. https://doi.org/10.4161/auto.26506

Querfurth, H. W., & Laferla, F. M. (2010). *Alzheimer's Disease*. *362*(4), 329–344. http://doi.org/10.1056/NEJMra0909142.

Quina, L. A., Wang, S., Ng, L., & Turner, E. E. (2009). Brn3a and Nurr1 Mediate a Gene Regulatory Pathway for Habenula Development. *Journal of Neuroscience*, *29*(45), 14309–14322. https://doi.org/10.1523/JNEUROSCI.2430-09.2009

Rahman, M. M., Zetterberg, H., Lendel, C., & Hard, T. (2015). Binding of human proteins to amyloid-β protofibrils. *ACS Chemical Biology*, *10*(3), 766–774. https://doi.org/10.1021/cb5008663

Rammes, G., Hasenjäger, A., Sroka-Saidi, K., Deussing, J. M., & Parsons, C. G. (2011). Therapeutic significance of NR2B-containing NMDA receptors and mGluR5 metabotropic glutamate receptors in mediating the synaptotoxic effects of β-amyloid oligomers on long-term potentiation (LTP) in murine hippocampal slices. *Neuropharmacology*, *60*(6), 982–990. https://doi.org/10.1016/j.neuropharm.2011.01.051

Ramos, L. L. P., Monteiro, F. P., Sampaio, L. P. B., Costa, L. A., Ribeiro, M. D. O., Freitas, E. L., … Kok, F. (2019). Heterozygous loss of function of NR4A2 is associated with intellectual deficiency, rolandic epilepsy, and language impairment. *Clinical Case Reports*, *7*(8), 1582–1584. https://doi.org/10.1002/ccr3.2260

Ranhotra, H. S. (2015). The NR4A orphan nuclear receptors: Mediators in metabolism and diseases. *Journal of Receptors and Signal Transduction*, *35*(2), 184–188. https://doi.org/10.3109/10799893.2014.948555

Rapoport, M., Dawson, H. N., Binder, L. I., Vitek, M. P., & Ferreira, A. (2002). Tau is essential to β-amyloid-induced neurotoxicity. *Proceedings of the National Academy of Sciences of the United States of America*, *99*(9), 6364–6369. https://doi.org/10.1073/pnas.092136199

Readhead, B., Haure-Mirande, J. V., Funk, C. C., Richards, M. A., Shannon, P., Haroutunian, V., … Dudley, J. T. (2018). Multiscale Analysis of Independent Alzheimer's Cohorts Finds Disruption of Molecular, Genetic, and Clinical Networks by Human Herpesvirus. *Neuron*, *99*(1), 64-82.e7. https://doi.org/10.1016/j.neuron.2018.05.023

Reinders, N. R., Pao, Y., Renner, M. C., Da Silva-Matos, C. M., Lodder, T. R., Malinow, R., & Kessels, H. W. (2016). Amyloid-β effects on synapses and memory require AMPA receptor subunit GluA3. *Proceedings of the National Academy of Sciences of the United States of America*, *113*(42), E6526–E6534. https://doi.org/10.1073/pnas.1614249113

Reinhardt, S., Schuck, F., Grösgen, S., Riemenschneider, M., Hartmann, T., Postina, R., … Endres, K. (2014). Unfolded protein response signaling by transcription factor XBP-1 regulates ADAM10 and is affected in Alzheimer's disease. *FASEB Journal*, *28*(2), 978–997. https://doi.org/10.1096/fj.13-234864

Reitz, C., Honig, L., Vonsattel, J. P., Tang, M.-X., & Mayeux, R. (2009). Memory performance is related to amyloid and tau pathology in the hippocampus. *Journal of Neurology, Neurosurgery & Psychiatry*, *80*(7), 715–721. https://doi.org/10.1136/jnnp.2008.154146

Renner, M., Lacor, P. N., Velasco, P. T., Xu, J., Contractor, A., Klein, W. L., & Triller, A. (2010). Deleterious Effects of Amyloid β Oligomers Acting as an Extracellular Scaffold for mGluR5. *Neuron*, *66*(5), 739–754. https://doi.org/10.1016/j.neuron.2010.04.029

Roberson, E. D., Halabisky, B., Yoo, J. W., Yao, J., Chin, J., Yan, F., … Mucke, L. (2011). Amyloid-β/fyn-induced synaptic, network, and cognitive impairments depend on tau levels in multiple mouse models of alzheimer's disease. *Journal of Neuroscience*, *31*(2), 700–711. https://doi.org/10.1523/JNEUROSCI.4152-10.2011

Robert, J., Button, E. B., Yuen, B., Gilmour, M., Kang, K., Bahrabadi, A., … Wellington, C. L. (2017). Clearance of beta-amyloid is facilitated by apolipoprotein E and circulating high-density lipoproteins in bioengineered human vessels. *ELife*, *6*. https://doi.org/10.7554/eLife.29595

Roberts, R., & David S. Knopman. (2013). Classification and Epidemiology of MCI. *Clin Geriatr*

Med., *29*(4), 1–19. https://doi.org/10.1016/j.cger.2013.07.003

Rodgers, R. J., & Dalvi, A. (1997). Anxiety, defence and the elevated plus-maze. *Neuroscience and Biobehavioral Reviews*, *21*(6), 801–810. https://doi.org/10.1016/s0149-7634(96)00058-9

Rodrigues, E. M., Scudder, S. L., Goo, M. S., & Patrick, G. N. (2016). Aβ-induced synaptic alterations require the E3 ubiquitin ligase Nedd4-1. *Journal of Neuroscience*, *36*(5), 1590–1595. https://doi.org/10.1523/JNEUROSCI.2964-15.2016

Rodríguez-Calvo, R., Tajes, M., & Vázquez-Carrera, M. (2017). The NR4A subfamily of nuclear receptors: potential new therapeutic targets for the treatment of inflammatory diseases. *Expert Opinion on Therapeutic Targets*, *21*(3), 291–304. https://doi.org/10.1080/14728222.2017.1279146

Rojas, P., Joodmardi, E., Hong, Y., Perlmann, T., & Ögren, S. O. (2007). Adult mice with reduced Nurr1 expression: An animal model for schizophrenia. *Molecular Psychiatry*, *12*(8), 756–766. https://doi.org/10.1038/sj.mp.4001993

Rojas, Patricia, Joodmardi, E., Perlmann, T., & Ögren, S. O. (2010). Rapid increase of Nurr1 mRNA expression in limbic and cortical brain structures related to coping with depression-like behavior in mice. *Journal of Neuroscience Research*, *88*(10), 2284–2293. https://doi.org/10.1002/jnr.22377

Rönicke, R., Mikhaylova, M., Rönicke, S., Meinhardt, J., Schröder, U. H., Fändrich, M., … Reymann, K. G. (2011). Early neuronal dysfunction by amyloid β oligomers depends on activation of NR2B-containing NMDA receptors. *Neurobiology of Aging*, *32*(12), 2219–2228. https://doi.org/10.1016/j.neurobiolaging.2010.01.011

Rosa, S. G., Quines, C. B., Stangherlin, E. C., & Nogueira, C. W. (2016). Diphenyl diselenide ameliorates monosodium glutamate induced anxiety-like behavior in rats by modulating hippocampal BDNF-Akt pathway and uptake of GABA and serotonin neurotransmitters. *Physiology and Behavior*, *155*, 1–8. https://doi.org/10.1016/j.physbeh.2015.11.038

Roselli, F., Tirard, M., Lu, J., Hutzler, P., Lamberti, P., Livrea, P., … Almeida, O. F. X. (2005). Soluble β-amyloid1-40 induces NMDA-Dependent Degradation of Postsynaptic Density-95 at Glutamatergic Synapses. *Journal of Neuroscience*, *25*(48), 11061–11070. https://doi.org/10.1523/JNEUROSCI.3034-05.2005

Roth, M., Tomlinson, B. E., & Blessed, G. (1966). Correlation between scores for dementia and counts of “senile plaques” in cerebral grey matter of elderly subjects. *Nature*, *209*(5018), 109–110. https://doi.org/10.1038/209109a0

Rudenko, L. K., Wallrabe, H., Periasamy, A., Siller, K. H., Svindrych, Z., Seward, M. E., … Alonso, A. (2019). Intraneuronal Tau Misfolding Induced by Extracellular Amyloid-β Oligomers. *Journal of Alzheimer’s Disease*, *71*(4), 1125–1138. https://doi.org/10.3233/JAD-190226

Safe, S., Jin, U.-H., Morpurgo, B., Abudayyeh, A., Singh, M., & Tjalkens, R. B. (2016). Nuclear receptor 4A (NR4A) family – orphans no more. *The Journal of Steroid Biochemistry and Molecular Biology*, *157*, 48–60. https://doi.org/10.1016/j.jsbmb.2015.04.016

Saganich, M. J., Schroeder, B. E., Galvan, V., Bredesen, D. E., Koo, E. H., & Heinemann, S. F. (2006). Deficits in Synaptic Transmission and Learning in Amyloid Precursor Protein (APP) Transgenic Mice Require C-Terminal Cleavage of APP. *Journal of Neuroscience*, *26*(52), 13428–13436. https://doi.org/10.1523/JNEUROSCI.4180-06.2006

Saijo, K., Winner, B., Carson, C. T., Collier, J. G., Rosenfeld, M. G., Gage, F. H., & Glass, C. K. (2009). A Nurr1/CoREST transrepression pathway attenuates neurotoxic inflammation in activated microglia and astrocytes. *Cell*, *137*(1), 47–59. https://doi.org/10.1016/j.cell.2009.01.038.A

Salloway, S., Sperling, R., Fox, N. C., Blennow, K., Klunk, W., Raskind, M., … Brashear, H. R. (2014). Two Phase 3 Trials of Bapineuzumab in Mild-to-Moderate Alzheimer’s Disease. *New England Journal of Medicine*, *370*(4), 322–333. https://doi.org/10.1056/NEJMoa1304839

Saman, S., Kim, W. H., Raya, M., Visnick, Y., Miro, S., Saman, S., … Hall, G. F. (2012). Exosome-associated tau is secreted in tauopathy models and is selectively phosphorylated in cerebrospinal fluid in early Alzheimer disease. *Journal of Biological Chemistry*, *287*(6), 3842–3849. https://doi.org/10.1074/jbc.M111.277061

Sanderson, J. L., Gorski, J. A., & Dell'Acqua, M. L. (2016). NMDA Receptor-Dependent LTD Requires Transient Synaptic Incorporation of Ca2+-Permeable AMPARs Mediated by AKAP150-Anchored PKA and Calcineurin. *Neuron*, *89*(5), 1000–1015. https://doi.org/10.1016/j.neuron.2016.01.043

Santoso, D. I. I., Yolanda, S., Redjeki, S., Andraini, T., & Ivanali, K. (2020). Continuous environmental enrichment and aerobic exercise improves spatial memory: focus on rat hippocampal BDNF and NGF. *Comparative Exercise Physiology*, *16*(2), 121–128. https://doi.org/10.3920/CEP190036

Saucedo-Cardenas, O, & Conneely, O. M. (1996). Comparative distribution of NURR1 and NUR77 nuclear receptors in the mouse central nervous system. *Journal of Molecular Neuroscience : MN*, *7*(1), 51–63. https://doi.org/10.1007/BF02736848

Saucedo-Cardenas, Odila, Quintana-Hau, J. D., Le, W. D., Smidt, M. P., Cox, J. J., De Mayo, F., … Conneely, O. M. (1998). Nurr1 is essential for the induction of the dopaminergic phenotype and the survival of ventral mesencephalic late dopaminergic precursor neurons. *Proceedings of the National Academy of Sciences of the United States of America*, *95*(7), 4013–4018. https://doi.org/10.1073/pnas.95.7.4013

Saura, C. A., Choi, S. Y., Beglopoulos, V., Malkani, S., Zhang, D., Rao, B. S. S., … Shen, J. (2004). Loss of presenilin function causes impairments of memory and synaptic plasticity followed by age-dependent neurodegeneration. *Neuron*, *42*(1), 23–36. https://doi.org/10.1016/S0896-6273(04)00182-5

Saura, C. A., Parra-Damas, A., & Enriquez-Barreto, L. (2015). Gene expression parallels synaptic excitability and plasticity changes in Alzheimer's disease. *Frontiers in Cellular Neuroscience*, *9*(AUG), 1–14. https://doi.org/10.3389/fncel.2015.00318

Saura, C. A., & Valero, J. (2011). The role of CREB signaling in Alzheimer's disease and other cognitive disorders. *Reviews in the Neurosciences*, *22*(2), 153–169. https://doi.org/10.1515/RNS.2011.018

Scheff, S W, Price, D. A., Schmitt, F. A., DeKosky, S. T., & Mufson, E. J. (2007). Synaptic alterations in CA1 in mild Alzheimer disease and mild cognitive impairment. *Neurology*, *68*(18), 1501–1508. https://doi.org/10.1212/01.wnl.0000260698.46517.8f

Scheff, Stephen W., Price, D. A., Schmitt, F. A., & Mufson, E. J. (2006). Hippocampal synaptic loss in early Alzheimer's disease and mild cognitive impairment. *Neurobiology of Aging*, *27*(10), 1372–1384. https://doi.org/10.1016/j.neurobiolaging.2005.09.012

Schwenk, J., Harmel, N., Zolles, G., Bildl, W., Kulik, A., Heimrich, B., … Klocker, N. (2009). Functional Proteomics Identify Cornichon Proteins as Auxiliary Subunits of AMPA Receptors. *Science*, *323*(5919), 1313–1319. https://doi.org/10.1126/science.1167852

Schwenk, Jochen, Boudkkazi, S., Kocylowski, M. K., Brechet, A., Zolles, G., Bus, T., … Fakler, B. (2019). An ER Assembly Line of AMPA-Receptors Controls Excitatory Neurotransmission and Its Plasticity. *Neuron*, *104*(4), 680-692.e9. https://doi.org/10.1016/j.neuron.2019.08.033

Sebollela, A., Freitas-Correa, L., Oliveira, F. F., Paula-Lima, A. C., Saraiva, L. M., Martins, S. M., … Ferreira, S. T. (2012). Amyloid-β oligomers induce differential gene expression in adult human brain slices. *Journal of Biological Chemistry*, *287*(10), 7436–7445. https://doi.org/10.1074/jbc.M111.298471

Selkoe, D. J. (2011). Resolving controversies on the path to Alzheimer's therapeutics. *Nature Medicine*, *17*(9), 1060–1065. https://doi.org/10.1038/nm.2460

Selkoe, D. J., & Hardy, J. (2016). The amyloid hypothesis of Alzheimer's disease at 25 years. *EMBO Molecular Medicine*, *8*(6), 595–608. https://doi.org/10.15252/emmm.201606210

Serrano-Pozo, A., Frosch, M. P., Masliah, E., & Hyman, B. T. (2011). Neuropathological alterations in Alzheimer disease. *Cold Spring Harbor Perspectives in Medicine*, *1*(1), 1–24. https://doi.org/10.1101/cshperspect.a006189

Setti, S. E., Hunsberger, H. C., & Reed, M. N. (2017). Alterations in hippocampal activity and Alzheimer's disease. *Translational Issues in Psychological Science*, *3*(4), 348–356. https://doi.org/10.1037/tps0000124

Shankar, G. M., Bloodgood, B. L., Townsend, M., Walsh, D. M., Selkoe, D. J., & Sabatini, B. L. (2007). Natural oligomers of the Alzheimer amyloid-β protein induce reversible synapse loss by modulating an NMDA-type glutamate receptor-dependent signaling pathway. *Journal of Neuroscience*, *27*(11), 2866–2875. https://doi.org/10.1523/JNEUROSCI.4970-06.2007

Shankar, G. M., Li, S., Mehta, T. H., Garcia-Munoz, A., Shepardson, N. E., Smith, I., … Selkoe, D. J. (2008). Amyloid-β protein dimers isolated directly from Alzheimer's brains impair synaptic plasticity and memory. *Nature Medicine*, *14*(8), 837–842. https://doi.org/10.1038/nm1782

Shen, J., & Kelleher, R. J. (2007). The presenilin hypothesis of Alzheimer's disease: Evidence for a loss-of-function pathogenic mechanism. *Proceedings of the National Academy of Sciences of the United States of America*, *104*(2), 403–409. https://doi.org/10.1073/pnas.0608332104

Sheng, M., & Kim, E. (2011). The postsynaptic organization of synapses. *Cold Spring Harbor Perspectives in Biology*, *3*(12). https://doi.org/10.1101/cshperspect.a005678

Sheng, M., Sabatini, B. L., & Südhof, T. C. (2015). Synapses and Alzheimer's Disease.*Cold Spring Harbor Perspectives in Biology, 4*(5). http://doi.org/10.1101/cshperspect.a005777.

Sheng, N., Bemben, M. A., Díaz-Alonso, J., Tao, W., Shi, Y. S., & Nicoll, R. A. (2018). LTP requires postsynaptic PDZ-domain interactions with glutamate receptor/auxiliary protein complexes. *Proceedings of the National Academy of Sciences*, *115*(15), 3948–3953. https://doi.org/10.1073/pnas.1800719115

Shepherd, J. D., & Huganir, R. L. (2007). The Cell Biology of Synaptic Plasticity: AMPA Receptor Trafficking. *Annual Review of Cell and Developmental Biology*, *23*(1), 613–643. https://doi.org/10.1146/annurev.cellbio.23.090506.123516

Shi, Y., Yamada, K., Liddelow, S. A., Smith, S. T., Zhao, L., Luo, W., … Holtzman, D. M. (2017). ApoE4 markedly exacerbates tau-mediated neurodegeneration in a mouse model of tauopathy. *Nature*, *549*(7673), 523–527. https://doi.org/10.1038/nature24016

Shrestha, B. R., Vitolo, O. V., Joshi, P., Lordkipanidze, T., Shelanski, M., & Dunaevsky, A. (2006). Amyloid β peptide adversely affects spine number and motility in hippocampal neurons. *Molecular and Cellular Neuroscience*, *33*(3), 274–282. https://doi.org/10.1016/j.mcn.2006.07.011

Silva, A. R. T., Grinberg, L. T., Farfel, J. M., Diniz, B. S., Lima, L. A., Silva, P. J. S., … Brentani, H. (2012). Transcriptional Alterations Related to Neuropathology and Clinical Manifestation of Alzheimer's Disease. *PLoS ONE*, *7*(11). https://doi.org/10.1371/journal.pone.0048751

Simpson, J. E., Ince, P. G., Shaw, P. J., Heath, P. R., Raman, R., Garwood, C. J., … Wharton, S. B. (2011). Microarray analysis of the astrocyte transcriptome in the aging brain: Relationship to Alzheimer's pathology and APOE genotype. *Neurobiology of Aging*, *32*(10), 1795–1807. https://doi.org/10.1016/j.neurobiolaging.2011.04.013

Skerrett, R., Malm, T., & Landreth, G. (2014). Nuclear receptors in neurodegenerative diseases. *Neurobiology of Disease*, *72*(Part A), 104–116. https://doi.org/10.1016/j.nbd.2014.05.019

Sleiman, P. M. A., Healy, D. G., Muqit, M. M. K., Yang, Y. X., Van Der Brug, M., Holton, J. L., … Wood, N. W. (2009). Characterisation of a novel NR4A2 mutation in Parkinson's disease brain. *Neuroscience Letters*, *457*(2), 75–79. https://doi.org/10.1016/j.neulet.2009.03.021

Smith, D. L., Pozueta, J., Gong, B., Arancio, O., & Shelanski, M. (2009). Reversal of long-term dendritic spine alterations in Alzheimer disease models. *Proceedings of the National Academy of Sciences of the United States of America*, *106*(39), 16877–16882. https://doi.org/10.1073/pnas.0908706106

Smith, G. A., Rocha, E. M., Rooney, T., Barneoud, P., McLean, J. R., Beagan, J., … Isacson, O. (2015). A Nurr1 agonist causes neuroprotection in a parkinson's disease lesion model primed with the toll-like receptor 3 dsRNA inflammatory stimulant poly(I:C). *PLoS ONE*, *10*(3), 1–14. https://doi.org/10.1371/journal.pone.0121072

Snyder, E. M., Nong, Y., Almeida, C. G., Paul, S., Moran, T., Choi, E. Y., … Greengard, P. (2005). Regulation of NMDA receptor trafficking by amyloid-β. *Nature Neuroscience*, *8*(8), 1051–1058. https://doi.org/10.1038/nn1503

Soderling, T. R. (2000). CaM-kinases: Modulators of synaptic plasticity. *Current Opinion in*

Neurobiology, *10*(3), 375–380. https://doi.org/10.1016/S0959-4388(00)00090-8

Song, I., & Huganir, R. L. (2002). Regulation of AMPA receptors during synaptic plasticity. *Trends in Neurosciences*, *25*(11), 578–588. https://doi.org/10.1016/s0166-2236(02)02270-1

Song, X., Liu, B., Cui, L., Zhou, B., Liu, W., Xu, F., … Ikejima, T. (2017). Silibinin ameliorates anxiety/depression-like behaviors in amyloid β-treated rats by upregulating BDNF/TrkB pathway and attenuating autophagy in hippocampus. *Physiology & Behavior*, *179*, 487–493. https://doi.org/10.1016/j.physbeh.2017.07.023

Sousa, K. M., Mira, H., Hall, A. C., Jansson-Sjöstrand, L., Kusakabe, M., & Arenas, E. (2007). Microarray Analyses Support a Role for Nurr1 in Resistance to Oxidative Stress and Neuronal Differentiation in Neural Stem Cells. *Stem Cells*, *25*(2), 511–519. https://doi.org/10.1634/stemcells.2006-0238

Spathis, A. D., Asvos, X., Ziavra, D., Karampelas, T., Topouzis, S., Cournia, Z., … Vassilatis, D. K. (2017). Nurr1:RXRα heterodimer activation as monotherapy for Parkinson's disease. *Proceedings of the National Academy of Sciences of the United States of America*, *114*(15), 3999–4004. https://doi.org/10.1073/pnas.1616874114

Sperling, R. A., Dickerson, B. C., Pihlajamaki, M., Vannini, P., LaViolette, P. S., Vitolo, O. V., … Johnson, K. A. (2010). Functional alterations in memory networks in early alzheimer's disease. *NeuroMolecular Medicine*, *12*(1), 27–43. https://doi.org/10.1007/s12017-009-8109-7

Sperling, R., Mormino, E., & Johnson, K. (2014). The Evolution of Preclinical Alzheimer's Disease: Implications for Prevention Trials. *Neuron*, *84*(3), 608–622. https://doi.org/10.1016/j.neuron.2014.10.038

Spires-Jones, T., & Knafo, S. (2012). Spines, plasticity, and cognition in Alzheimer's model mice. *Neural Plasticity*, *2012*. https://doi.org/10.1155/2012/319836

Spires, T. L., Meyer-Luehmann, M., Stern, E. A., McLean, P. J., Skoch, J., Nguyen, P. T., … Hyman, B. T. (2005). Dendritic spine abnormalities in amyloid precursor protein transgenic mice demonstrated by gene transfer and intravital multiphoton microscopy. *Journal of Neuroscience*, *25*(31), 7278–7287. https://doi.org/10.1523/JNEUROSCI.1879-05.2005

Steen, E., Terry, B. M., Rivera, E. J., Cannon, J. L., Neely, T. R., Tavares, R., … de la Monte, S. M. (2005). Impaired insulin and insulin-like growth factor expression and signaling mechanisms in Alzheimer's disease--is this type 3 diabetes? *Journal of Alzheimer's Disease : JAD*, *7*(1), 63–80. https://doi.org/10.3233/jad-2005-7107

Sturchler, E., Galichet, A., Weibel, M., Leclerc, E., & Heizmann, C. W. (2008). Site-specific blockade of RAGE-Vd prevents amyloid-β oligomer neurotoxicity. *Journal of Neuroscience*, *28*(20), 5149–5158. https://doi.org/10.1523/JNEUROSCI.4878-07.2008

Sun, H., Zhang, J., Zhang, L., Liu, H., Zhu, H., & Yang, Y. (2010). Environmental enrichment influences BDNF and NR1 levels in the hippocampus and restores cognitive impairment in chronic cerebral hypoperfused rats. *Current Neurovascular Research*, *7*(4), 268–280. https://doi.org/10.2174/156720210793180819

Sun, M. K., & Alkon, D. L. (2019). Neuro-regeneration Therapeutic for Alzheimer's Dementia: Perspectives on Neurotrophic Activity. *Trends in Pharmacological Sciences*, *40*(9), 655–668. https://doi.org/10.1016/j.tips.2019.07.008

Sun, X., Zhao, Y., & Wolf, M. E. (2005). Dopamine receptor stimulation modulates AMPA receptor synaptic insertion in prefrontal cortex neurons. *Journal of Neuroscience*, *25*(32), 7342–7351. https://doi.org/10.1523/JNEUROSCI.4603-04.2005

Tai, H. C., Serrano-Pozo, A., Hashimoto, T., Frosch, M. P., Spires-Jones, T. L., & Hyman, B. T. (2012). The synaptic accumulation of hyperphosphorylated tau oligomers in alzheimer disease is associated with dysfunction of the ubiquitin-proteasome system. *American Journal of Pathology*, *181*(4), 1426–1435. https://doi.org/10.1016/j.ajpath.2012.06.033

Takeda, S., Hashimoto, T., Roe, A. D., Hori, Y., Spires-Jones, T. L., & Hyman, B. T. (2013). Brain interstitial oligomeric amyloid β increases with age and is resistant to clearance from brain in a mouse model of Alzheimer's disease. *The FASEB Journal*, *27*(8), 3239–3248.

https://doi.org/10.1096/fj.13-229666

Tan, M. G., Chua, W. T., Esiri, M. M., Smith, A. D., Vinters, H. V., & Lai, M. K. (2010). Genome wide profiling of altered gene expression in the neocortex of Alzheimer's disease. *Journal of Neuroscience Research*, *88*(6), 1157–1169. https://doi.org/10.1002/jnr.22290

Terry, R. D. (1996). The pathogenesis of Alzheimer disease: an alternative to the amyloid hypothesis. *Journal of Neuropathology and Experimental Neurology*, *55*(10), 1023–1025.

Terry, R. D., Masliah, E., Salmon, D. P., Butters, N., DeTeresa, R., Hill, R., … Katzman, R. (1991). Physical basis of cognitive alterations in Alzheimer's disease: synapse loss is the major correlate of cognitive impairment. *Annals of Neurology*, *30*(4), 572–580. https://doi.org/10.1002/ana.410300410

Terzioglu-Usak, S., Negis, Y., Karabulut, D. S., Zaim, M., & Isik, S. (2017). Cellular Model of Alzheimer's Disease: Aβ1-42 Peptide Induces Amyloid Deposition and a Decrease in Topo Isomerase IIβ and Nurr1 Expression. *Current Alzheimer Research*, *14*(6), 636–644. https://doi.org/10.2174/1567205014666170117103217

Thakur, A., Wang, X., Siedlak, S. L., Perry, G., Smith, M. A., & Zhu, X. (2007). c-Jun phosphorylation in Alzheimer disease. *Journal of Neuroscience Research*, *85*(8), 1668–1673. https://doi.org/10.1002/jnr.21298

Tokuoka, H., Hatanaka, T., Metzger, D., & Ichinose, H. (2014). Nurr1 expression is regulated by voltage-dependent calcium channels and calcineurin in cultured hippocampal neurons. *Neuroscience Letters*, *559*, 50–55. https://doi.org/10.1016/j.neulet.2013.11.033

Tomita, S., Chen, L., Kawasaki, Y., Petralia, R. S., Wenthold, R. J., Nicoll, R. A., & Bredt, D. S. (2003). Functional studies and distribution define a family of transmembrane AMPA receptor regulatory proteins. *Journal of Cell Biology*, *161*(4), 805–816. https://doi.org/10.1083/jcb.200212116

Tomiyama, T., Matsuyama, S., Iso, H., Umeda, T., Takuma, H., Ohnishi, K., … Mori, H. (2010). A mouse model of amyloid β oligomers: Their contribution to synaptic alteration, abnormal tau phosphorylation, glial activation, and neuronal loss in vivo. *Journal of Neuroscience*, *30*(14), 4845–4856. https://doi.org/10.1523/JNEUROSCI.5825-09.2010

Torres-Lista, V., & Giménez-Llort, L. (2013). Impairment of nesting behaviour in 3xTg-AD mice. *Behavioural Brain Research*, *247*, 153–157. https://doi.org/10.1016/j.bbr.2013.03.021

Torres-Lista, V., López-Pousa, S., & Giménez-Llort, L. (2015). Marble-burying is enhanced in 3xTg-AD mice, can be reversed by risperidone and it is modulable by handling. *Behavioural Processes*, *116*, 69–74. https://doi.org/10.1016/j.beproc.2015.05.001

Torretta, S., Rampino, A., Basso, M., Pergola, G., Di Carlo, P., Shin, J. H., … Bertolino, A. (2020). NURR1 and ERR1 Modulate the Expression of Genes of a DRD2 Coexpression Network Enriched for Schizophrenia Risk. *The Journal of Neuroscience : The Official Journal of the Society for Neuroscience*, *40*(4), 932–941. https://doi.org/10.1523/JNEUROSCI.0786-19.2019

Treit, D., & Fundytus, M. (1988). Thigmotaxis as a test for anxiolytic activity in rats. *Pharmacology, Biochemistry, and Behavior*, *31*(4), 959–962. https://doi.org/10.1016/0091-3057(88)90413-3

Trinczek, B., Biernat, J., Baumann, K., Mandelkow, E., & Mandelkow, E. M. (1995). Domains of tau protein, differential phosphorylation, and dynamic instability of microtubules. *Molecular Biology of the Cell*, *6*(12), 1887–1902. https://doi.org/10.1091/mbc.6.12.1887

Tseng, B. P., Green, K. N., Chan, J. L., Blurton-Jones, M., & LaFerla, F. M. (2008). Aβ inhibits the proteasome and enhances amyloid and tau accumulation. *Neurobiology of Aging*, *29*(11), 1607–1618. https://doi.org/10.1016/j.neurobiolaging.2007.04.014

Tsien, J. Z., Huerta, P. T., & Tonegawa, S. (1996). The essential role of hippocampal CA1 NMDA receptor-dependent synaptic plasticity in spatial memory. *Cell*, *87*(7), 1327–1338. https://doi.org/10.1016/S0092-8674(00)81827-9

Tsokas, P., Grace, E. A., Chan, P. M., Ma, T., Sealfon, S. C., Iyengar, R., … Blitzer, R. D. (2005). Local protein synthesis mediates a rapid increase in dendritic elongation factor 1A after induction of late long-term potentiation. *Journal of Neuroscience*, *25*(24), 5833–5843.

https://doi.org/10.1523/JNEUROSCI.0599-05.2005

Tu, S., Okamoto, S., Lipton, S. A., & Xu, H. (2014). Oligomeric Aβ-induced synaptic dysfunction in Alzheimer's disease. *Molecular Neurodegeneration 9*(48), 1–12. https://doi.org/10.1186/1750-1326-9-48.

Tzeng, N. S., Chung, C. H., Lin, F. H., Chiang, C. P., Yeh, C. Bin, Huang, S. Y., … Chien, W. C. (2018). Anti-herpetic Medications and Reduced Risk of Dementia in Patients with Herpes Simplex Virus Infections—a Nationwide, Population-Based Cohort Study in Taiwan. *Neurotherapeutics*, *15*(2), 417–429. https://doi.org/10.1007/s13311-018-0611-x

Umeda, T., Tomiyama, T., Sakama, N., Tanaka, S., Lambert, M. P., Klein, W. L., & Mori, H. (2011). Intraneuronal amyloid β oligomers cause cell death via endoplasmic reticulum stress, endosomal/lysosomal leakage, and mitochondrial dysfunction in vivo. *Journal of Neuroscience Research*, *89*(7), 1031–1042. https://doi.org/10.1002/jnr.22640

Varvel, N. H., Bhaskar, K., Patil, A. R., Pimplikar, S. W., Herrup, K., & Lamb, B. T. (2008). Aβ oligomers induce neuronal cell cycle events in Alzheimer's disease. *Journal of Neuroscience*, *28*(43), 10786–10793. https://doi.org/10.1523/JNEUROSCI.2441-08.2008

Vassar, R., Bennett, B. D., Babu-Khan, S., Kahn, S., Mendiaz, E. A., Denis, P., … Citron, M. (1999). β-Secretase cleavage of Alzheimer's amyloid precursor protein by the transmembrane aspartic protease BACE. *Science*, *286*(5440), 735–741. https://doi.org/10.1126/science.286.5440.735

Vecsey, C. G., Hawk, J. D., Lattal, K. M., Stein, J. M., Fabian, S. A., Attner, M. A., … Wood, M. A. (2007). Histone deacetylase inhibitors enhance memory and synaptic plasticity via CREB: CBP-dependent transcriptional activation. *Journal of Neuroscience*, *27*(23), 6128–6140. https://doi.org/10.1523/JNEUROSCI.0296-07.2007

Vitolo, O. V., Sant'Angelo, A., Costanzo, V., Battaglia, F., Arancio, O., & Shelanski, M. (2002). Amyloid -peptide inhibition of the PKA/CREB pathway and long-term potentiation: Reversibility by drugs that enhance cAMP signaling. *Proceedings of the National Academy of Sciences*, *99*(20), 13217–13221. https://doi.org/10.1073/pnas.172504199

Vogel-Ciernia, A., Matheos, D. P., Barrett, R. M., Kramár, E. A., Azzawi, S., Chen, Y., … Wood, M. A. (2013). The neuron-specific chromatin regulatory subunit BAF53b is necessary for synaptic plasticity and memory. *Nature Neuroscience*, *16*(5), 552–561. https://doi.org/10.1038/nn.3359

Voisin, T., & Vellas, B. (2009). Diagnosis and treatment of patients with severe Alzheimer's disease. *Drugs and Aging*, *26*(2), 135–144. https://doi.org/10.2165/0002512-200926020-00005

Volakakis, N., Kadkhodaei, B., Joodmardi, E., Wallis, K., Panman, L., Silvaggi, J., … Perlmann, T. (2010). NR4A orphan nuclear receptors as mediators of CREB-dependent neuroprotection. *Proceedings of the National Academy of Sciences of the United States of America*, *107*(27), 12317–12322. https://doi.org/10.1073/pnas.1007088107

Volpicelli, F., Caiazzo, M., Greco, D., Consales, C., Leone, L., Perrone-Capano, C., … Porzio, U. Di. (2007). Bdnf gene is a downstream target of Nurr1 transcription factor in rat midbrain neurons in vitro. *Journal of Neurochemistry*, *102*(2), 441–453. https://doi.org/10.1111/j.1471-4159.2007.04494.x

Von Hertzen, L. S. J., & Giese, K. P. (2005). Memory reconsolidation engages only a subset of immediate-early genes induced during consolidation. *Journal of Neuroscience*, *25*(8), 1935–1942. https://doi.org/10.1523/JNEUROSCI.4707-04.2005

Vuillermot, S., Joodmardi, E., Perlmann, T., Ove Ögren, S., Feldon, J., & Meyer, U. (2011). Schizophrenia-relevant behaviors in a genetic mouse model of constitutive Nurr1 deficiency. *Genes, Brain and Behavior*, *10*(5), 589–603. https://doi.org/10.1111/j.1601-183X.2011.00698.x

Walsh, D. M., Klyubin, I., Fadeeva, J. V., Cullen, W. K., Anwyl, R., Wolfe, M. S., … Selkoe, D. J. (2002). Naturally secreted oligomers of amyloid β protein potently inhibit hippocampal long-term potentiation in vivo. *Nature*, *416*(6880), 535–539. https://doi.org/10.1038/416535a

Walsh, D. M., & Selkoe, D. J. (2007). Aβ oligomers - A decade of discovery. *Journal of Neurochemistry*, *101*(5), 1172–1184. https://doi.org/10.1111/j.1471-4159.2006.04426.x

Walsh, D. M., Townsend, M., Podlisny, M. B., Shankar, G. M., Fadeeva, J. V., El Agnaf, O., … Selkoe, D. J. (2005). Certain inhibitors of synthetic amyloid β-peptide (Aβ) fibrillogenesis block oligomerization of natural Aβ and thereby rescue long-term potentiation. *Journal of Neuroscience*, *25*(10), 2455–2462. https://doi.org/10.1523/JNEUROSCI.4391-04.2005

Wang, J. Q., Guo, M. L., Jin, D. Z., Xue, B., Fibuch, E. E., & Mao, L. M. (2014). Roles of subunit phosphorylation in regulating glutamate receptor function. *European Journal of Pharmacology*, *728*(1), 183–187. https://doi.org/10.1016/j.ejphar.2013.11.019

Wang, Jian, Yang, J., Zou, Y., Huang, G.-L., & He, Z.-W. (2013). Orphan Nuclear Receptor Nurr1 as a Potential Novel Marker for Progression in Human Prostate Cancer. *Asian Pacific Journal of Cancer Prevention*, *14*(3), 2023–2028. https://doi.org/10.7314/APJCP.2013.14.3.2023

Wang, Jun, Bi, W., Zhao, W., Varghese, M., Koch, R. J., Walker, R. H., … Pasinetti, G. M. (2016a). Selective brain penetrable Nurr1 transactivator for treating Parkinson's disease. *Oncotarget*, *7*(7). https://doi.org/10.18632/oncotarget.7191

Wang, M., Qin, L., & Tang, B. (2019). MicroRNAs in Alzheimer's disease. *Frontiers in Genetics*, *10*(MAR), 1–13. https://doi.org/10.3389/fgene.2019.00153

Wang, Q., Walsh, D. M., Rowan, M. J., Selkoe, D. J., & Anwyl, R. (2004). Block of Long-Term Potentiation by Naturally Secreted and Synthetic Amyloid β-Peptide in Hippocampal Slices Is Mediated via Activation of the Kinases c-Jun N-Terminal Kinase, Cyclin-Dependent Kinase 5, and p38 Mitogen-Activated Protein Kinase as well as M. *Journal of Neuroscience*, *24*(13), 3370–3378. https://doi.org/10.1523/JNEUROSCI.1633-03.2004

Wang, X., Zhuang, W., Fu, W., Wang, X., Lv, E., Li, F., … Wang, X. (2018). The lentiviral-mediated Nurr1 genetic engineering mesenchymal stem cells protect dopaminergic neurons in a rat model of Parkinson's disease. *American Journal of Translational Research*, *10*(6), 1583–1599.

Wang, Z., Benoit, G., Liu, J., Prasad, S., Aarnisalo, P., Liu, X., … Perlmann, T. (2003). Structure and function of Nurr1 identifies a class of ligand-independent nuclear receptors. *Nature*, *423*(6939), 555–560. https://doi.org/10.1038/nature01645

Wang, Z. H., Xiang, J., Liu, X., Yu, S. P., Manfredsson, F. P., Sandoval, I. M., … Ye, K. (2019). Deficiency in BDNF/TrkB Neurotrophic Activity Stimulates δ-Secretase by Upregulating C/EBPβ in Alzheimer's Disease. *Cell Reports*, *28*(3), 655-669.e5. https://doi.org/10.1016/j.celrep.2019.06.054

Wang, Z. X., Tan, L., Liu, J., & Yu, J. T. (2016b). The Essential Role of Soluble Aβ Oligomers in Alzheimer's Disease. *Molecular Neurobiology*, *53*(3), 1905–1924. https://doi.org/10.1007/s12035-015-9143-0

Wansa, K. D. S. A., Harris, J. M., Yan, G., Ordentlich, P., & Muscat, G. E. O. (2003). The AF-1 Domain of the Orphan Nuclear Receptor NOR-1 Mediates Trans-activation, Coactivator Recruitment, and Activation by the Purine Anti-metabolite 6-Mercaptopurine. *Journal of Biological Chemistry*, *278*(27), 24776–24790. https://doi.org/10.1074/jbc.M300088200

Watson, J. F., Ho, H., & Greger, I. H. (2017). Synaptic transmission and plasticity require AMPA receptor anchoring via its N-terminal domain. *ELife*, *6*, 1–20. https://doi.org/10.7554/eLife.23024

Wei, X., Gao, H., Zou, J., Liu, X., Chen, D., Liao, J., … Wang, Q. (2016b). Contra-directional Coupling of Nur77 and Nurr1 in Neurodegeneration: A Novel Mechanism for Memantine-Induced Anti-inflammation and Anti-mitochondrial Impairment. *Molecular Neurobiology*, *53*(9), 5876–5892. https://doi.org/10.1007/s12035-015-9477-7

Wei, Z., Meng, X., El Fatimy, R., Sun, B., Mai, D., Zhang, J., … Li, S. (2020). Environmental enrichment prevents Aβ oligomer-induced synaptic dysfunction through mirna-132 and hdac3 signaling pathways. *Neurobiology of Disease*, *134*(October 2019). https://doi.org/10.1016/j.nbd.2019.104617

Wesson, D. W., & Wilson, D. A. (2011). Age and gene overexpression interact to abolish nesting behavior in Tg2576 amyloid precursor protein (APP) mice. *Behavioural Brain Research*, *216*(1), 408–413. https://doi.org/10.1016/j.bbr.2010.08.033

West, A. E., & Greenberg, M. E. (2011). Neuronal activity-regulated gene transcription in synapse

development and cognitive function. *Cold Spring Harbor Perspectives in Biology*, *3*(6), 1–21. https://doi.org/10.1101/cshperspect.a005744

Widagdo, J., Guntupalli, S., Jang, S. E., & Anggono, V. (2017). Regulation of AMPA receptor trafficking by protein ubiquitination. *Frontiers in Molecular Neuroscience*, *10*(OCT), 1–10. https://doi.org/10.3389/fnmol.2017.00347

Wilson, E. N., Abela, A. R., Do Carmo, S., Allard, S., Marks, A. R., Welikovitch, L. A., … Cuello, A. C. (2016). Intraneuronal Amyloid Beta Accumulation Disrupts Hippocampal CRTC1-Dependent Gene Expression and Cognitive Function in a Rat Model of Alzheimer Disease. *Cerebral Cortex*, *27*(2). https://doi.org/10.1093/cercor/bhv332

Winblad, B., & Poritis, N. (1999). Memantine in severe dementia: results of the9M-best study (benefit and efficacy in severly demented patients during treatment with memantine). *International Journal of Geriatric Psychiatry*, *14*(2), 135–146. https://doi.org/10.1002/(SICI)1099-1166(199902)14:2<135::AID-GPS906>3.0.CO;2-0

Wong, J., Higgins, M., Halliday, G., & Garner, B. (2012). Alternative Transcript Expression With Implications for Alzheimer ' S Disease. *Nsc*, *210*, 363–374. https://doi.org/10.1016/j.neuroscience.2012.02.037

Wozniak, M. A., Mee, A. P., & Itzhaki, R. F. (2009). Herpes simplex virus type 1 DNA is located within Alzheimer's disease amyloid plaques. *The Journal of Pathology*, *217*(1), 131–138. https://doi.org/10.1002/path.2449

Wright, A. L., Zinn, R., Hohensinn, B., Konen, L. M., Beynon, S. B., Tan, R. P., … Vissel, B. (2013). Neuroinflammation and Neuronal Loss Precede Aβ Plaque Deposition in the hAPP-J20 Mouse Model of Alzheimer's Disease. *PLoS ONE*, *8*(4), e59586. https://doi.org/10.1371/journal.pone.0059586

Wu, H. Y., Kuo, P. C., Wang, Y. T., Lin, H. T., Roe, A. D., Wang, B. Y., … Tai, H. C. (2018). B-Amyloid Induces Pathology-Related Patterns of Tau Hyperphosphorylation At Synaptic Terminals. *Journal of Neuropathology and Experimental Neurology*, *77*(9), 814–826. https://doi.org/10.1093/jnen/nly059

Xiang, J., Wang, Z. H., Ahn, E. H., Liu, X., Yu, S. P., Manfredsson, F. P., … Ye, K. (2019). Delta-secretase-cleaved Tau antagonizes TrkB neurotrophic signalings, mediating Alzheimer's disease pathologies. *Proceedings of the National Academy of Sciences of the United States of America*, *116*(18), 9094–9102. https://doi.org/10.1073/pnas.1901348116

Xie, X., Peng, L., Zhu, J., Zhou, Y., Li, L., Chen, Y., … Zhao, Y. (2017). MiR-145-5p/Nurr1/TNF-α signaling-induced microglia activation regulates neuron injury of acute cerebral ischemic/reperfusion in rats. *Frontiers in Molecular Neuroscience*, *10*(NOV). https://doi.org/10.3389/fnmol.2017.00383

Xu, P.-Y., Liang, R., Jankovic, J., Hunter, C., Zeng, Y.-X., Ashizawa, T., … Le, W.-D. (2002). Association of homozygous 7048G7049 variant in the intron six of Nurr1 gene with Parkinson's disease. *Neurology*, *58*(6), 881–884. https://doi.org/10.1212/wnl.58.6.881

Yamada, K., Cirrito, J. R., Stewart, F. R., Jiang, H., Finn, M. B., Holmes, B. B., … Holtzman, D. M. (2011). In vivo microdialysis reveals age-dependent decrease of brain interstitial fluid tau levels in P301S human tau transgenic mice. *Journal of Neuroscience*, *31*(37), 13110–13117. https://doi.org/10.1523/JNEUROSCI.2569-11.2011

Yang, K.-L., Chen, M.-F., Liao, C.-H., Pang, C.-Y., & Lin, P.-Y. (2009). A simple and efficient method for generating Nurr1-positive neuronal stem cells from human wisdom teeth (tNSC) and the potential of tNSC for stroke therapy. *Cytotherapy*, *11*(5), 606–617. https://doi.org/10.1080/14653240902806994

Yao, P. J., Zhu, M., Pyun, E. I., Brooks, A. I., Therianos, S., Meyers, V. E., & Coleman, P. D. (2003). Defects in expression of genes related to synaptic vesicle trafficking in frontal cortex of Alzheimer's disease. *Neurobiology of Disease*, *12*(2), 97–109. https://doi.org/10.1016/S0969-9961(02)00009-8

Yin, Y., Gao, D., Wang, Y., Wang, Z. H., Wang, X., Ye, J., … Wang, J. Z. (2016). Tau accumulation induces synaptic impairment and memory deficit by calcineurin-mediated inactivation of nuclear CaMKIV/CREB signaling. *Proceedings of the National Academy of Sciences of the*

United States of America, *113*(26), E3773–E3781. https://doi.org/10.1073/pnas.1604519113

Yiu, A. P., Rashid, A. J., & Josselyn, S. A. (2011). Increasing CREB function in the CA1 region of dorsal hippocampus rescues the spatial memory deficits in a mouse model of alzheimer's disease. *Neuropsychopharmacology*, *36*(11), 2169–2186. https://doi.org/10.1038/npp.2011.107

Yue, P., Gao, L., Wang, X., Ding, X., & Teng, J. (2018). Ultrasound-triggered effects of the microbubbles coupled to GDNF- and Nurr1-loaded PEGylated liposomes in a rat model of Parkinson's disease. *Journal of Cellular Biochemistry*, *119*(6), 4581–4591. https://doi.org/10.1002/jcb.26608

Yuste, R., & Bonhoeffer, T. (2001). Morphological Changes in Dendritic Spines Associated with Long-Term Synaptic Plasticity. *Annual Review of Neuroscience*, *24*(1), 1071–1089. https://doi.org/10.1146/annurev.neuro.24.1.1071

Zagrebelsky, M., & Korte, M. (2014). Form follows function: BDNF and its involvement in sculpting the function and structure of synapses. *Neuropharmacology*, *76*(PART C), 628–638. https://doi.org/10.1016/j.neuropharm.2013.05.029

Zempel, H., Thies, E., Mandelkow, E., & Mandelkow, E. M. (2010). Aβ oligomers cause localized Ca2+ elevation, missorting of endogenous Tau into dendrites, Tau phosphorylation, and destruction of microtubules and spines. *Journal of Neuroscience*, *30*(36), 11938–11950. https://doi.org/10.1523/JNEUROSCI.2357-10.2010

Zetterström, R. H., Williams, R., Perlmann, T., & Olson, L. (1996). Cellular expression of the immediate early transcription factors Nurr1 and NGFI-B suggests a gene regulatory role in several brain regions including the nigrostriatal dopamine system. *Molecular Brain Research*, *41*(1–2), 111–120. https://doi.org/10.1016/0169-328X(96)00074-5

Zhang, H., Zhang, C., Vincent, J., Zala, D., Benstaali, C., Sainlos, M., … Choquet, D. (2018). Modulation of AMPA receptor surface diffusion restores hippocampal plasticity and memory in Huntington's disease models. *Nature Communications*, *9*(1). https://doi.org/10.1038/s41467-018-06675-3

Zhang, S. J., Steijaert, M. N., Lau, D., Schütz, G., Delucinge-Vivier, C., Descombes, P., & Bading, H. (2007). Decoding NMDA Receptor Signaling: Identification of Genomic Programs Specifying Neuronal Survival and Death. *Neuron*, *53*(4), 549–562. https://doi.org/10.1016/j.neuron.2007.01.025

Zhang, X., Odom, D. T., Koo, S. H., Conkright, M. D., Canettieri, G., Best, J., … Montminy, M. (2005). Genome-wide analysis of cAMP-response element binding protein occupancy, phosphorylation, and target gene activation in human tissues. *Proceedings of the National Academy of Sciences of the United States of America*, *102*(12), 4459–4464. https://doi.org/10.1073/pnas.0501076102

Zhang, Z., Li, X., Xie, W., Tuo, H., Hintermann, S., Jankovic, J., & Le, W. (2012). Anti-parkinsonian effects of Nurr1 activator in ubiquitin-proteasome system impairment induced animal model of Parkinson's disease. *CNS & Neurological Disorders Drug Targets*, *11*(6), 768–773. https://doi.org/10.2174/187152712803581155

Zhao, L. G., Tang, Y., Tan, J. Z., Wang, J. W., Chen, G. J., & Zhu, B. L. (2018). The effect of NR4A1 on APP metabolism and tau phosphorylation. *Genes and Diseases*, *5*(4), 342–348. https://doi.org/10.1016/j.gendis.2018.04.008

Zhao, W. Q., Santini, F., Breese, R., Ross, D., Zhang, X. D., Stone, D. J., … Ray, W. J. (2010). Inhibition of calcineurin-mediated endocytosis and α-amino-3-hydroxy- 5-methyl-4-isoxazolepropionic acid (AMPA) receptors prevents amyloid β oligomer-induced synaptic disruption. *Journal of Biological Chemistry*, *285*(10), 7619–7632. https://doi.org/10.1074/jbc.M109.057182

Zheng, H., & Koo, E. H. (2006). The amyloid precursor protein: Beyond amyloid. *Molecular Neurodegeneration*, *1*(1), 1–12. https://doi.org/10.1186/1750-1326-1-5

Zhou, Q., Homma, K. J., & Poo, M. M. (2004). Shrinkage of dendritic spines associated with long-term depression of hippocampal synapses. *Neuron*, *44*(5), 749–757. https://doi.org/10.1016/j.neuron.2004.11.011

Zhou, Z., Liu, A., Xia, S., Leung, C., Qi, J., Meng, Y., … Jia, Z. (2018). The C-terminal tails of endogenous GluA1 and GluA2 differentially contribute to hippocampal synaptic plasticity and learning. *Nature Neuroscience*, *21*(1), 50–62. https://doi.org/10.1038/s41593-017-0030-z

Zucchella, C., Sinforiani, E., Tamburin, S., Federico, A., Mantovani, E., Bernini, S., … Bartolo, M. (2018). The Multidisciplinary Approach to Alzheimer's Disease and Dementia. A Narrative Review of Non-Pharmacological Treatment. *Frontiers in Neurology*, *9*(DEC), 1–22. https://doi.org/10.3389/fneur.2018.01058